

Swan View Coalition

Nature and Human Nature on the Same Path



3165 Foothill Road, Kalispell, MT 59901

swanview.org & swanrange.org

ph/fax 406-755-1379

December 12, 2023

Chris Dowling
Swan Lake District Ranger
200 Ranger Station Road
Bigfork, MT 59911

Submission via <https://www.fs.usda.gov/project/flathead/?project=64924> and via email to Christopher.Dowling@usda.gov and jeffrey.durkin@usda.gov

Re: Comments on Rumbling Owl Fuels Reduction Project/Proposed Action

Dear Ranger Dowling and Silviculturist Durkin;

Please accept these comments in the above matter into the public record. We incorporate by reference the comments being submitted by Friends of the Wild Swan and Alliance for the Wild Rockies in this matter. Due to the size and scope of this Project, the vague nature of the Scoping/Proposed Action (PA) document, and the substantial uncertainty regarding the effects of the PA in the face of climate change, we discuss a number of issues that must be addressed in an Environmental Impact Statement.

Moreover, the PA proposes logging “beyond the WUI” and outside a public drinking water source area. This disqualifies the Project from the emergency exemption it seeks under the Infrastructure Investment and Jobs Act. The requisite public comment period must be provided for the DEIS, followed by the requisite Objection period when the FEIS and draft ROD are issued. Moreover, you must clearly describe and demonstrate that the WUI for the Project area was properly determined according to the requirements of the Healthy Forest Restoration Act and all other applicable laws and regulations.

1. Old-growth is barely mentioned in the PA and only then to indicate logging will occur in old-growth. The PA claims a priority is to favor ponderosa pine, western white pine and western larch, claiming this “**may** provide for long-term persistence of old growth in the future as they can achieve very large sizes, are resilient to fire when [they] achieve sufficient size, and are high value to wildlife as snags or downed wood.” (Emphasis added).

The PA proposes disturbance and damage to old-growth, with no real assurance it will help nurture existing and potential old-growth in the future. Indeed, SLRD logging has

greatly reduced the number and size of snags in its logging units in the Swan Valley, in spite of its Forest Plan standards and the requirements of the Migratory Bird Treaty Act. Please find attached, as Exhibit A, Mark Benedict's 11/25/23 letter to the Regional Forester documenting his monitoring of the logging of numerous units in the Cold Jim Project and his call for a halt to logging of Unit 8 due to inadequate marking for the protection of a known great gray owl nest, snags and other habitats for birds protected under the MBTA. The facts and photos presented by Mr. Benedict show that logging in old-growth and potential old-growth forests in fact destroys much of the potential for those stands to remain or become old-growth and to harbor the full array of associated and dependent species.

The PA maps do not show the location of old-growth or mature stands that should serve as recruitment old-growth. This must be remedied in an EIS.

Moreover, the PA states that the Project "would make progress towards improving forest health by reducing stocking levels . . ." This would destroy essential old-growth characteristics, especially those dependent on higher stocking levels. Moreover, logging and thinning would reduce the forest's carbon storage capacity, which is critical to maintain in the face of climate change.

As Dr. Beverley Law testified in 2021:

Impacts of tree removals on forest carbon stocks should be assessed as part of a strategic decision-making process. Preemptive broad-scale thinning will create a multi-decade carbon deficit that conflicts with carbon climate goals.

Deforestation and degradation reduce carbon stocks and other ecosystem benefits, create habitat loss that is a major cause of species extinctions, and are major sources of greenhouse gas emissions that further contributes to warming that amplifies risk of species extinction. Mature and old forests store more carbon in trees and soil than do young forests, and continue to accumulate it over decades to centuries making them the most effective forest-related climate mitigation strategy. High carbon density forests also have high biodiversity (species, critical habitat), promoting resilience to climate change.

Law, Beverly E., April 29, 2021, Statement Before the United States House of Representatives Subcommittee on National Parks, Forests and Public Lands <https://www.congress.gov/117/meeting/house/112540/witnesses/HHRG-117-II10-Wstate-LawB-20210429.pdf> and attached as Exhibit B.

The treatment of this issue in the revised Forest Plan and its FEIS is wholly inadequate. The environmental analyses for this Project must remedy that, not simply tier to it.

2. The PA's logging and thinning would render stands more susceptible to wind-driven fire as air movement is able to increase within the opened stands. We include in our attachments research papers demonstrating that the effects of the PA are highly controversial and uncertain, which mandates the preparation of an EIS (see the Ninth Circuit opinion in *Bark v. USFS*, Attachment C). We summarize here the expert findings

of Dr. Joseph Werne, extracted from his 4/4/21 Declaration regarding the inadequacy of current fire models and fuels management prescriptions (Attachment D):

- a. When ladder fuels are removed (by thinning), ground-level wind speed and turbulent mixing both increase, leading to faster fire spread and greater oxygen-transport efficiency; this, in turn, results in increased fire intensity.
- b. In many cases this aerodynamic effect is more important than the fire-dampening effects of the fuels reduction being evaluated.
- c. Two recent studies demonstrate just how consequential neglecting canopy wind-drag effects can be, leading to potentially disastrous results if aggressive ladder-fuel removal is applied. See Atchley et al. 2021, and Banerjee et al. 2020 (attached to declaration).
- d. Both papers demonstrate that the removal of ladder fuels reduces the sub-canopy wind drag, ultimately leading to increased fire spread.
- e. In other words, they both show how fuels-reduction treatments can increase fire spread, which is the opposite of what currently-used operational model studies predict.
- f. Furthermore, the Banerjee et al. 2020 paper goes further and also shows that aggressive ladder fuel removal increases the likelihood of overstory crown fires compared to more modest ladder fuel reductions, which is again opposite to operational model-run predictions.
- g. Other recent studies also confirm these findings. Coen et al. 2018 (attached to declaration) demonstrate that drought and fuel load were secondary effects compared to fire-induced atmospheric motions, which operational fire-behavior models neglect.
- h. Bradley et al. (2016) (attached to declaration) analyzed satellite data for 1500 fires from 1984 to 2014, affecting 23.5 million acres of forestland. Their results show that the more heavily forestland is managed, the more severely it burns, and the least-managed land (i.e., our National Parks and Wilderness Areas) are the most firesafe.
- i. By omitting atmospheric dynamics and wind-drag effects associated with vegetation treatments, fuels reductions designed to reduce fire intensity and fire spread are undoubtedly producing the opposite effect.

The PA is controversial and its effects are uncertain because it proposes to log and thin mature stands, some of which are old-growth. The PA is also controversial and its effects are uncertain because it proposes fuels reduction activities where past management activities have reduced fuels but vegetation growth in the project area reportedly creates a need for further treatment. In other words, areas that haven't been disturbed in the past need to be disturbed now and those that have been disturbed in the recent past need to be disturbed again, using methods that the research cited above indicates will have the opposite of intended effects on fire spread. An EIS is required as these fuels reduction treatments must be repeated over and over if one follows the logic under which they are proposed.

3. Whitebark pine is not even mentioned in the PA. Whitebark pine was recently listed under the ESA as a “threatened” species. This proposal must undergo Section 7 consultation with Fish and Wildlife Service to determine if whitebark pine is present in the area and, if so, what the effects will be on the species. A key aspect of that consultation must be to resolve the fact that whitebark pine utilize stand-replacement fire to reproduce, yet the Project’s intent is to limit or eliminate stand-replacement fires.

4. An EIS is also required to adequately assess cumulative effects in the Project area and beyond. The PA makes no mention of other past, current and future projects in the Swan Valley that in one way or another affect fire fuels, such as Mid-Swan Landscape, Cooney-McKay, Summit Mtn Salvage, Swan Bottom Burning, Beaver Creek, Glacier Loon, Cold Jim, Chilly James, Hemlock-Elk, Mid-Swan Blowdown, Mission Wilderness Burn, FNF Precommercial Thinning, Sixmile Fuels Reduction, Weed Lake Landscape Restoration, and Bug Creek Project, among others. An EA is not sufficient to adequately address the individual or cumulative effects of what essentially boils down to an agency agenda to “treat fuels” in these areas in perpetuity. Rumbling-Owl is clearly not a one-off project, yet it is being proposed as some minor project that should be exempt from full public review in an EIS and exempt from formal Objections.

You must adequately consider in an EIS the cumulative effects of these and all other activities that have occurred, are occurring and are expected to occur in the PA Project area and its surrounding area. Should you fail to do so, you face the prospect of an adverse court opinion like the one found in Attachment C. What is the status of these other projects? What monitoring data have you collected from them? What have you learned from these other projects? What are their cumulative impacts?

5. The Project area “supports populations of federally threatened bull trout, grizzly bear, and Canada Lynx, as well as gray wolves, elk, moose, deer, mountain lions and wolverines.” This is why Land and Water Conservation Funds were used to bring Section 33 near Holland Lake into public/Forest Service ownership in 2017. (See the Flathead NF web page in Attachment E). We note, however, that wolverine was listed under the ESA as a threatened species on 11/30/23, meaning the FS must undergo formal consultation with FWS regarding the impacts of this Project and the cumulative effects of this and other projects on wolverine.

Moreover, it is disturbing to read on page 5 of the PA that timber management prescription MA 6b “was selected to be applied to Section 33 . . . effective in September 2023.” Where was the public notice and public comment period provided so the public had some say in how this largely cutover section of land should be managed? If roadless lands are so important to wildlife conservation, as bragged by the Flathead NF in Exhibit E, why not remove all roads from Section 33, give it a rest, and let it recover naturally from past abuses?

6. The Project also proposes to bring some old Plum Creek roads in Section 33 into the FS road “system” while only mentioning “potential road decommissioning” for other roads there. This would appear to violate Forest Plan standard FW-STD-IFS-02 by

increasing total motorized route density over what it was in the 2011 baseline. This is because the definition of TMRD includes “Federal, State, and tribal roads and motorized trails that do not meet the definition of impassable road.” (Forest Plan Glossary).

In other words, the old Plum Creek roads and other private roads were apparently not counted in TMRD in the 2011 baseline, but must now be counted in TMRD if brought into the road system and not rendered “impassable” or decommissioned, thus increasing TMRD above the baseline. The FS may argue that the effects of the baseline remain unchanged because the on-the-ground effects of the old Plum Creek roads do not change, even if the TMRD numbers increase. But that would be to argue against the very “reason” the revised Forest Plan changed the definition of TMRD to allow roads to remain on the landscape as “impassable,” rather than requiring them to be decommissioned in order to not be counted in TMRD – as was the case under Amendment 19 to the former Forest Plan because even closed roads continue to displace grizzly bears.

Simply put, TMRD under the revised Forest Plan has limited relevance to impacts to grizzly bears because it ignores the prior requirement to fully decommission roads in order to remove them from TMRD. The revised Forest Plan and the Project also ignore the need to decommission an offsetting mileage of roads in order to bring new roads into the system without increasing TMRD.

Page 8 of the PA states that there will be 8 miles of new road construction, not counting the 4 miles of temporary road construction. Page 10 says only 3 miles of road decommissioning are proposed. That’s a net increase of 5 miles of new roads, yet this somehow doesn’t violate the requirement to not increase TMRD? Page 8 makes one wonder if planners of the Project fully understand the requirements of the Forest Plan:

All the new [road] construction is proposed to take place on existing road templates which would increase the amount of system roads in the Project Area. These road segments would not be open to the public and have barriers to limit vehicle access.

This indicates that TMRD would indeed be increased in the Project area because these new system roads would not be rendered “impassable,” as required by the Forest Plan to not be counted in TMRD. Page 8 of the PA instead requires the making of roads impassable for temporary roads only:

All temporary roads would be rehabilitated and made impassable following project activities with drain dips, out-sloping, scarifying, seeding, and /or recontouring . . . Temporary roads would meet the definition of “impassable” when no longer needed.”

The notion that roads not counted in TMRD can be closed simply with “barriers to limit vehicle access” is either a misunderstanding of the treatments necessary to render a road “impassable” or a confirmation that a reading of the minimum treatments necessary to qualify a road as “impassable” is to simply install barriers on the first 50 feet of the road.

7. The U.S. District Court in Missoula, on 6/24/23, ruled regarding the revised Flathead Forest Plan and its attendant Biological Opinion (BiOp) that:

The science indicates that, even where ‘permanent barriers’ are used, road closures may be ineffective and use may occur or continue. Both the [2004] Swan View Coalition Study and the Forest Service Study support that argument . . . Fish and Wildlife Service’s failure to consider the effect of ineffective road closures was arbitrary and capricious [violating] the ESA by not considering the impact of ineffective road closures in its 2017 BiOp.

The PA makes no mention of road closure effectiveness or what measure will be taken to make road closures effective, even though it emphasizes the extensive road network that will be necessary to carry out the Project. The Flathead NF is using an outdated description of its road closure effectiveness monitoring. It then relies on outdated effectiveness data (2019-2020) to conclude Forest-wide effectiveness of 92%, as does the revised Biological Opinion on the Flathead Forest Plan (Plan BiOp). The Project environmental analyses must not provide the same boilerplate language used in the Plan BiOp to discount, rather than account for, the effects of ineffective road closures on grizzly bears.

This boilerplate discounting of the effects on grizzly bears has been deemed inadequate and unlawful in a number of U.S. District Court rulings on the Kootenai NF and on the Helena-Lewis and Clark NF. See, for example, the Kootenai NF Knotty Pine decision at <http://www.swanview.org/reports/Knotty-Pine-preliminary-injunction-order-04242023.pdf> and the Helena-Lewis and Clark NF decision at: http://www.swanview.org/reports/Helena_illegal_roads_order_filed_8.03.23.pdf.

It does no good for the Project environmental analyses to add, as did the Dry Riverside EA at 54, that “Effects of past illegal use of roads on grizzly bears are part of the baseline conditions that have supported the expanding population and distribution of grizzly bears in the NDCE recovery zone” and deem the problem “inconsequential.” The Flathead is adding more miles to its road System as “impassable” by not counting them in calculations of TMRD, even though they will continue to function as roads – thus increasing the number of roads and the number of ineffective road closures over what was included in the 2011 baseline. See the above court orders and our discussion that follows.

Please also see our 2023 “Road Hunt” road closure effectiveness report based on data collected while inspecting 303 FS road closures in the Swan Valley Geographic Area in 2022. (https://www.swanview.org/reports/Road_Hunt_Hammer_2023.pdf and submitted separately via email to Chris Dowling and Jeff Durkin). We found only 53% of the closures showed no sign of motorized vehicles behind them and, after allowing for administrative and logging contractor use, found that effectiveness rose to only 68%. Our report discusses reasons for the disparity between the Flathead’s previous finding of 92% effectiveness, shows that the Flathead’s 2021 and 2022 data indicate a lower effectiveness, discusses flaws in the Flathead’s road closure monitoring program, demonstrates how road closure violations can persist for many years before the closure

device is repaired, reports on how dense vegetation contributes to road closure effectiveness (something which will be greatly diminished by the Project fuels reduction, thinning, and use of roads as fuel breaks), and discusses how the Flathead has not followed through with promises made to FWS during consultation on the revised Plan BiOp.

The environmental analyses must not rely on old data and procedures and must use the best available data and science available, as required by law. Some of that best available data would be the Flathead's own 2021 – 2023 road closure effectiveness data as well as our 2022 Swan Valley GA data and 2023 report. Moreover, the environmental analyses must include detailed road closure effectiveness data for each road in the analysis area. This data must include when each closure has been inspected and whether it was found effective or not, and a clear accounting of how rebuilding previously abandoned or decommissioned roads (often overgrown with vegetation) and then simply closing them as "impassable" or with "barriers" lowers closure effectiveness and grizzly bear security. Similar analyses must be performed to assess and disclose the negative effects on road closure effectiveness due to clearing along roads to broaden their use as fuel breaks.

In our "Road Hunt" report, road closure effectiveness data for the Project area can be viewed in Appendix C, using the list of abbreviations provided in Appendix B and by viewing the listings for serial Form numbers 150-176. These are the road closure inspections conducted in the geographic area from Rumble Creek south to the Swan-Clearwater divide/FNF boundary east of Highway 83. Of these 27 road closures in the Project area, we found 16 to be ineffective (59%) and 11 of them effective (41%) at prohibiting use by motorized vehicles, lower than the 53% overall effectiveness found for the entire Swan Valley Geographic Area.

The Project would rebuild 8 miles of previously abandoned or decommissioned roads and apparently return them to the road System with only "barriers to limit vehicle access – plus 4 miles of "temporary" roads to be rendered "impassable." Our Road Hunt report provides visual examples of where motor vehicles are detouring around closure devices for distances in excess of the 50' of closure treatment required to be "impassable" (page 17). The Project environmental analyses need to detail the current condition of each of the non-system roads intended to be rebuilt, including its current ability to prohibit motorized trespass, then detail to what degree rebuilding each road and simply putting a "barrier" on it or rendering it "impassable" will increase its vulnerability to motorized trespass.

We find the revised BiOp to suffer the same legal inadequacies Judge Molloy found in the 2017 BiOp, especially in regards to the abandonment of Amendment 19's requirements. The revised BiOp emphasizes several times in bold face that the Forest Plan and its implementing projects will and must maintain the 2011 **"on the ground"** grizzly bear habitat conditions. Yet it still allows the construction of new roads and the reconstruction of old roads without them showing up/being counted in TMRD.

It appears this Project, like Dry Riverside and others, can build new roads and rebuild historic roads and then simply close them as "impassable" roads - rather than have to reclaim and/or decommission them in order to omit them from TMRD. Rebuilding

historic road templates in this Project and then simply putting a “barrier” on the road or rendering the road “impassable” to motor vehicles for the first 50’ does not provide the grizzly bear security that the previous status of historic road and “existing template” provided. Brand new road templates and old templates newly cleared of vegetation do not provide the previously existing impediments to human travel nor the resulting **“on the ground”** habitat conditions and security that previously existed for grizzly bear.

By not requiring that “impassable” roads be included in TMRD, the Project, Plan and Plan BiOp allow unlimited miles of roads to be constructed without increasing TMRD above 2011 levels. While this sleight of hand may maintain 2011 numbers, it most certainly does not maintain 2011 **“on the ground”** habitat conditions” and habitat security – premises and promises upon which the Plan and its BiOps are based.

“Impassable” roads and those simply closed with gates or barriers continue to function as roads for non-motorized public access that has documented negative impacts on grizzly bears. These roads also provide for additional impacts by wheel-driven motorized trespass of the “impassable” barrier and the lawful use of motorized over-snow vehicles. Page 60 of the Dry Riverside EA, for example, indeed finds “Overgrown roads cleared for project activities may indirectly allow for easier winter snowmobile access in the project area.” But those impacts and those contemplated for Rumbling Owl are not accounted for by showing the actual increase in total road density / TMRD – they are instead dismissed / omitted as though the new roads don’t exist and have no impacts. How will this fact affect wolverine, among other species?

8. The PA’s “Purpose and Need” fails to even mention fish, wildlife or the Forest Plan’s specific requirements to conserve them. It instead talks about protecting human structures and the recreation tourism economy. If the purpose is to protect the recreation tourism economy, then why trash the natural setting along the East Foothill Trail 192 via deceptively named “improvement cuts” in units 100 and units in the lower 200s, apparently turning the trail into a fuel break corridor instead. Unlike the PA maps, the environmental analyses must clearly show the area trail locations and disclose the effects upon those trails and the public’s use and enjoyment of them.

The PA fails to adequately distinguish between, let alone mention, the risks to grizzly bears and other wildlife by decommissioned, abandoned, temporary, open, gated, and barricaded roads, as well as non-motorized but admittedly high-use trails. As a result, by suggesting it will comply with the Forest Plan, it draws arbitrary and capricious conclusions to support the building and rebuilding of more roads in areas already suffering from too many roads and culverts. An EIS is required which includes an alternative that would meet the 19/19/68 “research benchmarks” for OMAD, TMAD and Secure Core – which are still used by the FS and FWS to determine the levels of incidental take of grizzly bear.

Moreover, the PA builds and rebuilds roads in order to support specious logging and other “vegetation management” that will make the fire risk situation worse and do anything but improve the diversity and resiliency of terrestrial ecosystems. On the whole, the PA does not “maintain the on-the-ground [2011] conditions that have contributed to the growth and expansion of the NCDE grizzly bear population,” as required by the 2018 revised Forest Plan (see the 10/31/17 Biological Assessment on the

revised Forest Plan, at 127, and the 2/16/22 revised Biological Opinion of the revised Forest Plan).

Thank you for this opportunity to comment and please keep us informed about this project.

Sincerely,

A handwritten signature in black ink that reads "Keith". The letters are cursive and slightly slanted to the right.

Keith J. Hammer
Chair

Attachments A-E
Keith Hammer's 2023 "Road Hunt" road closure report sent via separate message.

ATTACHMENT A

November 25, 2023

Ms. Leanne Marten, Regional Forester
U.S. Forest Service, Region 1
26 Fort Missoula Road
Missoula, MT 59804

Dear Ms. Marten,

I am writing to call for an **immediate halt to the scheduled logging of Unit #8** (at a minimum) within the COLD JIM FUELS REDUCTION AND FOREST HEALTH PROJECT on the Swan Lake Ranger District, pending an onsite review by your agency. This delay is warranted because **Flathead National Forest will be out-of-compliance with your own Decision Notice, Appendix 2 - Selected Alternative Design Criteria, specifically: “Snag Retention for Snag Associated Wildlife Species and for Forest Vegetation”** if logging proceeds based on the existing presale marking work that was done in Unit #8 this past summer. **I also believe that the U.S. Forest Service is in violation of the Migratory Bird Treaty Act and subject to enforcement action** if you continue logging without compliance with the snag retention requirements (see enclosed Department of Interior Director’s Order No. 225).

This letter follows up on a meeting that was held March 15, 2023 at the Swan Lake Ranger District Offices (Bigfork) between your Cold Jim Project responsible staff, staff from the Owl Research Institute (ORI-Charlo) and me:

- John Harmon (Sale Administrator)
- Mark Ruby (Wildlife Biologist)
- Michele Mavor (NEPA Interdisciplinary Team Leader)
- Cory Anderson (SO Timber Sales Manager)
- Beth Mendelsohn (ORI Wildlife Researcher)
- Denver Holt (ORI President and Director)

The meeting was held at the request of ORI to discuss Great Gray Owl habitat requirements and the impacts of industrial timber harvesting on owl habitat generally and specifically related to snag and other nest site protection. During that meeting Beth Mendelsohn (ORI) presented her paper “Great Gray Owl (*Strix nebulosa*) Nesting Habitat Report – Cold Jim Fuels Project” (copy enclosed). ORI staff members have been studying Great Gray Owls and other owl species that live in the forest surrounding my property that is located at the south end of Salmon Prairie near Condon, MT for two years.

The Flathead National Forest re-marked Unit #8 and (I think) #9 (map enclosed) this summer and I wanted to understand exactly what protection was being provided to wildlife habitat after our meeting earlier in the year during which we had detailed discussions on this subject. Unit #8 includes nesting habitat for Great Gray owls as well as many other snag-dependent species and there was an active Great

ATTACHMENT A

Gray Owl nest there in spring and summer of 2023. The presence of that active nest was reported to your responsible staff by Beth Mendelsohn on April 30, 2023 via email (copy enclosed). Following the March 15th meeting, Ms. Mendelsohn followed up with several email and phone contacts to exchange technical assistance and information but she has communicated to me that none of those messages were returned.

Beginning in late September I initiated environmental monitoring by surveying all of Unit #8 (33 acres) to identify and document all snags over 12 inches DBH and compare my findings with the new USFS orange “leave” markings. My Excel data is enclosed in hardcopy and on disk along with photographs of the 47 snags that I found and inventoried on-site as well as pertinent photos of other Cold Jim units after they were logged.

The Cold Jim - Appendix A2 Management Criteria for snags greater than 12 “ DBH is as follows, titled: Snag Retention for Snag Associated Wildlife Species and for Forest Vegetation

“In treatment units, where available, a minimum average of 6 snags per acre that are 12 to 20 inches DBH would be left, and all snags greater than 20 inches would be left. If existing snag densities are below these densities, substitute live trees would be left. All standing dead western larch, ponderosa pine, and Douglas-fir trees 16 inches DBH or greater should be retained. Generally, snags to be left would be further than 150 feet from open roads and private land boundaries. Snags that pose a safety hazard to the Contractor’s operation would be felled and left on site.”

Based on my data and the above forest management criteria (performance standard) these are my findings:

- Unit #8 is listed as being 33 acres so there should be a minimum of 198 snags 12-20” DBH (6 x 33) plus all snags > 20” DBH (26 snags per my data) = 224 snags over 12” DBH.
- My survey of Unit #8 found only 47 snags total > 12” DBH and of these, **only 7 were marked by the USFS marking crew as “leave” trees (less than 15%).**
- There are 34 snags greater than or equal to 16 inch DBH (western larch, ponderosa pine, and Douglas-fir).
- The broken top live larch tree (w/old osprey nest) that contained the Great Gray Owl nest in spring 2023 was not marked as a “leave” tree (snag #30) and is currently unprotected. No buffer zone is established around it.
- It is impossible to distinguish “substitute” live trees from the mature “residual” (leave) trees under the USFS marking system but there should be at least 177 of them painted orange based on your criteria.
- Since these “substitute” trees are live it will likely be many years (decades to centuries) before they can become nesting habitat for cavity-nesting wildlife. **So, the comparative value of the 47 existing snags that are already providing wildlife habitat is much greater.**

ATTACHMENT A

- The 150 ft. road setback criteria does not apply here because all these roads are closed to the public.
- FYI, all the snags were photographed for future reference.

Migratory Bird Treaty Act (MBTA)

The destruction of standing dead trees (snags) violates the intent of the Migratory Bird Treaty Act (MBTA). Due to the fact that Flathead National Forest appears to be violating your own “Management Criteria”, I assert that you are also violating the MBTA “incidental takings” provision and are therefore subject to enforcement by U.S. Department of the Interior’s Fish & Wildlife Service (**cc’d via email**).

Many species of birds nest in dead or live trees during their breeding season. The list of protected snag-dependent and cavity nesting species in the Flathead National Forest includes:

Wood Duck, Hooded Merganser, Common Merganser, Bufflehead, Common Goldeneye, Northern Flicker, Williamson’s Sapsucker, Red-naped Sapsucker, Black-backed Woodpecker, Downy Woodpecker, Hairy Woodpecker, Pileated Woodpecker, Lewis’ Woodpecker, American Three-toed Woodpecker, Flammulated Owl, Western Screech Owl, Northern Pygmy Owl, Barred Owl, Great Gray Owl, Boreal Owl, Northern Saw-whet Owl, Northern Hawk Owl, American Kestrel, Merlin, Osprey, Black-capped Chickadee, Mountain Chickadee, Chestnut-backed Chickadee, Red-breasted Nuthatch, White-breasted Nuthatch, Pygmy Nuthatch, Brown Creeper, House Wren, Tree Swallow, Violet Green Swallow, Vaux’s Swift, Western Bluebird, and Mountain Bluebird.

Resident birds that live in tree cavities during the winter are killed when their homes are destroyed during logging activities. Migrants returning in the spring to former nest sites that find their nesting trees and the contiguous habitat logged, can not “move to another area” because those other areas are usually already occupied. They will simply fail to reproduce, resulting in a net decline in their species population.

Mammal species that are snag-dependent include: some bats (there are 15 bat species in Montana), Northern Flying Squirrel, Red Squirrel, Racoons, and Black Bears.

Observations on Harvested Cold Jim Project Units and Timber Sale Contract

I visited several other units near Salmon Prairie (#10, #11, #12) after they were harvested during winter 2022-2023. Standing snags of any size are now very scarce in these units. Deciduous trees that were few in number but present in Unit #10 and were supposed to be protected under your Management Criteria are now non-existent. Several photographs that I took of downed marked trees, downed snags, and a stack of logs that included many snags are included in the photo folders on the enclosed SD disk.

The choice of logging equipment (32-ton excavator-harvesters and 22-ton skidders) and whole tree harvesting creates multiple large landings in the relatively small units that equate to small clear-cuts within the “commercial thinning” units. After pile burning, broadcast burning and wind storms result in

ATTACHMENT A

further mortality to the 'residual' trees, these units will look a lot like urban parks for many years to come.

The timber sale contract contains a provision (K-C.3.0.3#) that directly conflicts with your snag retention Management Criteria. It reads as allowing the contractor to avoid protection of any snags less than 15 ft. tall, whereas the snag retention Management Criteria does not specify a height for snags. Ecological reality is that snags of any height (and less than 12" DBH) are used by wildlife and even stumps from previous logging have habitat value.

Applicability

While my field work focused on Unit #8 of the Cold Jim Fuels Project (33 out of a total of ~1100 acres) based on my observations of Units 9, 10, 11, & 12, I believe my findings reflect current U.S. Forest Service policy and management intent with respect to dead trees elsewhere in the other project units and probably the same is planned for the landscape scale Mid-Swan Projects that total ~75,000 acres.

[Elemental, Reimagine Wildfire](#)

This new documentary (2022) presents rebuttals to several assumptions that current U.S. Forest Service "fuels reduction/forest restoration" strategy is based upon. Everyone who has not already viewed this film should do so. It is a contribution towards sustainable forest management as well as sustainable/fire-resistant home building. The scientists interviewed in the film include:

- Dr. Jack Cohen, Scientist, USFS Fire Lab
- Dr. Tania Schoenagel, Fire Ecologist, University of Colorado
- Dr. Alexandra Syphard, Fire Ecologist, Conservation Biology Institute
- Dr. Beverly Law, Emeritus Professor - Oregon State University

Sustainable Forestry & Forest Stewardship Council (FSC)

The U.S. Forest Service's forest management practices need to be aligned to a legitimate sustainable forestry model starting with the [Forest Stewardship Council](#) principles and criteria. Staff at FSC have communicated to me that former USFS Chief Thomas Tidwell (from 2009-2017) indicated an interest in exploring FSC certification of USFS lands in 2013. The Chequamegon-Nicolet NF in northern Wisconsin was the USFS unit primarily involved in the development of the original USFS supplementary requirements that were approved in 2019. Maybe Flathead National Forest needs to pick up the ball, adopt FSC principles and criteria and then explore FSC certification.

Expectations

At a minimum, the Flathead National Forest needs to review their on-the-ground design, implementation, and post-harvest verification processes for the snag retention Management Requirement starting with Cold Jim Unit #8. I have sent copies of this letter (including enclosures) to a number of organizations listed below. Most are NGOs and some are enforcement-capable agency

ATTACHMENT A

oversight units. Success in any environmental endeavor can only come from science-based design, hard work, and a commitment to continuous improvement... so let's see some!

Sincerely,

Mark B. Benedict

Bigfork, MT 59911

Cc:

USDA, Office of the Inspector General
U.S. Fish & Wildlife Service, Law Enforcement
Ms. Carol Hatfield, Acting Supervisor, Flathead National Forest
Ms. Kristine M. Akland, Center for Biological Diversity
Mr. Keith Hammer, Swan View Coalition
Mr. Mike Garrity, Alliance for the Wild Rockies
Friends of the Wild Swan
Flathead Audubon Society
Ms. Beth Mendelsohn, Owl Research Institute
Swan Valley Connections

Enclosures:

*Cold Jim Unit #8 Compliance Letter
Great Gray Owl (*Strix nebulosa*) Nesting Habitat Report – Cold Jim Fuels Project
Great Gray Owl Active Nest Notification email from Beth Mendelsohn (ORI)
Excel spreadsheet of Unit #8 snag data and notes (Mark Benedict)
Map of Cold Jim Selected Alternative North Half with Great Gray owl nest site marked
Migratory Bird Treaty Act – Director's Order No. 225
2 GB SD memory card containing numbered snag images, other Cold Jim unit photos, and electronic copies of some enclosures.

**STATEMENT OF
DR. BEVERLY LAW
PROFESSOR EMERITUS
OREGON STATE UNIVERSITY
BEFORE THE
UNITED STATES HOUSE OF REPRESENTATIVES
SUBCOMMITTEE ON NATIONAL PARKS, FORESTS AND PUBLIC LANDS
APRIL 29, 2021
CONCERNING
“WILDFIRE IN A WARMING WORLD: OPPORTUNITIES TO IMPROVE COMMUNITY COLLABORATION,
CLIMATE RESILIENCE, AND WORKFORCE CAPACITY”**

Mr. Chairman and members of the subcommittee, thank you for inviting me today to discuss wildfires and opportunities to improve climate resilience. I am Professor Emeritus of Global Change Biology & Terrestrial Systems Science at Oregon State University, where I have been working for 25 years. I am appearing today in my person capacity, not representing OSU. I am a Fellow of the American Geophysical Union. I served on the US Carbon Cycle Science Steering Group, and on IPCC expert panels. I was an editor for 8 years with Global Change Biology, one of the leading peer-reviewed journals. I have been a lead author of the National Climate Assessment, and co-author of National Research Council reports on verifying greenhouse gas emissions and air quality management. My research topics include multi-scale analysis of the effects of drought, fire and management on forest carbon and water processes, and land use strategies to mitigate climate change and benefit biodiversity. I will focus my remarks on forest carbon and biodiversity conservation for climate resilience and effects of fire and management on carbon.

Forest carbon stocks and accumulation have an important role in climate mitigation

Atmospheric carbon dioxide is 50% higher than preindustrial levels. The next 10 to 30 years are a critical window for climate action (IPCC 2018). We need to simultaneously reduce carbon dioxide emissions and increase carbon accumulation in land reservoirs of forests and other terrestrial ecosystems. Annual emissions from forest harvesting are slightly greater than emissions from the entire building sector in the U.S. Reducing this source of emissions could help the U.S. meet its climate goals.

Further, regional studies have shown that preserving western U.S. temperate forest with high carbon density and lower vulnerability to mortality would account for about 8 years of the region's fossil fuel emissions, supporting US climate goals (Buotte et al. 2019). This provides near-term opportunities to reduce carbon dioxide emissions and increase carbon storage and accumulation.

Forest protections are part of Nationally Determined Contribution (NDC) strategies, recognizing that increasing forest carbon stocks is important to the intent of the Paris climate treaty. The goal is “...

stabilization of greenhouse gas concentrations in the atmosphere at a level that would prevent dangerous anthropogenic interference with the climate system” [Article 2 UNFCCC 1992]. When allowed to grow longer, natural forests do more to mitigate climate than management activities that keep forest carbon stocks at a level below the potential carbon stock over time; a level that is insufficient to meet climate goals.

The ability of forests to pull carbon from the atmosphere and accumulate it in living trees and soil for decades to centuries will continue to play a major role in reducing the severity of climate consequences. Preserving high carbon density forests like those of the Pacific Northwest, and allowing them to continue to accumulate carbon could increase forest carbon stocks substantially by 2100 (Hudiburg et al. 2009, Law et al. 2018, Buotte et al. 2020). A comparison of strategies showed that restricting harvest by 50% on public forests to allow them to continue growing while lengthening current harvest cycles in forests with low vulnerability to drought and fire under future climate conditions contribute the most to increasing forest carbon and reduce emissions. Less effective are reforestation and lastly afforestation, which can have competing land uses for agriculture and urban development (Law et al. 2018). Thus, temperate forests with high carbon density and lower vulnerability to mortality have substantial potential for climate mitigation.

Reforestation can be part of the climate solutions, but is not the only solution. Young trees will eventually grow to have large carbon stocks that contribute to climate mitigation, but allowing some existing forests with their large carbon stocks to continue to accumulate carbon will accumulate far more carbon out of the atmosphere during the critical coming decades. It is also far more difficult and expensive to initiate a forest than to grow additional carbon stocks in existing forests.

Harvesting forests for wood products and bioenergy that is as carbon intensive as coal results in depletion of ecosystem carbon stocks and the regrowth of these stocks takes many decades to centuries into the future, creating a long-term carbon debt. More carbon is stored longer in forests than in wood products because about half of the harvested carbon is emitted soon after logging (Harmon 2019, Hudiburg et al. 2019, Harris et al. 2016). Of the accumulated carbon harvested from west coast U.S. forests since 1900, 65% has returned to the atmosphere while only 19% is in long-lived wood products, and the remaining 16% is in landfills. That is, 81% of the wood removed from west coast forests since 1900 has been emitted to the atmosphere as carbon dioxide or is in landfills (Hudiburg et al. 2019). Increased harvesting adds additional carbon dioxide to the atmosphere, accelerating climate change.

Forests with medium and high carbon per acre also have medium and high biodiversity, promoting ecosystem resilience to climate change

We are in the midst of an emergency to address both climate change and biodiversity loss (Ripple et al. 2019). We must consider both forest carbon *and* biodiversity when determining management strategies in forests. Studies estimate that at least one-third of American wildlife, more than 12,000 species, are at increased risk of extinction, with extinction risk being highest in the largest and smallest vertebrates (Ripple et al. 2017).

Under future climate projections, medium to high carbon density western U.S. forests with relatively low to moderate vulnerability of mortality from fire or drought also have high amounts of critical habitat and high species diversity (Buotte et al. 2020). If protected, these forests have a strong potential to support biodiversity into the future and to promote ecosystem resilience to a changing climate. These

areas are primarily in the Pacific Northwest and northern Rocky Mountains in Idaho and Montana. A recent global study also strongly confirmed the spatial coincidence of areas important for carbon storage and biodiversity protection (Dinerstein et al. 2020).

Vulnerability to wildfire varies across the western US region in the next decades. Broad-scale thinning to reduce severity results in more carbon emissions than would be released by fire, creating a multi-decade carbon deficit that conflicts with climate goals.

Forests account for only about 40% of the area burned in wildfires in the U.S. Wet forests like the coastal forests of the PNW have longer fire return intervals (100-300 years). Strategically focusing on homes and communities is a smart place to start in fire-prone areas. At subregional to regional levels, roughly 1% of treatments (thinning, prescribed fires) experiences wildfire each year, and the effectiveness of treatments is only 10-20 year, so the treatments likely have little effect on wildfire (Campbell et al. 2012, Schoennagel et al. 2017).

Vulnerability of forests to wildfire varies spatially in the next decades. Wildfire is mainly a function of dryness, heat and wind. The warm, dry regions are expected to get warmer and drier. Projections show that burn area is expected to increase in the next few decades. Vulnerability to future fire is projected to be highest in the Sierra Nevada and portions of the Rocky Mountains, while high carbon-density forests in the coastal forests are expected to experience low vulnerability to fire (Buotte et al. 2018).

Wildfires have relatively little impact on forest carbon stocks as fires mainly combust surface litter and duff. If trees are killed, most of the carbon remains in the forest as dead wood that takes decades to centuries to decompose. Only a small portion of the total forest carbon is emitted to the atmosphere in wildfires – less than 10% of the total ecosystem carbon in live and dead trees, litter and soils combined has been found to enter the atmosphere as carbon dioxide in Pacific Northwest forest fires (Campbell et al. 2012; Law & Waring 2015).

Thinning to reduce fire severity or intensity is usually 30-50% of live tree biomass, and it puts much of the harvested carbon into the atmosphere quickly. A thinning study in a drought-prone young ponderosa pine plantation in Idaho found that removal of 40% of the live biomass from the forest would subsequently release about 60% of that carbon over the next 30 years (Stenzel et al. 2021). Enlarging the treated area more than would burn would further increase the carbon losses.

Local reduction of seedlings and saplings may be useful to protect the large trees in some fire-prone dry forests with high future vulnerability to fire. It will reduce whole ecosystem carbon, but can protect the large trees that store and accumulate the most carbon and are more drought- and fire-resistant than young trees (Irvine et al. 2004, Hurteau et al. 2019). Increasing the use of prescribed fires and managing wildland fires may promote resilience to more frequent fire (Schoennagel et al. 2017). Because climate change mitigation is expected to be part of decision-making, potential impacts of treatment options on forest carbon stocks should be assessed as part of a strategic decision-making process.

Broad-scale thinning of forests conflicts with carbon climate goals. The amount of carbon removed by thinning is much larger than that saved, and more area is harvested than would actually burn (Mitchell et al. 2009, Rhodes et al. 2009, Law & Harmon 2011, Campbell et al. 2012). The multi-decadal biomass carbon deficit following moderate to heavy thinning is supported by most analyses of mid to long-term thinning impacts on forest structure and carbon storage (Zhou et al. 2013). *There is no evidence that thinning forests increases biomass stored.*

Fire emissions are small relative to harvest emissions. Harvest-related emissions in the Oregon, Washington and California average about 5 times fire emissions (Hudiburg et al. 2019). In California, fire emissions are just a few percent of California's fossil fuel emissions.

Post-fire reforestation. Many western US forest fires are mixed-severity, meaning that a large portion of the fire burns at low and moderate severity in patches and a smaller portion burns at high severity where a majority of trees are killed (Law & Waring 2015). After fires, remaining trees and those on the periphery of burn areas provide seed source for natural regeneration (Donato et al. 2009). It is important to allow natural regeneration to occur because it provides the genetic and species diversity that existed prior to the fire, and that diversity makes the ecosystem more resilient. The complex early seral forest habitat that develops in the high severity patches is important to a host of species associated with these conditions (Donato et al. 2012). That is, both early- and late-successional forest canopies can support equally complex functioning and biodiversity. We can supplement with planting where regeneration fails.

Summary

The next 10 to 20 years are a critical window for climate action. Wildfires are an essential ecological process. They have relatively little impact on the total ecosystem carbon stock as fires mainly combust surface litter and duff, and if there is tree mortality the deadwood takes decades to centuries to decompose. In dry fire-prone forests projected to be vulnerable to fire-related mortality under future climate, it may be necessary to remove small trees in places. It would decrease ecosystem carbon but protect the large trees that are more fire-resistant and accumulate the most carbon. Impacts of tree removals on forest carbon stocks should be assessed as part of a strategic decision-making process. Preemptive broad-scale thinning will create a multi-decade carbon deficit that conflicts with carbon climate goals.

Deforestation and degradation reduce carbon stocks and other ecosystem benefits, create habitat loss that is a major cause of species extinctions, and are major sources of greenhouse gas emissions that further contributes to warming that amplifies risk of species extinction. Mature and old forests store more carbon in trees and soil than do young forests, and continue to accumulate it over decades to centuries making them the most effective forest-related climate mitigation strategy. High carbon density forests also have high biodiversity (species, critical habitat), promoting resilience to climate change.

Forest carbon, biodiversity and ecosystem type and integrity need to be considered concurrently when determining what to do with forests in the face of climate change. To meet zero net carbon goals and eventually halt climate change while also meeting biodiversity goals, some forests need to be protected.

Citations

Buotte, P.C., B.E. Law, W.J. Ripple, L.T. Berner. 2020. Carbon sequestration and biodiversity co-benefits of preserving forests in the western United States. *Ecol. Applic.* 30(2):e02039. Doi: 10.1002/eap.2039

Buotte, P.C., S. Levis, B.E. Law, T.W. Hudiburg, D.E. Rupp, J.J. Kent. 2018. Near-future vulnerability to drought and fire varies across the western United States. *Global Change Biol.* 25:290-303. Doi:10.1111/gcb.14490

- Campbell, J., M.E. Harmon, S.R. Mitchell. 2012. Can fuel-reduction treatments really increase forest carbon storage in the western US by reducing future fire emissions? *Front. Ecol. Env.* Doi:10.1890/110057
- Dinerstein, E., A.R. Joshi, C. Vynne, A.T.L. Lee, F. Pharand-Deschenes, et al. 2020. A “global safety net” to reverse biodiversity loss and stabilize Earth’s climate. *Science Adv.* 6 no. 36, eabb2824. Doi: 10.1126/sciadv.abb2824.
- Donato, D., J.B. Fontaine, J.L. Campbell, W.D. Robinson, J.B. Kaufmann, B.E. Law. 2009. Conifer regeneration in stand replacement portions of a landscape-scale mixed-severity fire. *Can. J. For. Res.* 39:823-838.
- Donato, D., J.L. Campbell, J.F. Franklin. 2012. Multiple successional pathways and precocity in forest development: Can some forests be born complex? *J. Veg. Sci.* 23: 576-584.
- Griscom, B.W., J. Adams, P.W. Ellis, R.A. Houghton, G. Lomax, D.A. Metiva, W.H. Schlesinger et al. 2017. Natural climate solutions. *Proc. Nat. Acad. Sci.* 114:11645-11650. Doi:10.1073/pnas.1704651114.
- Harmon, M.E. 2019. Have product substitution carbon benefits been overestimated? A sensitivity analysis of key assumptions. *Environ. Res. Lett.* **14** 065008.
- Harris, N.L., Hagen, S.C., Saatchi, S.S. et al. 2016. Attribution of net carbon change by disturbance type across forest lands of the conterminous United States. *Carbon Bal. Manage.* **11**, 24. Doi: 10.1186/s13021-016-0066-5
- Hudiburg, T.W., B.E. Law, W.R. Moomaw, M.E. Harmon, J.E. Stenzel. 2019. Meeting GHG reduction targets requires accounting for all forest sector emissions. *Env. Res. Lett.* 14: 095005.
- Hudiburg, T., B.E. Law, D.P. Turner, J. Campbell, D. Donato, M. Duane. 2009. Carbon dynamics of Oregon and Northern California forests and potential land-based carbon storage. *Ecol. Applic.* 19:163-180.
- Hurteau, M., M.P. North, G.W. Koch, B. Hungate. 2019. Managing for disturbance stabilizes forest carbon. *Proc. Nat. Acad. Sci. Opinion* 116: 10193-10195.
- IPCC. 2018. Global Warming of 1.5°C. An IPCC Special Report on the impacts of global warming of 1.5°C. [Masson-Delmotte, V., P. Zhai, H.-O. Pörtner, et al. (eds.)].
- Irvine, J., B.E. Law, M. Kurpius, P. Anthoni, D. Moore, P. Schwarz. 2004. Age related changes in ecosystem structure and function and the effects on carbon and water exchange in ponderosa pine. *Tree Physiol.* 24, 753-763.
- Kline, J.D., M.E. Harmon, T.A. Spies, A.T. Morzillo, R.J. Pabst, B.C. McComb, F. Schneckenger, K.A. Olsen, B. Csuti, J.C. Vogeler. 2016. Evaluating carbon storage, timber harvest, and habitat possibilities for a western Cascades (USA) forest landscape. *Ecol. Applic.* 26:2044-2059.
- Law, B.E. and M. Harmon. 2011. Forest sector carbon management, measurement and verification, and discussion of policy related to climate change. *Carbon Management* 2:73-84.

ATTACHMENT B

- Law, B.E., T.W. Hudiburg, L.T. Berner, J.J. Kent, P.C. Buotte, and M. Harmon. 2018. Land use strategies to mitigate climate change in carbon dense temperate forests. *Proc. Nat. Acad. Sci.* 115:3663-3668. Doi: 10.1073/pnas.1720064115
- Law, B.E., R.H. Waring. 2015. Carbon implications of current and future effects of drought, fire and management on Pacific Northwest forests. *For. Ecol. Manag.* 355:4-14.
- Mitchell, S., M.E. Harmon, K.B. O'Connell. 2009. Forest fuel reduction reduces both fire severity and long-term carbon storage in three Pacific Northwest ecosystems. *Ecol. Applic.* 19: 643-655.
- Ripple, W.J., C. Wolf, T.M. Newsome, P. Barnard, W.R. Moomaw. 2019. World scientists' warning of a climate emergency. *BioSci.* 70:8-12. <https://doi.org/10.1093/biosci/biz088>
- Ripple, W.J., C. Wolf, T.M. Newsome, M. Hoffmann, A.J. Wirsing et al. 2017. Extinction risk is most acute for the world's largest and smallest vertebrates. *Proc. Nat. Acad. Sci.* 114:10678-10683. Doi:10.1073/pnas.1702078114
- Rhodes, J.J., W.I. Baker. 2009. Fire probability, fuel treatment effectiveness and ecological tradeoffs in Western US public forests. *Open Forest Sci. J.* 1: 1-7.
- Schoennagel, T., J.K. Balch, H. Brenkert-Smith, P.E. Dennis,, et al. 2017. Adapt to more wildfire in western North American forests as climate changes. *Proc. Nat. Acad. Sci.* 114:4582-4590. Doi:10.1073/pnas.1617464114
- Stenzel, J.E., D.M. Berardi, E.S. Walsh, T.W. Hudiburg. 2021. Restoration thinning in a drought-prone Idaho forest creates a persistent carbon deficit. *JGR Biogeosci.* Doi:10.1029/2020JG005815
- Zhou, D., S. Liu, S. Zhao, J. Oeding. 2013. A meta-analysis on the impacts of partial cutting on forest structure and carbon storage. *Biogeosci.* 10:3691-3703. Doi: 10.5194/bg-10-3691-2013

ATTACHMENT C

FOR PUBLICATION

UNITED STATES COURT OF APPEALS
FOR THE NINTH CIRCUIT

BARK; CASCADIA WILDLANDS;
OREGON WILD,
Plaintiffs-Appellants,

v.

UNITED STATES FOREST SERVICE, a
federal agency,
Defendant-Appellee,

HIGH CASCADE, INC.,
Intervenor-Defendant-Appellee.

No. 19-35665

D.C. No.
3:18-cv-01645-
MO

ORDER AND
OPINION

Appeal from the United States District Court
for the District of Oregon
Michael W. Mosman, District Judge, Presiding

Argued and Submitted December 10, 2019
Seattle, Washington

Filed May 4, 2020

Before: Susan P. Graber, Marsha S. Berzon,
and Stephen A. Higginson,* Circuit Judges.

* Stephen A. Higginson, United States Circuit Judge for the U.S.
Court of Appeals for the Fifth Circuit, sitting by designation.

ATTACHMENT C

Order;
Opinion by Judge Higginson;
Concurrence by Judge Graber

SUMMARY**

Environmental Law

The panel granted appellants' request to publish the unpublished Memorandum Disposition with modifications; and reversed the district court's summary judgment in favor of the U.S. Forest Service in an action alleging violations of the National Environmental Policy Act and National Forest Management Act.

The Crystal Clear Restoration ("CCR") Project is a forest management effort and timber sale affecting 11,742 acres in Mt. Hood National Forest.

The panel held that the Forest Service's determination that the CCR Project did not require an Environmental Impact Statement ("EIS") was arbitrary and capricious for two independent reasons. First, the effects of the Project were highly controversial and uncertain, thus mandating the creation of an EIS. *See* 40 C.F.R. § 1508.27(b)(4) & (5). Second, the Forest Service failed to identify and meaningfully analyze the cumulative impacts of the Project.

** This summary constitutes no part of the opinion of the court. It has been prepared by court staff for the convenience of the reader.

ATTACHMENT C

Because an EIS was required, and because the findings in the EIS could prompt the Forest Service to change the scope of the Project or the methods it planned to use, the panel did not reach the appellants' other claims. The panel remanded to the Forest Service for further proceedings.

Judge Graber concurred in full in the judgment and in all but section III-B of the majority opinion. She agrees that an EIS was required, but would not reach whether the environmental assessments' discussion of cumulative impacts also was arbitrary and capricious.

COUNSEL

Brenna Bell (argued), Portland, Oregon; Nick Cady, Eugene, Oregon; for Plaintiffs-Appellants.

Jeffrey S. Beelaert (argued), Shaun M. Pettigrew, and Krystal-Rose Perez, Attorneys; Eric Grant, Deputy Assistant Attorney General; Jeffrey Bossert Clark, Assistant Attorney General; Environment and Natural Resources Division, United States Department of Justice, Washington, D.C.; Stephen A. Vaden, General Counsel; Val J. McLam Black, Senior Counsel, United States Department of Agriculture, Washington, D.C.; for Defendant-Appellee.

Lawson E. Fite (argued), and Sara Ghafouri, American Forest Resource Council, Portland, Oregon, for Intervenor-Defendant-Appellee.

ATTACHMENT C

ORDER

Appellants' request to publish the unpublished Memorandum disposition, Docket No. 37, is **GRANTED**. The Memorandum disposition filed April 3, 2020, is redesignated as an authored Opinion by Judge Higginson, with modifications. The time for filing a petition for rehearing and petition for rehearing en banc shall start anew as of the filed date of this Opinion.

OPINION

HIGGINSON, Circuit Judge:

Appellants Bark, Cascadia Wildlands, and Oregon Wild timely appeal the district court's summary judgment in favor of Appellees, the United States Forest Service (USFS) and High Cascade, for claimed violations of the National Environmental Policy Act (NEPA) and the National Forest Management Act (NFMA). We hold that the USFS's determination that the Crystal Clear Restoration (CCR) Project did not require an Environmental Impact Statement (EIS) was arbitrary and capricious and so reverse. We do not reach the NFMA claims.

I.

The CCR Project is a forest management effort and timber sale affecting 11,742 acres in Mt. Hood National Forest. The Project area is partly a moist "transition" climate, and partly a dry "eastside" climate. According to the USFS, forest stands in the area tend to be overstocked as a result of past management practices. When trees are closer together, they are more susceptible to insects and disease and

ATTACHMENT C

to high-intensity wildfires. The USFS undertook the CCR Project in order to “provide forest products from specific locations within the planning area where there is a need to improve stand conditions, reduce the risk of high-intensity wildfires, and promote safe fire suppression activities.” The USFS plans to achieve these goals in part using a technique called “variable density thinning.” This process gives the agency flexibility in choosing which trees to cut, thereby allowing the USFS to create variation within an area of forest so that the stands “mimic more natural structural stand diversity.” The USFS plans to leave an average canopy cover of 35–60%, with a minimum of 30% where the forest is more than 20 years old.

“NEPA imposes procedural requirements designed to force agencies to take a ‘hard look’ at environmental consequences” of their proposed actions. *League of Wilderness Defs./Blue Mountains Biodiversity Project v. Connaughton*, 752 F.3d 755, 763 (9th Cir. 2014) (internal quotation marks omitted). Agencies must prepare an EIS for federal actions that will “significantly affect[] the quality of the human environment.” 42 U.S.C. § 4332(2)(C). To determine whether a proposed action will have a significant effect on the quality of the human environment, agencies must prepare an Environmental Assessment (EA) that “[b]riefly provide[s] sufficient evidence and analysis for determining whether to prepare an environmental impact statement or a finding of no significant impact.” 40 C.F.R. § 1508.9(a)(1). An EIS is required when this process raises “substantial questions” about whether an agency action will have a significant effect. *Blue Mountains Biodiversity Project v. Blackwood*, 161 F.3d 1208, 1212 (9th Cir. 1998); *see also Native Ecosystems Council v. U.S. Forest Serv.*, 428 F.3d 1233, 1238–39 (9th Cir. 2005). “If the agency concludes in the EA that there is no significant effect from

ATTACHMENT C

the proposed project, the federal agency may issue a finding of no significant impact ('FONSI') in lieu of preparing an EIS." *Native Ecosystems Council*, 428 F.3d at 1239 (citing 40 C.F.R. § 1508.9(a)(1); *id.* § 1508.13).

After conducting an EA, the USFS determined that the CCR Project had no significant effects. It therefore issued a FONSI and did not prepare an EIS.

Appellants filed a complaint against the USFS bringing claims under NEPA and the NFMA. The NEPA claim alleged that the USFS did not undertake a proper analysis of the environmental impacts of the Project or of alternatives to the Project. The NFMA claim alleged that the USFS failed to comply with two forest plans and other guidance documents governing the Project area as required by the NFMA. The district court granted summary judgment to Appellees on all claims. Appellants timely appealed.

II.

We review the district court's grant of summary judgment de novo. *Ctr. for Biological Diversity v. Ilano*, 928 F.3d 774, 779 (9th Cir. 2019). The Administrative Procedure Act (APA), 5 U.S.C. § 706(2)(A), provides the governing standard for courts reviewing an agency's compliance with NEPA and the NFMA. *Native Ecosystems Council*, 428 F.3d at 1238. Under the APA, we may overturn an agency's conclusions when they are "arbitrary, capricious, an abuse of discretion, or otherwise not in accordance with law." 5 U.S.C. § 706(2)(A). "An agency action is arbitrary and capricious if the agency has: relied on factors which Congress has not intended it to consider, entirely failed to consider an important aspect of the problem, offered an explanation for its decision that runs counter to the evidence before the agency, or is so implausible that it could not be

ATTACHMENT C

ascribed to a difference in view or the product of agency expertise.” *WildEarth Guardians v. U.S. E.P.A.*, 759 F.3d 1064, 1069–70 (9th Cir. 2014) (quoting *Ctr. for Biological Diversity v. U.S. Bureau of Land Mgmt.*, 698 F.3d 1101, 1109 (9th Cir. 2012)). An agency’s factual determinations “must be supported by substantial evidence.” *Connaughton*, 752 F.3d at 759.

In reviewing an agency’s finding that a project has no significant effects, courts must determine whether the agency has met NEPA’s hard look requirement, “based [its decision] on a consideration of the relevant factors, and provided a convincing statement of reasons to explain why a project’s impacts are insignificant.” *In Def. of Animals v. U.S. Dep’t of Interior*, 751 F.3d 1054, 1068 (9th Cir. 2014) (alteration in original) (quoting *Env’tl. Prot. Info. Ctr. v. U.S. Forest Serv. (EPIC)*, 451 F.3d 1005, 1009 (9th Cir. 2006)). The term “significant” includes considerations of both the context and the intensity of the possible effects. 40 C.F.R. § 1508.27. “Context simply delimits the scope of the agency’s action, including the interests affected.” *In Def. of Animals*, 751 F.3d at 1068 (quoting *Nat’l Parks & Conservation Ass’n v. Babbitt*, 241 F.3d 722, 731 (9th Cir. 2001), *abrogated in part on other grounds by Monsanto Co. v. Geertson Seed Farms*, 561 U.S. 139, 157 (2010)). Consideration of context involves analysis “in several contexts such as society as a whole (human, national), the affected region, the affected interests, and the locality.” 40 C.F.R. § 1508.27(a). “[I]n the case of a site-specific action, significance . . . usually depend[s] upon the effects in the locale rather than in the world as a whole.” *Id.*

Consideration of intensity “refers to the severity of impact.” *Id.* § 1508.27(b). NEPA regulations list ten non-exhaustive factors that inform an agency’s intensity

ATTACHMENT C

determination, including “[t]he degree to which the effects on the quality of the human environment are likely to be highly controversial,” *id.* § 1508.27(b)(4), “[t]he degree to which the possible effects on the human environment are highly uncertain or involve unique or unknown risks,” *id.* § 1508.27(b)(5), and “[w]hether the action is related to other actions with individually insignificant but cumulatively significant impacts,” *id.* § 1508.27(b)(7). The regulations explain that “[s]ignificance exists if it is reasonable to anticipate a cumulatively significant impact on the environment,” and “cannot be avoided by . . . breaking [an action] down into small component parts.” *Id.* “When substantial questions are raised as to whether a proposed project ‘may cause significant degradation of some human environmental factor,’ an EIS is required.” *In Def. of Animals*, 751 F.3d at 1068.

III.

The USFS’s decision not to prepare an EIS was arbitrary and capricious for two independent reasons.

A.

First, the effects of the Project are highly controversial and uncertain, thus mandating the creation of an EIS. *See* 40 C.F.R. § 1508.27(b)(4) & (5) (listing relevant factors for whether an EIS is required, including if the project’s effects are “highly controversial” and “highly uncertain”). The stated primary purpose of the CCR Project is to reduce the risk of wildfires and promote safe fire-suppression activities, but Appellants identify considerable scientific evidence showing that variable density thinning will not achieve this purpose. Considering both context and intensity, as required by 40 C.F.R. § 1508.27, this evidence raises substantial questions about the Project’s environmental impact, and an

ATTACHMENT C

EIS is required. *See, e.g., Blackwood*, 161 F.3d at 1212; *Native Ecosystems Council*, 428 F.3d at 1238–39.

“A project is ‘highly controversial’ if there is a ‘substantial dispute [about] the size, nature, or effect of the major Federal action rather than the existence of opposition to a use.’” *Native Ecosystems Council*, 428 F.3d at 1240 (alteration in original) (quoting *Blackwood*, 161 F.3d at 1212). “A substantial dispute exists when evidence . . . casts serious doubt upon the reasonableness of an agency’s conclusions.” *In Def. of Animals*, 751 F.3d at 1069 (quoting *Babbitt*, 241 F.3d at 736). “[M]ere opposition alone is insufficient to support a finding of controversy.” *WildEarth Guardians v. Provencio*, 923 F.3d 655, 673 (9th Cir. 2019).

The EA explained that the CCR Project will use “variable density thinning” to address wildfire concerns. “In variable density thinning, selected trees of all sizes . . . would be removed.” This process would assertedly make the treated areas “more resilient to perturbations such as . . . large-scale high-intensity fire occurrence because of the reductions in total stand density.” Variable density thinning will occur in the entire Project area.

Substantial expert opinion presented by the Appellants during the administrative process disputes the USFS’s conclusion that thinning is helpful for fire suppression and safety. For example, Oregon Wild pointed out in its EA comments that “[f]uel treatments have a modest effect on fire behavior, and could even make fire worse instead of better.” It averred that removing mature trees is especially likely to have a net negative effect on fire suppression. Importantly, the organization pointed to expert studies and research reviews that support this assertion.

ATTACHMENT C

Bark also raised this issue: “It is becoming more and more commonly accepted that reducing fuels does not consistently prevent large forest fires, and seldom significantly reduces the outcome of these large fires,” citing an article from *Forest Ecology and Management*. Bark also directed the USFS to a recent study published in *The Open Forest Science Journal*, which concluded that fuel treatments are unlikely to reduce fire severity and consequent impacts, because often the treated area is not affected by fire before the fuels return to normal levels. Bark further noted that, while “Bark discussed [during the scoping process] the studies that have found that fuel reduction may actually exacerbate fire severity in some cases as such projects leave behind combustible slash, open the forest canopy to create more ground-level biomass, and increase solar radiation which dries out the understory[,] [t]he EA did not discuss this information.”

Oregon Wild also pointed out in its EA comments that fuel reduction does not necessarily suppress fire. Indeed, it asserted that “[s]ome fuel can actually help reduce fire, such as deciduous hardwoods that act as heat sinks (under some conditions), and dense canopy fuels that keep the forest cool and moist and help suppress the growth of surface and ladder fuels” Oregon Wild cited more than ten expert sources supporting this view. Importantly, even the Fuels Specialist Report produced by the USFS itself noted that “reducing canopy cover can also have the effect of increasing [a fire’s rate of spread] by allowing solar radiation to dry surface fuels, allowing finer fuels to grow on . . . the forest floor, and reducing the impact of sheltering from wind the canopy provides.”

The effects analysis in the EA did not engage with the considerable contrary scientific and expert opinion; it

ATTACHMENT C

instead drew general conclusions such as that “[t]here are no negative effects to fuels from the Proposed Action treatments.” Appellants thus have shown a substantial dispute about the effect of variable density thinning on fire suppression. Although it is not our role to assess the merits of whether variable density thinning is indeed effective in the project area to prevent fires, or to take sides in a battle of the experts, *see Greenpeace Action v. Franklin*, 14 F.3d 1324, 1333 (9th Cir. 1992), NEPA requires agencies to consider all important aspects of a problem. *See WildEarth Guardians*, 759 F.3d at 1069–70. Throughout the USFS’s investigative process, Appellants pointed to numerous expert sources concluding that thinning activities do not improve fire outcomes. In its responses to these comments and in its finding of no significant impact, the USFS reiterated its conclusions about vegetation management but did not engage with the substantial body of research cited by Appellants. This dispute is of substantial consequence because variable density thinning is planned in the entire Project area, and fire management is a crucial issue that has wide-ranging ecological impacts and affects human life. When one factor alone raises “substantial questions” about whether an agency action will have a significant environmental effect, an EIS is warranted. *See Ocean Advocates v. U.S. Army Corps of Eng’rs*, 402 F.3d 846, 865 (9th Cir. 2005) (“We have held that one of [the NEPA intensity] factors may be sufficient to require preparation of an EIS in appropriate circumstances.”). Thus, the USFS’s decision not to prepare an EIS was arbitrary and capricious. *See Blackwood*, 161 F.3d at 1213 (holding that conflicting evidence on the effects of ecological intervention in post-fire landscapes made a proposed project highly uncertain, thus requiring an EIS).

ATTACHMENT C

B.

The USFS also failed to identify and meaningfully analyze the cumulative impacts of the Project. “Cumulative impact is the impact on the environment which results from the incremental impact of the action when added to other past, present, and reasonably foreseeable future actions regardless of what agency . . . undertakes such other actions.” 40 C.F.R. § 1508.7. “Cumulative impacts can result from individually minor but collectively significant actions taking place over a period of time.” *Id.* “[I]n considering cumulative impact, an agency must provide ‘some quantified or detailed information; . . . [g]eneral statements about possible effects and some risk do not constitute a hard look absent a justification regarding why more definitive information could not be provided.’” *Ocean Advocates*, 402 F.3d at 868 (alterations in original) (quoting *Neighbors of Cuddy Mountain v. U.S. Forest Serv.*, 137 F.3d 1372, 1379–80 (9th Cir. 1998)). “This cumulative analysis ‘must be more than perfunctory; it must provide a useful analysis of the cumulative impacts of past, present, and future projects.’” *Id.* (quoting *Kern v. U.S. Bureau of Land Mgmt.*, 284 F.3d 1062, 1075 (9th Cir. 2002)) (internal quotation marks omitted). We have held that cumulative impact analyses were insufficient when they “discusse[d] only the direct effects of the project at issue on [a small area]” and merely “contemplated” other projects but had “no quantified assessment” of their combined impacts. *Klamath-Siskiyou Wildlands Ctr. v. Bureau of Land Mgmt.*, 387 F.3d 989, 994 (9th Cir. 2004).

The EA ostensibly analyzed the cumulative effects of the CCR Project, and included a table of other projects that were “considered in the cumulative effects analyses.” The cumulative impact analysis is insufficient because there is no

ATTACHMENT C

meaningful analysis of any of the identified projects. The table gave no information about any of the projects listed; it merely named them. The section of the EA actually analyzing the cumulative effects on vegetation resources did not refer to any of these other projects. Nor are there any specific factual findings that would allow for informed decision-making. The EA simply concluded that “there are no direct or indirect effects that would cumulate from other projects due to the minimal amount of connectivity with past treatments” and that the Project “would have a beneficial effect on the stands by moving them toward a more resilient condition that would allow fire to play a vital role in maintaining stand health, composition and structure.” These are the kind of conclusory statements, based on “vague and uncertain analysis,” that are insufficient to satisfy NEPA’s requirements. *Ocean Advocates*, 402 F.3d at 869.

The EA also mentioned the possibility of cumulative effects in sections on other specific sub-topics such as fuels management, transportation resources, and soil productivity. These sections similarly relied on conclusory assertions that the Project has “no cumulative effects.” When the EA did acknowledge the possibility of the Project’s impact, such as in the section that analyzed the Project’s effects on spotted owls, it noted only that “[t]imber harvest on federal, tribal, and private land, and utility corridor operations have reduced the amount of suitable habitat . . . on the landscape and could continue to do so in the future,” without attempting to quantify the cumulative loss or naming other projects. Yet there were other relevant timber projects to discuss. Appellants pointed out at least three other recent or future timber projects in their comments responding to the EA, but the relevant section of the document limited its analysis to only the Project area and a 1.2-mile buffer surrounding it. Such a small buffer zone fails to distinguish the EA’s

ATTACHMENT C

cumulative impact analysis from an analysis of the direct effects of the Project. *See Klamath-Siskiyou Wildlands Ctr.*, 387 F.3d. at 997 (assessing cumulative effects at the critical habitat unit scale). The USFS's failure to engage with the other projects identified by Appellants leaves open the possibility that several small forest management actions will together result in a loss of suitable owl habitat. Preventing or adequately mitigating this potential loss is the fundamental purpose of NEPA's requirement that agencies analyze cumulative impacts, and we have no basis in the record to assess whether the USFS has taken the necessary steps to consider this possibility.

Overall, there is nothing in the EA that could constitute "quantified or detailed information" about the cumulative effects of the Project. *Ocean Advocates*, 402 F.3d at 868 (internal quotation marks omitted). The USFS's analysis creates substantial questions about whether the action will have a cumulatively significant environmental impact. Therefore, this factor also requires the USFS to conduct an EIS. *See* 40 C.F.R. § 1508.27(b)(7).

IV.

Because an EIS is required, and because the findings in the EIS could prompt the USFS to change the scope of the Project or the methods it plans to use, we do not reach the Appellants' other claims. We reverse the district court's judgment and remand to the district court with instructions to remand to the USFS for further proceedings consistent with this opinion.

REVERSED and REMANDED.

ATTACHMENT C

GRABER, Circuit Judge, concurring:

I concur in full in the judgment and in all but section III-B of the majority opinion. The project's proposed methodology of variable density thinning is both highly controversial and highly uncertain, so an environmental impact statement is required. I would not reach whether the environmental assessment's discussion of cumulative impacts also was arbitrary and capricious.

ATTACHMENT D

Deborah A. Sivas (CA Bar No. 135446)
Matthew J. Sanders (CA Bar No. 222757)
Sidni M. Frederick (CA Bar Student Cert. No. 00650615)
Catherine H. Rocchi (CA Bar Student Cert. No. 00648085)
ENVIRONMENTAL LAW CLINIC
Mills Legal Clinic at Stanford Law School
559 Nathan Abbott Way
Stanford, California 94305-8610
Telephone: (650) 723-0325
Facsimile: (650) 723-4426
Email: dsivas@stanford.edu
Email: matthewjsanders@stanford.edu

Attorneys for Plaintiff Unite the Parks

René P. Voss (CA Bar No. 255758)
NATURAL RESOURCES LAW
15 Alderney Road
San Anselmo, CA 94960
Phone: (415) 446-9027
Email: renepvoss@gmail.com

*Attorney for Plaintiffs Sequoia ForestKeeper
and Earth Island Institute*

UNITED STATES DISTRICT COURT
FOR THE EASTERN DISTRICT OF CALIFORNIA
FRESNO DIVISION

UNITE THE PARKS; SEQUOIA
FORESTKEEPER; and EARTH ISLAND
INSTITUTE,

Plaintiffs,

v.

UNITED STATES FOREST SERVICE, an
agency of the U.S. Department of Agriculture;
and UNITED STATES FISH AND
WILDLIFE SERVICE, an agency of the U.S.
Department of the Interior,

Defendants.

Case No. 1:21-CV-00518-DAD-HBK

**DECLARATION OF DR. JOSEPH
WERNE IN SUPPORT OF PLAINTIFFS'
MOTION FOR PRELIMINARY
INJUNCTION**

Date: May 18, 2021
Time: 9:30 am
Courtroom: 5

ATTACHMENT D

1 I, Joseph Werne, declare as follows:

2 SUMMARY OF QUALIFICATIONS

3 1. I submit this declaration in support of the Plaintiffs' Motion for Preliminary
4 Injunction in this case regarding Defendants' plans to continue logging and vegetation-
5 management activities in the range of the Southern Sierra Nevada Pacific Fisher (SSN fisher) on
6 the Sierra, Sequoia, and Stanislaus National Forests. I have personal knowledge of the matters
7 stated herein and, if called as a witness, would and could competently testify thereto.

8 2. I am a research scientist with a Ph.D. in Physics (1993) from the University of
9 Chicago. I have a 34-year science career with a primary emphasis on high-resolution numerical
10 modeling and simulation of atmospheric dynamics. I have 78 scientific publications in refereed
11 journals, book chapters, and conference proceedings. My most-frequently cited works center on
12 two dominant themes: simulation and modeling of buoyant convection (which was my thesis
13 work), and accurate modeling of atmospheric turbulence. Both of these subjects are important for
14 understanding the atmospheric response and feedback to wildland fire. I have co-hosted
15 workshops at the National Center for Atmospheric Research (NCAR) and at the University of
16 Colorado at Boulder on the theory and modeling of atmospheric dynamics. I have presented
17 invited lectures on atmospheric turbulence theory and modeling and high-performance computing
18 across the U.S., in Japan, Italy, England, and elsewhere in Europe. I have served as either the
19 principle investigator or co-investigator on over 20 research and high-performance-computing
20 projects related to atmospheric simulation and modeling. A true and correct copy of my
21 Curriculum Vitae (CV) is attached as Exhibit A.

22 3. I am currently the co-lead of a working group of assembled experts in wildland-fire
23 theory and modeling. The group's expertise includes fire physics, high-resolution numerical
24 weather-fire simulation, forest ecology, wildlife ecology, and wildfire insurance. The goals of the
25 working group are to: a) integrate and incorporate the current state of the art in each of these
26 disciplines into an improved Wildland-Fire Behavior Assessment tool to aid land-management
27 decision making, and b) apply the results of our wildland-fire-behavior work to improved fire-
28 resilience assessments in California.

ATTACHMENT D

1 halted until we better understand their consequences, because claimed increased fire resilience
2 remains unproven. In fact, current practices may be reducing the fire resilience of our forests.

3 9. Below I provide background information for context related to Pacific fishers and
4 the large trees they need. I describe the primary threat to large trees from fire, namely, crown fires,
5 and I detail how current land-management practices designed to protect large trees from fire can
6 lead to the opposite effect. Finally, I present the latest science, which shows how current fuels-
7 reduction practices can make our forests less firesafe, and I show how operational fire models can
8 mislead us into believing vegetation treatments are effective, when they actually are not.

9 Background

10 10. The Pacific fisher is a member of the weasel family with quick reflexes, excellent
11 climbing skills, and exceptional fur. It is a midsize forest carnivore that eats small mammals and is
12 eaten by cougars, bobcats, and coyote. Fisher population numbers have been decimated by historic
13 fur trapping and logging of its old-growth forest habitat, and on May 15, 2020 the Distinct
14 Population Segment (DPS) of the Pacific fisher in the Southern Sierra Nevada (SSN) was listed as
15 endangered by the USFWS (U.S. Fish and Wildlife Service) under the Endangered Species Act.

16 11. In the forests where Pacific fishers live, fire occurs naturally; and the large trees
17 fishers need for reproduction also help make the forest firesafe. It is well established that large,
18 old-growth trees are able to resist burning because of their thick bark and large-diameter trunks;
19 also, their high canopies create cool microclimate environments that help protect surrounding
20 habitat by blocking the wind, shading the soil, retaining moisture, and significantly lowering
21 surface temperatures (e.g., Binkley et al. 2007, Lesmeister et al. 2019). True and correct copies of
22 the Binkley and Lesmeister papers are attached as Exhibits B and C, respectively. Though they
23 typically number less than 2% of the individual trees in a forest, trees larger than 40 inches in
24 diameter can account for nearly half of a forest's biomass (Lutz et al. 2012). A true and correct
25 copy of this paper is attached as Exhibit D. Unfortunately, for every old-growth tree that remains
26 today, more than seven have already been logged. Compared to historical abundances, only 12%
27 of Sierra Nevada old-growth trees remain (Erman et al. 1996, Vol. II). Therefore, safeguarding our
28 last large trees is critically important for protecting both the fisher's ability to reproduce and the
forest's ability to survive wildfire.

ATTACHMENT D

Crown Fires Threaten Our Remaining Large Trees

12. Major threats to large trees are overstory crown fires, which occur when treetops ignite during severe burns. Analysis of severe-burn patches in the 2013 Rim Fire found that crown fire disproportionately kills larger trees compared to smaller trees (Lydersen et al. 2016). Removing “ladder fuels” that connect the ground to the overstory is therefore a common-sense practice designed to prevent fires on the forest floor from climbing to the treetops (e.g., PSW-GTR-220). Nevertheless, recent research using detailed high-resolution numerical simulations reports that removing ladder fuels can easily increase the likelihood of crown-fire occurrence, despite being designed to reduce it (Banerjee et al. 2020). The reason for this seemingly counter-intuitive result involves the important role atmospheric motions play, and it demonstrates how focusing solely on forest fuels can make matters worse, if one neglects to also consider how vegetation treatments can increase the oxygen supply to a fire.

Accurate Fire Modeling Must Include Atmospheric Dynamics

13. Current operational fire models are incomplete, because they attempt to characterize complex fire behavior across a landscape using limited resources. In contrast, detailed high-resolution numerical fire simulations on high-performance supercomputers do a much better job, but they are too slow and too expensive for operational use. This is because operational models must rapidly obtain and compare a large number of different ignition and vegetation-treatment scenarios if they are to be useful. Nevertheless, fast models that produce unrealistic results can have catastrophic consequences for forestland management, and below I discuss two examples that demonstrate serious deficiencies with application of all of the USFS (U.S. Forest Service) operational models, including BehavePlus, FARSITE, FlamMap, FVS-FFE, and FSPro.

14. The first example concerns inadequate handling of the wind resistance associated with ladder fuels. When ladder fuels are removed, the ground-level windspeed and turbulent mixing both increase, leading to faster fire spread and greater oxygen-transport efficiency; this, in turn, results in increased fire intensity. As recent high-resolution numerical fire simulations show (e.g., Banerjee et al. 2020, Atchley et al. 2021), in many cases this aerodynamic effect is more important than the fire-dampening effects of the fuels reduction being evaluated. Nevertheless, comparisons using operational fire models do not predict this result because they ignore

ATTACHMENT D

1 aerodynamic differences between model runs with and without ladder fuels, using the same
2 specified windspeed for both cases. For example, see the USFS tutorial, Jones et al. 2010 at page
3 15, where a constant 20 mph windspeed is specified. (A true and correct copy of this paper is
4 attached as Exhibit E.) The model results are discussed in detail for varying degrees of ladder-fuel
5 removal (e.g., 0, 10, 20, 25, and 100 percent), but all cases are computed with exactly the same 20
6 mph windspeed. In reality, increasing levels of fuels reduction will be accompanied by higher
7 windspeeds as the sub-canopy wind drag drops, but this is not considered by Jones et al., and this
8 is typical of operational fire-model use. This mistake is repeated in the next example Jones et al.
9 discuss, where on page 22 they state, “The fire scenario was the same,” meaning the same constant
10 20 mph windspeed was again used.

11 15. Two recent studies using high-resolution numerical fire simulations demonstrate
12 just how consequential neglecting canopy wind-drag effects can be, leading to potentially
13 disastrous results if aggressive ladder-fuel removal is applied. One study is by Atchley et al. 2021,
14 sponsored by the USFS (a true and correct copy of which is included as Exhibit F), and the other
15 is by Banerjee et al. 2020 (a true and correct copy of which is included as Exhibit G). In both
16 papers, separate simulations are performed to compare different fuels configurations, and both
17 papers demonstrate that the removal of ladder fuels reduces the sub-canopy wind drag, ultimately
18 leading to increased fire spread. In other words, they both show how fuels-reduction treatments
19 can increase fire spread, which is the opposite of what the operational model studies predict.
20 Furthermore, the Banerjee et al. 2020 paper goes further and also shows that aggressive ladder-
21 fuel removal increases the likelihood of overstory crown fires compared to more modest ladder-
22 fuel reductions, which is again opposite to operational model-run predictions.

23 16. From these results, it is clear that evaluating wildland fire resilience using current
24 USFS operational fire-modeling theory is suspect, especially since operational models fail to
25 properly include all of the important effects associated with specified fuels treatments, especially
26 canopy wind resistance, which both Atchley et al. (2021) and Banerjee et al. (2020) show are
27 extremely important. Until operational fire models are updated to include the latest and best-
28 available science, claims of improved fire resilience should be viewed with skepticism, and

ATTACHMENT D

1 treatments should stop until they are carefully validated against more accurate simulation methods.

2 Our forests and the fisher may very-well depend on it.

3 Missing Fire Physics Can Be More Important than Fuel Load and Severe Weather

4 17. In addition to the focused process studies like those of Atchley et al. 2021 and
5 Banerjee et al. 2020, realistic high-resolution numerical fire simulations are also used to study the
6 details of real-world fires. Since the simulations require significant computer time, they are done
7 after the fact, but they are helpful for learning aspects of fire behavior that would be otherwise
8 difficult to determine. For example, Coen et al. 2018, also sponsored by the USFS (a true and
9 correct copy of which is included here as Exhibit H) uses high-resolution simulations to
10 deconstruct the 2014 King Fire, and its authors show that fire-induced winds were primarily
11 responsible for the fire's rapid growth and size. In their study, Coen et al. demonstrate that drought
12 and fuel load were secondary effects compared to fire-induced atmospheric motions, which
13 operational fire-behavior models neglect. Two important conclusions from the study are: 1. "...
14 extreme fires need not arise from extreme fire environment conditions," and 2. "... models used in
15 operations do not capture fire-induced winds and dynamic feedbacks so [they] can underestimate
16 megafire events." In other words, the inability of operational models to simulate plume-driven
17 megafires like the 2014 King Fire is not due to climate change or extreme weather events, but
18 instead because of known missing physics in the operational models.

19 18. Additional evidence that vegetation treatments may be excluding important fire
20 physics is suggested by the most comprehensive study to-date of wildland-fire data, which was
21 conducted by Bradley et al. (2016), a true and correct copy of which is included as Exhibit I. They
22 analyze satellite data for 1500 fires from 1984 to 2014, affecting 23.5 million acres of forestland.
23 Their results show that the more heavily forestland is managed, the more severely it burns, and the
24 least-managed land (i.e., our National Parks and Wilderness Areas) are the most firesafe
25 (correcting for forest type, topography, and climate variables). Other scientific studies find similar
26 results (e.g., Donato et al., 2006; Thompson et al., 2007; Cruz et al., 2014; Zald and Dunn, 2018).
27 This suggests our land-management activities may be making our forestlands less firesafe, not
28 more.

ATTACHMENT D

Long-Term Landscape-Resilience Claims are Unproven, and Sometimes They are Wrong

19. Current vegetation treatments advocated by the USFS were defined in 2009 in technical report PSW-GTR-220, and then later they were clarified in 2012 in PSW-GTR-237. Their efficacy for increased long-term, i.e., 30-year, landscape resilience is therefore not directly proven, since they were not practiced 30 years ago. Hence, claims of long-term resilience are theoretical, and they are only as credible as the models used to predict them. Given the results of Atchley et al. 2021, Banerjee et al. 2020, Coen et al. 2018, and Bradley et al. 2016, are we willing to bet the Pacific fisher's future on them?

20. Attempts to evaluate these claimed long-term benefits demonstrate that a) they are *not* based on the best available science and b) they exaggerate or mischaracterize the findings in the references used to justify them. In contrast, the most comprehensive scientific study to date examining forestland-fire data demonstrates that land-management practices are producing forestlands that are less firesafe, not more; see paragraphs 13-18. Though this may seem counter-intuitive, the reason is straightforward: the fire-behavior theory being used to guide vegetation treatments is incomplete because it does not sufficiently consider atmospheric motions, neither those induced by the fire, nor those induced by the vegetation treatments being analyzed. Until operational fire models are updated to address these deficiencies by including the latest available science, claims of improved long-term landscape resilience remain unproven, and the known harm being done to the Pacific fisher is therefore not justified.

21. Unfortunately, appropriate caution when interpreting operational model results is not apparent when long-term improvements are asserted by the Services. For example, in its June 12 addendum to its 2020 Programmatic Biological Opinion (2020 PBO), the USFWS justifies anticipated negative impacts to the SSN DPS of the Pacific fisher, and its habitat, including its permitted Incidental Take of twelve individuals, by asserting planned vegetation treatments would "be beneficial for the fisher in the long-term by increased resilience of habitat" (2020 PBO addendum at 6). Similarly, in its February 23, 2021 Amendment to the Programmatic Biological Assessment (2020 PBA), the USFS makes similar claims, stating "Many of the management activities analyzed here and in the May 19, 2020 PBA are designed to reduce fuels and the risk of high-severity fires within the SSNDPS. Management activities that reduce the risk of high-severity

ATTACHMENT D

1 fire confer a long-term benefit to the SSNDPS resilience to fire” (2020 PBA Amendment at 5-
2 6, February 23, 2021). Similar claims are repeated throughout the project documents associated
3 with the 45 vegetation-treatment projects approved by USFWS.

Conclusion

4
5 22. Recent high-resolution numerical fire simulations demonstrate important
6 deficiencies in the current USFS fire-behavior theory being used to analyze and design vegetation
7 treatments that are known by USFS and USFWS to be harming Pacific fisher habitat. By omitting
8 atmospheric dynamics and wind-drag effects associated with vegetation treatments, fuels
9 reductions designed to reduce fire intensity and fire spread are undoubtedly producing the opposite
10 effect. Also, poorly designed ladder-fuel removal is likely increasing the incidence of crown-fire
11 events that are killing our last large, old-growth trees.

12 23. Furthermore, the most comprehensive study to-date of forestland-fire data shows
13 that more heavily managed forestland burns more severely, and the least-managed land (i.e., our
14 National Parks and Wilderness Areas) are the most firesafe (correcting for forest type, topography,
15 and climate variables).

16 24. Claims of long-term fire resilience are theoretical, and they are only as credible as
17 the operational models being used to predict them. Assertions of long-term landscape resilience
18 should be viewed with skepticism, and given the best-available science, including Atchley et al.
19 2021, Banerjee et al. 2020, Coen et al. 2018, and Bradley et al. 2016, are we willing to bet the
20 Pacific fisher’s future on unproven assertions being made by the Services?

21 25. Given recent trends in California of ever-increasing fire size and severity, the desire
22 to take decisive action to make things better is understandable. However, if our actions are ill-
23 informed by flawed application of operational fire-behavior models that are guiding us to make an
24 already dire situation worse, until we fully understand the consequences of the actions we take, no
25 action is preferred.

26 I declare, under penalty of perjury, that the foregoing is true and correct to the best of my
27 knowledge and recollection. Executed on April 4, 2021 in Lafayette, Colorado.

28 

Joseph Werne

ATTACHMENT D

1 References

- 2 Atchley, A.L., R. Linn, A. Jonko, C. Hoffman, J.D. Hyman, F. Pimont, C. Sieg, R.S. Middleton,
3 2021. Effects of fuel spatial distribution on wildland fire behavior. *International Journal of*
4 *Wildland Fire*. doi:10.1071/WF20096.
- 5 Balch, J.K., B.A. Bradley, J.T. Abatzoglou, R.C. Nagy, E.J. Fusco, A.L. Mahood, 2017. Human-
6 started wildfires expand the fire niche across the United States. *Proc. Nat'l Acad. Sci.* 114(11),
7 pp.2946-2951.
- 8 Banerjee, T., W. Heilman, S. Goodrick, J.K. Hiers, and R. Linn, 2020. Effects of canopy midstory
9 management and fuel moisture on wildfire behavior. *Nature, Sci Reps* 10:17312.
10 <https://doi.org/10.1038/s41598-020-74338-9>
- 11 Bradley, C.M., C.T. Hanson, and D.A. DellaSalla, 2016. Does increased forest protection
12 correspond to higher fire severity in frequent-fire forests of the western USA? *Ecosphere* 7: article
13 e01492.
- 14 Coen, J.L., E.N. Stavros, and J.A. Fites-Kaufman, 2018. Deconstructing the King megafire.
15 *Ecological Applications*, 28(6), 2018, pp.1565-1580.
- 16 Cruz ,M.G., M.E. Alexander, and J.E. Dam, 2014. Using modeled surface and crown fire behavior
17 characteristics to evaluate fuel treatment effectiveness: a caution. *Forest Science* 60:1000-1004.
- 18 Donato, D.C., J.B. Fontaine, J.L. Campbell, W.D. Robinson, J.B. Kauffman, B.E. Law, 2006.
19 Post-Wildfire Logging Hinders Regeneration and Increases Fire Risk. *Science* 311 (5759), 352.
- 20 Erman, D.C. et al. 1996. Sierra Nevada Ecosystem Project, Final Report to Congress, Vol. II,
21 Assessment and Scientific Basis for Management Options. Wildland Resources Center Report No.
22 37, ISBN 1-887673-01-6, Center for Water and Wildland Resources, University of California,
23 Davis, CA 627-657.
- 24 Jones, J.G., W. Chung, C. Seielstad, J. Sullivan, K. Krueger, 2010. Optimizing spatial and
25 temporal treatments to maintain effective fire and non-fire fuels treatments at landscape scales.
26 Final Report, JFSP Project 06-3-3-14. U.S. Department of Agriculture/U.S. Department of the
27 Interior, Joint Fire Science Program. 33p.
- 28 Lutz, J.A., A.J. Larson, M.E. Swanson, J.A. Freund, 2012. Ecological Importance of Large-
Diameter Trees in a Temperate Mixed-Conifer Forest. *PLoS ONE* 7(5):e36131.
- Lydersen, J.M., B.M. Collins, J.D. Miller, D.L. Fry, S.L. Stephens, 2016. Relating Fire-Caused
Change in Forest Structure to Remotely Sensed Estimates of Fire Severity. *Fire Ecology*, 12(3),
pp.99-116.
- PSW-GTR-220: North, M., P. Stine, K. O'Hara, W. Zielinski, S. Stephens, 2009. An Ecosystem
Management Strategy for Sierran Mixed-Conifer Forests. USDA, FS General Technical Report.
- PSW-GTR-237: North, M., ed. 2012, Managing Sierra Nevada Forests. USDA, FS, General

ATTACHMENT D

- 1 Technical Report.
- 2 Thompson, J.R., T.A. Spies, and L.M. Ganio, 2007. Reburn severity in managed and unmanaged
3 vegetation in a large wildfire. Proc. Nat'l Academy of Sciences, 104(25).
- 4 USFS. 2021. Amendment to the Programmatic Biological Assessment for the Southern Sierra
5 Nevada DPS of Pacific fisher. U.S. Forest Service, Pacific Southwest Region, Vallejo, CA, 23
6 February 2021.
- 7 USFWS. 2020. Batch 1 Appendage to the Programmatic Biological Opinion on the Proposed U.S.
8 Forest service Management Programs for the Endangered Southern Sierra Nevada Distinct
9 Population Segment of the Fisher. U.S. Fish and Wildlife Service, Sacramento Fish and Wildlife
10 Office, Sacramento, CA, 12 June 2020.
- 11
- 12
- 13
- 14
- 15
- 16
- 17
- 18
- 19
- 20
- 21
- 22
- 23
- 24
- 25
- 26
- 27
- 28
- Zald, H.S.J. and C.J. Dunn. 2018. Sever fire weather and intensive forest management increase
fire severity in a multi-ownership landscape. Ecological Apps, 28(4), doi:10.1002/eap.1710.

ATTACHMENT D

EXHIBIT A

Institutional Address:

NorthWest Research Associates

3380 Mitchell Lane, Boulder, CO 80301, 303-415-9701 x207, werne@nwra.com

Education:

Old Dominion University

B.S. (summa), Physics (1987)

B.S. (summa), Mech. Eng'g & Mechanics (1987)

The University of Chicago, Ph.D., Physics (1993)

Positions Held:

1985-87 Engineering Co-op, Reactor Plant Planning Yard, Newport News Shipbuilding

1987-89 Teaching Assistant, Physics Department, The University of Chicago

1989-92 Research Assistant, Department of Astronomy and Astrophysics, The University of Chicago

1992-94 Postdoctoral Fellow, Advanced Study Program, National Center for Atmospheric Research

1994-95 Visiting Scientist, National Center for Atmospheric Research

1995-96 Research Associate, Joint Institute for Laboratory Astrophysics & Laboratory for Atmospheric and Space Physics, Univ. of Colorado

1997-01 Research Scientist, NorthWest Research Associates

2001-08 Assistant Division Manager, NorthWest Research Associates

2006-18 Vice President, NorthWest Research Associates

1998- Affiliated Faculty, Department of Applied Mathematics, Univ. of Colorado

2001- Senior Research Scientist, NorthWest Research Associates

2003- Director on the Board, NorthWest Research Associates

Professional Societies:

American Physical Society

American Astronomical Society

Professional Activities:

Presentations: Gordon Conference on Modeling in Solar Terrestrial Physics (1990); Gordon Conference on Solar Plasma and MHD Processes (1991); Army High Performance Computing Research Center, Workshop on Visualization and Statistical Analysis in Hard Turbulence (1992); The James Franck Institute, The University of Chicago, Turbulence Meeting (1993); Pittsburgh Supercomputing Center, Supercomputing Techniques: Parallel Processing/Cray T3D (1994); Woods Hole Oceanographic Institution Summer Program in Geophysical Fluid Dynamics (1995); NCAR Geophysical and Astrophysical Convection (1995); American Physical Society 43th, 44th, 46th, 47th, 48th, 58th, 60th & 66th Annual Meetings of the Division of Fluid Dynamics (1990-91, 1993-95, 2005, 2007, 2013); University of California 12th Annual Conference in Nonlinear Science (1996); National Center for Supercomputing Applications, Parallel Computing Workshop; SGI Origin (1997); DoD HPCMO User Group Conference (1998, 1999, 2000, 2001, 2002, 2003, 2004, 2005, 2006, 2007, 2008, 2009, 2010, 2011); Global Grid Forum 2 and 3, Washington, D.C. (2001) and Frascati, Italy (2001); EUROMECH Workshop 428 "Transport by coherent structures in environmental and geophysical flows," Torino, Italy (2001); Department of Energy, Environmental Meteorology Program, "Vertical Transport and Mixing," Salt Lake City (2001, 2002); Center for Turbulence Research, "30 Years of Dynamic Modeling," Stanford University (2002); Invited Speaker, Center for Nonlinear Studies, Los Alamos National Laboratory (2003); Invited Speaker, "Helio- and Asteroseismology: Towards a Golden Future," Yale University, New Haven, Connecticut (2004); "Turbulence and Waves," Lighthill Institute of Mathematical Sciences, London, UK (2004); Visiting Scientist Colloquium, NASA Langley Research Center (2005); Invited Speaker, "Turbulent Mixing and Beyond," Trieste, Italy (2007); Co-organizer, NCAR 2008 Theme of the Year Workshop "Petascale Computing: Its Impact on Geophysical Modeling and Simulation" (2008). Invited Speaker, 20th DoD HPCMO User Group Conference, Schaumburg, IL (2010); Invited Speaker, "Turbulent Mixing and Beyond TMB-2011," Trieste, Italy (2011); Invited Speaker, Fundamental Aspects of Geophysical Turbulence II (2015); VIII International Symposium on Stratified Flows (2016); Invited Speaker, "McWilliams Symposium" National Center for Atmospheric Research, Boulder, CO (2016).

Software: Principle Architect & Author, *Practical Supercomputing Toolkit*, used by the Department of Defense (DoD) High Performance Computing and Modernization Program (HPCMP) to define a uniform command-line interface that streamlines use of disparate supercomputer platforms, high-speed networks, and archival data storage systems at all of the DoD HPC centers: <https://pstoolkit.nwra.com>. Principle Architect & Author, *Werne-NWRA Triple Code*, a highly accurate pseudo-spectral fluid-dynamics solver designed to run efficiently on modern massively parallel supercomputer platforms: <https://cora.nwra.com/~werne/triple/>.

Teaching: Instructor, Summer MCAT Program, The University of Chicago, Biological Sciences Division and the Pritzker School of Medicine (1989-92). Principal Lecturer, NCAR 2008 Summer School: Geophysical Turbulence. Instructor, University of Colorado at Boulder 2009 Supercomputing Workshop, Fluid Instabilities, Waves, and Turbulence, as part of Professor Juri Toomre's ASTR/ATOC 5410 Graduate Course

Awards: A.D. Morgan Scholarship (1986-87); Faculty Award in Mechanical Engineering and Mechanics (1987); Outstanding Senior Award in Physics (1987); Gregor Wentzel Prize for Excellence as Graduate Student Tutor (1988).

Societies: Phi Kappa Phi; Pi Tau Sigma; Tau Beta Pi.

General Fields of Investigation:

Theoretical and numerical turbulence process, dynamics, and transport mechanisms in geophysical and astrophysical applications, including both stable and unstable stratification. Specific research areas include high-Rayleigh-number convection, penetrative convection, rotating convection, stratified shear turbulence, gravity-wave breaking, wave-wave interactions, multi-scale shear and wave dynamics, magnetohydrodynamic instability and turbulence processes, and optimal-perturbation theory. Applications have included ocean- and atmosphere-dynamics modeling, aircraft-wakes evolution and ground interactions, plasma dynamics for space-weather applications, solar-interior modeling, helioseismic analysis of the solar interior, and Bayesian-hierarchical turbulence-process modeling in the troposphere and stratosphere. A primary emphasis has been on efficient and accurate spectral numerical methods, large-scale and high-performance computing, and massively parallel computing on a wide range of architectures, starting with the Cray XMP and YMP vector machines, the modestly parallel Cray C90, and then larger-scale and massively parallel platforms, including the Cray T3D, T3E, XT3, XT4, XT5, XE6, XC40; IBM SP, P4+, P5+, P6; SGI O2k, O3k, Altix; Compaq SC40/45.

Business Development:

Developed, analyzed, and helped implement the 2000 NWRA Business Model, which encourages Research Scientists to become Principal-Investigator (PI) Partners in a successful research-science company. This model is novel, maximizes PI compensation, minimizes corporate taxes, has proven to be an invaluable recruiting tool for NWRA, and has worked successfully since 2000.

Publications:

1. *Design of a Mars Oxygen Processor:* Ash, R., J. Werne and M. B. Haywood 1989, in *The Case for Mars III* edited by C. Stoker, AAS Science and Technology Series, **75**, 479-487.
2. *Numerical Simulations of Soft and Hard Turbulence: Preliminary Results for Two-Dimensional Convection:* DeLuca, E. E., J. Werne, R. Rosner, and F. Cattaneo 1990, Phys. Rev. Letters, **64**(20), 2370-3.
3. *The Development of Hard-Turbulent Convection in Two Dimensions: Numerical Evidence:* Werne, J., E. E. DeLuca, R. Rosner and F. Cattaneo 1991, Phys. Rev. Letters, **67**(25), 3519.
4. *The Structure of Hard-Turbulent Convection in Two Dimensions: Numerical Evidence:* Werne, J. 1993, Phys. Rev. E, **48**, 1020.
5. *Plume Model for the Boundary-Layer Dynamics in Hard Turbulence :* Werne, J. 1994, Phys. Rev. E, **49**, 4072.
6. *Incompressibility and No-Slip Boundaries in the Chebyshev-Tau Approximation: Correction to Kleiser and Schumann's Influence-Matrix Solution:* Werne, J. 1995, J. Comput. Phys., **120**, 260.
7. *Penetrative Convection in Rapidly Rotating Flows: Preliminary Results from Numerical Simulation:* Julien, K., S. Legg, J. McWilliams, and J. Werne 1996, Dyn. Atmos. Oceans, **24**, 237.
8. *Turbulent Rotating Rayleigh-Benard Convection with Comments on 2/7:* Werne, J. 1995, Woods Hole Oceanog. Inst. Tech. Rept. WHOI-95-27.
9. *Hard turbulence in rotating Rayleigh-Benard convection:* Julien, K., S. Legg, J. McWilliams, and J. Werne 1996, Phys. Rev. E, **53**, 5557R.
10. *Rapidly Rotating Turbulent Rayleigh-Benard Convection:* Julien, K., S. Legg, J. McWilliams and J. Werne 1996, J. Fluid Mech., **322**, 243.
11. *Dynamics and Scaling in Quasi Two-Dimensional Turbulent Convection:* Bizon, C., A. A. Predtechensky, J. Werne, K. Julien, W. D. McCormick, J. B. Swift and H. Swinney 1997, Physica A., **239**, 204.
12. *Plume Dynamics in Quasi 2D Turbulent Convection:* Bizon, C., J. Werne, A. A. Predtechensky, K. Julien, W. D. McCormick, J. B. Swift and H. L. Swinney 1997, Chaos, **7**, 1.
13. *Turbulent convection: what has rotation taught us?:* Werne, J. 2000 in *Geophysical and Astrophysical Convection*, Eds. P. A. Fox and R. M. Kerr. Gordon and Breach Science Publishers, 221.
14. *The effects of rotation on the global dynamics of turbulent convection:* Julien, K., J. Werne, S. Legg and J. McWilliams 1997 in *SCORe'96: Solar Convection and Oscillations and their Relationship*. Eds. J. Christensen-Dalsgaard and F. P. Pijpers. Kluwer Academic Publ., 227-230.
15. *The effect of rotation on convective overshoot:* Julien, K., J. Werne, S. Legg and J. McWilliams 1996, in *SCORe'96: Solar Convection and Oscillations and their Relationships*. Eds. J. Christensen-Dalsgaard and F. P. Pijpers. Kluwer Academic Publ., 231-234.
16. *Comment on "There is no Error in the Kleiser-Schumann Influence-Matrix Method":* Werne, J. 1998, J. Comput. Phys. **141**, 88.

17. *Turbulence in Stratified and Shear Fluids: T3E Simulations*: Werne, J. and D. C. Fritts 1998, 8th DoD HPC User Group Conference, Houston, TX.
18. *2-D Convection in Tall, Narrow Containers: Implications for Theories of Heat Transport in Hard Turbulence*: Werne, J. 1996, (in preparation).
19. *High Rayleigh number convective transport: testing theories by modifying boundary conditions*: Brummell, N., K. Julien, and J. Werne 1996, (in preparation).
20. *Plumes in rotating convection: Part 1. Ensemble statistics and dynamical balances*: Julien, K., S. Legg, J. McWilliams, and J. Werne 1999, *J. Fluid Mech.* **391**, 151-187.
21. *Statistical Analysis of the Influence of Rotation in Rayleigh-Benard Convection*: Julien, K., S. Legg, J. McWilliams, and J. Werne 1996, (in preparation).
22. *On the linear stability of Hele-Shaw Convection*: Julien, K. and J. Werne 1996, *Int. J. Heat and Mass Transfer*, (to be submitted).
23. *A new class of equations for rotationally constrained flows*: Julien, K., E. Knobloch and J. Werne 1998, *Theoret. and Comput. Fluid Dynamics*, **11**, 251-261.
24. *Reduced Equations for Rotationally Constrained Convection*: Julien, K., E. Knobloch and J. Werne 1999, In the International Symposium on Turbulence and Shear Flow Phenomena, v.1, pp. 101-106, Begel House.
25. *A Reduced Description for Rapidly Rotating Turbulent Convection*: Julien, K., E. Knobloch and J. Werne 1998, In *Advances in Turbulence VII*, Eds U. Frisch, pp. 472-482, Kluwer Academic Publishers.
26. *Dynamics of counter-rotating vortex pairs in stratified and sheared environments*: Garten, J. F., S. Arendt, D. C. Fritts and J. Werne 1998, *J. Fluid Mech.* **361**, 189-236.
27. *Anisotropy in Stratified Shear Turbulence*: Werne, J. and D. C. Fritts 1999, 9th DoD HPC User Group Conference, Monterey, CA.
28. *Stratified shear turbulence: Evolution and statistics*: Werne, J. and D. C. Fritts 1999, *Geophys. Res. Letters* **26**, 439.
29. *Turbulence-induced fluctuations in ionization and application to PMSE*: Hill, R. J., D. Gibson-Wilde, J. Werne and D. C. Fritts 1999, *Earth Planets Space*, **51**, 499.
30. *Structure Functions in Stratified Shear Turbulence*: Werne, J. and D. C. Fritts 2000, 10th DoD HPC User Group Conference, Albuquerque, NM.
31. *Turbulence Dynamics and Mixing due to Gravity Waves in the Lower and Middle Atmosphere*: Fritts, D. C. and J. Werne 2000, in *Atmospheric Science across the Stratopause*, Geophysical Monograph 123, American Geophys. Union, 143-159.
32. *Hierarchical Data Structuring: an MPP I/O How-to*: Werne, J., P. Adams and D. Sanders 2000, *Scientific Computing at NPACI*, June 14, Volume 4 Issue 12.
33. *Linear scaling during production runs: conquering the I/O bottleneck*: Werne, J., P. Adams and D. Sanders 2000, in *ARSC CRAY T3E Users' Group Newsletter* **193**, April 14, eds. T. Baring & G. Robinson.
34. *Numerical modeling of turbulent zero momentum late wakes in density stratified fluids*: Gourlay, M. J., S.C. Arendt, D.C. Fritts, and J. Werne 2000, 10th DoD HPC User Group Conference, June 5-9, Albuquerque, NM.
35. *Numerical modeling of turbulent non-zero momentum late wakes in density stratified fluids*: Gourlay, M. J., S.C. Arendt, D.C. Fritts, and J. Werne 2000, Fifth International Symposium on Stratified Flows, July 10-13, Vancouver, Canada.
36. *Numerical modeling of initially turbulent wakes with net momentum*: Gourlay, M. J., S.C. Arendt, D.C. Fritts, and J. Werne 2001, *Phys. Fluids* **13**, 3783.
37. *Numerical simulation of late wakes in stratified and sheared flows*: Fritts, D., M. Gourlay, W. Orlando, C. Meyer, J. Werne, and T. Lund 2003, 13th DoD HPC User Group Conference, DOI:10.1109/DODUGC.2001.1253394
38. *Direct numerical simulation of VHF radar measurements of turbulence in the mesosphere*: Gibson-Wilde, D., J. Werne, D. C. Fritts and R. J. Hill 2000, *Radio Science* **35**, 783.
39. *Anisotropy in a stratified shear layer*: Werne, J. and D. C. Fritts 2001, *Physics and Chemistry of the Earth*, **26**, 263.
40. *Direct numerical simulations of the Crow instability and subsequent vortex reconnection in a stratified fluid*: Garten, J. F., J. Werne, D. C. Fritts, and S. Arendt 2001, *J. Fluid Mech.* **426**, 1.
41. *Wave-breaking and shear turbulence simulations in support of the Airborne Laser*: Werne, J., C. Bizon, C. Meyer, and D. C. Fritts 2001, 11th DoD HPC User Group Conference, June, Biloxi, MS.
42. *Vertical transport by convection plumes: Modification by rotation*: Legg, S., K. Julien, J. McWilliams, and J. Werne 2001, *Phys. Chem. of the Earth*, **B, 26** (4), 259-262.
43. *The Effects of Ambient Stratification on the Crow Instability and Subsequent Vortex Reconnection*: Garten, J. F., J. Werne, D. C. Fritts and S. Arendt 1999 in *European Series in Applied and Industrial Mathematics*, ESAIM Proceedings, Third International Workshop on Vortex Flow and Related Numerical Methods, Vol 7 Eds: A. Giovannini, G. H. Cottet, Y. Gagnon, A. Ghoniem, E. Meiburg.
44. *Application of turbulence simulations to the mesosphere*: Gibson-Wilde, D., J. Werne, D. C. Fritts, and R. Hill 2000, *Proc. MST 9 Radar Workshop*, Toulouse, France.
45. *A new dynamical subgrid model for the planetary surface layer. I. The model and a priori tests*: Dubrulle, B., J.-P. Laval, P. P. Sullivan and J. Werne 2002, *J. Atmos. Sci.* **59**, 857.
46. *Entrainment-zone restratification and flow structures in stratified shear turbulence*: Pettersson-Reif, B.A., J. Werne, O. Andreassen, C. Meyer, M. Davis-Mansour 2002, *Studying Turbulence Using Numerical Simulation Databases -IX*, Proceedings of the 2002 Summer Program, Center for Turbulence Research, ed. P. Bradshaw, 245-256.

47. *Layering accompanying turbulence generation due to shear instability and gravity wave breaking*: Fritts, D.C., C. Bizon, J.A. Werne, and C.K. Meyer 2003, *J. Geophys. Res.* **108**, D8, 8452, doi:10.1029/2002JD002406.
48. *The Need for Control Experiments in Local Helioseismology*: Werne, J., A. Birch, and K. Julien 2004, SOHO 14/GONG 2004, Helio- and Asteroseismology: Towards a Golden Future, New Haven, CT., Es. D. Danesy, European Space Agency SP-559.
49. *Visualization of the Energy-Containing Turbulent Scales*: Helgeland, A., Ø. Andreassen, A. Ommundsen, B.A. Pettersson-Reif, J. Werne, T. Gaarder 2004, 2004 IEEE Symposium on Volume Visualization and Graphics (VV'04) 103-109., DOI:10.1109/SVVG.2004.15
50. *Persistence of a Kelvin-Helmholtz instability complex in the upper troposphere*: M.C. Kelley, C.Y. Chen, R.R. Beland, R. Woodman, J.L. Chau, and J. Werne 2005, *J. Geophys. Res.* **110**, D14, 106, doi:10.1029/2004JD005345.
51. *CAP Phase II Simulations for the Air Force HEL-JTO Project: Atmospheric Turbulence Simulations on NAVO's 3000-Processor IBM P4+ and ARL's 2000-Processor Intel Xeon EM64T Cluster*: Werne, J., T. Lund, B.A. Pettersson-Reif, P. Sullivan, and D.C. Fritts 2005, 15th DoD HPC User Group Conference, June, Nashville, TN., DOI:10.1109/DODUGC.2005.16
52. *Characterization of high altitude turbulence for Air Force platforms*: Ruggiero, F.H., J. Werne, T.S. Lund, D.C. Fritts, K. Wan, L. Wang, A. Mahalov, and B. Nichols 2005, 15th DoD HPC User Group Conference, June, Nashville, TN.
53. *Generalized quasi-geostrophy for spatially anisotropic rotationally constrained flows*: K. Julien, E. Knobloch, R. Milliff & J. Werne 2006, *J. Fluid Mech.*, **555**, 233-274.
54. *Mean and variable forcing of the middle atmosphere by gravity waves*: Fritts, D.C., S.L. Vadas, K. Wan, and J. Werne 2006, *J. Atmos. Solar-Terres. Phys.*, **68**, 247-265.
55. *Characterization of High Altitude Turbulence for Air Force Platforms*: Ruggiero, F.H., J. Werne, A. Mahalov, B. Nichols, and D.E. Wroblewski 2006, 16th DoD HPC User Group Conference, June, Denver, CO.
56. *Numerical simulation of an asymptotically reduced system for rotationally constrained convection*: Sprague, M., K. Julien, E. Knobloch, and J. Werne 2006, *J. Fluid Mech.*, **551**, 141-174.
57. *Characterization of High Altitude Turbulence for Air Force Platforms*: Ruggiero, F.H., A. Mahalov, B. Nichols, J. Werne, and D.E. Wroblewski 2007, 17th DoD HPC User Group Conference, June, Pittsburgh, PA., DOI:10.1109/HPCMP-UGC.2007.15
58. *High-Resolution Simulations and Atmospheric Turbulence Forecasting*: Werne, J., D.C. Fritts, L. Wang, T. Lund, and K. Wan 2008, 18th DoD HPC User Group Conference, July, Seattle, WA.
59. *Gravity Wave Instability Dynamics at High Reynolds Numbers. Part II: Turbulence Evolution, Structure, and Anisotropy*: D.C. Fritts, L. Wang, J. Werne, T. Lund, and K. Wan 2009, *J. Atmos. Sci.*, DOI:10.1175/2008JAS2727.1
60. *Gravity wave instability dynamics at high Reynolds numbers, 1: Wave field evolution at large amplitudes and high frequencies*: Fritts, D.C., L. Wang, J. Werne, T. Lund, and K. Wan 2009, *J. Atmos. Sci.* **66**, 1126-1148, doi:10.1175/2008JAS2726.1.
61. *Gravity wave instability dynamics at high Reynolds numbers, 2: Turbulence evolution, structure, and anisotropy*: Fritts, D.C., L. Wang, J. Werne, T. Lund, and K. Wan 2009, *J. Atmos. Sci.* **66** 1149-1171, doi:10.1175/2008JAS2727.1.
62. *High-Resolution Simulations of Internal Gravity-Wave Fine Structure Interactions and Implications for Atmospheric Turbulence Forecasting*: Werne, J., Fritts, D.C., L. Wang, T. Lund and K. Wan 2009, 19th DoD HPC User Group Conference, 15-19 June, San Diego, CA, DOI: 10.1109/HPCMP-UGC.2009.43
63. *Gravity wave fine-structure interactions: A reservoir of small-scale and large-scale turbulence energy*: Fritts, D.C., L. Wang and J. Werne 2009, *Geophys. Res. Lett.* **36**, L19805, doi:10.1029/2009GL039501.
64. *Numerical simulation of the linking of Kelvin-Helmholtz instabilities at adjacent shear layers*: Fritts, D.C., B. Laughman, J. Werne, D. Simkhada and M.J. Taylor 2009, *J. Geophys. Res.* (to be submitted).
65. *Numerical simulation of bore generation and morphology in thermal and Doppler ducts*: Laughman, B., D.C. Fritts, and J. Werne 2009, *Ann. Geophys.*, SpreadFEx special issue, **27**, 511-523.
66. *Atmospheric Turbulence Forecasts for Air Force and Missile Defense Applications*: Werne, J., D.C. Fritts, L. Wang, T. Lund, and K. Wan 2010, Invited Paper, 20th DoD HPC User Group Conference, 14-17 June, Schaumburg, IL, DOI:10.1109/HPCMP-UGC.2010.75
67. *Temperature and velocity structure functions in the upper troposphere and lower stratosphere from aircraft measurements (invited)*: Wroblewski, D.E., J. Werne, O. Cote, J. Hacker, and R. Dobosy 2010, *J. Geophys. Res.*, DOI:10.1029/2010JD014618
68. *Comparisons of predicted bore evolutions by the Benjamin-Davis-Ono and Navier-Stokes equations for idealized mesopause thermal ducts*: Laughman, B., D.C. Fritts, and J. Werne 2011, *J. Geophys. Res.*, DOI:10.1029/2010JD014409
69. *Computation of clear-air radar backscatter from numerical simulations of turbulence: 1. Numerical methods and evaluation biases*: Franke, P.M., S. Mahmoud, K. Raizada, K. Wan, D.C. Fritts, T. Lund, and J. Werne 2011, *J. Geophys. Res.*, DOI:10.1029/2011JD015895
70. *Computation of clear-air radar backscatter from numerical simulations of turbulence: 2. Backscatter moments throughout the lifecycle of a Kelvin-Helmholtz instability*: Fritts, D.C., P.M. Franke, K. Wan, T. Lund and J. Werne 2011, *J. Geophys. Res.*, DOI:10.1029/2010JD014618
71. *Interpretation of apparent simultaneous occurrences of Kelvin-Helmholtz instability in two airglow layers: Observations*: Simkhada, D., B. Laughman, D.C. Fritts, J. Werne, and A. Liu 2013, *J. Geophys. Res.* (submitted).
72. *Kelvin-Helmholtz instability in two airglow layers: Observations*: Simkhada, D., B. Laughman, D.C. Fritts, J. Werne, and A. Liu 2013, *J. Geophys. Res.* (submitted).
73. *Modeling the implications of Kelvin-Helmholtz instability dynamics for airglow observations*: Fritts, D.C., K. Wan, J. Werne, T. Lund, J.H. Hecht 2014, *J. Geophys. Res. Atmos.*, **119**, 8858-8871. doi:10.1002/2014JD021737.

74. *Gravity Wave-Fine Structure Interactions. Part I: Influences of Fine Structure Form and Orientation on Flow Evolution and Instability*: Fritts, D.C., L. Wang, and J.A. Werne 2013, J. Atmos. Sci. 70:12, 3710-3734, DOI:10.1175/JAS-D-13-055.1
75. *Coupled small scale mesospheric dynamics in a dual shear environment over Hawaii II: Modeling and interpretation*: Laughman, B., D.C. Fritts, J. Werne, D.B. Simkhada, M.J. Taylor, and A.Z. Liu 2013, J. Geophys. Res. (submitted).
76. *Quantifying Kelvin-Helmholtz Instability Dynamics Observed in Noctilucent Clouds: 2. Modeling and Interpretation of Observations*: Fritts, D.C., G. Baumgarten, K. Wan, J. Werne, T. Lund 2014, J. Geophys. Res., 119, 9359-9375, doi:10.1002/2014JD021833
77. *Numerical Modeling of Multiscale Dynamics at a High Reynolds Number: Instabilities, Turbulence, and an Assessment of Ozmidov and Thorpe Scales*: Fritts, D.C., L. Wang, M.A. Geller, D.A. Lawrence, J. Werne, B.B. Balsley 2016, J. Atmos. Sci., 73(2), 555-578, doi:10.1175/JAS-D-14-0343.1
78. *Fine Structure, Instabilities, and Turbulence in the Lower Atmosphere: High-Resolution in Situ Slant-Path Measurements with the DataHawk UAV and Comparisons with Numerical Modeling*: Balsley, B.B., D.A. Lawrence, D.C. Fritts, L. Wang, K. Wan, J. Werne, 2018, J. Atmos. and Oceanic Tech., 35(3), 619-642, doi:10.1175/JTECH-D-16-0037.1

ATTACHMENT D

EXHIBIT B

Synthesis, part of a Special Feature on [The Conservation and Restoration of Old Growth in Frequent-fire Forests of the American West](#)

The Role of Old-growth Forests in Frequent-fire Landscapes

[Daniel Binkley](#)¹, [Tom Sisk](#)^{2,3}, [Carol Chambers](#)⁴, [Judy Springer](#)⁵, and [William Block](#)⁶

ABSTRACT. Classic ecological concepts and forestry language regarding old growth are not well suited to frequent-fire landscapes. In frequent-fire, old-growth landscapes, there is a symbiotic relationship between the trees, the understory graminoids, and fire that results in a healthy ecosystem. Patches of old growth interspersed with younger growth and open, grassy areas provide a wide variety of habitats for animals, and have a higher level of biodiversity. Fire suppression is detrimental to these forests, and eventually destroys all old growth. The reintroduction of fire into degraded frequent-fire, old-growth forests, accompanied by appropriate thinning, can restore a balance to these ecosystems. Several areas require further research and study: 1) the ability of the understory to respond to restoration treatments, 2) the rate of ecosystem recovery following wildfires whose level of severity is beyond the historic or natural range of variation, 3) the effects of climate change, and 4) the role of the microbial community. In addition, it is important to recognize that much of our knowledge about these old-growth systems comes from a few frequent-fire forest types.

Key Words: *ecological processes; evolutionary adaptations; historic range of variation (HRV); human values; knowledge gaps; resilience; understory vegetation*

INTRODUCTION

Traditional forestry took decades to understand the unique features of frequent-fire forests. Early foresters in the Southwest were very concerned about the near-absence of young trees in forests dominated by older, widely spaced ponderosa pine (*Pinus ponderosa*) trees, and they realized that frequent fires prevented the development of closed-canopy, high-wood-producing forests. A young Aldo Leopold (1920) wrote:

...the prevention of light burning during the past 10 years... has brought in growth on large areas where reproduction was hitherto largely lacking. Actual counts show that the 1919 seedling crop runs as high as 100 000 per acre. It does not require any very elaborate argument to show that these tiny trees, averaging only 2 inches high, would be completely destroyed by even a light ground fire.

Leopold did not yet have the insight to understand the profound consequences of 100 000 seedlings per acre, although he later came to see the more subtle argument that fire prevention thwarted the processes necessary for the long-term health of the forest ecosystem.

Frequent fires challenge the survival of new tree seedlings and strongly shape the long-term development of all the components of a forest. Young trees often establish in clumps, as a legacy of patchy fuels and fire behavior; and this structural legacy may last for centuries. Gaps between clumps may result from a combination of competition with grasses and shrubs, from uneven distribution of seeds, and also the pattern of fire that interacts with the pattern of soils, vegetation, and fine fuels. The intimate mixture of shady clumps of trees and small open meadows provides a local-scale diversity that would be found only at much larger scales in landscapes without frequent fire. Indeed, some classic vocabulary in forestry is not well suited for frequent-fire forests. As noted by Kaufmann et al.

¹Colorado Forest Restoration Institute, ²Northern Arizona University, Environmental Sciences, ³ForestERA, ⁴Northern Arizona University, School of Forestry, ⁵Ecological Restoration Institute, ⁶U.S. Forest Service Rocky Mountain Research Station

ATTACHMENT D

in this issue, old-growth characteristics in dry, frequent-fire forests are remarkably different from the old-growth images developed in wetter areas. Even the concept of the forest “stand” as a part of a forest landscape with relatively uniform conditions and somewhat distinct boundaries may not be suitable for frequent-fire forests (Long and Smith 2000). The important details about the spatial arrangement of trees in the landscape relate to the clumping of trees into small groups, and to clusters of these groups, rather than to extensive, uniform areas of similar-size trees stretching across hundreds or thousands of hectares (Fig. 1).

The frequent recurrence of fires reinforces a spatial heterogeneity, promoting a forest with high, small-scale variety in plant species composition, animal habitat, and ecological processes. This pattern of local variety is a key defining feature of old-growth forests in frequent-fire landscapes. In this chapter, we consider some of the crucial ecological roles that might depend partially on the spatial arrangements of trees, and those that relate to the fully developed old-growth conditions.

EVOLUTIONARY ADAPTATIONS TO FIRE

The adaptations of large trees to surviving fire are fundamental in the ecology of old-growth forests in frequent-fire landscapes. Depending on the species, trees in these forests have developed a number of characteristics to withstand and survive fire. Although fire typically kills small conifers with thin bark by overheating or destroying the cambium layer (van Mantgem and Schwartz 2003), most coniferous tree species in the mature state have thick, insulating bark that is relatively nonflammable, long needles, self-pruning lower branches, and deep roots. Giant sequoia (*Sequoiadendron giganteum*) also experiences rapid growth that raises canopies off the ground quickly, as well as latent buds and serotinous cones (Stephenson 1999). Jeffrey pine (*Pinus jeffreyi*) develops buds with thick scales that help withstand heat. Sugar pine (*Pinus lambertiana*) has thick, fire-resistant bark and an open canopy that retards the spread of fire through the canopy. Gray pine (*Pinus sabiniana*) has thick bark and is self-pruning. Arizona pine (*Pinus arizonica*) has insulated buds, a high capacity to recover from crown scorch and an open crown. Ponderosa pine has thick bud scales; tight needle bunches that enclose and protect the meristems, then open into a loose arrangement that does not favor combustion

or propagation of flames; high foliar moisture; and a deep rooting habit. The foliage and buds are also usually elevated away from the flame zone. With its high foliar moisture content, ponderosa pine can withstand extensive scorching as long as the buds and twigs, which tolerate higher temperatures than needles, are not badly scorched.

USING PAST CONDITIONS AS A GUIDE

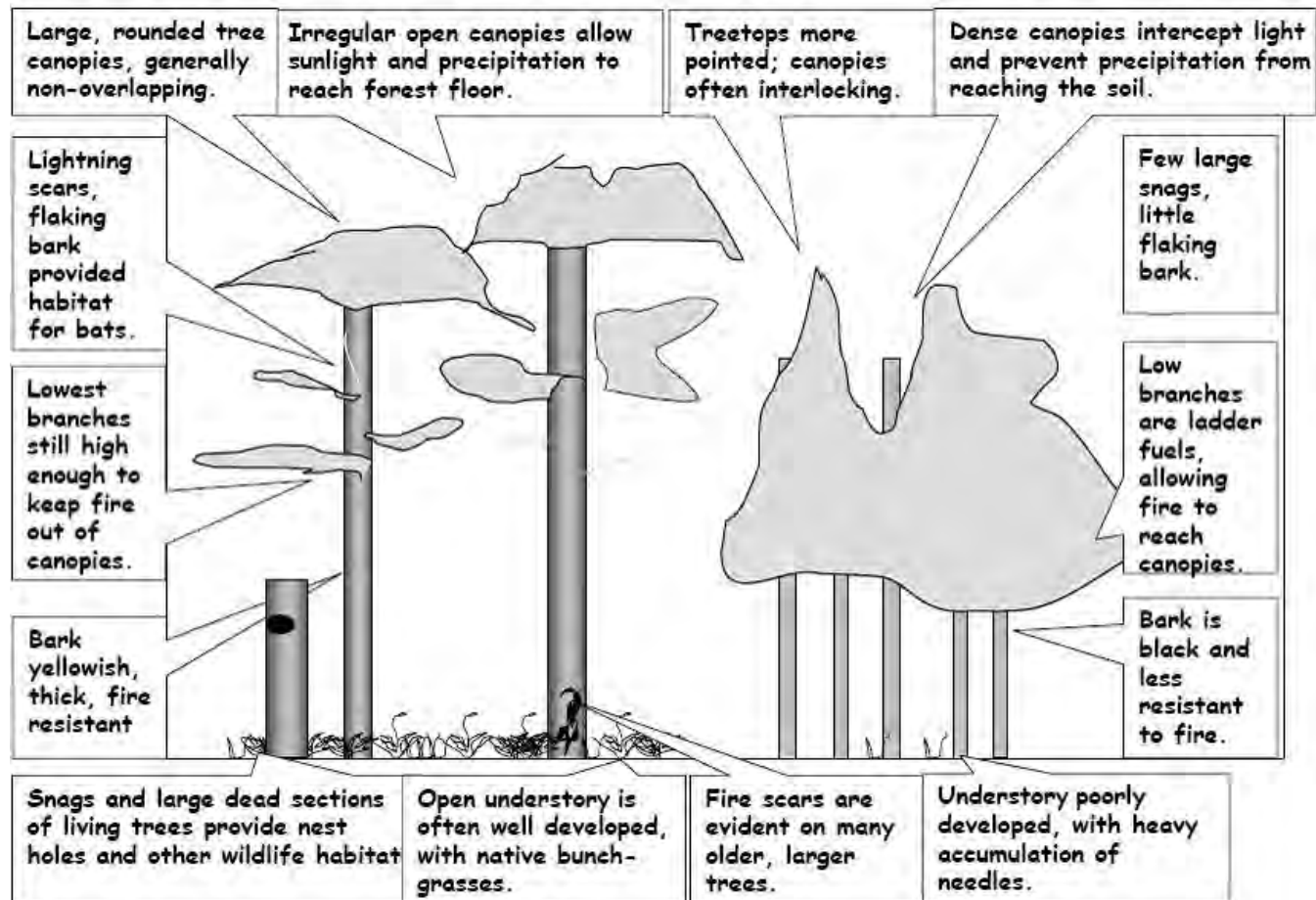
Historic range of variability (HRV) or natural range of variability are interchangeable terms along with natural variability, historical variation, and natural range of variability. These terms suggest that past conditions and processes can be used as guidance for managing present-day ecosystems, and that disturbance (and resultant variety) is a vital attribute of nearly every ecosystem (Landres et al. 1999). The HRV approach is just a first step in pondering possible future forests and landscapes, because it is difficult to deduce details about HRV (especially across large areas and long times), and because future climate conditions may not track historical trends. Because of changes in fire regimes, particularly caused by grazing and fire suppression, many frequent-fire forests now function well outside the HRV (see Moore et al. 1999, Veblen et al. 2000, Allen et al. 2002, Arno and Fiedler 2005, Zier and Baker 2006). For example, Sierra Nevada forests currently are undergoing fire-free periods that are much longer than at any time in the past two centuries (Keeley and Stephenson 2000).

Determining the Historic Structure and Function of Old-growth Forests

Almost all of the frequent-fire landscapes of the western United States have changed dramatically as a result of livestock grazing, timber harvesting, and fire suppression. Given the near absence of fully functioning, old-growth forests in frequent-fire landscapes, scientists have to use a variety of approaches to determine the structure and processes that characterize these forests (Swetnam et al. 1999, Egan and Howell 2001, Friederici 2003). Historical journals, photographs, and records provide information from some forests on the number and sizes of trees before major changes in land use, and the most detailed records even provide information on other features, such as downed logs and bunchgrass locations (Moore et al. 2004). In the absence of historical records, detailed characterizations

ATTACHMENT D

Fig. 1. A cartoon description of the key features of old-growth forests in frequent-fire landscapes (left), in contrast to younger forests lacking fire (right).



of tree ages, stump ages, and other field evidence can provide solid descriptions of previous conditions. A very few sites, such as the Powell Plateau in the Grand Canyon and some regions of northern Mexico, may have experienced so little change in land use and fire regimes that contemporary measurements are possible (Fulé et al. 2005). Some of the most detailed insights about the structure and function of old-growth forests come from intensive experiments that have reestablished historic forest structure. These treatments include harvesting (and removing) the excessive young trees, retaining most old trees, and reintroducing fire at intervals that match the frequency of historical fires (Bailey and Covington 2002, Fulé et al. 2002, 2006). Forest restoration

treatments may not redevelop historical old-growth conditions perfectly for a variety of reasons: 1) the seedbanks of native species may be depleted after decades without fire, 2) exotic species may invade, and 3) the animal communities may not be the same as in past centuries.

We know that historic frequent-fire, old-growth forests were not all alike. For example, Moore and her colleagues (2004), after studying a set of 11 research plots established in the early 1900s in Arizona and New Mexico, found that basal area ranged from 9 to 27 m²/ha, with an average of 15 m²/ha. By the end of the century, basal area had doubled on average, although some sites had changed little and others had tripled. Similarly,

ATTACHMENT D

Arno et al. (1995), using dendrochronological reconstructions of six old-growth ponderosa–Douglas-fir (*Pseudotsuga menziesii*) stands in Montana, found basal densities in 1900 ranging from 15 to 35 m²/ha. The variety of old-growth forest structures probably varied with environmental factors that influence tree establishment, growth, and mortality, including the interacting effects of fires. We also know that the return intervals for fires were longer for most of the ponderosa pine forests in eastern Montana (Morgan et al. 2002) and the Front Range of Colorado—and modestly longer for forests in western Montana (Arno 1980), eastern Oregon (Youngblood et al. 2004), and eastern Washington (Everett et al. 2000)—than for similar forests in Arizona and New Mexico. However, we don't know how this difference in fire regime led to differences in stand structure and function (for example, see Kaufmann et al. 2006)

PROCESSES

The most essential process in the development of old-growth conditions is time. Frequent-fire forests occur under relatively dry conditions, and the lack of abundant water limits the growth rates of trees. Forests with slow-growing trees take 100–200 years to begin to show the full spectrum of old-growth structure and processes.

However, time alone is not sufficient to encourage old growth in frequent-fire forests. Fundamental to the development of old-growth conditions is the interaction of forest processes with repeated fires. In the absence of repeated fire, tree density tends to remain high, and the fuel structure develops to the point where a very intense fire kills most of the trees. As a result, old-growth conditions are never reached.

Frequent surface fires allow larger trees to persist, limit the success of new trees, and foster the spatial pattern of open meadows mixed with tree clumps. Surface fires that recur every few years or decades kill most of the small trees that managed to establish during years with favorable precipitation and seed crops. The trees that survive the fires experience less competition for light and soil moisture, leading to higher rates of individual growth, thicker bark, and higher canopy base heights—all of which makes these trees more resistant to subsequent surface fires. The grasses, forbs, and shrubs that thrive between clumps of trees are typically burned

by surface fires, but these plants often resprout from surviving roots or reseed.

Without the recurring cultivation of the forest by fire, old-growth conditions may not develop. Fire suppression allows tree seedlings to recruit in large numbers, forming denser stands. Wildfire spreads more easily into the canopies of smaller trees with low branches, and from smaller trees into the crowns of previously fire-resistant old trees. With abundant small trees established among the more scattered old growth, fire may spread rapidly across large areas, with high mortality in all age and size classes.

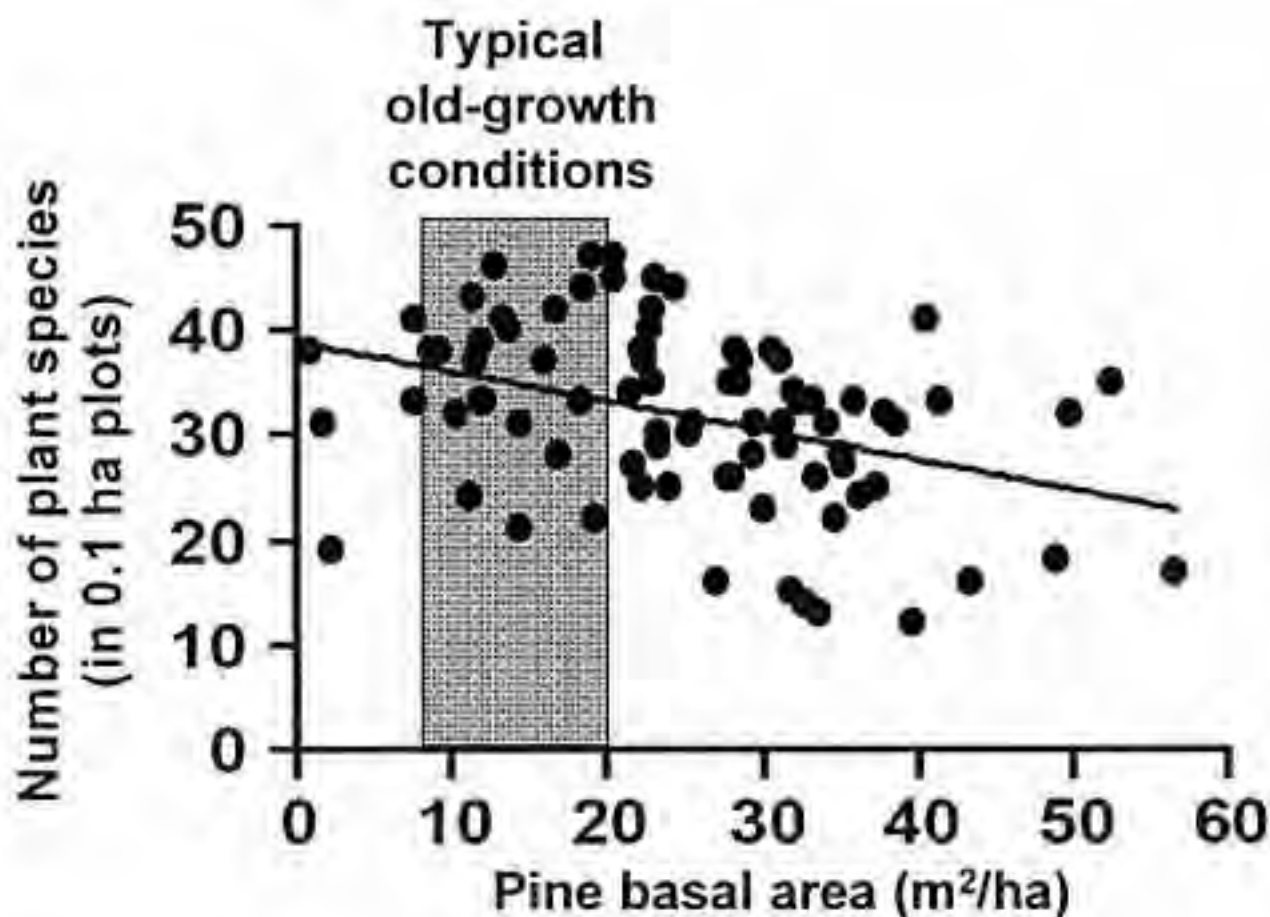
Productivity, Hydrology, and Nutrient Cycling

One of the most distinctive features of frequent-fire, old-growth forests is the major contribution that the understory vegetation (grasses, forbs, shrubs) makes to ecosystem diversity and productivity. In the absence of fire, the density of overstory trees increases, which reduces the diversity of understory vegetation 10–30% (Fig. 2, Laughlin and Grace 2006). This relationship between the density of trees and understory diversity is further influenced by the number of years between fires (the fire return interval). For example, a ponderosa pine forest on the Kaibab Plateau that burned in the past 10 years might have 35 species in the understory, compared with 28 species after 70 years without a fire, and 22 species after 120 years without a fire (Laughlin et al. 2005).

Restoration treatments reduce tree density and lower the total growth of trees in a forest, but increase the growth of residual (retained) trees and the biomass and productivity of the understory. In Montana, understory plant diversity declined the first year after a thinning and burning restoration treatment in a ponderosa pine–Douglas-fir forest, but increased significantly 2 years after treatment (Metlen and Fiedler 2006). Experiments around northern Arizona typically show understory biomass and growth increases of more than two-fold in response to thinning and prescribed burning (Fig. 3; Abella 2004, Gildar et al. 2004, Moore et al. 2004). Restoration treatments appear to have little effect on the total productivity of the forests, but they shift how the growth is allocated between the overstory and understory. A restoration experiment at Fort Valley near Flagstaff, Arizona showed that total production did not change, but the proportion accounted for by the understory rose from 10% to

ATTACHMENT D

Fig. 2. The richness of understory plant species declines with increasing density of overstory pine trees, on the Kaibab Plateau in northern Arizona (after Laughlin and Grace 2006). Typical historic conditions would have had about 35 species per 0.1-ha plot, but with changing land use and fire regimes, the most common species richness has declined to 25 to 30 species per 0.1-ha plot.

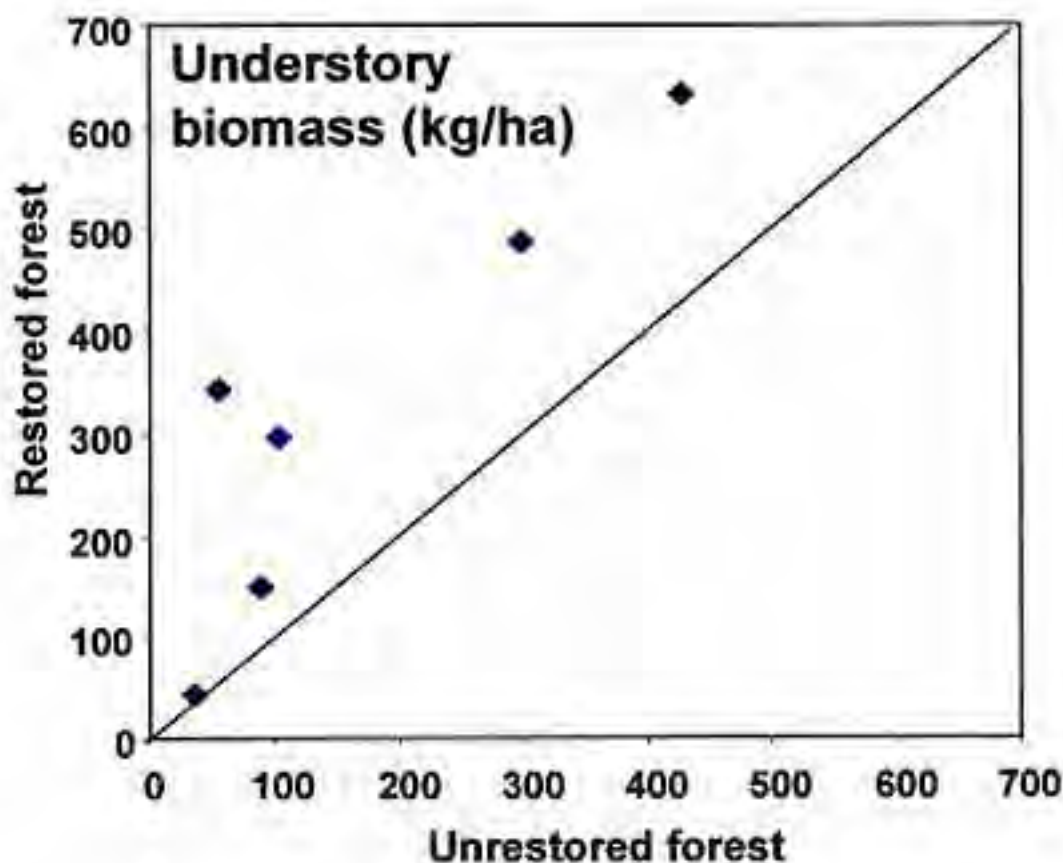


about 25%. The benefit of restoration treatments also differs among plant types. For example, the restoration responses at Fort Valley were greater for grasses than forbs (Moore et al. 2006), greater for leguminous forbs than other types, and greater for C_3 grasses (e.g., bottlebrush squirreltail (*Elymus elymoides* subsp. *elymoides*)) than C_4 grasses (e.g., mountain muhly (*Muhlenbergia montana*)). All of these trends might differ in response to major or minor differences in restoration prescriptions, site history, and current weather.

The higher productivity of understory plants in old-growth (and restored) forests in frequent-fire landscapes results in part from the low canopy leaf area of the overstory trees. Tree canopies cover less than half of the ground area (and commonly as little as 25%). Despite this patchy distribution of trees, the total amount of leaves in the tree canopy on 1 ha would still provide 2 or 3 ha of leaf surface area to intercept light. Forests in landscapes with higher supplies of water commonly have canopy surface areas of 4 to 6 ha displayed for each hectare of ground area.

ATTACHMENT D

Fig. 3. Understory biomass and growth were much higher in forests with restoration treatments than in control forests (from summary of Abella 2004, Gildar et al. 2004, Moore et al. 2006). The greatest proportional increases occur when the biomass in the unrestored forests is particularly low.



The amount of tree leaf area in a forest may have important effects on the supply of water in the soil that is available for both trees and understory vegetation. Precipitation falling on tree canopies may be intercepted, accumulating briefly on the needles before evaporating back to the atmosphere, never reaching the soil. Forests with high leaf area not only lose more precipitation from this interception loss, but they also have higher rates of water use by trees, with lower amounts of soil water available for use by understory plants. In wetter landscapes, changes in the amount of tree leaf area influence the amount of water reaching streams. For example, reducing tree cover in higher-elevation forests in the Rocky Mountains commonly increases

stream flow by 15 to 30% (MacDonald and Stednick 2003). The amount of water flowing in streams in frequent-fire landscapes depends less on the density and size of trees (and canopies) than in wetter areas, because drier conditions mean that water not used by trees will be used by understory plants. Restoring old-growth structure to forests in frequent-fire landscapes may lead to increased streamflow during wet periods and, perhaps, to some recharge of subsurface aquifers.

Forest restoration treatments generally improve the water status of large trees, reducing water stress, and increasing the volume of resin in stems (Wallin et al. 2004, Zausen et al. 2005). Improved water

ATTACHMENT D

status may enhance the overall vigor of trees, leading to lower rates of mortality from bark beetles and other insects and diseases.

Nutrient cycles in forests are influenced directly by fire, including losses (such as nitrogen converted to gas as biomass is consumed) and probably short-term increases in availability of some nutrients (including nitrogen). In the longer run, differences between old-growth and non-old-growth conditions may derive from the indirect effects of changes in vegetation composition than from the direct, cumulative effects of fires (Hart et al. 2005a).

EVOLUTION AND ADAPTATION

The biotic processes in forests develop from interactions between genes, organisms, and environmental factors. The genetics of a forest include those of trees, understory plants, wildlife, and the unimaginably diverse organisms in the soil. Although the interactions among genes, organisms, and environmental factors in a ponderosa pine forest are beyond the scope of this article (and indeed, beyond human comprehension!), we provide a few examples to illustrate the complexity and resilience of this system.

Bark Beetles

Bark beetles are an important, natural component of many conifer ecosystems. Bark beetles (and their fungal symbionts) routinely kill small numbers of pine trees and, occasionally, extremely high beetle populations lead to massive pine mortality across very large areas. A number of factors—drought, lightning strikes, root pathogens, large fire scars, severe defoliation, tree senescence, excessive competition—make an individual old tree or stand more susceptible to bark beetle outbreaks. Recent thinning may also contribute to increased wind turbulence in a stand, leading to root damage and, perhaps, making individual trees susceptible to attack (Christiansen et al. 1987).

Coniferous trees have developed two main mechanisms to counter beetle attacks. First, they have a system of resin ducts in the phloem and xylem that can pitch-out invading beetles. Second, they have developed a hypersensitive reaction to invasion by microorganisms (including fungi, bacteria, and viruses) that enter the tree along with

the beetles. A necrotic area, impregnated with resinous and phenolic compounds that prevent beetle gallery construction and fungal proliferation, then forms around the point of infection. This wound resin is highly toxic to beetle eggs and larvae and also inhibits fungal growth (Christiansen et al. 1987).

The ability of a large, old tree to resist an attack depends on its genetic makeup and physiological status (Franceschi et al. 2005). Independent of age, ponderosa pine trees grow slowly when stressed by competition. However, because most old trees are large in size and stature, they may have higher maintenance respiration demands because of the amount of living, non-photosynthetic tissue they maintain compared with younger trees (Skov et al. 2004). Another factor that may limit photosynthetic rate is that these large trees also tend to have more branch junctions and a longer root-leaf hydraulic path length that may decrease hydraulic conductance (Skov et al. 2004). Together, these factors may all contribute to slow growth of old ponderosa pine trees.

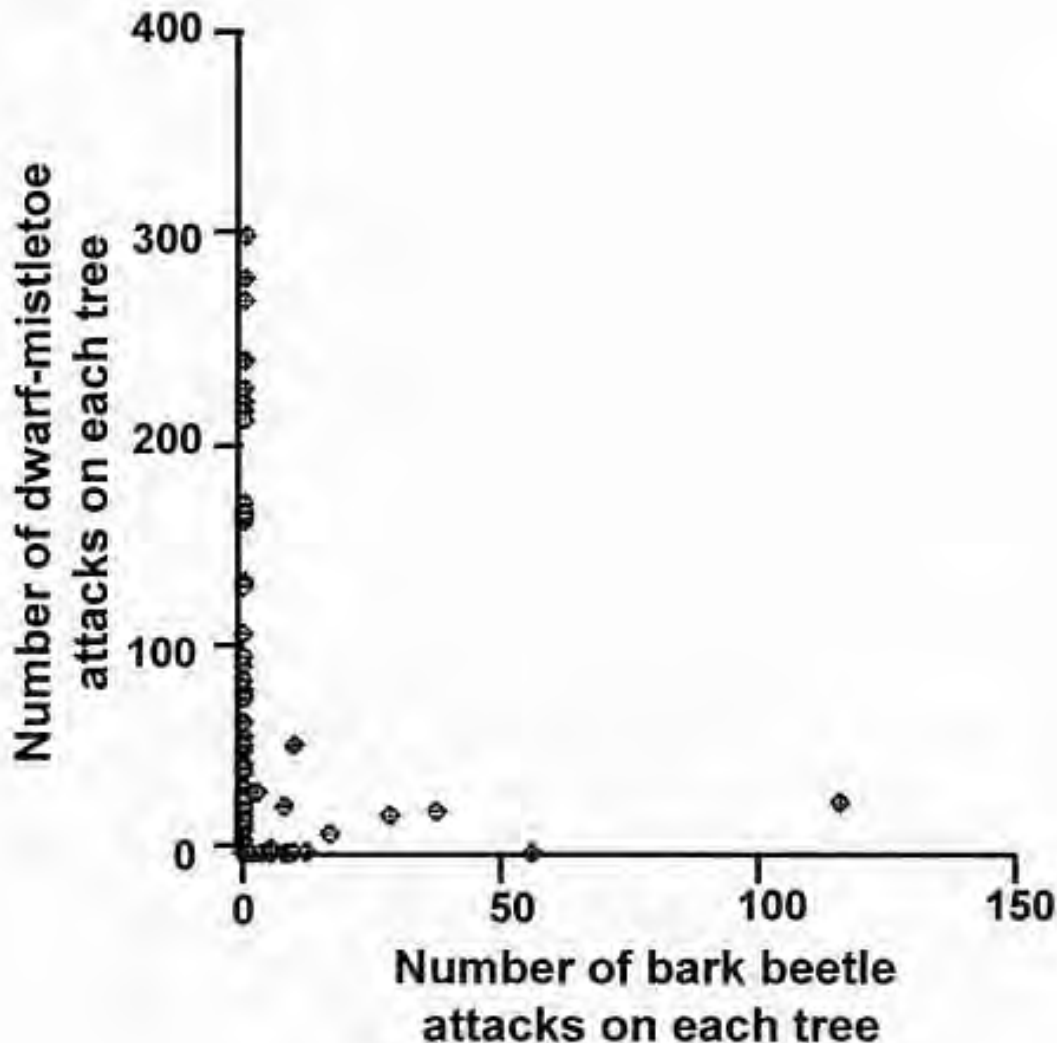
Bark beetles are only one of many potential threats to ponderosa pine trees, and the susceptibility to each threat differs among trees. For example, ponderosa pine trees may be attacked by bark beetles and infected by dwarf mistletoe (*Arceuthobium* spp.), but the success of each of these varies among individual ponderosa pines (Fig. 4). Trees that appear susceptible to beetles appear to be resistant to dwarf mistletoe, and vice versa. The continued survival, growth, and seed production of individual pine trees may depend in part on the local prevalence of parasites, which depends in turn on the local genotypes of pines and local environmental conditions.

Abert's Squirrels

Abert's squirrels (*Sciurus aberti*) are also highly dependent on ponderosa pine trees. Ponderosa pines provide them with places to live, nest, rest, and hide from predators as well as food in the form of bark, buds, flowers, and seeds (Hoffmeister 1986). Squirrels choose individual trees based on the (heritable) chemistry of tree phloem. As a result, different populations of Abert's squirrels are adapted to different populations of ponderosa pine (Snyder 1992, 1993; Snyder and Linhart 1994).

ATTACHMENT D

Fig. 4. Some ponderosa pine trees were heavily attacked by bark beetles, some heavily infected by dwarf mistletoe parasites, and some were unaffected—but no trees were heavily attacked by both bark beetles and dwarf mistletoe (after Linhart et al. 1994).



Yet another ecological interaction connects ponderosa pines and Abert's squirrels. Squirrels eat mycorrhizal fungi and help disperse it through their fecal pellets. Mycorrhizal fungi are very important to plant productivity, so if the fungi were rare, then squirrels could, perhaps, enhance forest productivity (Vireday 1982, Kotter and Farentinos 1984a, b).

Mooney and Linhart (2006) have recently developed an even more interwoven story about pines, growth, birds, ants, spiders, aphids, wasps, and dwarf mistletoe.

ATTACHMENT D

Genetics and Old Trees

The genotypes of pine trees are influenced by both selective pressures (Abert's squirrels, beetles, and dwarf mistletoes), and by the flow of genes in the neighborhood. The genes of paternal trees flood the local landscape as pollen drifts on the wind, but maternal genes disperse only as far as seeds can fall from a tree or be carried by animals (Latta et al. 1998). Old trees may be particularly important in a forest, as they have (by definition) survived centuries of changing environmental and biotic challenges. The presence of these trees in a landscape is critical for contributing both seeds and pollen to later generations of trees.

Resilience and Fire at the Landscape Scale

Just as individual trees have mechanisms that make them resistant to bark beetles and fire, a healthy, functioning forest will exhibit resilience on a large scale. Persistence, resilience, and resistance are all terms applied to the stability of an ecosystem (Holling 1973, Gunderson et al. 1995, Gunderson and Holling 2002). Ecosystem fragility is the opposite of stability and is expediently defined as "...the degree of change in species abundances and in species composition, following disturbance" (Nilsson and Grelsson 1995). Frequent-fire forests are highly stable in the long term, as long as fire is maintained in the system. However, they may be considered fragile in the short term following a fire. Moreover, many of these forests are now considered fragile in the long term, particularly following the catastrophic fires that result from long periods of fire suppression.

OLD-GROWTH FOREST COMPOSITION

Although processes are the driving forces behind any ecosystem, those processes are reflected and supported by the composition of the ecosystem, that is by the living and non-living entities that exist in the ecosystem. Old-growth forests, by definition, have old trees, but the presence of old trees is just the beginning of a description of the composition of an old-growth forest. The frequent return of fires provides the opportunity for a great range of plants, animals, and microbes to coexist in the same landscape.

Plant Composition and Structure

In frequent-fire landscapes, the diversity of plant species in the forest understory is much greater than the diversity of overstory species. Moreover, frequent fires strongly influence the composition of understory plant communities. The most striking feature of old-growth patches of ponderosa pine may be the towering "yellow-bellies"—the large-diameter giants with the yellowish, fire-resistant bark. However, these forests are characterized as much by the understory that develops in the diverse range of habitat conditions: near clumps of big trees, in small openings between clumps, and in the open meadows between groups of large trees. Native perennial graminoids, including several species of fescue (*Festuca* spp.) and sedges (*Carex* spp.), dropseed (*Blepharoneuron tricholepis*), *Sporobolus* spp.), Indian ricegrass (*Oryzopsis* spp.), and galleta (*Pleuraphis* spp.), as well as grazing-tolerant squirreltail and western wheatgrass (*Pascopyrum smithii*) and the ubiquitous grama grasses (*Bouteloua* spp.), form diverse understory communities that account for a large portion (more than half) of the net annual primary production in many old-growth ponderosa pine stands (Moore et al. 2004).

In addition to the native grasses, many annual and perennial forbs occur, usually as subdominants or rare components of the understory plant community. Native penstemon (*Penstemon* spp.), evening primrose (*Oenothera* spp.), and low-growing sages (*Artemisia* spp.) are complemented by diverse composites that flower throughout the growing season. Fire-resilient or -adapted shrubs, such as kinnikinnick (*Arctostaphylos uva-ursi*) and serviceberry (*Amelanchier* spp.) in the Inland Northwest, and cliffrose (*Purshia* spp.) and ceanothus in the Southwest, are characteristic of open-growing, old-growth pine forests. In many Southwest locations, Gambel oak (*Quercus gambelii*), which can be found from a low-growing shrub to subdominant tree, is the second most abundant woody plant.

This heterogeneity in species composition and structural types is characteristic of most types of old-growth forests that develop in frequent-fire landscapes. Large overstory trees typically occur in scattered clumps of several to several dozen individuals sometimes in a dense matrix of younger trees, and other times intermixed with grassland openings of several acres. In terms of species

ATTACHMENT D

composition, structural diversity, and ecological function, such old-growth forests contrast sharply with the dense stands that commonly develop when fires are suppressed. For example, Gambel oak and ceanothus are common shrubs in most Southwest ponderosa pine forests, but they typically are more common, and individual plants are larger and more developed, in open forests dominated by large pines. This diversity in the woody plant community has far-reaching implications, in part because these species support insect communities that are more diverse and abundant than those found in pure stands of ponderosa pine. Insect abundance, in turn, influences bird and bat populations, pollination rates, and the amount of wildlife forage. In this way, the composition and structural attributes of the ponderosa pine trees set the template for a potentially diverse plant community whose composition and function vary widely.

Animal Communities

Wildlife species respond in a host of ways to the structure of forests, and to boundaries between forests with different structures. Old-growth forests provide habitat for many wildlife species, but the critical habitat characteristics vary tremendously among species in both time and space. Some species are year-round residents, and others use old-growth forests only for breeding, wintering, or migration. Similarly, some species (e.g., pygmy nuthatch (*Sitta pygmaea*)) rely on specific old-growth structural components, such as large trees, whereas others (e.g., Abert's squirrel) need the structure of a whole patch of old-growth trees to facilitate their movements and provide food. Some species (e.g., northern goshawk (*Accipiter gentilis*)) require old-growth forest conditions within an entire landscape matrix that contains non-old-growth forests to meet all their ecological needs.

Starting at the small end of the scale, standing dead trees (snags) and partially dead trees (living snags) are an important part of a living forest ecosystem (Waskiewicz 2003, Chambers and Mast 2005). Dozens of species of birds and bats rely on living and dead trees for habitat, and many of these species in turn may influence the success (or failure) of other organisms (e.g., defoliating caterpillars). Resource managers are commonly required to provide a minimum number of snags, but more recent insights have indicated snags alone may not be the key to providing habitat for species such as bats,

nuthatches, and bluebirds because the longevity and number of dead snags is limited in frequent-fire forest. For instance, Saab et al. (2006) tested prescribed fire on more than 130 plots in the southwestern United States, and found an average loss of 35% of the downed wood and half of the standing snags (Saab et al. 2006). Boucher et al. (2000) pointed out that snags may not last long in frequent-fire forests because surface fires either ignite snags or topple them by burning the roots. The best long-term habitat may be provided by living snags, which are live trees with large dead limbs or tops. These living snags often develop after lightning strikes, beetle infestations, pathogen attack, or a combination of these factors.

Moving up to the scale of patches or stands, forest structure influences survival and population persistence of a variety of wildlife species. Very uniform spacing of trees, which is the typical result of traditional silvicultural thinning treatments, degrades habitats for Abert's squirrels (Dodd et al. 2003). Information on characteristics and sizes of patches needed by the squirrel and the spatial arrangement of these patches are necessary parts of silvicultural prescriptions that ensure viable populations of these squirrels. Similar silvicultural and management decisions are required for other old-growth-dependent species, including spotted owls (*Strix occidentalis*).

At the scale of entire landscapes, old-growth forests will likely be part of a landscape mosaic that includes forests that lack old-growth characteristics. These non-old-growth habitats (ranging from meadows to dense young stands to maturing second-growth stands) might support some aspect of an animal species' needs. For example, northern goshawks are habitat generalists and their populations are often limited by the availability of food, which causes them to move between different habitat types. Reynolds et al. (1992) developed a landscape model of goshawk habitat that identifies a landscape-scale mosaic of six vegetation structural stages, which provide habitat for a suite of northern goshawk prey species. These vegetation structural stages range from grass-forb regeneration conditions to old-growth forest. Although northern goshawks need old-growth forests, particularly for nesting, they also benefit from a diverse mosaic across the landscape.

There are also symbiotic, co-evolutionary relationships that animals have throughout old-

ATTACHMENT D

growth forests. As noted in the discussion above about Abert's squirrels, there is almost no limit to the nature of interactions in forests, and we are far from having a clear understanding of which interactions have major, cascading effects. Some wildlife species are considered keystone species in that other species depend on them to provide necessary conditions. For example, populations of hairy woodpeckers (*Picoides villosus*) increase after fire, just as populations of beetles increase (Covert-Bratland et al. 2006). In ponderosa pine forests in the Southwest, half of the species that nest in tree cavities cannot excavate cavities (secondary cavity-nesting species), so hairy woodpeckers may be critical in supporting a diversity of animals. The feedback cycle turns yet again because, without fires, the population of hairy woodpeckers may be low, reducing the habitat opportunities for other species, further changing the complex forest ecosystem.

Management activities that move a forest away from old-growth conditions change the opportunities for many species. For example, Szaro and Balda (1979) compared four treatments with an uncut control plot that had some characteristics of old-growth forests. Pygmy nuthatches, red-faced warblers (*Cardellina rubrifrons*), hermit thrushes (*Catharus guttatus*), cordilleran flycatchers (*Empidonax occidentalis*), and violet-green swallows (*Tachycineta thalassina*) lost habitat with treatments that moved the forests away from old-growth forest conditions.

Grazing alters herbaceous plant composition and structure, affecting habitat for species such as Mogollon voles (*Microtus mogollonensis*) (Chambers and Doucett 2008). Using a stable-isotope approach, these scientists found that herbivorous voles rely on grass and herbs for food, and that C₃ plants (e.g., yarrow (*Achillea millefolium*), lupine (*Lupinus* spp.), fescue, mulleins (*Verbascum* spp.), snakeweed (*Gutierrezia* spp.)) were a more important food source than C₄ plants (e.g., species of muhly (*Muhlenbergia* spp.) and grama grasses). Excessive ungulate grazing and introduction of invasive plant species that lead to changes in plant species composition or reductions in C₃ plants in montane grasslands and forests would reduce habitat quality for Mogollon voles. Mogollon voles are also important food for the threatened Mexican spotted owl (*Strix occidentalis lucida*) (Ward 2001). Recent research indicates that vole populations are reduced in pine-oak forests as the result of past logging and grazing practices (Block et al. 2005).

As noted throughout this special issue, the loss of old-growth structure in frequent-fire landscapes commonly leads to uncharacteristically severe wildfires, which, in turn, benefit some animal species and harm others. Bock and Block (2005), for instance, compared the bird communities in unburned and moderately and severely burned forests. Three years after the fires, the unburned forest had 31 species in the breeding season and 26 in the non-breeding season. Both levels of burn intensity increased the diversity of birds, with more than 40 species of breeding birds and 33 species of non-breeders. Species groups that increased in response to fire included woodpeckers, flycatchers, and thrushes.

Restoration treatments that move forests toward old-growth structure and composition appear to be effective in restoring bird habitat. Germaine and Germaine (2002) found that the fledgling rate (i.e., number of young to leave the nest) for western bluebirds (*Sialia mexicana*) in restored stands was 1.6 times greater than in dense, untreated stands. Converse et al. (2006a, b) evaluated effects of fuel-reduction treatments on small mammals and found that total biomass and population sizes of small mammals generally increased following thinning and fire. The most thorough assessments of post-restoration animal responses come from landscape-scale treatments near Mt. Trumbull in the Grand Canyon-Parashant National Monument in northern Arizona (Covington et al. 2005). Various aspects of wildlife habitat and populations were examined for up to 9 years, and demonstrated that restoring old-growth forest structure generally favored species or had much lower negative effects than stand-replacing fire. Mule deer (*Odocoileus hemionus*) tended to use restored portions of the landscape at night, although they used restored and control areas about equally during the day. Abert's squirrel populations declined in response to the lower density of pine trees, but the squirrels did continue living in trees in the restored areas. Breeding pairs of northern goshawks were found in control and restored areas, and fledglings were successful in both forest types. The densities of butterflies doubled in restored areas.

Microbial Communities

Given that microbial interactions and processes are the foundation of much of the forest ecosystem, surprisingly little is known about the differences in

ATTACHMENT D

microbial communities between old-growth forests and post-fire-cessation forests. The two microbial communities that we know the most about are wood-decaying fungi and mycorrhizal fungi.

A number of wood-decaying fungi infect primarily old trees, roots, and large branches. Several species of wood-decaying fungi found in unmanaged older forests are rare in younger stands (Romme et al. 1992). Aging trees tend to become increasingly vulnerable to wood-decaying fungi because fungi can enter through dead branch stubs, knots, broken tops, fire scars, and wounds such as those caused by bark beetles or woodpeckers (Farris et al. 2004). In addition to the vital role these pathogens play in the carbon cycle and in recycling nutrients for plants, they also create valuable habitat for numerous wildlife species (Marcot 2002).

Mycorrhizal fungi form symbiotic associations with tree roots, providing water and nutrients to roots in exchange for sugar. Experiments by various researchers have shown that fire may substantially affect these fungal associations, particularly near the soil surface. For example, a study by Pattinson et al. (1999) that simulated the effect of fire showed a decline in numbers of mycorrhizal propagules and a reduction in the hyphal network (the tiny, networked strands of fungus). Korb et al. (2003) found a rapid increase in arbuscular mycorrhizae following restoration treatments in northern Arizona, whereas Smith et al. (2005) reported a short-term reduction in ectomycorrhizal fungi (EMF) following prescribed fire in Oregon.

Researchers have also studied the effects of seasonal burning on the mycorrhizal community. Smith et al. (2004) detected that fall burning in dry ponderosa pine stands significantly reduced duff depth, live root biomass, and EMF species richness compared with spring burning. The probability of mature tree mortality was also greater after fall burning. Meyer et al. (2005) found that burning reduced litter depth and log volume as well as the frequency, biomass, and species richness of mycorrhizal truffles in an area of the Sierra Nevada. The authors posit that decaying woody debris forms an important reservoir of moisture and nutrients, especially in dry forests, for fruiting fungi. It also appears that mycorrhizal fungi are more likely to survive when the duff layer is thin or moist.

Hart et al. (2005a) report that repeated burning (every 2 years during a 20-year period) reduced fine

root length, fine root biomass, and mycorrhizal root biomass, as well as the amount of nitrogen and phosphorus stored in the belowground pools. The authors speculate that the change in these pools most likely occurred during the first few prescribed burns when the fuel loads and fire intensities would have been highest. Their results suggest that such frequent burning may have negative long-term effects on belowground biomass pools and nutrient cycling. They also postulate that these negative effects may be avoided by mechanically removing some of the accumulated fuel before prescribed burning.

Despite these descriptive studies and experiments, we essentially know very little about the critical changes that may (or may not) follow the loss of old-growth characteristics in a forest. A recent study (Hart et al. 2005b) found that a fire following a long, fire-free period reduced the diversity of the bacterial community by more than half, yet more than doubled the diversity of the fungal community. We do not know if these dramatic changes have important cascading effects in the forest.

HUMAN VALUES

Although this is covered in more depth by other authors in this special issue, we also want to say that old-growth forests in frequent-fire landscapes provide a host of human values that go beyond the list of species present, or economic and ecological functions. For instance, old-growth forests carry a legacy of information from earlier times. They can tell us a great deal about how climates have varied in past epochs, and how the forests (and fires) responded. Without the information held in tree rings, we would not know how the landscapes of the southwestern United States were influenced by patterns of El Niño/Southern Oscillation precipitation (Grissino-Mayer and Swetnam 2000) or to what degree the rise and fall of dryland civilizations related (or not) to climate (Dean 1988). We also recognize that many people see an inherent beauty in old-growth forests (Huckaby et al. 2003), and find personal sustenance from these “wilderness” or wild landscapes.

ATTACHMENT D

KNOWLEDGE GAPS

All forests are complicated ecosystems, making the potential list of gaps in our knowledge almost unbounded. Nevertheless, we can identify several key areas where studies and experiments are needed to fill major gaps that hinder restoration efforts of old growth in the frequent-fire forests of the American West.

Ability of Understory Vegetation to Respond to Restoration Treatments

How well can we recover the historical understory (and related animal habitat features) that characterized old-growth conditions? The absence of fire for a century has been coupled in many forests with a host of other land-use impacts, including intensive livestock grazing and logging. Long-term plots from northern Arizona have shown not only declines in total understory production and species diversity, but also shifts among vegetation types (such as greater losses of C_4 grasses than C_3 grasses). How well can the understory recover its former productivity and species composition in response to thinning or thinning plus fire? Does the season and/or frequency of burning have an effect on the understory? Will adding native seed from nearby areas be critical? How did use by Native Americans affect the understory of pre-European-settlement, old-growth forest understories? More experiments across a variety of landscape conditions are needed to answer these and other questions related to understory vegetation.

Ability of Frequent-fire Forests to Recover Following Catastrophic Wildfires

How does ecosystem recovery progress after severe wildfires that exceed the historical range of fire behavior in frequent-fire landscapes? We expect that recovery will be slow, but will recovery eventually occur or will the forests be converted to other vegetation types (grasslands or shrublands)? What restoration treatments would be most effective for recovering natural forest composition, structure, and function after large, severe fires? Which treatments can move forests toward old-growth conditions and also reduce risks of severe fires?

Ability to Extrapolate Knowledge of Certain Forests to Other Places and Forest Types

Much of our knowledge about old-growth conditions in frequent-fire landscapes comes from a very limited range of forest types, and detailed information comes from an even more restricted set of intensive study sites. How representative are the ponderosa pine landscapes of northern Arizona for ponderosa pine in other areas? How different are dry mixed-conifer forests from ponderosa pine forests, and how do they vary with landscape position locally and throughout the West? We have a good general understanding of the key questions and the important processes, but restoration of old-growth conditions in any local forest will depend on locally appropriate details.

The Uncertainty of Climate Change and its Effects on Forested Ecosystems

Climates have changed dramatically in the past 10 000 years, and the 21st century will likely differ from the 19th century. What do we need to know to foster old-growth forest conditions under various climate scenarios? If managers can only afford to restore a portion of a landscape (which is almost always the case), should restoration focus on lower-elevation sites (with the risk that climate changes would shift the ecotone upward)? This knowledge gap will probably not be filled by data collection or experimentation, but the potential effects of climate change need to be kept in mind.

Responses to this article can be read online at:
<http://www.ecologyandsociety.org/vol12/iss2/art18/responses/>

LITERATURE CITED

- Abella, S. R. 2004. Tree thinning and prescribed burning effects on ground flora in Arizona ponderosa pine forests: a review. *Journal of the Arizona-Nevada Academy of Science* 36:68–76.
- Allen, C. D., M. Savage, D. A. Falk, K. F. Suckling, T. W. Swetnam, T. Schulke, P. B. Stacey, P. Morgan, M. Hoffman, and J. T. Klingel. 2002. Ecological restoration of southwestern ponderosa pine ecosystems: a broad perspective. *Ecological Applications* 12:1418–1433.

ATTACHMENT D

- Arno, S. F.** 1980. Forest fire history in the northern Rockies. *Journal of Forestry* **78**:460–465.
- Arno, S. F., and C. E. Fiedler.** 2005. *Mimicking nature's fire: restoring fire-prone forests in the West*. Island Press, Washington, D.C., USA.
- Arno, S. F., J. Scott, and M. Hartwell.** 1995. *Age-class structure of old growth ponderosa pine/Douglas-fir stands and its relationship to fire history*. U.S. Forest Service Research Paper **481**.
- Bailey, J. D., and W. W. Covington.** 2002. Evaluating ponderosa pine regeneration rates following ecological restoration treatments in northern Arizona, USA. *Forest Ecology and Management* **155**:271–278.
- Block, W. M., J. L. Ganey, P. E. Scott, and R. King.** 2005. Prey ecology of Mexican spotted owls in pine-oak forests of northern Arizona. *Journal of Wildlife Management* **69**:618–629.
- Bock, C. E., and W. M. Block.** 2005. Response of birds to fire in the American southwest. Pages 1093–1099 in C. J. Ralph and T. D. Rich, editors. *Bird conservation implementation and integration in the Americas: Proceedings of the third international Partners in Flight conference. Volume 2*. U.S. Forest Service General Technical Report PSW-GTR-191.
- Boucher, P. F., W. M. Block, G. V. Benavidez, and L. W. Wiebe.** 2000. Implementing the expanded prescribed fire program on the Gila National Forest, New Mexico: implications for snag management. *Proceedings of the Tall Timbers Fire Ecology Conference* **21**:104–113.
- Chambers, C. L., and R. R. Doucett.** 2008. Diet of the Mogollon vole as indicated by stable isotope analysis (13 C and 15 N). *Western North American Naturalist* (In press).
- Chambers, C. L., and J. N. Mast.** 2005. Ponderosa pine snag dynamics and cavity excavation following wildfire in northern Arizona. *Forest Ecology and Management* **216**:227–240.
- Christiansen, E., R. H. Waring, and A. A. Berryman.** 1987. Resistance of conifers to bark beetle attack: searching for general relationships. *Forest Ecology and Management* **22**:89–106.
- Converse, S. J., W. M. Block, and D. C. White.** 2006a. Small mammal population and habitat responses to forest thinning and prescribed fire. *Forest Ecology and Management* **228**:263–273.
- Converse, S. J., G. C. White, and W. M. Block.** 2006b. Small mammal response to thinning and wildfire in ponderosa pine-dominated forests of the southwestern USA. *Journal of Wildlife Management* **70**(6):1711–1722.
- Covert-Bratland, K. A., W. M. Block, and T. Theimer.** 2006. Hairy woodpecker winter ecology in ponderosa pine forests representing different ages since wildfire. *Journal of Wildlife Management* **70** (5):1379–1392.
- Covington, W. W., D. Vosick, and K. A. Lowe.** 2005. *Southwest fire initiative final report*. Submitted to the Bureau of Land Management by the Ecological Restoration Institute, Flagstaff, Arizona, USA.
- Dean, J. S.** 1988. Dendrochronology and paleoenvironmental reconstruction on the Colorado Plateaus. Pages 119–167 in G. J. Gumerman, editor. *The Anasazi in a changing environment*. School of American Research Book, Cambridge University Press, New York, New York, USA.
- Dodd, N. L., J. S. States, and S. S. Rosenstock.** 2003. Tassel-eared squirrel population, habitat condition, and dietary relationships in north-central Arizona. *Journal of Wildlife Management* **67**:622–633.
- Egan, D. and E. A. Howell, editors.** 2001. *The historical ecology handbook: a restorationist's guide to reference ecosystems*. Island Press, Washington, D.C., USA.
- Everett, R. L., R. Schellhaas, D. Keenum, D. Spurbeck, and P. Ohlson.** 2000. Fire history in the ponderosa pine/Douglas-fir forests on the east slope of the Washington Cascades. *Fire Ecology and Management* **129**:207–225.
- Farris, K. L., M. J. Huss, and S. Zack.** 2004. The role of foraging woodpeckers in the decomposition of ponderosa pine snags. *The Condor* **106**:50–59.
- Franceschi, V. R., P. Krokene, E. Christiansen, and T. Krekling.** 2005. Anatomical and chemical defenses of conifer bark against bark beetles and other pests. *The New Phytologist* **167**:353–376.

ATTACHMENT D

- Friederici, P.**, editor. 2003. *Ecological restoration of southwestern ponderosa pine forests*. Island Press, Washington, D.C., USA.
- Fulé, P. Z., W. W. Covington, H. B. Smith, J. D. Springer, T. A. Heinlein, K. D. Huisinga, and M. M. Moore.** 2002. Comparing ecological restoration alternatives at Grand Canyon, Arizona. *Forest Ecology and Management* **170**:19–41.
- Fulé, P. Z., W. W. Covington, M. T. Stoddard, and D. Bertolette.** 2006. Minimal impact restoration treatments have limited effects on forest structure and fuels at Grand Canyon, USA. *Restoration Ecology* **14**(3):357–368.
- Fulé, P. Z., J. Villanueva-Díaz, and M. Ramos-Gómez.** 2005. Fire regime in a conservation reserve in Chihuahua, Mexico. *Canadian Journal of Forest Research* **35**:320–330.
- Germaine, H. L., and S. S. Germaine.** 2002. Forest restoration treatment effects on the nesting success of western bluebirds. *Restoration Ecology* **10**:362–367.
- Gildar, C. N., P. Z. Fulé, and W. W. Covington.** 2004. Plant community variability in ponderosa pine forest has implications for reference conditions. *Natural Areas Journal* **24**(2):101–111.
- Grissino-Mayer, H. D., and T. W. Swetnam.** 2000. Century-scale climate forcing of fire regimes in the American Southwest. *Holocene* **10**:213–220.
- Gunderson, L., and C. S. Holling, editors.** 2002. *Panarchy: understanding transformations in human and natural systems*. Island Press, Washington, D. C, USA.
- Gunderson, L., C. S. Holling, and S. Light, editors.** 1995. *Barriers and bridges to the renewal of ecosystems and institutions*. Columbia University Press, New York, New York, USA.
- Hart, S. C., A. T. Classen, and R. J. Wright.** 2005a. Long-term interval burning alters fine root and mycorrhizal dynamics in a ponderosa pine forest. *Journal of Applied Ecology* **42**:752–761.
- Hart, S. C., T. H. DeLuca, G. S. Newman, M. D. MacKenzie, and S. I. Boyle.** 2005b. Post-fire vegetative dynamics as drivers of microbial community structure and function in forest soils. *Forest Ecology and Management* **220**:166–184.
- Hoffmeister, D. F.** 1986. *Mammals of Arizona*. University of Arizona Press and Arizona Game and Fish Department, Tucson and Phoenix, Arizona, USA.
- Holling, C. S.** 1973. Resilience and stability of ecological systems. *Annual Review of Ecology and Systematics* **4**:1–23.
- Huckaby, L. S., M. R. Kaufmann, P. J. Fornwalt, J. M. Stoker, and C. Dennis.** 2003. Identification and ecology of old ponderosa pine trees in the Colorado Front Range. U.S. Forest Service General Technical Report **RMRS-GTR-110**.
- Kaufmann, M. R., T. T. Veblen, and W. H. Romme.** 2006. *Historical fire regimes in ponderosa pine forests of the Colorado Front Range, and recommendations for ecological restoration and fuels management*. Colorado Forest Restoration Institute, Colorado State University, and The Nature Conservancy, Fort Collins, Colorado, USA.
- Keeley, J. E., and N. L. Stephenson.** 2000. Restoring natural fire regimes to the Sierra Nevada in an era of global change. Pages 255–265 in D. N. Cole, S. F. McCool, W. T. Borrie, and J. O'Loughlin, compilers. *Wilderness science in a time of change conference—Volume 5: Wilderness ecosystems, threats, and management*. U.S. Forest Service Proceedings **RMRS-P-15-VOL-5**.
- Korb, J. E., N. C. Johnson, and W. W. Covington.** 2003. Arbuscular mycorrhizal propagule densities respond rapidly to ponderosa pine restoration treatments. *Journal of Applied Ecology* **40**:101–110.
- Kotter, M. M., and R. C. Farentinos.** 1984a. Formation of ponderosa pine ectomycorrhizae after inoculation with feces of tassel-eared squirrels. *Mycologia* **76**:758–760.
- — —. 1984b. Tassel-eared squirrels as spore dispersal agents of hypogeous mycorrhizal fungi. *Journal of Mammalogy* **65**:684–667.
- Landres, P. B., P. M. Morgan, and F. J. Swanson.** 1999. Overview of the use of natural variability concepts in managing ecological systems. *Ecological Applications* **9**(4):1179–1188.

ATTACHMENT D

- Latta, R. G., Y. B. Linhart, D. Fleck, and M. Elliot.** 1998. Direct and indirect estimates of seed versus pollen movement within a population of ponderosa pine. *Evolution* **52**:61–67.
- Laughlin, D. C., J. D. Bakker, and P. Z. Fulé.** 2005. Understory plant community structure in lower montane and subalpine forests, Grand Canyon National Park, USA. *Journal of Biogeography* **32**:2083–2102.
- Laughlin, D. C., and J. B. Grace.** 2006. A multivariate model of plant species richness in forested systems: old-growth montane forests with a long history of fire. *Oikos* **114**:60–70.
- Leopold, A.** 1920. Piute forestry vs. forest fire prevention. *Southwestern Magazine* **2**:12–13. (Reprinted as: Paiute forestry. 1990. Pages 139–142 in D.E. Brown and N.B. Carmony, editors. *Aldo Leopold's southwest*. University of New Mexico Press, Albuquerque, New Mexico, USA.
- Long, J. N., and F. W. Smith.** 2000. Restructuring the forest: goshawks and the restoration of southwestern ponderosa pine. *Journal of Forestry* **98**:25–30.
- MacDonald, L. H., and J. D. Stednick.** 2003. *Forests and water: a state-of-the-art review for Colorado*. Colorado Water Resources Research Institute Report No. 196.
- Marcot, B. G.** 2002. An ecological functional basis for managing decaying wood for wildlife. Pages 895–910 in W. F. Laudenslayer, Jr., P. J. Shea, B. E. Valentine, C. P. Weatherspoon, and T. E. Lisle, editors. *Proceedings of the symposium on the ecology and management of dead wood in western forests*. U.S. Forest Service General Technical Report PSW-GTR-181.
- Metlen, K. L., and C. E. Fiedler.** 2006. Restoration treatment effects on understory of ponderosa pine/Douglas-fir forests in western Montana. *Forest Ecology and Management* **222**:355–369.
- Meyer, M. D., M. P. North, and D. A. Kelt.** 2005. Short-term effects of fire and forest thinning on truffle abundance and consumption by *Neotamias speciosus* in the Sierra Nevada of California. *Canadian Journal of Forest Research* **35**:1061–1070.
- Mooney, K. A., and Y. B. Linhart.** 2006. Contrasting cascades: insectivorous birds increase pine but not parasitic mistletoe growth. *Journal of Animal Ecology* **75**:350–357.
- Moore, M. M., C. A. Casey, J. D. Bakker, J. D. Springer, P. Z. Fulé, W. W. Covington, and D. C. Laughlin.** 2006. Herbaceous vegetation responses (1992–2004) to restoration treatments in a ponderosa pine forest. *Rangeland Ecology and Management* **59**:135–144.
- Moore, M. M., W. W. Covington, and P. Z. Fulé.** 1999. Reference conditions and ecological restoration: a southwestern ponderosa pine perspective. *Ecological Applications* **9**(4):1266–1277.
- Moore, M. M., D. W. Huffman, P. Z. Fulé, W. W. Covington, and J. E. Crouse.** 2004. Comparison of historical and contemporary forest structure and composition of permanent plots in southwestern ponderosa pine forests. *Forest Science* **50**:162–176.
- Morgan, T. A., C. E. Fiedler, and C. W. Woodall.** 2002. Characteristics of dry site old-growth ponderosa pine in the Bull Mountains of Montana, USA. *Natural Areas Journal* **22**(1):11–19.
- Nilsson, C., and G. Grelsson.** 1995. The fragility of ecosystems: a review. *Journal of Applied Ecology* **32**: 677–692.
- Pattinson, G. S., K. A. Hammill, B. G. Sutton, and P. A. McGee.** 1999. Simulated fire reduces the density of arbuscular mycorrhizal fungi at the soil surface. *Mycological Research* **103**(4):491–496.
- Reynolds, R. T., T. G. Russel, M. H. Reiser, R. L. Bassett, P. L. Kennedy, D. A. Boyce, Jr., G. Goodwin, R. Smith, and E. L. Fisher.** 1992. *Management recommendations for the northern goshawk in the southwestern United States*. U.S. Forest Service General Technical Report RM-217.
- Romme, W. H., D. W. Jamieson, J. S. Redder, G. Bigsby, J. P. Lindsey, D. Kendall, R. Cowen, T. Kreykes, A. W. Spencer, and J. C. Ortega.** 1992. Old-growth forests of the San Juan National Forest in southwestern Colorado. Pages 154–165 in M. R. Kaufmann, W. H. Moir, and R. L. Bassett, editors. *Old-growth forests in the southwest and Rocky Mountain regions: Proceedings of a workshop*. U.

ATTACHMENT D

S. Forest Service General Technical Report RM-213.

Saab, V., L. Bate, J. Lehmkuhl, B. Dickson, S. Story, S. Jentsch, and W. Block. 2006. Changes in downed wood and forest structure after prescribed fire in ponderosa pine forests. U.S. Forest Service Proceedings RMRS-P-41.

Skov, K. R., T. E. Kolb, and K. F. Wallin. 2004. Tree size and drought affect ponderosa pine physiological response to thinning and burning treatments. *Forest Science* **50**(1):81–91.

Smith, J. E., D. McKay, G. Brenner, J. McIvers, and J. W. Spatafora. 2005. Early impacts of forest restoration treatments on the ectomycorrhizal fungal community and fine root biomass in a mixed conifer forest. *Journal of Applied Ecology* **42**:526–535.

Smith, J. E., D. McKay, C. G. Niwa, W. G. Thies, G. Brenner, and J. W. Spatafora. 2004. Short-term effects of seasonal prescribed burning on the ectomycorrhizal fungal community and fine root biomass in ponderosa pine stands in the Blue Mountains of Oregon. *Canadian Journal of Forest Research* **34**:2477–2491.

Snyder, M. A. 1992. Selective herbivory by Abert's squirrel mediated by chemical variability in ponderosa pine. *Ecology* **73**:1730–1741.

— — —. 1993. Interactions between Abert's squirrel and ponderosa pine: the relationship between selective herbivory and host plant fitness. *American Naturalist* **141**:866–879.

Snyder, M. A., and Y. B. Linhart. 1994. Nest-site selection by Abert's squirrel: chemical characteristics of nest trees. *Journal of Mammalogy* **75**:136–141.

Stephenson, N. L. 1999. Reference conditions for giant sequoia forest restoration: structure, process, and precision. *Ecological Applications* **9**:1253–1265.

Swetnam, T. W., C. D. Allen, and J. L. Betancourt. 1999. Applied historical ecology: using the past to manage for the future. *Ecological Applications* **9** (4):1189–1206.

Szaro, R. C., and R. P. Balda. 1979. Bird community dynamics in a ponderosa pine forest.

Studies in Avian Biology **3**.

van Mantgem, P., and M. Schwartz. 2003. Bark heat resistance of small trees in Californian mixed conifer forests: testing some model assumptions. *Forest Ecology and Management* **178**: 341–352.

Veblen, T. T., T. Kitzberger, and J. Donnegan. 2000. Climatic and human influences on fire regimes in ponderosa pine forests in the Colorado Front Range. *Ecological Applications* **10**(4):1178–1195.

Vireday, C. C. 1982. *Mycophagy in tassel-eared squirrels (Sciurus aberti aberti and S. a. kaibabensis) in northern Arizona*. Thesis. Northern Arizona University, Flagstaff, Arizona, USA.

Wallin, K. F., T. E. Kolb, K. R. Skov, and M. R. Wagner. 2004. Seven-year results of thinning and burning restoration treatments on old growth ponderosa pines at the Gus Pearson Natural Area. *Restoration Ecology* **12**:239–247.

Ward, J. P., Jr. 2001. *Ecological responses by Mexican spotted owls to environmental variation in the Sacramento Mountains, New Mexico*. Dissertation. Colorado State University, Fort Collins, Colorado, USA.

Waskiewicz, J. D. 2003. *Snags and partial snags in managed, relict, and restored ponderosa pine forests of the Southwest*. Thesis. Northern Arizona University, Flagstaff, Arizona, USA .

Youngblood, A., T. Max, and K. Coe. 2004. Stand structure in eastside old-growth ponderosa pine forests of Oregon and northern California. *Forest Ecology and Management* **228**:191–217.

Zausen, G. L., T. E. Kolb, J. D. Bailey, and M. R. Wagner. 2005. Long-term impacts of stand management on ponderosa pine physiology and bark beetle abundance in northern Arizona: a replicated landscape study. *Forest Ecology and Management* **218**:291–305.

Zier, J. L., and W. L. Baker. 2006. A century of vegetation change in the San Juan Mountains, Colorado: an analysis using repeat photography. *Forest Ecology and Management* **228**:251–262.

ATTACHMENT D

EXHIBIT C

Mixed-severity wildfire and habitat of an old-forest obligate

DAMON B. LESMEISTER^{1,2,†} STAN G. SOVERN,² RAYMOND J. DAVIS,³ DAVID M. BELL,¹
MATTHEW J. GREGORY,⁴ AND JODY C. VOGELER^{4,5}

¹USDA Forest Service, Pacific Northwest Research Station, Corvallis, Oregon 97331 USA

²Department of Fisheries and Wildlife, Oregon State University, Corvallis, Oregon 97331 USA

³USDA Forest Service, Pacific Northwest Region, Corvallis, Oregon 97331 USA

⁴Department of Forest Ecosystems and Society, Oregon State University, Corvallis, Oregon 97331 USA

⁵Natural Resources Ecology Lab, Colorado State University, Fort Collins, Colorado 80523 USA

Citation: Lesmeister, D. B., S. G. Sovern, R. J. Davis, D. M. Bell, M. J. Gregory, and J. C. Vogeler. 2019. Mixed-severity wildfire and habitat of an old-forest obligate. *Ecosphere* 10(4):e02696. 10.1002/ecs2.2696

Abstract. The frequency, extent, and severity of wildfire strongly influence the structure and function of ecosystems. Mixed-severity fire regimes are the most complex and least understood fire regimes, and variability of fire severity can occur at fine spatial and temporal scales, depending on previous disturbance history, topography, fuel continuity, vegetation type, and weather. During high fire weather in 2013, a complex of mixed-severity wildfires burned across multiple ownerships within the Klamath-Siskiyou ecoregion of southwestern Oregon where northern spotted owl (*Strix occidentalis caurina*) demographics were studied since 1990. A year prior to these wildfires, high-resolution, remotely sensed forest structural information derived from light detection and ranging (lidar) data was acquired for an area that fully covered the extent of these fires. To quantify wildfire impact on northern spotted owl nesting/roosting habitat, we fit a relative habitat suitability model based on pre-fire locations used for nesting and roosting, and forest structure variables developed from 2012 lidar data. Our pre-fire habitat suitability model predicted nesting/roosting locations well, and variable response functions followed known resource selection patterns. These forests had typical characteristics of old-growth forest, with high density of large live trees, high canopy cover, and complex structure in canopy height. We projected the pre-fire model onto lidar data collected two months post-fire to produce a post-fire suitability map, which indicated that >93% of pre-fire habitat that burned at high severity was no longer suitable forest for nesting and roosting. We also quantified the probability that pre-fire nesting/roosting habitat would burn at each severity class (unburned/low, low, moderate, high). Pre-fire nesting/roosting habitat had lower probability of burning at moderate or high severity compared to other forest types under high burning conditions. Our results indicate that northern spotted owl habitat can buffer the negative effects of climate change by enhancing biodiversity and resistance to high-severity fires, which are predicted to increase in frequency and extent with climate change. Within this region, protecting large blocks of old forests could be an integral component of management plans that successfully maintain variability of forests in this mixed-ownership and mixed-severity fire regime landscape and enhance conservation of many species.

Key words: forest structure; habitat; lidar; mixed-severity fire regime; northern spotted owl; old forest; pre-fire vegetation condition; *Strix occidentalis caurina*.

Received 20 September 2018; revised 6 December 2018; accepted 12 March 2019. Corresponding Editor: Joseph A. LaManna.

Copyright: © 2019 The Authors. This is an open access article under the terms of the Creative Commons Attribution License, which permits use, distribution and reproduction in any medium, provided the original work is properly cited.

† **E-mail:** dlesmeister@fs.fed.us

INTRODUCTION

Climate and land-use patterns are strong predictors of disturbance regimes that ultimately influence the structure and function of an ecosystem (Sousa 1984). Globally, forest ecosystems are at risk of large disturbance regime shifts (frequency and severity) and ultimately a range of possible alternative stable states due to climate change-induced drought and heat stress, and associated interactions with insect disease outbreaks and wildfire (Dale et al. 2001, Allen et al. 2010, Kitzberger et al. 2012). In the case of fire regimes, their frequency and severity are typically negatively correlated, such that frequent fires are of lower severity, and strongly influence community dynamics and successional pathways (Agee 2005). Fire regimes play a key role in species adaptations as well as community structure and distribution of ecosystems, including the availability of several key components of wildlife habitat (Bunnell 1995, Noss et al. 2006, Pausas and Keeley 2009). Persistence of native wildlife species that are adapted to historical fire regimes may be at risk given climate change and land management practices that alter patterns in fire frequency and intensity relative to historical patterns. For example, in many dry forests the extent of areas impacted by high-severity fire is increasing, with concern for sensitive wildlife species that rely on forest types altered by fire (Westerling et al. 2006, Miller et al. 2008, Miller and Safford 2012, Reilly et al. 2017, Rockweit et al. 2017).

The fire regime of an ecosystem is defined as the natural patterns of wildfire in a given area including fire frequency, seasonality, extent, severity, and synergistic effects with other disturbances (Agee 1993, Halofsky et al. 2011). Forest successional theory suggests that in most areas, the interval length between disturbances should influence outcomes of succession, such that early-seral stands, low stature, and open microclimates are common in ecosystems with short-interval fires, whereas those with long-interval fires generally are dominated by mature forests with relatively closed canopies (Donato et al. 2009, Halofsky et al. 2011). Low-severity regimes are most often associated with dry forest types which experience frequent and predominantly low-severity fires where loss of biomass due to

fire is low, and <30% mortality of trees is typical (Agee 1993). This disturbance regime results in stands with open canopies and an understory dominated by sprouting and rhizomatous shrubs and herbaceous plants, which are described in historical accounts as open, parklike forests (Agee 2013). The extent of these forest types was often overrepresented in historical records due to the ease of traveling through them and the opportunities for pleasing photographs (Van Pelt 2008). In truth, these open, parklike forest conditions do not represent many forests in western North America (Odion et al. 2014). Forests in high-severity fire regimes experience infrequent (>200-yr return intervals) but high-severity fires. Large patches of total mortality occur within the fire events and overall mortality is high (>70%), though areas of low- and moderate-severity fire are also common (Agee 1993, Turner and Romme 1994). In western North America, these forest types associated with high-severity fire regimes are characteristic of high-elevation, lodgepole pine (*Pinus contorta*)-dominated stands, some spruce (*Picea* spp.)-dominated forests, and moist Douglas-fir (*Pseudotsuga menziesii*)/western hemlock (*Tsuga heterophylla*) forests of the Pacific Northwest (Agee 1993).

Within mixed-severity fires, 30–70% tree mortality is common; however, the mixed-severity regime is not simply intermediate between low- and high-severity fire regimes (Agee 1993, Perry et al. 2011). The resulting pattern of low-, moderate-, and high-severity fire patches within a given area is highly variable and difficult to predict (Agee 2005), although at a large enough spatial scale (e.g., watersheds), nearly all fires are mixed-severity (Turner and Romme 1994, Baker et al. 2007, Halofsky et al. 2011). This variability can occur at fine spatial and temporal scales dependent on previous fire history, topography, fuel continuity, vegetation type, and weather (Heyerdahl et al. 2001, Donato et al. 2009, Thompson and Spies 2009, Krawchuk et al. 2016). Because of the spatiotemporal variability across the landscape, mixed-severity fire regimes are the most complex and least understood fire regimes, unique in terms of patch metrics and the life history attributes of native species (Schoennagel et al. 2004, Agee 2005, Halofsky et al. 2011). Fire histories in mixed-severity regimes, in particular, are difficult to determine

because most fire history techniques have been developed to study either the low- or high-severity extremes in fire regimes (Agee 2005). Short-interval severe fires are an important characteristic of mixed-severity fire regimes and are typically considered extreme events and expected to be deleterious to forest succession and diversity (Donato et al. 2009). However, many native plants within these forests possess functional traits (e.g., persistent seed banks, vegetative sprouting, rapid maturation) lending to resilience to short-interval severe fires that result in distinct vegetation assemblages that enhance landscape heterogeneity inherent to mixed-severity fire regimes (Donato et al. 2009). Furthermore, high diversity of vegetation types, driven by short-interval repeat fires in a mixed-severity fire regime landscapes, plays an important role in conservation and the structure of avian communities (Fontaine et al. 2009).

Fire behavior is most strongly influenced by weather, topography, and fuels (i.e., above-ground vegetation biomass) interacting through multiple pathways and at multiple spatial scales (Agee 1993). Weather is perhaps the most important factor controlling fire behavior and severity, especially in mixed-severity regimes (Bessie and Johnson 1995, Collins et al. 2007, Thompson and Spies 2009, Bradstock et al. 2010). In moderate fire weather, topographical complexity and position (east- and south-facing, upper- and mid-slopes) have been shown to strongly influence fire intensity, with pre-fire vegetation condition and fire history also important predictors of severity (Estes et al. 2017). Under these conditions, shrubs and younger forests were more likely to burn at higher intensity than mature forests. In very high and severe fire weather, the amount (fuel loads), type (e.g., younger vs. older forest), and vertical and horizontal spatial arrangement of fuels (contiguous vs. unconnected) can be the primary driver of spatial patterns in mixed-severity fire (Zald and Dunn 2018). Furthermore, previous fires and post-fire management can set up the landscape for patterns of self-perpetuating high-severity fire in mixed-severity regimes (Donato et al. 2009, Thompson and Spies 2010). Even in drier forest types with high frequency of fire, certain topographic settings have lower fire frequencies where patches of dense, old forest can develop

and persist as islands in a matrix of open, older forests (Camp et al. 1997, Krawchuk et al. 2016). With changing climates and land management practices, the size of patches of high-severity fire is increasing relative to historical patterns, with concern for sensitive species that rely on forests dramatically altered by fire (Westerling et al. 2006, Miller et al. 2008, Miller and Safford 2012, Reilly et al. 2017, Rockweit et al. 2017).

Northern spotted owls (*Strix occidentalis caurina*) are an obligate species of old forests in the Pacific Northwest of the United States and southwest Canada and typically nest in large old conifer trees (Wilk et al. 2018). The subspecies was listed as threatened under the U.S. Endangered Species Act because populations declined primarily as result of habitat loss due to large-scale harvest of late-successional forests (USFWS 1990). A variety of forest types are used by northern spotted owls for foraging, but nesting and roosting primarily occur in forests older than 125 yr of age. These older forests have average tree diameters above 50 cm and many trees exceed 75 cm diameter, canopy cover is usually >60%, and the forest has multiple canopy layers (Davis et al. 2016). The Northwest Forest Plan (NWFP) was designed to protect most remaining old forest and, after several decades, provide enough habitat on federal lands for viable populations of several old-forest species, primarily through a network of late-successional forest reserves (USDA and USDI 1994). On federal lands, loss of northern spotted owl habitat due to timber harvest has declined, but losses due to wildfires have increased in recent decades (Davis et al. 2016). Studies focused on the subspecies of northern spotted owls suggest that occupancy and survival generally decline after fire, especially if post-fire logging occurs (Clark et al. 2011, 2013, Rockweit et al. 2017). The effects of fire on individual northern spotted owls and habitat quality are complex and not fully understood (Lesmeister et al. 2018), but clearly suitability of forests for nesting and roosting decreases if canopy cover is reduced and with spatial aggregation of high-severity fire (Davis et al. 2016, Rockweit et al. 2017, Sovern et al. 2019).

Fire regimes within the range of northern spotted owls range from infrequent/high severity in the northern and coastal regions to frequent/low

severity in the eastern and southern regions (Spies et al. 2018). In between these two extremes is a broad area of mixed-severity regimes, including the Oregon Klamath, where recent wildfires have caused high rates of loss of old forests and threaten species associated with them (Spies et al. 2006, 2018). Wildfires within this regime are comprised of a mix of burn severities, with low-severity ranging from 45% to 54% of the burned area, moderate-severity from 24% to 36%, and high-severity fire from 23% to 26% (Reilly et al. 2017). While the frequency and extent of high-severity fire have been increasing due to a general increase in large wildfires within the owls range, there is no strong evidence that high-severity wildfire comprises a higher proportion of burned areas than it did historically (Miller and Safford 2012, Reilly et al. 2017).

Within the Klamath-Siskiyou ecoregion of southwestern Oregon, an area characterized as moderate-frequency, mixed-severity fire regime (Spies et al. 2018), northern spotted owl demographics have been studied on the Klamath demographic study area since 1990 (Dugger et al. 2016). In and near the study area, lightning from a thunderstorm on 26 July 2013 started 54 fires that burned under very high fire weather conditions and were managed as the Douglas Complex and Big Windy Fires (Zald and Dunn 2018). Most of the fires joined into several large fires that burned with mixed severity over an area of about 38,000 ha. Within the fire perimeter were large patches of high-severity fire and subsequent salvage logging, primarily on private lands and along roads on federal lands. The non-overlapping—but nearby—large mixed-severity wildfires burning simultaneously in a mixed-ownership and management landscape presented a unique landscape experiment to evaluate interactions between severity classes (unburned/low, low, moderate, and high) and vegetation condition (e.g., suitable or unsuitable forest for nesting and roosting by northern spotted owls). Further, the study area provided an exceptional opportunity to study responses of vegetation to fire because high-resolution remote sensing data of vegetation height provided by aerial light detection and ranging (lidar) were available pre- and post-fire, which provided an unprecedented ability to measure forest attributes before and immediately following the fires.

Our objectives were to (1) quantify the immediate impact of various wildfire severities on northern spotted owl nesting/roosting habitat, which has typical characteristics of old-growth forests in the Pacific Northwest; and (2) analyze the relative susceptibility of northern spotted owl nesting/roosting habitat to higher or lower severity fire. We hypothesized that northern spotted owl nesting/roosting habitat would be degraded as severity increased, but the relationship would be non-linear where habitat would not be degraded at low severity, only slightly degraded with moderate severity, and highly degraded with high severity. Because the area was in drought and fire weather was very high to severe, we expected the high fuel loading of northern spotted owl nesting/roosting habitat may cause these stands to burn at higher or equal severity than other forest types with less fuel (Weatherspoon et al. 1992). However, several lines of evidence suggest older forests with dense, multi-storied canopies are more resistant to high-severity wildfire during severe fire weather (e.g., Countryman 1955).

METHODS

Study site

The study was conducted in the Klamath-Siskiyou ecoregion, which extends from northwestern California into southwestern Oregon (Fig. 1). The Douglas Complex and Big Windy Fires burned mostly within the boundary of the Klamath northern spotted owl demography study area (1422 km²; Fig. 1) with elevations ranging from 610 to 1680 m. Annual precipitation ranged from 1500 to 3000 mm over the study area (<http://prism.oregonstate.edu/>), with <15% falling from May to September. The region is among the top global hotspots of species rarity and richness, identified as a global center of biodiversity, a World Wildlife Fund globally outstanding ecoregion (www.worldwildlife.org/publications/global-200), and an IUCN area of global botanical significance (Olson and Dinerstein 1998, Noss 2000). The complexities of climate, topography, biogeographic patterns, geology, and mixed-severity fire regime in the Klamath and Siskiyou Mountains create one of the four richest temperate coniferous forests in the world with high endemism, species richness, and unique community assemblages (Noss et al. 1999, Vance-Borland

1999). Forests were dominated by Douglas-fir, ponderosa pine (*P. ponderosa*), sugar pine (*P. lambertiana*), and incense cedar (*Calocedrus decurrens*) and mixed with a variety of other conifers (*Pinus* spp. and grand fir *Abies grandis*) and hardwoods (e.g., Pacific madrone *Arbutus menziesii*, golden chinquapin *Castanopsis chrysophylla*, and oak *Quercus* spp.).

Within the Klamath-Siskiyou ecoregion, a complex and variable fire regime prevails, dominated by frequent mixed-severity and very frequent mixed-severity fires (Fig. 1; Spies et al. 2018). Historical fire severity varied in spatial scale, patchiness, and fire-return intervals (c. 5–75 yr), but overall exhibiting mixed severity over

time and space (Agee 1993, Taylor and Skinner 1998, Perry et al. 2011). When a stand-replacing fire occurs, rapid recovery of vegetation and fuel continuity, coupled with dry summers and frequent lightning, create the potential for recurrent high-severity fires over decadal timescales (Thompson et al. 2007). Thus, short-interval severe fires have likely been a component of the complex fire regime and a factor structuring vegetation in the region (Agee 1993, Donato et al. 2009).

Fire data

We used daily fire perimeter map data for the Douglas Complex Fires that burned with mixed

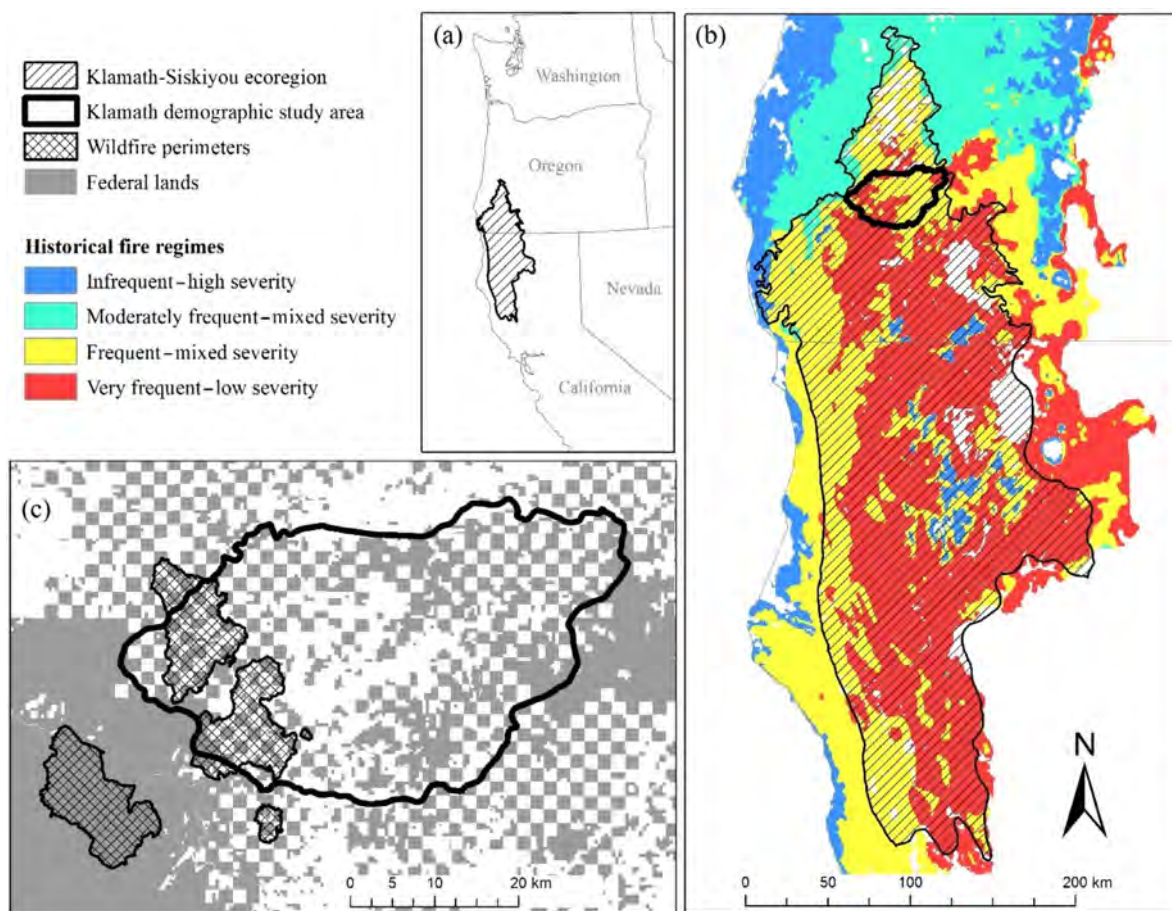


Fig. 1. Maps showing (a) the Klamath-Siskiyou ecoregion of California and Oregon, USA (hatched area); (b) historical fire regimes in the Klamath-Siskiyou ecoregion (Spies et al. 2018), Klamath northern spotted owl demography study area (1422 km²; center = 123.315° W, 42.782° N, heavy black border); and (c) landownership (federal land, gray; private land, white) and the 2013 Douglas Complex and Big Windy Fires (cross-hatched area).

severity: Dads Creek (final perimeter = 9890 ha), Rabbit Mountain (9706 ha), and Brimstone (928 ha); and for the Big Windy Fire (10,799 ha; Fig. 2). Low precipitation in 2013 resulted in moderate-to-severe drought conditions in southern Oregon (NDMC 2018) and contributed to active fire behavior in the early burning period of these fires. Zald and Dunn (2018; and unpublished data) summarized weather data for the first 4 d of the Douglas and Big Windy Complexes (see Fig. 2 for fourth-day fire perimeters)

from three Remote Automatic Weather Stations near fires and found maximum temperature was 25–32°C, minimum relative humidity was 17–30%, and maximum wind speed was 19–29 kmh. After the fourth day of the fire, a temperature inversion developed—a common occurrence in this region (Estes et al. 2017)—which dramatically changed fire behavior and greatly improved the effectiveness of suppression efforts. Mean daily burning index (BI) for the first 4 d of the fire was 52–76, which was above the

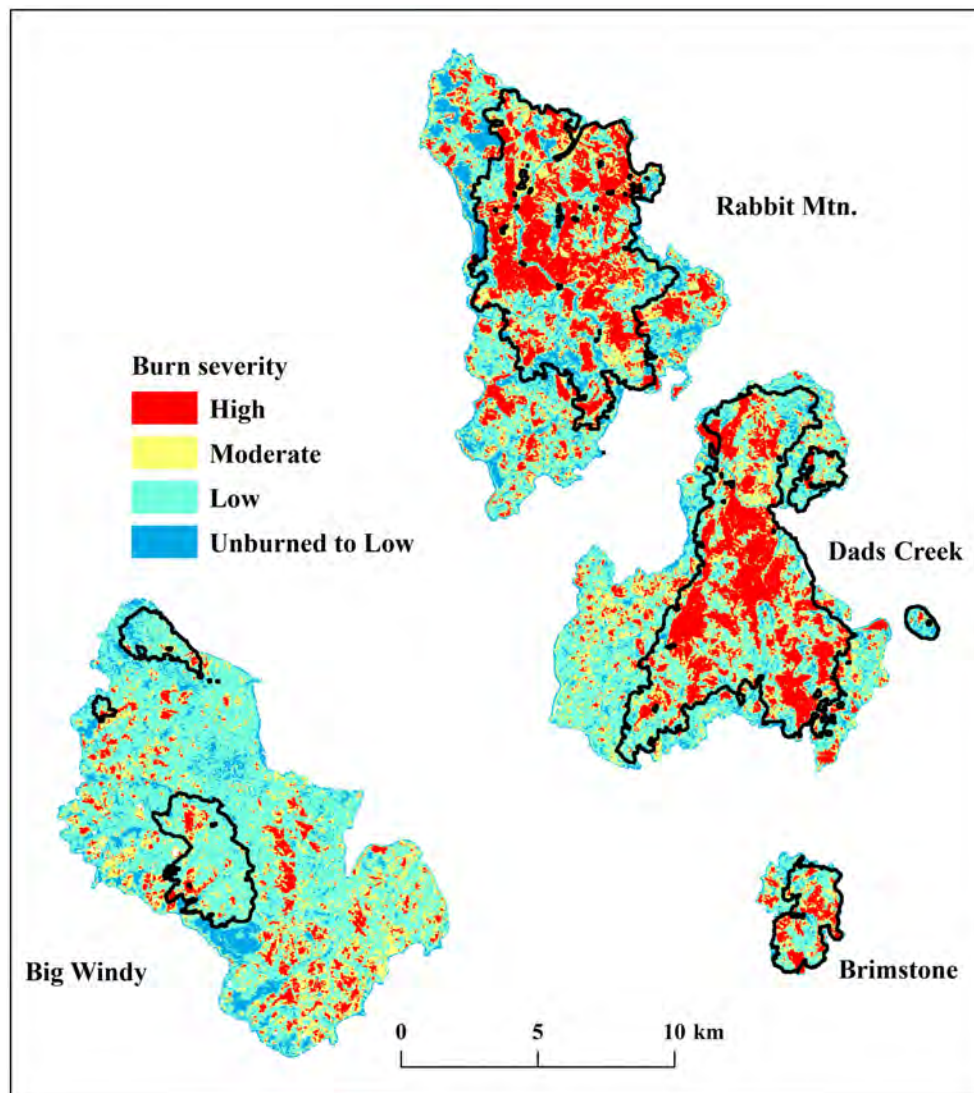


Fig. 2. Map of monitoring trends in burn severity (Eidenshink et al. 2007) data for the Big Windy and Douglas Complex Fires in southwest Oregon, USA, 2013. Severity is based on change in normalized burn ratio (dNBR) from Landsat-8 images from pre- and post-fire. The perimeter of the fires after the fourth day is outlined in black.

historic (1991–2017 1 June–30 September) 90th percentile for this period (Zald and Dunn 2018). Mean daily energy release component (ERC) values ranged from 49 to 67, also above the 90th percentile for this area (Dalton et al. 2015) for 3 of 4 d. Burning index is a fire behavior index proportional to flame length that incorporates wind speed estimates, and ERC is an index of fire energy that includes the cumulative drying effect of weather in the days prior to the estimate and measures live and dead fuel moisture (Bradshaw et al. 1983, Cohen and Deeming 1985). Post-fire logging occurred over much of the high-severity portions of the private lands, but most federal land was unlogged post-fire because the area was designated as a late-successional reserve under the NWFP. The areas of the Douglas Complex Fires were primarily composed of Oregon and California Railroad Lands with federal lands, managed by the U.S. Bureau of Land Management, in a checkerboard pattern with private lands (Fig. 1; Zald and Dunn 2018). The Big Windy Fire burned within an intact landscape of federally managed forest lands (Fig. 1).

Pre- and post-fire habitat suitability

We used program MaxEnt version 3.3.3k (Phillips et al. 2006) to produce a pre-fire relative nesting/roosting habitat suitability model of forests used by northern spotted owls and applied the model algorithm to post-fire forest conditions to map post-fire suitability. MaxEnt is based on the maximum information entropy theory and is widely used to develop resource selection functions through the use of machine learning applied to known species locations (i.e., model training data) and relevant environmental predictor variables (Harte and Newman 2014). Previous efforts also used machine learning to develop nesting/roosting cover type models in several northern spotted owl studies and monitoring reports (Davis et al. 2011, 2016, Glenn et al. 2017). We followed Ackers et al. (2015) by using lidar-derived forest structure variables to develop a model of suitable forest for northern spotted owl nesting and roosting.

We used site locations where northern spotted owls nested and roosted within the demographic study area as training and testing data for relative habitat suitability models. These location data were collected during long-term research of

northern spotted owl demography, including survival rates, reproductive rates, and annual rate of population change. The protocol used to determine site occupancy, nesting, and reproductive status for this study followed the guidelines specified by monitoring effectiveness of the NWFP (Franklin et al. 1996, Dugger et al. 2016).

We derived our pre- and post-fire model predictor variables from multiple-return discrete lidar data acquired in 2012 (1 yr pre-fire) and 2013 (2 months post-fire) by Quantum Spatial (previously Watershed Sciences, Corvallis, Oregon, USA) using aircraft-mounted Leica ALS 50 and/or Leica ALS 60 sensors with an average point density of ≥ 10 points per square meter. The 2012 data were collected as part of the Oregon Lidar Consortium (OLC) Rogue River lidar acquisition, covering an area of $\sim 567,000$ ha. Within this OLC Rogue River collection area, $\sim 50,000$ ha of lidar data were acquired again in 2013 post-wildfire, encompassing the Douglas complex and Big Windy Fires. We processed all lidar metrics from delivered point clouds, creating 1-m-resolution models of highest (i.e., first) return and bare earth digital elevation models (DEMs) with FUSION/LDV software (McGaughey 2015).

Following Ackers et al. (2015), we derived four metrics from the lidar data known to be important drivers in northern spotted owl nesting and roosting ecology: percentage overstory canopy cover (CANOPY), mean overstory canopy height (HEIGHT), density of large live trees (LARGE TREES), and rumple index (RUMPLE; Parker et al. 2004). We calculated the percent CANOPY taller than 2 m and the mean vegetation height using only first returns at 30 m resolution. We calculated RUMPLE, a measure of stand structure diversity where higher values represent stands with more horizontal and vertical complexity, using a 3×3 window focal mean of the 1-m canopy height model (CHM; Ackers et al. 2015). We matched the resolution of the HEIGHT and CANOPY metrics using a cell multiplier of 30 and then derived RUMPLE from the surface area ratio output. We calculated LARGE TREES from point files representing large live tree (≥ 31 m tall) locations from the 1-m CHM and CanopyMaxima in FUSION/LDV (McGaughey 2015). The tree height threshold of 31 m was the average height of 80-yr-old trees based on a

height–age relationship of trees in forest inventory plots from the study area. To minimize the chance of having multiple points for the same tree, we created 10 m radius buffers around all points in ArcGIS 10.1 (ESRI, Redlands, California, USA), dissolved overlapping buffers, and then created a new point layer from the centers of the dissolved buffers. Any trees that were mapped only in the post-fire LARGE TREES map were added to the pre-fire model (with the assumption that large trees present after the fire were present prior to fires).

Northern spotted owl presence data for model training and testing were based on 107 nesting or roosting locations from 27 territories. Given that presence data originated from a long-term northern spotted owl study area, we were confident that we met sampling assumptions of minimal sampling bias and high probability of detecting owls when they were present. We followed standard procedures for presence-only modeling to avoid multi-collinearity between model variables by restricting modeling response functions that were overly complex, using stepwise calibration, and testing of bootstrapped model replicates (O'Brien 2007, Phillips and Elith 2013, Merow et al. 2014). We followed the model selection method used by Ackers et al. (2015) by using a random subset of our owl location data (75%) and 10,000 random modeling region locations to develop bootstrapped replicate models that related location data to random environmental conditions. We used the held-out 25% of northern spotted owl locations to test model predictions. We made stepwise adjustments to the model regularization multipliers that serve as a penalty parameter in machine learning by eliminating model coefficients and keeping only those that increase model gain, which relates to the likelihood ratio of an average species location to average background environmental conditions. Higher gains produce better differentiation of species locations from background conditions. The best model was based on balancing two criteria: (1) minimizing the difference between regularized training gain and test gain to avoid over-fitting the models, while (2) maximizing model test statistics (area under the curve [AUC] and Spearman rank correlation [Rs]). Once the best model was selected, we used the predicted vs. expected (P/E) curve to classify the model

into a binary map of suitable and unsuitable nesting/roosting habitat (Hirzel et al. 2006).

Burn severity and change in suitability

We assumed most of the negative effects of wildfire on northern spotted owl nesting/roosting habitat would result from loss of canopy cover and mortality of large trees. To capture changes in the large, live tree component (LARGE TREES), we needed to estimate the proportion of LARGE TREES that suffered mortality by fire severity to adjust our post-fire LARGE TREES variable for the post-fire nesting/roosting habitat model. However, initial examination of the lidar data indicated that the post-fire lidar data could not differentiate live vs. dead trees ≥ 31 m height, leading to a bias in the lidar-based LARGE TREES variable. Previous research has indicated that lidar variables are better predictors for live and total basal area while multispectral imagery variables (e.g., Landsat data) are better predictors for dead and percent dead basal area (Bright et al. 2014). For example, changes in normalized burn ratio (NBR) are commonly used for mapping forest disturbance, especially timber harvest and wildfire (Miller and Thode 2007, Kennedy et al. 2010, 2012, Schroeder et al. 2011). In particular, changes in NBR have been widely used to assess fire severity (Miller et al. 2009, 2012, Cansler and McKenzie 2012, Lydersen et al. 2016). Furthermore, changes in NBR have been effectively related to changes in canopy cover (Miller et al. 2009) and basal area (Reilly et al. 2017). In this study, we used changes in satellite-based NBR from Landsat-8 to assess changes in canopy cover, and thus tree mortality, in live trees ≥ 31 m height to avoid biases produced by directly calculating changes in LARGE TREES from pre- and post-fire lidar data.

To assess canopy cover losses, and thus large live tree mortality associated with the fire, we acquired two spatial datasets to be used for mapping vegetation change within the fire perimeters: (1) We used Google Earth Engine (Google Earth Engine Team 2015, Gorelick et al. 2017) to collect 30-m-resolution Landsat-8 LaSRC imagery for the study area from 1 May to 1 August of 2013 and 2014 to generate pre- and post-fire NBR maps; and (2) we used post-fire high-resolution (7.62 cm) imagery acquired concurrently with lidar acquisition to estimate tree canopy

cover. For all 30×30 m (900 m^2) pixels in the study area, we calculated NBR in 2013 (pre-fire) and 2014 (post-fire) as the normalized differences between near-infrared and shortwave-infrared bands (bands 5 and 7, respectively; Li et al. 2013) for each Landsat-8 image. For our study area, no single image was optimal (e.g., cloud cover over part of the area on a given date), so we created a median composite image of NBR for each growing season (May–August; Kennedy et al. 2012). Large, live trees represented by LARGE TREES were only located in older forests; therefore, we measured live tree canopy cover visible in the high-resolution aerial photographs at 200 randomly generated 30×30 m (900 m^2) plots within older forests (95th percentile lidar return height ≥ 30.8 m) inside the study area snapped to the 2014 Landsat-8 pixel boundaries. Within each plot, 36 systematically distributed sampling points were established and tree canopy cover was measured as the proportion of sampling points where we observed live tree crowns in the high-resolution imagery. Plots co-located with roads, timber salvage, young plantations, or lacking clear imagery (e.g., steep slope in shadow) were excluded from our analysis, resulting in a final sample size of $n = 181$ that included post-fire canopy cover in forests experiencing a variety of fire severity conditions. Note that canopy cover measurements collected at these sample locations represent only live tree canopy cover and were independent from lidar-based canopy cover estimates that include both live and dead trees.

Statistical models relating NBR change and forest change (e.g., basal area mortality; Reilly et al. 2017) are available, but we did not have reliable measurements of canopy cover change based on both pre- and post-fire aerial photographs upon which we could parameterize a model. Pre-fire aerial imagery could not be used in conjunction with post-fire aerial imagery to calculate change in canopy cover directly because of the lower resolution images and differing parallax (i.e., an apparent shift in the position of objects as viewed from differing vantage points) between pre- and post-fire images. Therefore, an accurate assessment of cover change between photographs was unreliable. Additionally, published models were not parameterized for our landscape, but rather broad regional

datasets for California (Miller et al. 2009) or Oregon and Washington (Reilly et al. 2017). Because only post-fire reference data for canopy cover (high-resolution aerial photographs) were available, we developed a mortality algorithm based on changes in forest canopy cover predicted from NBR data. The algorithm (1) predicted live canopy cover based on post-fire NBR and canopy cover measurements from aerial photography, (2) calculated the change in predicted canopy cover from the pre-fire to post-fire conditions, and (3) assigned mortality to LARGE TREES with probability proportional to the change in Landsat-based canopy cover.

Because tree canopy cover data were non-negative, we modeled tree canopy cover as a function of NBR with a zero-truncated regression model (Fig. 3). The model was fit to the 2014 NBR (post-fire) and tree canopy cover data in the R statistical environment version 3.3.1 (R Core Team 2016) with the function `tobit` (AER package; Kleiber and Zeileis 2009). For each 30-m Landsat pixel, tree canopy cover predictions for pre- and post-fire were generated by applying the fitted model to 2013 (before fire ignition) and

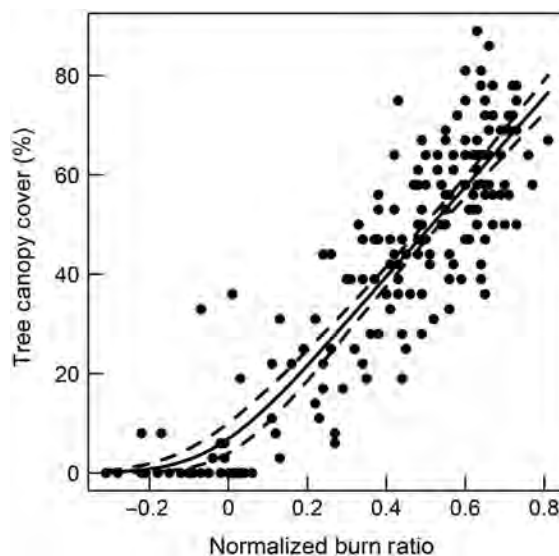


Fig. 3. Mean (solid line) and 95% confidence intervals (dashed lines) for predicted live tree canopy cover as a function of normalized burn ratio within the Douglas Complex and Big Windy Fires in southwest Oregon, USA, in 2013 based on the zero-truncated regression model.

2014 NBR data, respectively. To minimize differences between 2013 and 2014 canopy cover maps, we normalized the 2013 NBR data so that the differences between 2013 and 2014 NBR outside the fire perimeter were minimized. We transformed the 2013 NBR image by creating a mask of high NBR (stable forest, both 2013 and 2014 NBR were >0.75) outside the fire boundaries, and within the study area, which served as the population for creating a normalization between the two image dates. We then created a simple least-squares linear fit between NBR 2013 and NBR 2014 based on all pixels in the mask population, with a slope of 0.845 and intercept of 0.119 based on estimated coefficients. We created the transformed NBR 2013 by applying slope/intercept from linear fit, thereby transforming the 2013 image calibrated to the values in the 2014 image and quantified differences.

Pre- and post-fire predictions of canopy cover were differenced and divided by the predicted pre-fire canopy cover to calculate the proportional change in canopy cover (ΔC). The probability of mortality for a given 30-m pixel on the landscape was taken to be $1 - \Delta C$ (i.e., canopy cover-weighted tree mortality). Areas with canopy cover increases (i.e., $\Delta C > 0$) were assumed to have no tree mortality. We assessed the performance of the canopy cover-weighted mortality by comparing our predictions for each pixel with a large live tree with an independent basal area-weighted mortality prediction generated using existing models (Appendix S1; Reilly et al. 2017). We use these data for validation because the models produced by Reilly et al. (2017) predict basal area-weighted tree mortality from a regional forest inventory network based on RdNBR ($r^2 = 0.68$) and perform particularly well in identifying patches of forest experiencing basal area-weighted mortality $>75\%$ (classification accuracy = 82.8%).

Large tree mortality within each pixel was assigned proportional to $1 - \Delta C$. For a given pixel with n canopy dominant trees identified based on lidar imagery, a sample $n \times (1 - \Delta C)$ trees, rounded to the nearest integer, was taken and recorded as having died during the fire, with the remaining $n \times \Delta C$ trees surviving. This assumes that the number of trees dying during the fire was proportional to the canopy cover losses and that the identity of trees dying does

not matter. For canopy dominant trees examined in this paper, such an assumption seems reasonable. We, therefore, used the mortality algorithm to modify our post-fire point file of tree stems to estimate which trees mapped by lidar suffered mortality. We then used the post-fire live tree point file to generate our post-fire LARGE TREES density variable for nesting/roosting habitat modeling.

We recognize that by leveraging multiple datasets and modeling techniques—lidar-based LARGE TREES and satellite-based canopy cover-weighted mortality—there is the opportunity to propagation of error from one step to another. For example, errors in estimating forest carbon stocks may arise from field data collection, allometric equations, and modeling errors (Clough et al. 2016). In the case of this study, errors associated with canopy cover modeling, the calculation of canopy cover-weighted mortality, and the application of that mortality to attribute tree death to individual trees all contribute to overall errors.

Pre-fire vegetation vs. fire severity analysis

Our main interest was to examine the relationship between fire severity and nesting/roosting habitat with limited confounding effects of fire suppression activities and differences in fire weather during the time the fire burned. Though it is difficult to separate the confounding effects of suppression efforts when analyzing almost all fires, we reasoned we could minimize this effect by examining the early days of the fire before more extensive backfiring occurred and suppression activities had limited effect. Thus, we used the spatial extent of daily fire growth (as mapped using aerial IR technology each night) throughout the first 4 d after ignition. Starting at approximately day 5 of the fire, changes in atmospheric temperature altered fire weather conditions and suppression efforts included igniting backfires in some areas (K. Kosel, *personal communication*; Fig. 2). Additionally, by focusing on these rapid fire growth days we believe there is little to no alteration of natural fire behavior or severity across the spectrum of northern spotted owl nesting/roosting habitat suitability. To quantify the odds of forest types burning in 1 of 4 severity types, we evaluated the ratios of the proportion of suitable and unsuitable nesting/roosting

habitat that burned (B) at each fire severity to what was available to burn (A). Fire severity types were taken from Monitoring Trends in Burn Severity (MTBS 2017) data, a map product based on changes in NBR commonly used by forest management agencies. The types include high severity, moderate severity, low severity, and unburned to low severity. By using the same fire severity classifications commonly used by land managers, communication and application of results from this research will be more straightforward. A value of $B/A < 1$ indicates that the forest type burned less than would have been expected by chance, and a ratio $B/A > 1$ indicates it burned more than would be expected by chance (Moreira et al. 2001, 2009, Manly et al. 2010). While the canopy cover-weighted mortality modeling we used to attribute large tree mortality depends on NBR and is thus likely related to the MTBS fire severity classes, we use the

MTBS classes for summarizing across severity classes because of their widely accepted use in forest planning.

RESULTS

Pre- and post-fire habitat suitability

Our best model of nesting/roosting habitat suitability predicted nesting/roosting locations well with an AUC statistic of 0.89 and a P/E curve Spearman rank correlation of 0.92. The binary classification of the habitat model into suitable and unsuitable was based on $P/E = 1$ (0.32). Model variable response functions (Fig. 4) followed known resource selection patterns by owls (Ackers et al. 2015, Glenn et al. 2017).

Burn severity and change in suitability

Post-fire nesting/roosting habitat suitability decreased with increasing fire severity (Table 1),

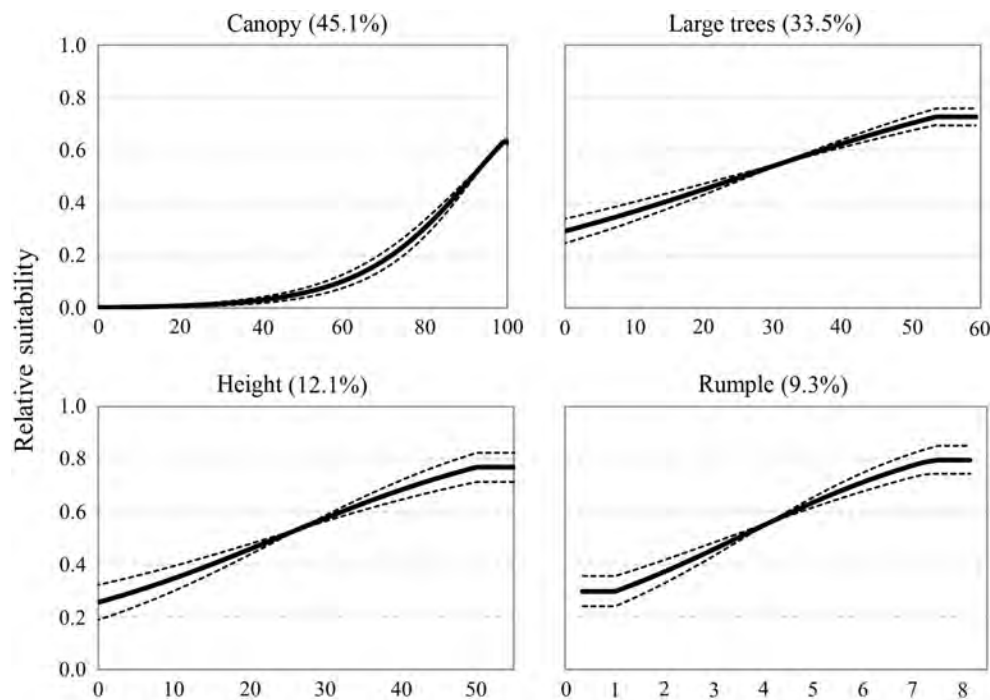


Fig. 4. Variable response functions with percent contribution (%) to pre-fire nesting/roosting habitat suitability model for northern spotted owls in the Klamath demographic study area in southwest Oregon, USA, where the Douglas Complex and Big Windy Fires burned in 2013. The solid line represents the mean, and the dashed lines represent 95% confidence intervals. Variables were derived from lidar data, and the variables included were CANOPY (percent canopy cover), LARGE TREES (large live trees per hectare), RUMPLE (rump index), and HEIGHT (mean tree height [m]).

ATTACHMENT D

LESMEISTER ET AL.

Table 1. Metrics within areas burned at four severity classes based on Monitoring Trends in Burn Severity (MTBS) measurements.

Fire severity	Pre-fire live trees	Trees killed	% Mort	Mean pre-fire NBR	Mean post-fire NBR	Δ Mean NBR (%)	Mean pre-fire suitability	Mean post-fire suitability	% Loss suitable habitat
Unburned to low	66,015	2830	4	0.75	0.68	-9.2	0.22	0.20	4.5
Low	251,356	49,413	20	0.74	0.56	-24.6	0.22	0.21	25.5
Moderate	71,826	40,038	56	0.72	0.30	-58.3	0.10	0.08	63.9
High	67,897	62,348	92	0.75	-0.04	-104.9	0.12	0.03	93.7

Notes: Reported are estimated number of large live trees pre-fire, estimated number large live trees killed during fire, percentage of large live trees killed, mean normalized burn ratio (NBR) pre (2013)- and post-fire (2014), percent change in NBR, pre (2012)- and post-fire (2013) mean nesting/roosting habitat suitability, and percent loss of suitable nesting/roosting habitat for northern spotted owls in the Douglas Complex and Big Windy wildfires in southwest Oregon during 2013.

mainly owing to fire-caused decreases in LARGE TREES and CANOPY. Low-severity fire had little effect on nesting/roosting habitat suitability. High-severity fire resulted in 75% decrease in mean suitability and >93% loss of suitable nesting/roosting habitat (Table 1) and commonly converted pre-fire suitable forests to conditions that were unsuitable for nesting and roosting (Fig. 5). Overall, most pre-fire habitat was lost if it burned at moderate severity (Table 1), but depending on the pre-fire suitability, moderate-severity fire produced mixed effects on nesting/roosting habitat suitability and did not consistently result in a loss of suitability. The forests that burned at unburned to low severities had pre-fire suitability values approximately two times higher than suitability of forests that burned at moderate or high severity (Table 1); thus, moderate- to high-severity fire had the greatest effect on pre-fire areas with low habitat suitability for northern spotted owls (Fig. 6).

Tree mortality and pre-fire vegetation vs fire severity

Canopy cover-weighted mortality (Appendix S1: Fig. S1) generated as the basis of attributing post-fire tree mortality for large trees exhibited a slight positive bias (mean error = 2.42% mortality) and root mean square deviation of 5.82% compared to an existing basal area-weighted mortality model based on regional forest inventory datasets co-located with large wildfires (Reilly et al. 2017). Despite these errors, our canopy cover-weighted mortality predictions were highly correlated with the existing basal area-weighted mortality predictions (Pearson correlation = 0.99).

Based on lidar tree mapping and the post-fire NBR analysis, we estimated the fires directly killed a total of 154,629 large live trees (51.1% of total pre-fire estimate). Tree mortality increased with fire severity and percent change in NBR (Table 1). There were 2.27 times more large live trees in areas that experienced unburned to low-severity fire compared to those areas that burned at moderate and high severity (Table 1). The susceptibility of forests to moderate- and high-severity fire was lower in suitable nesting/roosting habitat and higher in unsuitable forest than would be expected by chance (Fig. 6). The differences between low and moderate/high severity were more pronounced in suitable nesting/roosting habitat than unsuitable forest. The odds that suitable nesting/roosting habitat would burn at lower severity was 2–3 times higher than the odds it would burn at moderate-to-high severity. There were significant differences (based on non-overlapping 95% confidence intervals) between odds of burning at low severity and burning at moderate/high severity among forest types. There was no evidence for a difference between the odds (i.e., B/A index) of burning at moderate or high severity within suitable nesting/roosting habitat or unsuitable forest types, but there were differences between suitable and unsuitable forest types (Fig. 6). The odds that unsuitable forest burned at moderate-to-high severity was about twice that of suitable nesting/roosting habitat.

DISCUSSION

Here, we used newly developed tools and lidar data to examine the interaction between mixed-severity fires and northern spotted owl

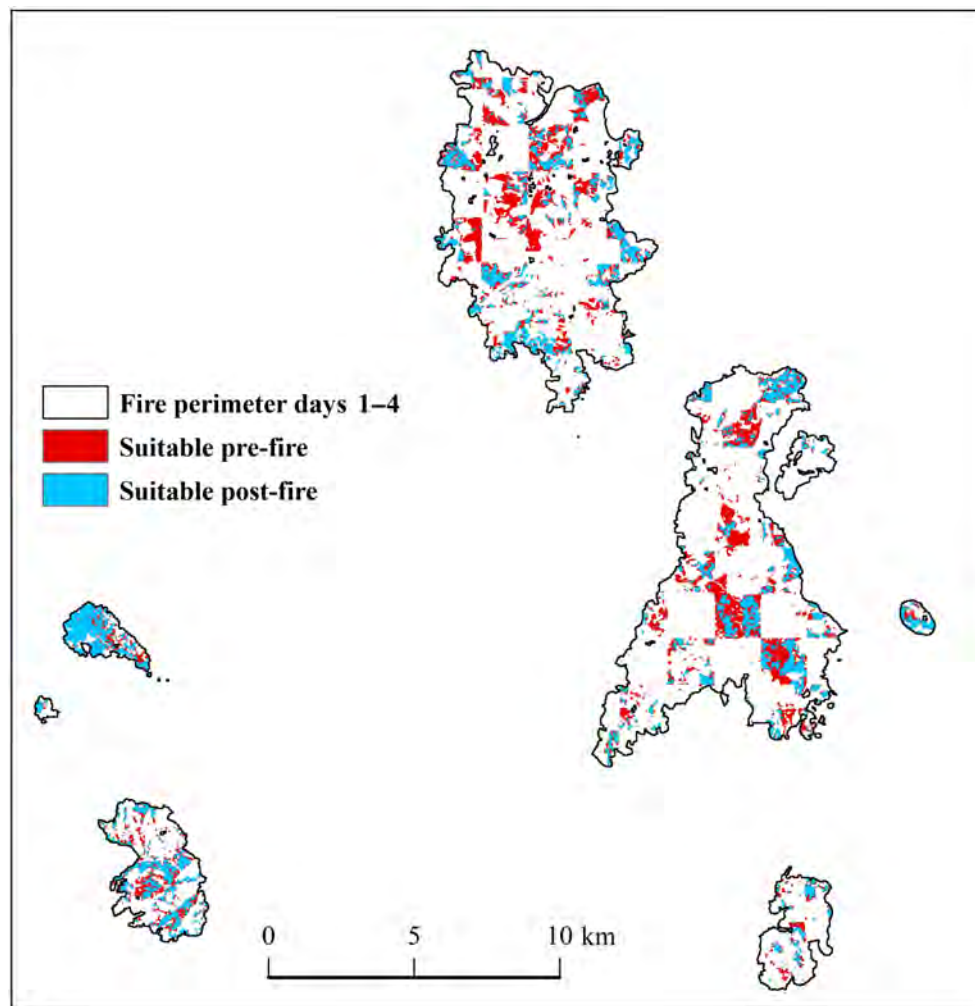


Fig. 5. Patterns of conversion from suitable habitat to unsuitable conditions for northern spotted owl nesting and roosting in the Douglas Complex and Big Windy Fires that burned in southwestern Oregon, USA. Binary classification of nesting/roosting habitat was based on predicted vs. expected ratio threshold of 0.32, and lidar metrics of live vegetation height, canopy cover, stand complexity (rumple index), and large tree density. Area shown is the perimeter of the fires 4 d after the fire ignited on 26 July 2013.

nesting/roosting habitat under high fire weather conditions in a landscape characterized by the interactions between land-use patterns and a mixed-severity fire regime. Because of high site fidelity, northern spotted owls may continue to use areas if suitable nesting/roosting cover remains and prey are available. However, survival decreases through time in areas with a high proportion of high-severity fire likely because post-fire habitat quality decreases to the point that territories are only marginally capable of supporting northern spotted owls (Rockweit

et al. 2017). Within a few years post-fire, areas opened up by tree mortality change structurally (i.e., standing dead trees transitioning to fallen logs) and prey may be less accessible with high density of shrubs and herbaceous understory in high-severity burn areas. As expected, in our study the suitability of northern spotted owl nesting/roosting habitat decreased with increasing fire severity, to the degree that much of the pre-fire habitat that burned at high severity was no longer suitable cover for nesting or roosting. The greatest impacts from moderate- and high-severity fire

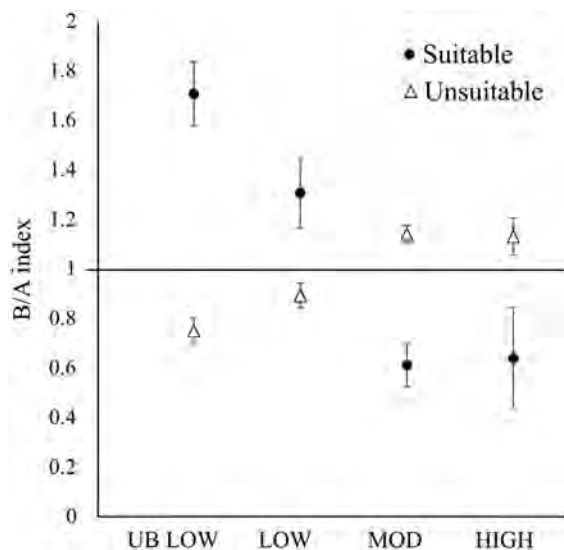


Fig. 6. Ratio of proportion of suitable and unsuitable nesting/roosting habitat that burned (B) at each fire severity to what was available (A) to burn (B/A index) with 95% confidence intervals, Douglas Complex and Big Windy Fires, southwestern Oregon, USA, 2013. We used Monitoring Trends in Burn Severity (MTBS 2017) to determine fire severity types (UB LOW, unburned to low severity; LOW, low severity; MOD, moderate severity; HIGH, high severity) and separated into suitable nesting/roosting habitat for northern spotted owls or unsuitable forest types based on lidar metrics. B/A index < 1 indicates that the forest type (suitable or unsuitable) burned at the severity class less than would have been expected by chance, and B/A index > 1 indicates forest type burned at the class more than by chance alone.

were observed in those forests exhibiting low habitat suitability for northern spotted owl nesting and roosting before the fire.

We found that the old-forest conditions associated with northern spotted owl habitat burned at lower severity despite having higher fuel loading than other forest types on the landscape. The microclimate and forest structure likely played a key role in lower fire severity in nesting/roosting habitat compared to other forest types. As succession progresses and canopy cover of shade-tolerant tree species increases, forests eventually gain old-growth characteristics and become less likely to burn because of higher relative humidity in soil and air, less heating of the forest floor

due to shade, lower temperatures, lower wind speeds, and more compact litter layers (Countryman 1955, Chen et al. 1996, Kitzberger et al. 2012, Frey et al. 2016, Spies et al. 2018). In addition, as the herbaceous and shrub layer is reduced by shading from lower to mid-layer canopy trees, the connection between surface fuels and the canopy declines, despite possible increases in canopy layering (Halofsky et al. 2011, Odion et al. 2014). Alexander et al. (2006) found that in the Klamath-Siskiyou ecoregion, southern aspects tended to burn with greater severity, but exogenous factors also played an important role because areas with large trees burned less and had less fire damage than areas dominated by smaller trees. On the 2002 Biscuit Fire that burned near our study area, Thompson and Spies (2009) concluded that weather and pre-fire vegetation conditions were the primary determinants of crown damage. They found that forests with small-stature vegetation and areas of open tree canopies and dense shrubs experienced the highest levels of tree crown damage, while older, closed-canopy forests with high levels of large conifer cover were associated with the lowest levels of tree crown damage. The moisture content of air and soil in a forest affects the amount of fuel moisture, and thus the probability of ignition and burning temperature (Heyerdahl et al. 2001). In addition to the potential to mitigate negative effects of climate warming at local scales by creating refugia and enhancing biodiversity (Frey et al. 2016), we suggest that northern spotted owl nesting/roosting habitat also has the potential to function as fire refugia (i.e., areas with higher probability of escaping high-severity fire compared to other areas on landscape) in areas with mixed-severity fire regimes under most weather conditions. Thus, in these landscapes, management strategies to conserve old-growth characteristics may also reduce risk of high-severity wildfire (Bradley et al. 2016) and serve as buffer to negative effects of climate change (Betts et al. 2018).

Although it has long been recognized that older forests have lower flammability than other forest types (Countryman 1955), federal agencies are often criticized for not extensively managing old forests to reduce risk of high-severity fire (OFRI 2010). The perception is that forest succession leads to increased flammability with age

(Kitzberger et al. 2012, Duff et al. 2017). Where this view may be correct is in dry forests with historically very frequent fire-return intervals (<10 yr), and contemporary increased fuel continuity has resulted from fire exclusion and led to increased sizes of high-severity patches when fires burn under extreme weather (Reilly et al. 2017). In the driest forest types, fire exclusion converts open forests with grassy understories to dense forests with high fuel loads, and the increased fuel continuity can result in larger patches of high-severity fire than would have occurred historically. In other forest types, succession likely decreases risk of high-severity fire. Compared to older forest, younger forests have lower canopies and thinner barked trees that reduce resistance to fire, and thinned young forests can be susceptible to high mortality from fire unless surface fuels are treated with prescribed fire (Raymond and Peterson 2005). Thinned forests have more open conditions, which are associated with higher temperatures, lower relative humidity, higher wind speeds, and increasing fire intensity. Furthermore, live and dead fuels in young forest or thinned stands with dense saplings or shrub understory will be drier, making ignition and high heat more likely, and the rate of spread higher because of the relative lack of wind breaks provided by closed canopies with large trees.

Primarily as inputs to fire models that estimate likely fire behavior, fuel models involve typing forested stands according to fuel loading and are often used to explore or inform management directions because fuels are under the purview of forest managers (Deeming and Brown 1975, Anderson 1982, Bradshaw et al. 1983, Finney 2004, Scott and Burgan 2005, Andrews 2009). Suitable nesting/roosting habitat often falls in classes rated as highly burnable, with fast rates of fire spread, high flame lengths, and intense fire behavior (Anderson 1982). Thus, fire model results can show nesting/roosting habitat has higher burn probabilities and higher crown fire potential than adjacent areas (Ager et al. 2007, 2012). The results of this study as well as other recent studies show that these older forests in mixed-conifer forest environments are less susceptible to high-severity fire than other successional stages, even under high fire weather conditions and with short return intervals <15 yr (Donato et al. 2009). Running fire models for our

study area based on conditions during the Douglas Complex and Big Windy Fires would be a worthwhile exercise to evaluate model predictions relative to the actual behavior of those fires. However, based on the findings of this study and many others (see review by Duff et al. 2017), we contend that fire models that continue to use fuel models that rate older forests with higher relative fire behavior will likely overestimate fire severity and inflate estimated loss of old forests in the Pacific Northwest. An alternative is to consider forest fuels in a more holistic manner and alternative age-flammability models (Kitzberger et al. 2012, Duff et al. 2017).

Intensive management (especially on timber industry lands) that results in reduced fuel loading does not always equate to less frequent or severe fire. Results by Charnley et al. (2017) in southcentral Oregon showed that private industry lands had more than three times the percentage area of open-canopy forest compared to U.S. Forest Service-managed lands that included thinning trees <53.3 cm diameter, prescribed fire, and no active management. Federal land management practices resulted in forests with more resilience to high-severity wildfire as opposed to management on private lands (Charnley et al. 2017). Furthermore, Zald and Dunn (2018) found that ownership patterns were the best predictor for high-severity fire in the Douglas Complex Fires, where federal lands, with primarily older forests in late-successional reserves, burned at lower severity than non-federal forests that were primarily private timber industry lands.

Gradual changes in temperature or precipitation patterns may have little effect until a disturbance-driven threshold is reached at which a large shift occurs that might be difficult or impossible to reverse (Scheffer and Carpenter 2003). Peterson (2002) described “ecological memory” and how previous patterns of disturbance can predispose an area to follow a certain disturbance pathway. For example, a landscape that experiences severe disturbance (e.g., high-severity fire, clear-cut logging, post-fire salvage logging) can be predisposed to high-severity fire in a mixed-severity fire regime (Thompson et al. 2007, Donato et al. 2009, Thompson and Spies 2009, Zald and Dunn 2018). High-severity wildfire can alter soil and successional pathways and potentially shift the system into an alternative stable state (Peterson 2002). A

key component of overall ecosystem function and sustainability occurs belowground, and with high-severity fire, changes in the soil physical, chemical, and biological functions can be deleterious to the entire ecosystem caused by changes in successional rates and species composition (Neary et al. 1999). Conversely, low-severity fire effects on soil can promote herbaceous flora, increase plant diversity, increase available nutrients, and thin over-crowded forests, all of which can enhance healthy forest ecosystems (Neary et al. 1999). The time for recovery of belowground systems is a key driver of ecosystem processes and depends on burning intensity and on previous land-use practices. Soils are greatly altered and degraded in young intensively managed forest and post-salvage logged sites, which are more susceptible to repeat and short-interval high-severity wildfire, and these forests that experience multiple rapid successions of natural and human-derived disturbances may cross thresholds and be changed catastrophically (Lindenmayer and Noss 2006).

The Klamath-Siskiyou ecoregion is currently dominated by biodiverse temperate coniferous forest and may be near a tipping point toward an alternative stable state (shrub/hardwood chaparral) with extensive loss of conifer forest, dominance by deciduous trees and shrubs, and recurring early-seral and young forest conditions (Tepley et al. 2017, Serra-Diaz et al. 2018). The region has experienced short intervals between recent high-severity fires coupled with intensive timber management in this mixed-severity fire regime area, and the likelihood of further shortening of fire-return intervals with climate change (Davis et al. 2017). Even where climate is suitable to sustain dense mature forests, early-seral and non-forest conditions may perpetuate because of a cycle of short-interval repeat burning and timber harvest and have dramatic impacts on biodiversity and wildlife habitats (Lindenmayer et al. 2011, Tepley et al. 2017). Under this scenario, the persistence of old-forest associated species, including northern spotted owls, within the Klamath-Siskiyou ecoregion would be further threatened.

It was recognized early in the history of northern spotted owl conservation that fire would play a major role in determining the success of management plans (Agee and Edmunds 1992). The 2011 federal northern spotted owl recovery

plan calls for increasing fire resiliency in dry forests with focus on active management outside of northern spotted owl core areas to meet project goals (USFWS 2011). For many dry forests in the western United States that historically experienced frequent, low- to moderate-severity fire regimes, prescribed fire and mechanical treatments have been effective at reducing surface fuel loads, forest structure, and potential fire severity (Stephens et al. 2009). In mixed-severity landscapes, the fire severity mosaic is highly variable and the effects of topography and climate are strong predictors for this regime, but forest conditions also are important and much less predictable and stable (Beaty and Taylor 2001), further complicating management decisions aimed at increasing fire resiliency of forests. Management actions employed in dry forest types to reduce wildfire risk may not work equivalently in mixed-severity regimes. Active management actions that include mechanical treatments degrade suitability of forests for nesting and roosting by northern spotted owls (Lesmeister et al. 2018) and may not always decrease risk of high-severity fire. Further, considering trends and forecasts for earlier spring snowmelt and longer fire seasons, climate change may exacerbate the effects of wildfire (Dale et al. 2001, Westerling et al. 2006), and thus the framed conundrum between northern spotted owl habitat and fire management in mixed-severity regimes. Our results indicate that older forest in late-successional reserves (i.e., northern spotted owl nesting/roosting habitat) with no active management can serve as a buffer to the effects of climate change and associated increase in wildfire occurrence. These multi-storied old forests in these environments enhance biodiversity and have the highest probability to persist through fire even in weather conditions associated with high fire activity.

Fuel-reduction treatments such as mechanical thinning can effectively reduce fire severity in the short term, but these treatments, by themselves, may not effectively mitigate long-term dynamics of fire behavior under severe weather conditions and may not restore the natural complexity of historical stand and landscape structure (Schoenagel et al. 2004). On the other hand, prescribed fire that mimics severity and return intervals of natural fire regimes in forests that historically

experienced fire can result in landscapes that are both self-regulating and resilient to fire (Parks et al. 2015). Prescribed fire is generally considered to be the most effective way to reduce the likelihood of high-severity fire in combination with mechanical treatments (Stephens et al. 2009). The 2013 Rim Fire in the Sierra Nevada, California, USA, burned with low severity in areas previously treated with prescribed fires, suggesting that prescribed burning was an effective management tool to reduce fire severity (Harris and Taylor 2017). Many fire-prone forests will require active management to restore ecosystem function, but no single prescription will be appropriate for all areas and, in some portions of the forests, minimal maintenance may be more sustainable in the long term (Noss et al. 2006). Within the Klamath-Siskiyou ecoregion, flexible and multi-scale land management approaches that promote diversity of forest types will likely enhance conservation of a range of species requiring different forest conditions for long-term persistence. An integral component of these approaches could include resistance strategies (i.e., no active management) to protect high-value older forest (Millar et al. 2007) and prescribed fire to promote and maintain a mix of forest conditions in this landscape characterized by mixed-ownership and mixed-severity fire regime. Ultimately, spatial heterogeneity that includes the buffering effects of northern spotted owl nesting/roosting habitat may serve as a stabilizing mechanism to climate change and reduce tendency toward large-scale catastrophic regime shifts.

ACKNOWLEDGMENTS

We are deeply indebted to R. Horn and many other field biologists for the long-term collection of northern spotted owl data presented here. We are grateful to G. McFadden and B. Hollen for support and facilitating primary funding from USDI Bureau of Land Management. Additional support was provided by USDA Forest Service Region 6 and Pacific Northwest Research Station. K. Kosel provided background information on fire suppression efforts for the fires. We thank T. Spies and two anonymous reviewers, whose suggested edits and comments on an earlier version greatly improved the manuscript. This publication represents the views of the authors, and any use of trade, firm, or product names is for descriptive purposes only and does not imply endorsement by the U.S. Government.

LITERATURE CITED

- Ackers, S. H., R. J. Davis, K. A. Olsen, and K. M. Dugger. 2015. The evolution of mapping habitat for northern spotted owls (*Strix occidentalis caurina*): a comparison of photo-interpreted, Landsat-based, and lidar-based habitat maps. *Remote Sensing of Environment* 156:361–373.
- Agee, J. K. 1993. Fire ecology of Pacific Northwest Forests. Island Press, Washington, D.C., USA.
- Agee, J. K. 2005. The complex nature of mixed severity fire regimes. In L. Taylor, J. Zelnik, S. Cadwallader, and B. Hughes, editors. Mixed severity fire regimes: ecology and management. Association for Fire Ecology, Spokane, Washington, USA.
- Agee, J. K. 2013. Historical range of variability in eastern Cascades forests, Washington, USA. *Landscape Ecology* 18:725–740.
- Agee, J. K., and R. L. Edmunds. 1992. Forest protection guidelines for the northern spotted owl, vol. 2. Pages 181–244 in USDI, editor. Recovery plan for the northern spotted owl-final draft. Volume 2. US Government Printing Office, Washington, D.C., USA.
- Ager, A. A., M. A. Finney, B. K. Kerns, and H. Maffei. 2007. Modeling wildfire risk to northern spotted owl (*Strix occidentalis caurina*) habitat in Central Oregon, USA. *Forest Ecology and Management* 246:45–56.
- Ager, A. A., N. M. Vaillant, M. A. Finney, and H. K. Preisler. 2012. Analyzing wildfire exposure and source-sink relationships on a fire prone forest landscape. *Forest Ecology and Management* 267:271–283.
- Alexander, J. D., N. E. Seavy, C. J. Ralph, and B. Hoggboom. 2006. Vegetation and topographical correlates of fire severity from two fires in the Klamath-Siskiyou region of Oregon and California. *International Journal of Wildland Fire* 15:237–245.
- Allen, C. D., et al. 2010. A global overview of drought and heat-induced tree mortality reveals emerging climate change risks for forests. *Forest Ecology and Management* 259:660–684.
- Anderson, H. E. 1982. Aids to determining fuel models for estimating fire behavior. INT-GTR-122. USDA Forest Service, Intermountain Forest and Range Experiment Station, Ogden, Utah, USA.
- Andrews, P. L. 2009. BehavePlus fire modeling system, version 5.0. Variables. RMRS-GTR-213. USDA Forest Service, Rocky Mountain Research Station, Fort Collins, Colorado, USA.
- Baker, W. L., T. T. Veblen, and R. L. Sherriff. 2007. Fire, fuels and restoration of ponderosa pine-Douglas fir forests in the Rocky Mountains, USA. *Journal of Biogeography* 34:251–269.

- Beatty, R. M., and A. H. Taylor. 2001. Spatial and temporal variation of fire regimes in a mixed conifer forest landscape, Southern Cascades, California, USA. *Journal of Biogeography* 28:955–966.
- Bessie, W. C., and E. A. Johnson. 1995. The relative importance of fuels and weather on fire behavior in subalpine forests. *Ecology* 76:747–762.
- Betts, M. G., B. Phalan, S. J. K. Frey, J. S. Rousseau, Z. Yang, and T. Albright. 2018. Old-growth forests buffer climate-sensitive bird populations from warming. *Diversity and Distributions* 24:439–447.
- Bradley, C. M., C. T. Hanson, and D. A. DellaSala. 2016. Does increased forest protection correspond to higher fire severity in frequent-fire forests of the western United States? *Ecosphere* 7:e01492.
- Bradshaw, L. S., J. E. Deeming, R. E. Burgan, and J. D. Cohen. 1983. The 1978 National Fire-Danger Rating System: technical Documentation. General Technical Report INT-169. USDA Forest Service, Intermountain Forest and Range Experiment Station, Ogden, Utah, USA.
- Bradstock, R. A., K. A. Hammill, L. Collins, and O. Price. 2010. Effects of weather, fuel and terrain on fire severity in topographically diverse landscapes of south-eastern Australia. *Landscape Ecology* 25:607–619.
- Bright, B. C., A. T. Hudak, R. E. Kennedy, and A. J. H. Meddens. 2014. Landsat time series and lidar as predictors of live and dead basal area across five bark beetle-affected forests. *IEEE Journal of Selected Topics in Applied Earth Observations and Remote Sensing* 7:3440–3452.
- Bunnell, F. L. 1995. Forest-dwelling vertebrate faunas and natural fire regimes in British Columbia: patterns and implications for conservation. *Conservation Biology* 9:636–644.
- Camp, A., C. Oliver, P. Hessburg, and R. Everett. 1997. Predicting late-successional fire refugia pre-dating European settlement in the Wenatchee Mountains. *Forest Ecology and Management* 95:63–77.
- Cansler, C. A., and D. McKenzie. 2012. How robust are burn severity indices when applied in a new region? Evaluation of alternate field-based and remote-sensing methods. *Remote Sensing* 4:456–483.
- Charnley, S., T. A. Spies, A. M. G. Barros, E. M. White, and K. A. Olsen. 2017. Diversity in forest management to reduce wildfire losses: implications for resilience. *Ecology and Society* 22:22.
- Chen, J., J. F. Franklin, and T. A. Spies. 1996. Growing-season microclimate gradients from clearcut edges into old-growth Douglas-fir forests. *Ecological Applications* 5:74–86.
- Clark, D. A., R. G. Anthony, and L. S. Andrews. 2011. Survival rates of northern spotted owls in post-fire landscapes of southwest Oregon. *Journal of Raptor Research* 45:38–47.
- Clark, D. A., R. G. Anthony, and L. S. Andrews. 2013. Relationship between wildfire, salvage logging, and occupancy of nesting territories by northern spotted owls. *Journal of Wildlife Management* 77:672–688.
- Clough, B. J., M. B. Russel, G. M. Domke, and C. W. Woodall. 2016. Quantifying allometric model uncertainty for plot-level live tree biomass stocks with a data-driven, hierarchical framework. *Forest Ecology and Management* 372:176–188.
- Cohen, J. D., and J. E. Deeming. 1985. The National Fire-Danger Rating System: basic equations. Pacific Southwest Forest and Range Experiment Station, Berkeley, California, USA.
- Collins, B. M., M. Kelly, J. W. van Wagtendonk, and S. L. Stephens. 2007. Spatial patterns of large natural fires in Sierra Nevada wilderness areas. *Landscape Ecology* 22:545–557.
- Countryman, C. M. 1955. Old-growth conversion also converts fire climate. *USDA Forest Service Fire Control Notes* 17:15–19.
- Dale, V. H., et al. 2001. Climate change and forest disturbances. *BioScience* 51:723.
- Dalton, M. M., J. T. Abatzoglou, L. Evers, and K. Hege-wisch. 2015. Projected changes in the energy release component under climate change in north-west predictive services areas. The Oregon Climate Change Research Institute (OCCRI), Corvallis, Oregon, USA.
- Davis, R. J., K. M. Dugger, S. Mohoric, L. Evers, and W. C. Aney. 2011. Northwest Forest Plan—the first 15 years (1994–2008): status and trends of northern spotted owl populations and habitat. General Technical Report PNW-GTR-850, USDA Forest Service, Pacific Northwest Research Station, Portland, Oregon, USA.
- Davis, R. J., B. Hollen, J. Hobson, J. E. Gower, and D. Keenum. 2016. Northwest Forest Plan—the first 20 years (1994–2013): status and trends of northern spotted owl habitats. PNW-GTR-929. USDA Forest Service, Pacific Northwest Research Station, Portland, Oregon, USA.
- Davis, R., Z. Yang, A. Yost, C. Belongie, and W. Cohen. 2017. The normal fire environment—Modeling environmental suitability for large forest wildfires using past, present, and future climate normals. *Forest Ecology and Management* 390:173–186.
- Deeming, J. E., and J. K. Brown. 1975. Fuel models in the national fire-danger rating system. *Journal of Forestry* 73:347–350.
- Donato, D. C., J. B. Fontaine, W. D. Robinson, J. B. Kauffman, and B. E. Law. 2009. Vegetation response to a short interval between high-severity

- wildfires in a mixed-evergreen forest. *Journal of Ecology* 97:142–154.
- Duff, T., R. Keane, T. Penman, and K. Tolhurst. 2017. Revisiting wildland fire fuel quantification methods: the challenge of understanding a dynamic, biotic entity. *Forests* 8:351.
- Dugger, K. M., et al. 2016. The effects of habitat, climate and Barred Owls on the long-term population demographics of Northern Spotted Owls. *Condor* 118:57–116.
- Eidenshink, J., B. Schwind, K. Brewer, Z. Ahu, B. Quayle, and S. Howard. 2007. A project for monitoring trends in burn severity. *Fire Ecology Special Issue* 3:3–21.
- Estes, B. L., E. E. Knapp, C. N. Skinner, J. D. Miller, and H. K. Preisler. 2017. Factors influencing fire severity under moderate burning conditions in the Klamath Mountains, northern California, USA. *Ecosphere* 8:e01794.
- Finney, M. A. 2004. FARSITE: fire area simulator—model development and evaluation. RMRS-RP-4 revised. USDA Forest Service, Rocky Mountain Research Station, Fort Collins, Colorado, USA.
- Fontaine, J. B., D. C. Donato, W. D. Robinson, B. E. Law, and J. B. Kauffman. 2009. Bird communities following high-severity fire: response to single and repeat fires in a mixed-evergreen forest, Oregon, USA. *Forest Ecology and Management* 257:1496–1504.
- Franklin, A. B., D. R. Anderson, E. D. Forsman, K. P. Burnham, and F. W. Wagner. 1996. Methods for collecting and analyzing demographic data on the Northern Spotted Owl. *Studies in Avian Biology* 17:12–20.
- Frey, S. J. K., A. S. Hadley, S. L. Johnson, M. Schulze, J. A. Jones, and M. G. Betts. 2016. Spatial models reveal the microclimatic buffering capacity of old-growth forests. *Science Advances* 2:e1501392.
- Glenn, E. M., D. B. Lesmeister, R. J. Davis, B. Hollen, and A. Poopatanapong. 2017. Estimating density of a territorial species in a dynamic landscape. *Landscape Ecology* 32:563–579.
- Google Earth Engine Team. 2015. Google Earth Engine: a planetary-scale geospatial analysis platform. <https://earthengine.google.com/>
- Gorelick, N., M. Hancher, M. Dixon, S. Ilyushchenko, D. Thau, and R. Moore. 2017. Google Earth Engine: planetary-scale geospatial analysis for everyone. *Remote Sensing of Environment* 202:18–27.
- Halofsky, J. E., et al. 2011. Mixed-severity fire regimes: lessons and hypotheses from the Klamath-Siskiyou Ecoregion. *Ecosphere* 2:art40.
- Harris, L., and A. H. Taylor. 2017. Previous burns and topography limit and reinforce fire severity in a large wildfire. *Ecosphere* 8:e02019.
- Harte, J., and E. A. Newman. 2014. Maximum information entropy: a foundation for ecological theory. *Trends in Ecology and Evolution* 29:384–389.
- Heyerdahl, E. K., L. B. Brubaker, and J. K. Agee. 2001. Spatial controls of historical fire regimes: a multi-scale example from the interior west, USA. *Ecology* 82:660–678.
- Hirzel, A. H., G. Le Lay, V. Helfer, C. Randin, and A. Guisan. 2006. Evaluating the ability of habitat suitability models to predict species presences. *Ecological Modelling* 199:142–152.
- Kennedy, R. E., Z. Yang, and W. B. Cohen. 2010. Detecting trends in forest disturbance and recovery using yearly Landsat time series: 1. LandTrendr—Temporal segmentation algorithms. *Remote Sensing of Environment* 114:2897–2910.
- Kennedy, R. E., Z. Yang, W. B. Cohen, E. Pfaff, J. Braaten, and P. Nelson. 2012. Spatial and temporal patterns of forest disturbance and regrowth within the area of the Northwest Forest Plan. *Remote Sensing of Environment* 122:117–133.
- Kitzberger, T., E. Araoz, J. H. Gowda, M. Mermoz, and J. M. Morales. 2012. Decreases in fire spread probability with forest age promotes alternative community states, reduced resilience to climate variability and large fire regime shifts. *Ecosystems* 15:97–112.
- Kleiber, C., and A. Zeileis. 2009. AER: applied Econometrics with R. R package version 1.1.
- Krawchuk, M. A., L. Haire, J. Coop, M.-A. Parisien, E. Whitman, G. Chong, and C. Miller. 2016. Topographic and fire weather controls of fire refugia in forested ecosystems of northwestern North America. *Ecosphere* 7:e01632.
- Lesmeister, D. B., R. J. Davis, P. H. Singleton, and J. D. Wiens. 2018. Northern spotted owl habitat and populations: status and threats. In T. Spies, P. Stine, R. Gravenmier, J. Long, and M. Reilly, editors. *Synthesis of science to inform land management within the northwest forest plan area*. PNW-GTR-966. USDA Forest Service, Pacific Northwest Research Station, Portland, Oregon, USA.
- Li, P., L. Jiang, and Z. Feng. 2013. Cross-comparison of vegetation indices derived from Landsat-7 enhanced thematic mapper plus (ETM+) and Landsat-8 operational land imager (OLI) sensors. *Remote Sensing* 6:310–329.
- Lindenmayer, D. B., R. J. Hobbs, G. E. Likens, C. J. Krebs, and S. C. Banks. 2011. Newly discovered landscape traps produce regime shifts in wet forests. *Proceedings of the National Academy of Sciences* 108:15887–15891.
- Lindenmayer, D. B., and R. F. Noss. 2006. Salvage logging, ecosystem processes, and biodiversity conservation. *Conservation Biology* 20:949–958.

- Lydersen, J. M., B. M. Collins, J. D. Miller, D. L. Fry, and S. L. Stephens. 2016. Relating fire-caused change in forest structure to remotely sensed estimates of fire severity. *Fire Ecology* 12:99–116.
- Manly, B. F. J., L. L. McDonald, D. L. Thomas, T. L. McDonald, and W. P. Erickson. 2010. Resource selection by animals: statistical design and analysis for field studies, 2nd edition.. Kluwer Academic Publishers, Dordrecht, The Netherlands.
- McGaughey, R. J. 2015. FUSION/LDV: providing fast, efficient, and flexible access to LiDAR, IFSAR and terrain datasets. U.S. Department of Agriculture, Forest Service, Pacific Northwest Research Station, Portland, Oregon, USA.
- Merow, C., M. J. Smith, T. C. Edwards, A. Guisan, S. M. McMahon, S. Normand, W. Thuiller, R. O. Wüest, N. E. Zimmermann, and J. Elith. 2014. What do we gain from simplicity versus complexity in species distribution models? *Ecography* 37:1267–1281.
- Millar, C. I., N. L. Stephenson, and S. L. Stephens. 2007. Climate change and forests of the future: managing in the face of uncertainty. *Ecological Applications* 17:2145–2151.
- Miller, J. D., E. E. Knapp, C. H. Key, C. N. Skinner, C. J. Isbell, R. M. Creasy, and J. W. Sherlock. 2009. Calibration and validation of the relative differenced Normalized Burn Ratio (RdNBR) to three measures of fire severity in the Sierra Nevada and Klamath Mountains, California, USA. *Remote Sensing of Environment* 113:645–656.
- Miller, J. D., and H. Safford. 2012. Trends in wildfire severity: 1984 to 2010 in the Sierra Nevada, Modoc Plateau, and Southern Cascades, California, USA. *Fire Ecology* 8:41–57.
- Miller, J. D., H. D. Safford, M. Crimmins, and A. E. Thode. 2008. Quantitative evidence for increasing forest fire severity in the Sierra Nevada and southern Cascade Mountains, California and Nevada, USA. *Ecosystems* 12:16–32.
- Miller, J. D., C. N. Skinner, H. D. Safford, E. E. Knapp, and C. M. Ramirez. 2012. Trends and causes of severity, size, and number of fires in northwestern California, USA. *Ecological Applications* 22:184–203.
- Miller, J. D., and A. E. Thode. 2007. Quantifying burn severity in a heterogeneous landscape with a relative version of the delta Normalized Burn Ratio (dNBR). *Remote Sensing of Environment* 109:66–80.
- Moreira, F., F. C. Rego, and P. G. Ferreira. 2001. Temporal (1958–1995) pattern of change in a cultural landscape of northwestern Portugal: implications for fire occurrence. *Landscape Ecology* 16:557–567.
- Moreira, F., P. Vaz, F. Catry, and J. S. Silva. 2009. Regional variations in wildfire susceptibility of land-cover types in Portugal: implications for landscape management to minimize fire hazard. *International Journal of Wildland Fire* 18:563–574.
- MTBS. 2017. MTBS Data Access: fire Level Geospatial Data. USDA Forest Service and USDI Geological Survey.
- NDMC. 2018. National Drought Mitigation Center, Drought Impact Summary. <https://droughtmonitor.unl.edu/DroughtSummary.aspx>
- Neary, D. G., C. C. Klopatek, L. F. DeBano, and P. F. Ffolliott. 1999. Fire effects on belowground sustainability: a review and synthesis. *Forest Ecology and Management* 122:51–71.
- Noss, R. F. 2000. High-risk ecosystems as foci for considering biodiversity and ecological integrity in ecological risk assessments. *Environmental Science & Policy* 3:321–332.
- Noss, R. F., J. F. Franklin, W. L. Baker, T. Schoennagel, and P. B. Moyle. 2006. Managing fire-prone forests in the western United States. *Frontiers in Ecology and the Environment* 4:481–487.
- Noss, R. F., J. R. Strittholt, P. Frost, K. Vance-Borland, and C. Carroll. 1999. A conservation plan for the Klamath-Siskiyou Ecoregion. *Natural Areas Journal* 19:392–411.
- O'Brien, R. M. 2007. A caution regarding rules of thumb for variance inflation factors. *Quality & Quantity* 41:673–690.
- Odion, D. C., et al. 2014. Examining historical and current mixed-severity fire regimes in ponderosa pine and mixed-conifer forests of western North America. *PLoS ONE* 9:e87852.
- OFRI. 2010. Federal Forestland in Oregon: coming to terms with active forest management of federal forestland. A Special Report of the Oregon Forest Resources Institute, Portland, Oregon, USA.
- Olson, D. M., and E. Dinerstein. 1998. The global 200: a representation approach to conserving the earth's most biologically valuable ecoregions. *Conservation Biology* 12:502–515.
- Parker, G. G., M. E. Harmon, M. A. Lefsky, J. Chen, R. V. Pelt, S. B. Weis, S. C. Thomas, W. E. Winner, D. C. Shaw, and J. F. Franklin. 2004. Three-dimensional structure of an old-growth *Pseudotsuga-Tsuga* canopy and its implications for radiation balance, microclimate, and gas exchange. *Ecosystems* 7:440–453.
- Parks, S. A., L. M. Holsinger, C. Miller, and C. R. Nelson. 2015. Wildland fire as a self-regulating mechanism: the role of previous burns and weather in limiting fire progression. *Ecological Applications* 25:1478–1492.
- Pausas, J. G., and J. E. Keeley. 2009. A burning story: the role of fire in the history of life. *BioScience* 59:593–601.

- Perry, D. A., P. F. Hessburg, C. N. Skinner, T. A. Spies, S. L. Stephens, A. H. Taylor, J. F. Franklin, B. McComb, and G. Riegel. 2011. The ecology of mixed severity fire regimes in Washington, Oregon, and Northern California. *Forest Ecology and Management* 262:703–717.
- Peterson, G. D. 2002. Contagious disturbance, ecological memory, and the emergence of landscape pattern. *Ecosystems* 5:329–338.
- Phillips, S. J., R. P. Anderson, and R. E. Schapire. 2006. Maximum entropy modeling of species geographic distributions. *Ecological Modelling* 190:231–259.
- Phillips, S. J., and J. Elith. 2013. On estimating probability of presence from use–availability or presence–background data. *Ecology* 94:1409–1419.
- R Core Team. 2016. R: a language and environment for statistical computing. R Foundation for Statistical Computing, Vienna, Austria.
- Raymond, C. L., and D. L. Peterson. 2005. Fuel treatments alter the effects of wildfire in a mixed-evergreen forest, Oregon, USA. *Canadian Journal of Forest Research* 35:2981–2995.
- Reilly, M. J., C. J. Dunn, G. W. Meigs, T. S. Spies, R. E. Kennedy, J. D. Bailey, and K. Briggs. 2017. Contemporary patterns of fire extent and severity in forests of the Pacific Northwest, USA (1985–2010). *Ecosphere* 8:e01695.
- Rockweit, J. T., A. B. Franklin, and P. C. Carlson. 2017. Differential impacts of wildfire on the population dynamics of an old-forest species. *Ecology* 98:1574–1582.
- Scheffer, M., and S. R. Carpenter. 2003. Catastrophic regime shifts in ecosystems: linking theory to observation. *Trends in Ecology & Evolution* 18:648–656.
- Schoennagel, T., T. T. Veblen, and W. H. Romme. 2004. The interaction of fire, fuels, and climate across Rocky Mountain forests. *BioScience* 54:661–676.
- Schroeder, T. A., M. A. Wulder, S. P. Healey, and G. G. Moisen. 2011. Mapping wildfire and clearcut harvest disturbances in boreal forests with Landsat time series data. *Remote Sensing of Environment* 115:1421–1433.
- Scott, J. H., and R. E. Burgan. 2005. Standard fire behavior fuel models: a comprehensive set for use with Rothermel's surface fire spread model. RMRS-GTR-153. USDA Forest Service, Rocky Mountain Research Station, Fort Collins, Colorado, USA.
- Serra-Diaz, J. M., C. Maxwell, M. S. Lucash, R. M. Scheller, D. M. Laflower, A. D. Miller, A. J. Tepley, H. E. Epstein, K. J. Anderson-Teixeira, and J. R. Thompson. 2018. Disequilibrium of fire-prone forests sets the stage for a rapid decline in conifer dominance during the 21st century. *Scientific Reports* 8:6749.
- Sousa, W. P. 1984. The role of disturbance in natural communities. *Annual Review of Ecology and Systematics* 15:353–359.
- Sovern, S. G., D. B. Lesmeister, K. M. Dugger, M. S. Pruett, R. J. Davis, and J. M. Jenkins. 2019. Activity center selection by northern spotted owls. *Journal of Wildlife Management Early View*. <https://doi.org/10.1002/jwmg/21632>
- Spies, T. A., M. A. Hemstrom, A. Youngblood, and S. Hummel. 2006. Conserving old-growth forest diversity in disturbance-prone landscapes. *Conservation Biology* 20:351–362.
- Spies, T. A., P. F. Hessburg, C. N. Skinner, K. J. Puettmann, M. J. Reilly, R. J. Davis, J. A. Kertis, J. W. Long, and D. C. Shaw. 2018. Old growth, disturbance, forest succession, and management in the area of the Northwest Forest Plan. In T. A. Spies, P. Stine, R. Gravenmier, J. W. Long, and M. J. Reilly, editors. *Synthesis of Science to inform land management within the northwest forest plan area*. PNW-GTR-966. USDA Forest Service, Pacific Northwest Research Station, Portland, Oregon, USA.
- Stephens, S. L., et al. 2009. Fire treatment effects on vegetation structure, fuels, and potential fire severity in western U.S. forests. *Ecological Applications* 19:305–320.
- Taylor, A. H., and C. N. Skinner. 1998. Fire history and landscape dynamics in a late-successional reserve, Klamath Mountains, California, USA. *Forest Ecology and Management* 111:285–301.
- Tepley, A. J., J. R. Thompson, H. E. Epstein, and K. J. Anderson-Teixeira. 2017. Vulnerability to forest loss through altered postfire recovery dynamics in a warming climate in the Klamath Mountains. *Global Change Biology* 23:4117–4132.
- Thompson, J. R., and T. A. Spies. 2009. Vegetation and weather explain variation in crown damage within a large mixed-severity wildfire. *Forest Ecology and Management* 258:1684–1694.
- Thompson, J. R., and T. A. Spies. 2010. Factors associated with crown damage following recurring mixed-severity wildfires and post-fire management in southwestern Oregon. *Landscape Ecology* 25:775–789.
- Thompson, J. R., T. A. Spies, and L. M. Ganio. 2007. Reburn severity in managed and unmanaged vegetation in a large wildfire. *Proceedings of the National Academy of Sciences* 104:10743–10748.
- Turner, M. G., and W. H. Romme. 1994. Landscape dynamics in crow fire ecosystems. *Landscape Ecology* 9:59–77.
- USDA and USDI. 1994. Final supplemental environmental impact statement on management of habitat for late-successional and old-growth forest

- related species within the range of the northern spotted owl. USFS, Portland, Oregon, USA.
- USFWS. 1990. Endangered and threatened wildlife and plants: determination of threatened status for the northern spotted owl. Federal Register 55:26114–26194.
- USFWS. 2011. Revised recovery plan for the northern spotted owl (*Strix occidentalis caurina*). USDI Fish and Wildlife Service, Portland, Oregon, USA.
- Van Pelt, R. 2008. Identifying old trees and forest in Eastern Washington. Washington State Department of Natural Resources, Olympia, Washington, USA.
- Vance-Borland, K. W. 1999. Physical habitat classification for conservation planning in the Klamath Mountains region. Thesis. Oregon State University, Corvallis, Oregon, USA.
- Weatherspoon, C. P., S. J. Husari, and J. W. van Wagtenonk. 1992. Fire and fuels management in relation to owl habitat in forests of the Sierra Nevada and southern California. In J. Verner, K. S. McKelvey, B. R. Noon, R. J. Gutierrez, G. I. Gould Jr., and T. W. Beck, editors. The California spotted owl: a technical assessment of its current status. PSW-GTR-133. USDA Forest Service, Pacific Southwest Research Station, Albany, California, USA.
- Westerling, A. L., H. G. Hidalgo, D. R. Cayan, and T. W. Swetnam. 2006. Warming and earlier spring increase western U.S. forest wildfire activity. Science 313:940–943.
- Wilk, R. J., D. B. Lesmeister, and E. D. Forsman. 2018. Nest trees of northern spotted owls (*Strix occidentalis caurina*) in Washington and Oregon, USA. PLoS ONE 13:e0197887.
- Zald, H. S. J., and C. J. Dunn. 2018. Severe fire weather and intensive forest management increase fire severity in a multi-ownership landscape. Ecological Applications 28:1068–1080.

SUPPORTING INFORMATION

Additional Supporting Information may be found online at: <http://onlinelibrary.wiley.com/doi/10.1002/ecs2.2696/full>

ATTACHMENT D

EXHIBIT D

ATTACHMENT D

Ecological Importance of Large-Diameter Trees in a Temperate Mixed-Conifer Forest

James A. Lutz^{1*}, Andrew J. Larson², Mark E. Swanson³, James A. Freund⁴

1 College of the Environment, University of Washington, Seattle, Washington, United States of America, **2** Department of Forest Management, University of Montana, Missoula, Montana, United States of America, **3** School of the Environment, Washington State University, Pullman, Washington, United States of America, **4** School of Environmental and Forest Sciences, University of Washington, Seattle, Washington, United States of America

Abstract

Large-diameter trees dominate the structure, dynamics and function of many temperate and tropical forests. Although both scaling theory and competition theory make predictions about the relative composition and spatial patterns of large-diameter trees compared to smaller diameter trees, these predictions are rarely tested. We established a 25.6 ha permanent plot within which we tagged and mapped all trees ≥ 1 cm dbh, all snags ≥ 10 cm dbh, and all shrub patches ≥ 2 m². We sampled downed woody debris, litter, and duff with line intercept transects. Aboveground live biomass of the 23 woody species was 507.9 Mg/ha, of which 503.8 Mg/ha was trees (SD = 114.3 Mg/ha) and 4.1 Mg/ha was shrubs. Aboveground live and dead biomass was 652.0 Mg/ha. Large-diameter trees comprised 1.4% of individuals but 49.4% of biomass, with biomass dominated by *Abies concolor* and *Pinus lambertiana* (93.0% of tree biomass). The large-diameter component dominated the biomass of snags (59.5%) and contributed significantly to that of woody debris (36.6%). Traditional scaling theory was not a good model for either the relationship between tree radii and tree abundance or tree biomass. Spatial patterning of large-diameter trees of the three most abundant species differed from that of small-diameter conspecifics. For *A. concolor* and *P. lambertiana*, as well as all trees pooled, large-diameter and small-diameter trees were spatially segregated through inter-tree distances < 10 m. Competition alone was insufficient to explain the spatial patterns of large-diameter trees and spatial relationships between large-diameter and small-diameter trees. Long-term observations may reveal regulation of forest biomass and spatial structure by fire, wind, pathogens, and insects in Sierra Nevada mixed-conifer forests. Sustaining ecosystem functions such as carbon storage or provision of specialist species habitat will likely require different management strategies when the functions are performed primarily by a few large trees as opposed to many smaller trees.

Citation: Lutz JA, Larson AJ, Swanson ME, Freund JA (2012) Ecological Importance of Large-Diameter Trees in a Temperate Mixed-Conifer Forest. PLoS ONE 7(5): e36131. doi:10.1371/journal.pone.0036131

Editor: Ben Bond-Lamberty, DOE Pacific Northwest National Laboratory, United States of America

Received: February 14, 2012; **Accepted:** March 28, 2012; **Published:** May 2, 2012

Copyright: © 2012 Lutz et al. This is an open-access article distributed under the terms of the Creative Commons Attribution License, which permits unrestricted use, distribution, and reproduction in any medium, provided the original author and source are credited.

Funding: Funding was received from the Smithsonian Institution Center for Tropical Forest Science (<http://www.ctfs.si.edu/>) and the University of Washington College of the Environment (<http://coenv.washington.edu/>). In-kind support was received from the University of Washington, the University of Montana, Washington State University, the US Geological Survey, and Yosemite National Park. The funders had no role in study design, data collection and analysis, decision to publish, or preparation of the manuscript.

Competing Interests: The authors have declared that no competing interests exist.

* E-mail: jlutz@uw.edu

Introduction

Large-diameter trees dominate the structure, dynamics, and function of many temperate and tropical forest ecosystems and are of considerable scientific and social interest. They comprise a large fraction of forest wood volume, biomass and carbon stocks [1,2], and modulate stand-level leaf area, transpiration, and microclimates [3,4]. Large-diameter trees contribute disproportionately to reproduction [5], influence the rate and pattern of tree regeneration and forest succession [6], and originate further disturbance by crushing or injuring neighboring trees when they fall to the ground [7,8]. Arboreal wildlife species preferentially occupy large trees as habitat (e.g. [9]), and the greater structural complexity of large tree crowns [10] supports habitat for obligate wildlife species (e.g. [11]), unique epiphyte communities [12], and soil development and water storage within the forest canopy [13].

Large-diameter trees continue to contribute disproportionately to forest ecosystem structure and function after they die. Dead large-diameter trees persist as standing snags for many years,

providing additional wildlife habitat. In temperate forests large-diameter logs may persist on the forest floor for centuries, where they continue to provide habitat for diverse assemblages of vertebrates and invertebrates and microorganisms, store carbon and other nutrients, serve as substrates for tree regeneration, and play numerous other functional roles [14,15].

Human societies derive many non-timber values from large-diameter trees. Tree ring chronologies from large trees provide long records of past forest development and disturbance [16], as well as proxy records of annual climatic variation [17]; they are an important source of the data required to test and refine ecological theories and models. Large trees are culturally [18] and spiritually important [19] in many societies; individuals and organizations maintain large tree registries (e.g., [20]), and government agencies manage parks and preserves dedicated to the conservation of exceptionally large trees, such as Redwood and Sequoia & Kings Canyon National Parks in California, USA.

Populations of large-diameter trees can be intractable study subjects. Large-diameter trees occur at low densities and estimates

ATTACHMENT D

of their abundance, spatial patterns, and contributions to ecosystem function (e.g. biomass) are subject to high rates of sampling error [21,22]. Consequently, descriptive statistics and hypothesis tests for large-diameter trees require very large sample plots [22]. The combination of low abundance and low mortality rates [8,23,24] make detecting changes in demographic rates or spatial patterns of large-diameter trees even more difficult, further underscoring the requirement for large sample plots. Conventional studies based on small (1 ha to 4 ha) plots often do not contain enough large-diameter trees to conduct even community-level (i.e., pooled across species) analyses (e.g., [24]). Consequently, despite their ecological and cultural significance, relatively less is known – and with greater uncertainty – about the abundance, distribution, and dynamics of large-diameter trees.

Predictions for large-diameter trees

Scaling theory and competition theory both provide frameworks for predictions about the relative contributions of large-diameter structures to aboveground biomass, the spatial distribution of large-diameter trees, and the spatial relationships between large-diameter and small-diameter trees. Scaling theory predicts that a relatively few trees in the largest diameter classes will dominate stand-level aboveground biomass [25,26], and that there are continuous relationships between tree diameter and density, and total forest biomass. However, scaling theory has been repeatedly shown to underpredict large tree densities and mortality rates [27,28]. This discrepancy likely arises because trees rarely die from competition once they reach large sizes but rather succumb to biological agents, physical disturbances, and combinations thereof [8,29]. Although scaling theory predicts dominance of biomass pools by a few large individuals, the simplifying assumptions about tree mortality embedded in the theory may render it inadequate to predict accurately either the aggregate large tree contributions to stand biomass or the local-scale variation. We were interested in quantifying the actual contribution of large-diameter pieces to aboveground biomass pools—which should be substantial [14]—because predictions from scaling theory alone may not be accurate enough to serve as inputs into ecosystem models or to support sound natural resource policies and management.

Tree spatial patterns integrate past tree-tree interactions. Competition theory predicts that distance and density-dependent growth and mortality during forest development will lead to increasingly uniform spatial patterns in larger diameter classes [30,31]. Therefore, the arrangement of large-diameter trees should be more uniform than small-diameter trees, and the largest trees should exhibit spatial regularity at the tree neighborhood scale. Competition theory also predicts spatial relationships between large and small-diameter trees. When large trees compete asymmetrically with small trees their respective spatial locations become segregated because seedlings preferentially survive and grow into understory trees where they are not suppressed by larger competitors [30,32,33].

Our study was motivated by three purposes: (1) determine the degree to which predictions from ecological theory hold for contemporary populations of large-diameter trees; (2) establish a permanent forest research plot of sufficient size to detect and attribute forest ecosystem change, including for the large-diameter component, in order to test future predictions against longitudinal data; and (3) support current management efforts to restore large-diameter tree populations in Sierra Nevada mixed-conifer forest, which were dramatically reduced by widespread logging throughout the range of this important forest type during the 19th and 20th centuries [34,35]. We established the Yosemite Forest Dynamics Plot (YFDP) in an old-growth Sierra Nevada mixed-conifer forest

and within the plot quantified the relative contribution of large-diameter trees, snags, and down woody debris to the aboveground biomass pools, the comparative spatial patterns of large-diameter and small-diameter trees, and spatial relationships between them.

Results

Species composition

In the 25.6 ha of the Yosemite Forest Dynamics Plot (YFDP), there were 34,458 live stems ≥ 1 cm dbh of 11 tree species (Table 1) and 3.87 ha (15.1%) of continuous shrub cover comprising 12 shrub species that reach 1 cm in diameter at 1.37 m height (Table 2). Eleven plant families were represented. All woody stems were native plants. Live tree basal area was 64.3 m²/ha and biomass was 503.8 Mg/ha (SD = 114.3 Mg/ha) (Table 3). Of the three principal species by biomass (*Pinus lambertiana*, *Abies concolor*, and *Calocedrus decurrens*), *P. lambertiana* had a much higher average biomass (Fig. 1) and exhibited a rotated-sigmoid diameter distribution, possibly reflecting lower mortality of middle-aged individuals (Fig. 2). Diameter distributions of *A. concolor* and *C. decurrens* followed negative exponential distributions (Fig. 2). Relative dominance of *Abies concolor* declines at diameters above ~ 90 cm (Fig. 2). *Calocedrus decurrens* exhibits almost an order of magnitude less biomass than either *P. lambertiana* or *A. concolor* (Fig. 2). However, some individuals do persist into large diameter classes (Fig. 2). Live shrub biomass was 4.1 Mg/ha (Table 2). There were 2,697 snags (19.9% of living trees of this diameter). Biomass of snags ≥ 10 cm dbh was 43.0 Mg/ha (Table 3). Biomass of the forest floor components (Table 3, Fig. 3) was 53.1 Mg/ha for down woody debris (SD = 102.9 Mg/ha) and 48.0 Mg/ha (SD = 22.5) for fine fuels (Table 3). Litter and duff averaged 1.05 cm (SD = 0.38) and 1.20 cm (SD = 0.68) in depth, respectively. A correlogram analysis of woody debris volumes as estimated by the 20 m line intercept segments showed no spatial correlation in fuel loads at any distance. Total above-ground biomass of living and dead components was 652.0 Mg/ha.

Large-diameter composition

The large diameter component dominated most biomass pools (Table 3). For living trees, 1.4% of individuals had dbh ≥ 100 cm dbh (19.1 large-diameter trees ha⁻¹), but these individuals comprised 49.4% of tree biomass. For snags, 12.4% were large-diameter, comprising 59.5% of snag biomass. Snags ≥ 100 cm dbh were about half as numerous (42.9%) as live trees ≥ 100 cm dbh. There were 10 pieces of woody debris ≥ 100 cm (3.8%) measured on the line intercepts, and the large debris component comprised 36.6% of down woody debris biomass. There is, by definition, no large-diameter component to shrubs, fine fuels, litter or duff. Overall, large-diameter structures constituted 44.9% of above-ground live and dead biomass.

Scaling theory was informative for the relationship between tree density and diameter class ($r^2 = 0.84$); the theoretical relationship under-predicted the density of medium and large trees, but over-predicted the density of trees ≥ 170 cm dbh (Fig. 2). Although informative, the relationship between tree density and diameter class was better explained by a negative exponential distribution ($r^2 = 0.99$). The theoretical relationship between tree radii and biomass was not informative ($r^2 = 0.00$) (Fig. 2).

Spatial patterns

Small-diameter subpopulations of *A. concolor*, *C. decurrens*, *P. lambertiana*, as well as all tree species combined, exhibited significant aggregation relative to the null model of complete spatial randomness (CSR) from 0–9 m (Monte Carlo goodness-of-

ATTACHMENT D

Table 1. Tree species within the Yosemite Forest Dynamics Plot in 2010.

Tree species	Family	Density (stems/ha)	Basal area (m ² /ha)	Stems ≥ 1 cm dbh	Stems ≥ 10 cm dbh	Stems ≥ 100 cm dbh	Large-diameter prop. (%)
Trees ≥1 cm dbh							
<i>Abies concolor</i>	Pinaceae	956.3	29.28	24,481	9,634	103	0.4
<i>Pinus lambertiana</i>	Pinaceae	185.5	28.75	4,748	2,166	339	7.1
<i>Cornus nuttallii</i>	Cornaceae	92.5	0.26	2,368	287	-	-
<i>Calocedrus decurrens</i>	Cupressaceae	62.2	4.78	1,592	685	45	2.8
<i>Quercus kelloggii</i>	Fagaceae	43.3	1.12	1,109	735	-	-
<i>Prunus</i> spp.	Rosaceae	5.0	t	128	-	-	-
<i>Abies magnifica</i>	Pinaceae	0.4	0.06	11	5	1	9.1
<i>Salix scouleriana</i>	Salicaceae	0.4	t	11	-	-	-
<i>Pseudotsuga menziesii</i>	Pinaceae	0.2	0.03	6	3	1	16.7
<i>Pinus ponderosa</i>	Pinaceae	t	0.01	2	1	-	-
<i>Rhamnus californica</i>	Rhamnaceae	t	t	1	-	-	-
Live tree total		1,346.0	64.32	34,458	13,516	489	1.4
Snags ≥10 cm dbh							
<i>Abies concolor</i>					1,971	64	3.2
<i>Pinus lambertiana</i>					530	133	25.1
<i>Quercus kelloggii</i>					127	-	-
<i>Calocedrus decurrens</i>					46	5	10.9
<i>Pseudotsuga menziesii</i>					1	1	100.0
<i>Cornus nuttallii</i>					1	-	-
Unknown					21	7	33.3
Dead tree total					2,697	210	7.8

t – trace; less than one tree per 10 ha; less than 0.01 m²/ha.
doi:10.1371/journal.pone.0036131.t001

Table 2. Shrub species occurring in patches of continuous cover ≥2 m² within the Yosemite Forest Dynamics Plot in 2010.

Species	Family	Cover (m ²)	Demography plot data		YFDP extrapolation	
			Density ^a (stems/m ²)	Biomass (kg/m ²)	Density (stems/ha)	Biomass (Mg/ha)
<i>Arctostaphylos patula</i>	Ericaceae	2,524	5.333	14.747	526	1.454
<i>Ceanothus cordulatus</i>	Rhamnaceae	1,220	1.667	1.189	79	0.057
<i>Ceanothus integerrimus</i>	Rhamnaceae	194	7.875	10.427	60	0.079
<i>Ceanothus parvifolius</i>	Rhamnaceae	187	3.250	1.527	24	0.011
<i>Chrysolepis sempervirens</i>	Fagaceae	13,082	3.167	1.464	1,618	0.748
<i>Corylus cornuta</i> var. <i>californica</i>	Betulaceae	13,310	1.000	1.565	520	0.814
<i>Cornus sericea</i>	Cornaceae	2,320	8.667	6.087	785	0.552
<i>Leucothoe davisiae</i>	Ericaceae	2,151	0.250	2.430	21	0.204
<i>Vaccinium uliginosum</i>	Ericaceae	2,937	0.083	1.069	10	0.123
<i>Sambucus racemosa</i> ^b	Adoxaceae	13	1.000	1.565	t	0.001
<i>Rhododendron occidentale</i> ^c	Ericaceae	687	0.083	1.069	2	0.029
<i>Ribes nevadense</i> ^c	Grossulariaceae	7	0.083	1.069	t	t
<i>Ribes roezlii</i> ^d	Grossulariaceae	66	0	0.534	0	0.001
Total		38,698			3,645	4.103

Baseline density and biomass equations were generated from 25, 2 m×2 m shrub demography plots, and allometric equations from [90].

^aStems ≥1 cm dbh.

^bSubstituted biomass and density for *Corylus cornuta* var. *californica*.

^cSubstituted biomass and density for *Vaccinium uliginosum*.

^dSubstituted one half the biomass of *Vaccinium uliginosum*. No stems reach 1 cm dbh.

t – trace; <1 stem/ha; <1 kg/ha.

doi:10.1371/journal.pone.0036131.t002

ATTACHMENT D

Table 3. Biomass within the Yosemite Forest Dynamics Plot in 2010.

Tree species	Biomass ≥1 cm (Mg/ha)		Biomass ≥10 cm (Mg/ha)		Biomass ≥100 cm (Mg/ha)		Large-diameter prop. (%)
Trees ≥1 cm							
<i>Abies concolor</i>	214.703	(37.505)	210.533	(36.916)	47.983	(8.950)	22.3
<i>Pinus lambertiana</i>	254.039	(66.623)	253.380	(66.508)	187.345	(47.594)	73.7
<i>Cornus nuttallii</i>	1.411	(0.301)	0.765	(0.199)	-	-	-
<i>Calocedrus decurrens</i>	24.978	(7.911)	24.764	(7.845)	12.964	(4.076)	51.9
<i>Quercus kelloggii</i>	7.849	(1.935)	7.736	(1.907)	-	-	-
<i>Prunus</i> spp.	0.005	(0.002)	-	-	-	-	-
<i>Abies magnifica</i>	0.609	(0.110)	0.609	(0.110)	0.469	(0.078)	77.0
<i>Salix scouleriana</i>	t	t	-	-	-	-	-
<i>Pseudotsuga menziesii</i>	0.146	(0.033)	0.144	(0.032)	0.134	(0.030)	91.8
<i>Pinus ponderosa</i>	0.064	(0.003)	0.064	(0.003)	-	-	-
<i>Rhamnus californica</i>	t	t	-	-	-	-	-
Live tree total	503.804	(114.346)	497.994	(113.444)	248.896	(60.651)	49.4
Snags ≥10 cm							
<i>Abies concolor</i>			20.276		6.708		33.1
<i>Pinus lambertiana</i>			21.167		17.959		84.8
<i>Quercus kelloggii</i>			0.244		-		-
<i>Calocedrus decurrens</i>			0.893		0.551		61.7
<i>Pseudotsuga menziesii</i>			0.196		0.196		100.0
<i>Cornus nuttallii</i>			t		-		-
Unknown			0.181		0.147		81.2
Dead tree total			42.958		25.562		59.5
Forest floor woody debris ≥10 cm			53.099	(102.897)	19.444	(78.977)	36.6
Shrubs total	4.103		-		-		-
Forest floor fine fuels [†]							
100-hour fuels	4.562	(4.820)	-		-		-
10-hour fuels	5.176	(3.487)	-		-		-
1-hour fuels	1.129	(0.834)	-		-		-
Litter	13.150	(6.244)	-		-		-
Duff	24.017	(16.517)	-		-		-
Total fine fuels	48.034	(22.495)	-		-		-

Biomass is shown to three significant figures (corresponding to 1 kg/ha) to facilitate comparison between less abundant, small-diameter species and more abundant species (standard deviation shown in parentheses). Standard deviation of tree biomass was based on the root mean squared error of the underlying allometric equations, and standard deviation of down woody debris biomass was based on Brown's method [89]. Biomass of shrubs and snags are derived from cover (m^2) or measured dimensions and fixed wood density values [see Methods]. Total of living and dead biomass pools was 652.0 Mg/ha.

t – trace; less than 1 kg/ha.

[†]Fine litter measured by fuel classifications [88]. 100-hour fuels are defined as twigs and fragments with diameter 1" to 3" (2.5 cm to 7.6 cm); 10-hour fuels have diameter 0.25" to 1" (0.6 cm to 2.5 cm); 1-hour fuels have diameter 0" to 0.25" (0 cm to 0.6 cm). Litter and duff are measured by depth.

doi:10.1371/journal.pone.0036131.t003

fit tests; *A. concolor*: $P=0.004$; *C. decurrens*: $P=0.001$; *P. lambertiana*: $P=0.001$, all trees: $P=0.004$). In other words, when averaged across all points in a given pattern, small-diameter trees of these species have more neighbors of the same type located within a circle with a radius of 9 m than would be expected if tree locations were completely independent of each other. $\hat{L}(r)$ values for small-diameter stems of both *P. lambertiana* and *A. concolor* rose steeply at small scales (Fig. 4), reaching a plateau at about 20 m, indicating that the strong spatial aggregation in these respective subpopulations primarily manifests at scales <20 m. The $\hat{L}(r)$ curves for small-diameter *C. decurrens* stems rose steadily from 0–80 m, indicating moderate but consistent clustering across the entire range of scales analyzed (Fig. 4).

The spatial arrangement of large-diameter *A. concolor*, *C. decurrens* and *P. lambertiana* individually, and for all species combined, were not different from complete spatial randomness from 0–9 m (Monte Carlo goodness-of-fit tests; *A. concolor*: $P=0.012$; *C. decurrens*: $P=0.074$; *P. lambertiana*: $P=0.132$; all trees: $P=0.057$). However, the behavior of the individual $\hat{L}(r)$ curves from 0–80 m reveals spatial structure within large-diameter *A. concolor* and *P. lambertiana* subpopulations at other interpoint distances (Fig. 4). The empirical $\hat{L}(r)$ curve (Fig. 4) for large-diameter *P. lambertiana* was negative and steadily decreased from 0–2 m, tracking the lower boundary of the simulation envelope, indicating spatial inhibition at these scales. From 2–4 m the large-diameter *P. lambertiana* $\hat{L}(r)$ curve sharply increased, providing evidence of

ATTACHMENT D

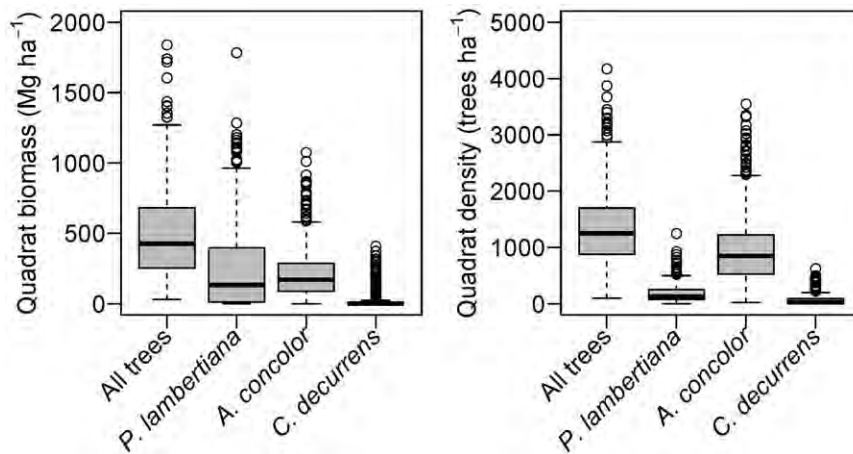


Figure 1. Heterogeneity in biomass and density of the principal tree species of the Yosemite Forest Dynamics Plot. Each boxplot represents values from the 640, 20 m×20 m quadrats of the plot.
doi:10.1371/journal.pone.0036131.g001

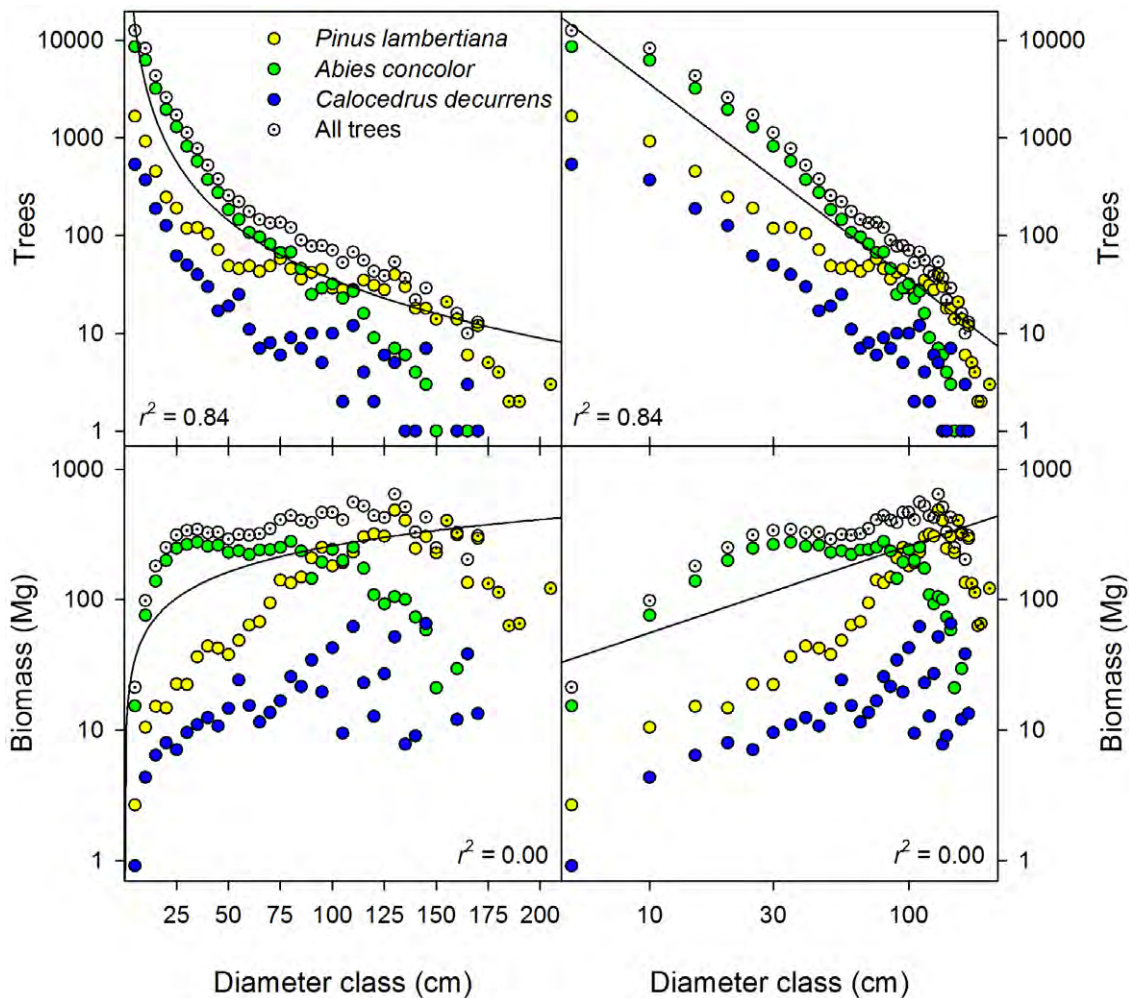


Figure 2. Diameter distribution of the number of trees and the biomass of trees in the Yosemite Forest Dynamics Plot. Each point represents a 5 cm diameter class (first bin; 1 cm≤dbh<5 cm) of the trees from the entire 25.6 ha plot (34,458 live stems ≥1 cm dbh totaling 12,897 Mg); identical data are shown with linear diameter bins (left) and log diameter (right). Solid lines represent the best fitting equation of the form specified by scaling theory, $tree\ density = Ar^{-2}$ ($r^2 = 0.84$) and $biomass = Br^{2/3}$ ($r^2 = 0.00$), where r is tree radius.
doi:10.1371/journal.pone.0036131.g002

ATTACHMENT D

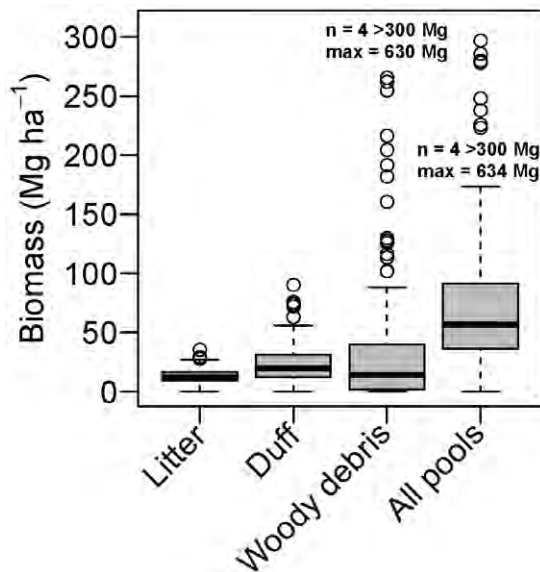


Figure 3. Biomass of forest floor components of the Yosemite Forest Dynamics Plot. Each boxplot represents values from 112 transects of 20 m (2.24 km of line transects). Outliers represent intercepted pieces of large-diameter debris.
doi:10.1371/journal.pone.0036131.g003

spatial clustering at these scales, with continued evidence for clustering occurring out to 22 m, where the empirical value reached the upper bound of the simulation envelope. Large-diameter *A. concolor* also exhibited rapid changes in spatial pattern at small scales, with steadily decreasing $\hat{L}(r)$ values from 0–3 m (evidence of spatial inhibition) then increasing sharply from 3–5.5 m, indicating strong spatial clustering over this short range of scales. A sustained increase in the $\hat{L}(r)$ curve for large-diameter *A. concolor* from 13–38 m provided further evidence for spatial aggregation at larger scales. The $\hat{L}(r)$ curves for large-diameter *C. decurrens* stems rose steadily from 0–80 m, reaching the upper bound of the simulation envelope at 30 m, indicating moderate but consistent clustering across these scales.

The relative spatial patterns of large- and small-diameter trees differed for all species combined, as well as for *P. lambertiana* and *A. concolor*, but not for *C. decurrens*. Small-diameter *P. lambertiana* were always more aggregated than large conspecifics at the same scale. Large-diameter *A. concolor* were less aggregated than conspecific small-diameter trees at scales of 0–3 m, then rapidly became more aggregated than small trees from 3–6 m, and remained so up to 80 m (Fig. 4). The spatial pattern of large and small *C. decurrens* subpopulations was similar from 0–80 m (Fig. 4).

We found evidence for negative associations between large-diameter and small-diameter *P. lambertiana* and *A. concolor*, and for all tree species combined, relative to the population independence hypothesis when evaluated from 0–9 m (Monte Carlo goodness-of-fit tests; *A. concolor*: $P=0.001$; *P. lambertiana*: $P=0.001$; all trees: $P=0.001$). Spatial locations of large-diameter and small-diameter *C. decurrens* were independent at the 9 m neighborhood scale (Monte Carlo goodness-of-fit test; $P=0.378$). The $\hat{L}_{1,2}(r)$ curve for *P. lambertiana* (Fig. 5) indicates spatial repulsion between large and small from 0–10 m, and modest attraction from 10–40 m. The $\hat{L}_{1,2}(r)$ curve for *A. concolor* decreased steadily from 0–80 m, but was only outside the simulation envelope at scales less than 10 m. Large and small stems of *C. decurrens* were spatially attracted from 15–80 m, with the empirical $\hat{L}_{1,2}(r)$ curve at or beyond the upper boundary of the simulation envelope (Fig. 5).

Discussion

The relative proportion of large trees varies in old-growth forests worldwide [28], and at 49.4%, the contribution that large-diameter trees make to the total biomass of the YFDP is higher than in most other forests. Although some forests have almost all of their biomass concentrated in large-diameter trees (most notably *Sequoia sempervirens*; [13,36]), the biomass of most forest types is concentrated in trees <100 cm dbh. In a 1 ha plot in tropical moist forests of Rondônia, Brazil, Brown et al. [1] found that three trees ≥ 100 cm dbh had biomass of 64.3 Mg compared to a total aboveground biomass of 285 Mg (22.6%). In 5.15 ha of neotropical lowland rain forest in Costa Rica, Clark & Clark [2] found that trees ≥ 70 cm dbh comprised 27% of the biomass of 241 Mg/ha ($\sim 18\%$ for trees ≥ 100 cm dbh; [2], Fig. 1). In semi-evergreen forests of northeast India, Baishya et al. [37] found $\sim 12\%$ of biomass in trees ≥ 100 cm dbh, and plantation forests or forests that are recovering from disturbance may have few or no large-diameter trees, even when stem density and diversity are high [37,38].

Within the Smithsonian Center for Tropical Forest Science network (<http://www.ctfs.si.edu/plots/>), only the *Gilbertiodendron deweyi* (mbau) forest of the Congo has a higher live biomass, with the dipterocarp forests of Malaysia having equivalent live biomass (Table 4, [39,40]). Other old-growth forest types have a biomass of $\sim 60\%$ of the YFDP [39]. When the live and dead biomass are considered together, the biomass of the YFDP is 652.0 Mg/ha, currently the highest in the CTFS network. Unlike either of the high-biomass tropical plots, live biomass in the YFDP is dominated by two tree species (both Pinaceae), *Pinus lambertiana* (50.4% biomass) and *Abies concolor* (42.6% biomass), while down woody debris biomass is similarly dominated by these two species (57% and 32%, respectively). Scaling theory did not describe the distribution of biomass in this system (Fig. 2). Differences between theory and this forest are likely driven by the reoccurrence of fire throughout the period of stand development, and because of mortality rates that vary with diameter class. However, the very high levels of heterogeneity in density and biomass at 20 m scales (Fig. 1) would make scaling theory even less informative in study areas smaller than the YFDP.

Although the YFDP has high biomass, the diversity of woody plants ≥ 1 cm dbh is the lowest among the CTFS plots ≥ 25 ha. The combination of summer drought and winter snow may reduce the species pool. Other temperate plots (Changbaishan, Wabikon, and the Smithsonian Ecological Research Center, SERC) have higher species diversity [41,42]. However, those plots either receive precipitation evenly distributed throughout the year (Wabikon and SERC), or the wet season coincides with the growing season (Changbaishan).

One almost ubiquitous difficulty in biomass analyses of large-diameter trees is the uncertainty of allometric equations. The use of previously published equations to predict biomass of large trees from ground-level measurement of DBH assumes that these equations were based on adequate sampling of large trees. However, most allometric equations for tree biomass have been developed from dissection of 10–50 trees [43], and the number of large trees used in formulating equations is very low. Some of the large-diameter *P. lambertiana*, *A. concolor*, and *C. decurrens* exceeded the maximum diameter of any that have been dissected, and for these individual trees, substitute species were used [see Appendix S1]. Moreover, DBH is often a poor predictor of whole-tree biomass as large tree DBH is a poor reflection of tree size [10]. Nonetheless, many comparative studies of primary forest biomass use allometric equations that probably predict large-diameter tree

ATTACHMENT D

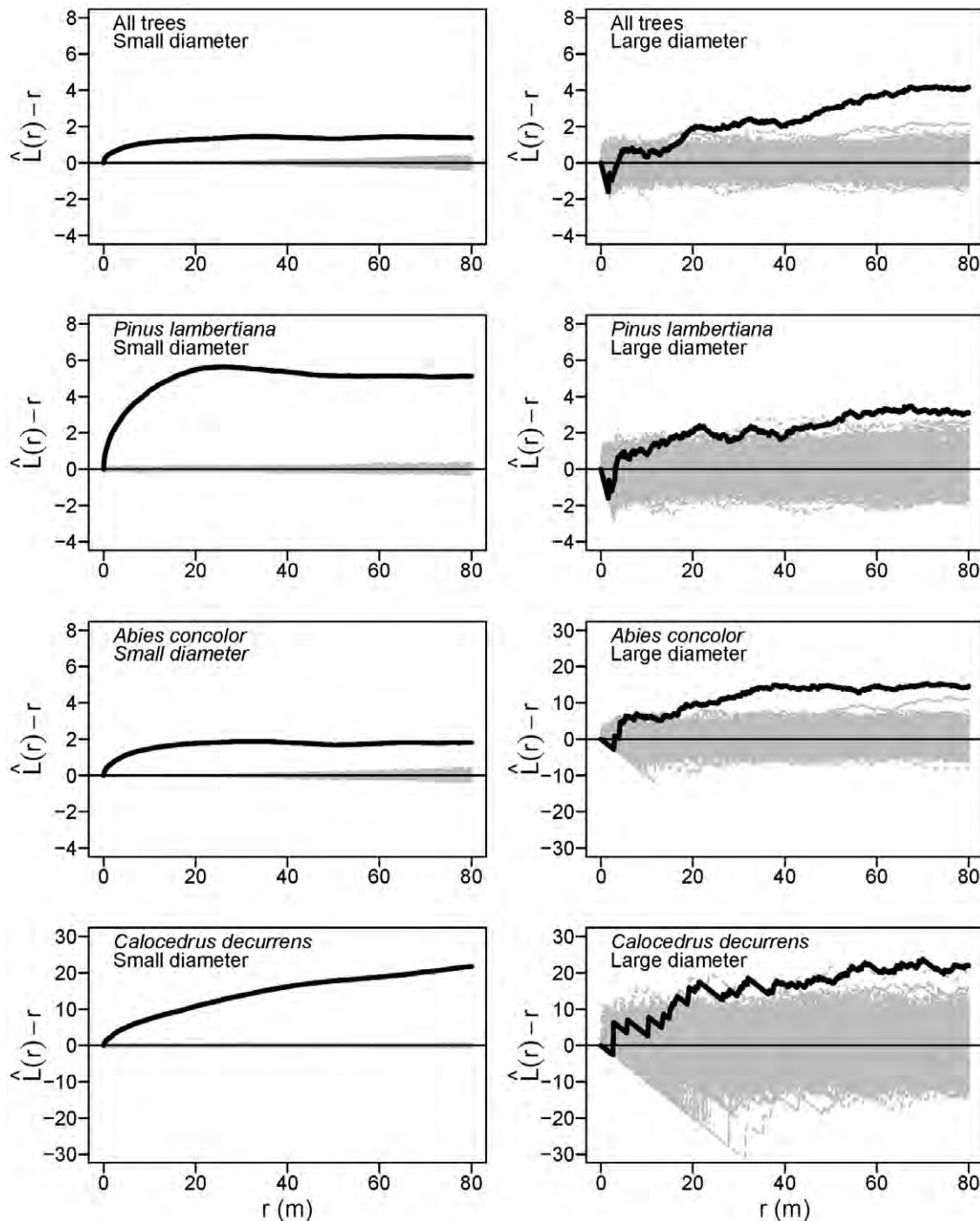


Figure 4. Univariate tree spatial patterns in the Yosemite Forest Dynamics Plot. Solid black lines show the $\hat{L}(r)$ statistic for the actual patterns, where r is the intertree distance; thin gray lines show $\hat{L}(r)$ curves for 999 simulations of complete spatial randomness. Positive values indicate spatial clumping and negative values indicate spatial regularity. Large-diameter trees are ≥ 100 cm dbh; small-diameter trees are < 100 cm dbh.

doi:10.1371/journal.pone.0036131.g004

biomass poorly (i.e. [39,40]). Our calculations (Table 3) have been presented to a level of 1 kg/ha to enable comparison of forest dominants with less common and smaller tree species and likely represent an underestimation of whole tree biomass. However, the SD of biomass for principal species in the YFDP is 17% to 32% of the calculated value (Table 3), so the uncertainty of the large-diameter biomass could be larger than the smaller biomass pools.

Biomass calculations for shrubs, snags, and woody debris also embody several simplifying assumptions (i.e. uniform stem density per unit area, single measures of diameter, simple geometry, no hollows in snags) that could lead to imprecise biomass totals.

Unlike the tropical forests where decomposition of snags and woody debris is rapid, the YFDP features considerable biomass of standing and down woody debris, also a characteristic of

ATTACHMENT D

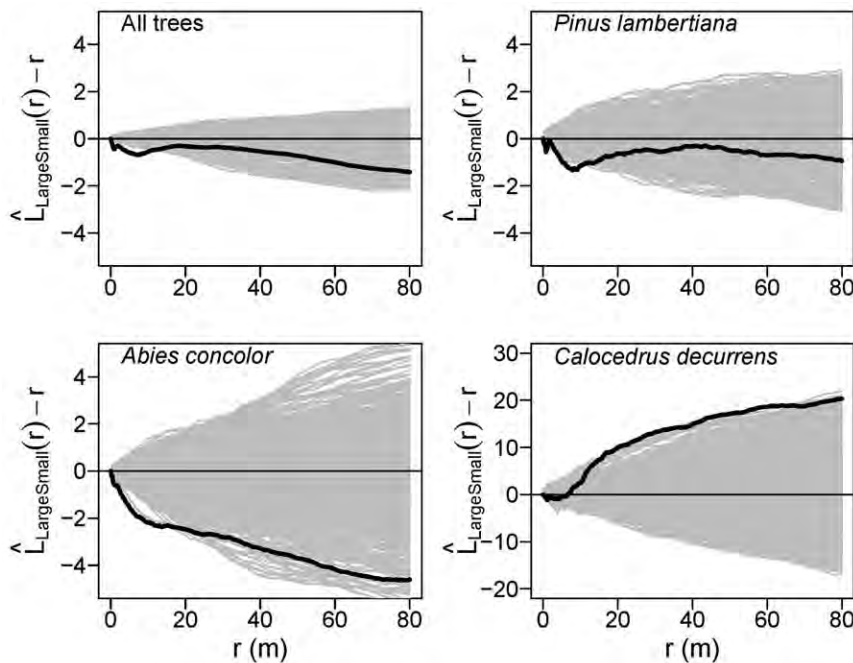


Figure 5. Spatial interactions between large-diameter and small-diameter trees. Solid black lines show the $\hat{L}_{1,2}(r)$ statistic for the actual pattern, where r is the intertree distance; thin gray lines show $\hat{L}(r)$ curves for 999 patterns simulated by synchronous random toroidal shifts of large and small tree subpopulations. Positive values indicate spatial attraction and negative values indicate spatial repulsion. Large-diameter trees are ≥ 100 cm dbh; small-diameter trees are < 100 cm dbh.

doi:10.1371/journal.pone.0036131.g005

temperate broadleaf forests [44]. The combination of snowy winters and dry summers contributes to slow decomposition, and even the fastest decomposing tree species (*A. concolor*) has a half-life of 14 years [14]. Large-diameter snags account for a relatively high proportion of total snag biomass, while large-diameter down woody debris accounted for a lower proportion of the woody debris. This may be due to low-severity fires in the historical period that might have consumed large-diameter woody debris via glowing combustion, decreasing the proportion relative to snag representation [45], or because small snags tend to fall over relatively quickly, thus being better represented in the woody debris pool. The lack of spatial correlation of the woody debris at any scale suggests that, while mortality may be non-random, tree and snag-fall events may result in loss of spatial pattern between standing individuals and the patterns of down wood they produce.

The observed univariate spatial patterns of large and small trees provide modest support for the inference that past competition

contributed to the present spatial distribution of large-diameter trees. In particular, the increasing spatial uniformity from small to large size classes is consistent with competition theory [30,31]. However, the observed random arrangement of large trees at neighborhood scales differs from spatial uniformity expected when competition is the dominant process affecting tree spatial patterns. Previous studies of large-diameter tree spatial patterns in Sierra Nevada mixed-conifer forests agree with our findings (N.B., with large-diameter thresholds differing somewhat from 100 cm). Van Pelt and Franklin [32] found that main canopy trees at Giant Forest in Sequoia National Park were not different from spatial randomness at scales < 9 m. In addition, their empirical $\hat{L}(r)$ curve [32] was similar to those for *P. lambertiana* and *A. concolor* in the YFDP: inhibited from 0–1.5 m. The observed small-scale (0–3 m) inhibition is most likely due to physical requirements for minimum hard core spacing due to the large size of the boles and limits to crown plasticity, although resource competition may

Table 4. Comparison of the Yosemite Forest Dynamics Plot with other Smithsonian CTFs-affiliated forest plots.

Location	Latitude	Forest type	Live biomass (Mg/ha)	Live and dead biomass (Mg/ha)	Woody species	Citation
Changbaishan, China	42.2°N	Korean pine mixed forest	318.9		52	Hao et al. [41]
Yosemite, USA	37.8°N	Mixed-conifer forest	507.9	652.0	23	This study
BCI, Panama	9.2°N	Lowland tropical moist forest	306.5		299	Chave et al. [39]
Lambir, Malaysia	4.2°N	Mixed dipterocarp forest	497.2		1,182	Chave et al. [39]
Lenda, Congo	1.3°N	Mbau forest	549.7		423	Makena et al. [40]

Live biomass includes woody stems ≥ 1 cm dbh. Live and dead biomass includes snags ≥ 10 cm dbh and forest floor components as well as live biomass (also see [38] for basal area comparisons among additional large forest plots.

doi:10.1371/journal.pone.0036131.t004

ATTACHMENT D

contribute as well. At Teakettle Experimental Forest (an old-growth, mixed-conifer forest 100 km south of the YFDP), stems ≥ 76 cm dbh were randomly arranged from 0–60 m [46]. However, Bonnicksen and Stone [47] found that main canopy *P. lambertiana* and *A. concolor* trees were uniformly spaced in a giant sequoia mixed-conifer forest in Kings Canyon National Park. Past competition and competitive mortality undoubtedly influenced the development of spatial patterning in large-diameter tree populations in some Sierra Nevada mixed-conifer forests [48,49]. However, it appears that the cumulative effects of any past self-thinning in the YFDP were not sufficient to completely override the effects of clustered or random tree regeneration [50], non-random mortality or other potential sources of heterogeneity in the distribution of large-diameter trees.

We must thus consider processes other than competition to explain spatial patterns of large-diameter trees in the YFDP. For the fire-tolerant and modestly shade-tolerant *P. lambertiana*, meso-scale aggregation (2–22 m) in the large-diameter subpopulation is most readily explained by clustered establishment, consistent with a disturbance-centric model of forest dynamics and spatial pattern formation in low and mixed severity fire regimes [51]. For *A. concolor* (fire intolerant when small) the strong clustering of large-diameter trees at local (3–5.5 m) and intermediate (13–38 m) scales may originate from fire refugia that allowed groups of *A. concolor* to survive and reach large diameters. Clustered establishment alone (e.g., in gaps or in moisture-receiving microtopographic features) could explain the aggregation of large *A. concolor* stems, but given the historical regime of frequent fire [51] it is likely that heterogeneous fire effects leading to patchy *A. concolor* survival also contributed.

The observed spatial segregation of large and small trees is consistent with inference that competitive interactions between these size classes influence their spatial relationships and overall forest structure. Spatial segregation of large and small trees has been documented in many other forest types (i.e. [33] and the studies reviewed therein), including Sierra Nevada mixed-conifer forests [32]. Spatial segregation between large and small trees may arise from asymmetrical competition for light and gap-phase regeneration [33]. However, we acknowledge that other mechanisms acting at the tree neighborhood scale potentially contribute to the observed spatial segregation between large and small *A. concolor* and *P. lambertiana*, including crushing mortality by falling limbs and bole fragments from live large-diameter trees [8,52], and the spatially heterogeneous buildup and subsequent burning of surface fuels. Additionally, in the absence of fire large-diameter *P. lambertiana* accumulate a deep mound of debris (bark and needles) at their base [53], a substrate not suitable for seedling establishment, which would also give rise to repulsion between large and small stems. Prior to fire exclusion, Sierra Nevada mixed-conifer forests had low densities of small-diameter trees [35,51]; the observed repulsion between tree diameter classes may also be due to preferential tree establishment in fire-maintained openings following disruption of the historical fire regime [54].

Conclusions

We assessed the degree to which scaling theory and competition theory explain variation of accumulated biomass and spatial patterns across the tree size spectrum. These respective bodies of theory were not sufficient to explain our empirical results. However, our results do not indicate the rejection of these theories. Scaling theory is clearly a powerful framework for developing novel ecological insights, but our results and those of others [21,27,28] show that the requisite simplifying assumptions render predictions from scaling theory inappropriate as inputs in

to ecosystem models or as a basis for natural resource decision making. A vast body of accumulated scientific literature details mechanisms and outcomes of plant competition; our results do not contradict this theory. Rather, competition theory alone was insufficient to explain our empirical measurements of tree spatial patterns, strengthening the conclusion that competition is not the dominant control of tree population dynamics and forest development in old-growth Sierra Nevada mixed-conifer forests [24].

We predict that long-term observations at our study site and other sites throughout the range of Sierra Nevada mixed-conifer forests will reveal strong top-down regulation of forest biomass and spatial structure by pathogens, insects and physical disturbances, especially in old-growth forests. We also suggest that, in forests with high functional inequality across the tree size spectrum, ecosystem function may be more sensitive to natural perturbations, environmental change or management actions – at least those affecting the large-diameter trees – than in forests where ecosystem function is distributed more equitably across the tree size spectrum. Sustaining ecological functions and services, such as carbon storage or provision of habitat for specialist species, will likely require different forest management strategies when the ecosystem services are provided primarily by a few large trees as opposed to many smaller trees.

Materials and Methods

Study area

The Yosemite Forest Dynamics Plot (YFDP) is located in the mixed-conifer forest of the western portion of Yosemite National Park (Fig. 6). The plot is approximately oriented to the cardinal directions with dimensions of 800 m east to west and 320 m north to south (25.6 ha) centered at 37.77°N, 119.82°W. Elevation ranges between 1774.1 m and 1911.3 m for a vertical relief of 137.2 m (Fig. S1). The YFDP is comprised of vegetation types within the *Abies concolor* – *Pinus lambertiana* Forest Alliance [55], including *Abies concolor*-*Pinus lambertiana*/*Ceanothus cordulatus* Forest, *Abies concolor*-*Pinus lambertiana*/*Maianthemum racemosum* (*Smilacina racemosa*, Hickman [56])-*Disporum hookeri* Forest, *Abies concolor*-*Calocedrus decurrens*-*Pinus lambertiana*/*Cornus nuttallii*/*Corylus cornuta* var. *californica* Forest, *Abies concolor*-*Calocedrus decurrens*-*Pinus lambertiana*/*Adenocaulon bicolor* Forest, and *Abies concolor*-*Pinus lambertiana*-*Calocedrus decurrens*/*Chrysolepis sempervirens* Forest, classified according to the U.S. National Vegetation Classification [57] (Fig. 7). Overall demographic rates in Sierra Nevada conifer forests between 1500 m and 2000 m elevation are approximately 1.5% [58,59]. Canopy emergents, principally *P. lambertiana* and *A. concolor*, reach 60 m to 67 m in height. The soils of the YFDP are derived from metamorphic parent material. Approximately 85% of the soils of the YFDP are metasedimentary soils of the Clarksledge-Ultic Palixeralfs complex with a water-holding capacity of 160 mm in the top 150 cm of the soil profile [60]. The soils of the northwest 15% of the YFDP are Humic Dystroxerepts-Typic Haploxeralfs-Inceptic soils of the Haploxeralfs complex with a water-holding capacity of 70 mm in the top 150 cm of the soil profile [60]. Plant nomenclature follows Hickman [56].

The climate at the YFDP is Mediterranean, with cool moist winters and long dry summers. Between 1971 and 2000, the modeled mean temperature range at the YFDP was from 12.2°C to 26.1°C in July and –2.7°C to 9.4°C in February; annual precipitation was 1061 mm, with most precipitation falling in the winter months as snow [61,62]. Snow depth on April 1st is generally 100 cm to 150 cm. The seasonality of precipitation

ATTACHMENT D

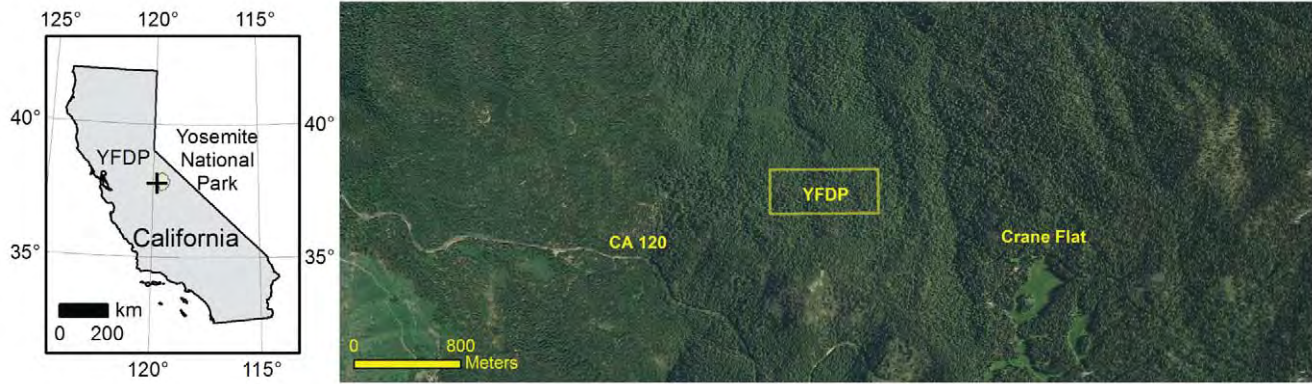


Figure 6. Location of the Yosemite Forest Dynamics Plot (YFDP). The YFDP is located near the western boundary of Yosemite National Park (left, green) in the lower montane, mixed-conifer zone of the Sierra Nevada, California, USA. The plot is located in relatively uniform, late-successional forest near Crane Flat (right). The area immediately north of the YFDP was logged in the early 1930s, as was the area comprising the western 1/3 of the image.

doi:10.1371/journal.pone.0036131.g006

yields a summer drought with a mean annual climatic water deficit of 200 mm [63] (Fig. S2).

Disturbance processes: fire, wind, insects, pathogens, vertebrates, and human use

Fire is the dominant natural disturbance process in Sierra Nevada mixed-conifer forests [64]. The fire regime is of mixed severity with fires burning in a mosaic of high, moderate, and low

severities. The pre-Euro-American fire return interval for the YFDP was 10–13 years [51]. The combination of repeated fire and other disturbances gives rise to a fine-grained mosaic structure [50,65]. During the Landsat TM period of record (1984–2011), most fires in this forest type have been either low severity management-ignited prescribed fires or moderate and high severity wildfires [66–68]. The YFDP has not burned since comprehensive park fire records were initiated in 1930. Mechan-



Figure 7. Structure and composition of the Yosemite Forest Dynamics Plot (YFDP). Four images from different parts of the YFDP illustrate defining characteristics of the ecosystem. Most precipitation falls in the winter as snow yielding a spring snowpack of approximately 1 m (upper left image, April 11, 2011). The forest is composed of an overstory of large-diameter trees with abundant but heterogeneous shrub and herbaceous layers (upper right image, June 22, 2009). Shrubs can be locally dense enough to reduce tree recruitment (lower left image, June 22, 2009). Although most trees and shrubs are evergreen, the presence of the deciduous species *Cornus nuttallii* and *Quercus kelloggii* results in seasonal openings in the canopy (lower right image, November 11, 2010). All photos by J. A. Lutz.

doi:10.1371/journal.pone.0036131.g007

ATTACHMENT D

ical damage, whether from wind, snow, or crushing of smaller individuals by falling trees or tree parts contributes to stand structural development [8,69]. Many of the larger trees in the YFDP have broken tops, or reiterated tops that have regrown following damage.

Insects are important agents of mortality, with most common conifer tree species having coevolved bark beetles (family Scolytidae) that are always present at low levels [70,71]. In particular, *Dendroctonus ponderosa* (mountain pine beetle) attacks *Pinus lambertiana* and *P. ponderosa* and *Scolytus ventralis* attacks *Abies concolor* and *A. magnifica*. Other bark beetles such as *S. subscaber*, *D. valens* (red turpentine beetle) and *Ips* spp. have been less abundant in the recent past but contribute to tree mortality. *Quercus kelloggii* (California black oak) also has associated bark beetles (*Pseudopityophthorus* spp.). *Conophthorus ponderosae* (ponderosa pine cone beetle) is present and can reduce the reproductive output of *P. lambertiana*.

Pathogens include the structural root rots *Armillaria* spp. [72], *Heterobasidion annosum* [73] and *Phaeolus schweinitzii* [71]. The root rots spread through roots and root contacts at rates of approximately 30 cm per year, and hence tend to occur in patches. *Armillaria* spp. are somewhat generalist pathogens and attack *Abies* spp., *Prunus* spp., and *Cornus nuttallii*. *Phaeolus schweinitzii* infects *Pinus lambertiana* and *Abies* spp., but tends to progress much more slowly than *Heterobasidion* and *Armillaria*. *Pinus lambertiana* is also affected by the introduced pathogen *Cronartium ribicola* [74]. *Calocedrus decurrens*, *Abies concolor*, and *Quercus kelloggii* are hosts to mistletoes: *Phoradendron libocedri* on *C. decurrens*, *Phoradendron pauciflorum* and *Arceuthobium abietinum* on *A. concolor*, and *Phoradendron villosum* on *Q. kelloggii* [75]. These mistletoes are distributed both by birds, and in the case of *Arceuthobium abietinum*, also by explosive discharge that can carry seeds up to 16 m (typically 10 m; [75]).

The YFDP has a rich fauna, with most species of herbivores and their predators present since prior to Euro-American settlement. Large mammals include *Ursus americanus* (black bear), *Felis concolor* (mountain lion), *Canis latrans* (coyote), and *Odocoileus hemionus* (mule deer). Altogether, vertebrate species observed within similar forest types within 5 km of the YFDP include 16 rodent species, 12 bat species, 7 carnivore species, one hooved mammal, 7 raptor species, 38 passerine species, 5 amphibian species, and 7 reptile species Table S1, [76–79]).

Yosemite has been inhabited at least since 100 AD [80]. Immediately prior to Euro-American discovery of the region in 1833 [81] and the subsequent entry of Euro-Americans into Yosemite Valley in 1851 [82], the area was occupied by the Central Sierra Miwok and the Southern Sierra Miwok [83]. Because the YFDP contains only intermittent streams and seeps, Native American use of the site was probably low, and modification of the fire regime at this site by Native Americans appears unlikely [84]. The YFDP is near the transit route from Hazel Green to Crane Flat used by sheepherders in the late 19th century. John Muir may have passed through or near the YFDP on July 9th, 1869 – the topography and vegetation are consistent with his journal entry [85].

The original Yosemite Grant (1864) placed Yosemite Valley and the Mariposa Grove of giant sequoia in protected status. The YFDP lies within what was a single parcel of land prior to its inclusion into Yosemite National Park in 1930. The parcel of land immediately to the north of the YFDP (~20 m from the plot boundary) was in different ownership and was logged in the early 1930s. The northwest corner of the YFDP contains four large stumps that appear to be associated with the logging of the parcel to the north. Logging outside the YFDP continued throughout the 1920s until the area was purchased by the National Park Service and John D. Rockefeller. The area of unlogged sugar pine

containing the YFDP is today termed the Rockefeller Grove in honor of J.D. Rockefeller's role in protecting this part of the park.

Surveying

We established a sampling grid using Total Stations with accuracies of at least 5 seconds of arc (Leica models 1100, Builder R200M Power, Builder 505, and TC 2003). We set permanent markers on nominal 20 m centers, offset for tree boles, coarse woody debris, or large rocks. Survey closure across the plot was 0.18 m northing, 0.05 m easting, and 0.03 m elevation (~1/5000). In addition to the sampling grid, we established control points in open areas near the plot where marginal Global Positioning System (GPS) reception was possible. Three survey-grade GPS receivers (Magellan Z-Extremes) were used to establish control to and across the plot, using a reference station approximately 2 km from the plot (MGROVE, PID DF8617 on the California State Plane Coordinate System and being described in the National Geodetic Survey Datasheets). The GPS receivers collected data at 10 second intervals for 2–6 hours. The static GPS measurements were post-processed with GNSS Solutions software (Magellan Navigation, Inc., pro.magellangps.com), with final accuracies in the range of 0.01 m horizontally and 0.02 m vertically. We transformed the plot grid to Universal Transverse Mercator coordinates with Lewis and Lewis Coordinated Geometry software (Lewis and Lewis Land Surveying Equipment, Inc., www.lewis-lewis.net). We augmented the ground survey with LiDAR-derived elevation data at 1 m horizontal resolution. Aerial LiDAR data were acquired on 22 July 2010 by Watershed Sciences Inc., Corvallis, Oregon with a density of 40 returns per square meter. Ground survey data and the LiDAR-derived ground model coincided with a root-mean-squared error of 0.15 m.

Field sampling of trees, shrubs, snags, and woody debris

In the summers of 2009 and 2010 we tagged and mapped all live trees ≥ 1 cm at breast height (1.37 m; dbh), following the methods of Condit [86], with some alterations. We measured tree diameter at 1.37 m (instead of 1.30 m), and trees large enough to accept a nail were nailed at the point of measurement, both in keeping with research methods of the western United States. We used stainless steel tags, nails and wire to increase tag longevity in this fire-dominated ecosystem. We measured tree locations from the surveyed grid points with a combination of hand-held lasers (Laser Technologies Impulse 200 LR), mirror compasses, and tapes. Tapes were laid south to north between adjacent grid points, and a perpendicular angle determined by sighting a target bole with a mirror compass. The distance from the tape to each tree was then measured with the hand-held lasers. We calculated the location of the tree center from the horizontal and perpendicular references to the surveyed grid points and dbh with the assumptions of cylindrical boles and linear interpolation of elevation between adjacent grid points. All measurements were slope corrected.

We mapped continuous patches of shrub cover ≥ 2 m² relative to the 20 m sampling grid with a combination of tapes, mirror compasses, and lasers. For each shrub patch we recorded the shape of the patch as a polygon, as well as average and maximum shrub heights. To convert between shrub cover and the number of stems and biomass in the YFDP, we established 25 shrub demography plots for nine species (*Arctostaphylos patula*, *Ceanothus cordulatus*, *Ceanothus integerrimus*, *Ceanothus parvifolius*, *Chrysolepis sempervirens*, *Corylus cornuta* var. *californica*, *Cornus sericia*, *Leucothoe davisiae*, and *Vaccinium uliginosum*). We tagged every woody stem in each of these 2 m×2 m plots. We measured basal diameter for

ATTACHMENT D

every woody stem. If stems were 1.37 m tall (or long), we made an additional measurement at 1.37 m.

We tagged and mapped dead trees ≥ 10 cm dbh and ≥ 1.8 m in height. For each snag, we collected height, top diameter (with a laser), and snag decomposition class data (following [87]; class 1 = least decayed, class 5 = most decayed). We did not collect data on trees < 10 cm dbh at the original census because of the difficulty in finding small stems a few years after they die.

To measure down woody debris, litter, and duff, we established four interior fuel transects totaling 2.24 km (112 transects of 20 m). We used the National Park Service fuel monitoring protocols [88], in turn based on Brown transects [89]. Litter included freshly fallen leaves, needles, bark, flakes, acorns, cones, cone scales, and miscellaneous vegetative parts [88]. Duff included the fermentation and humus layers, not the fresh material of the litter layer. Down woody material included branches, trunks of trees, and shrubs that had fallen on or within 2 m above the ground [88]. Intercept diameter and decay class were recorded for all intercepted woody debris ≥ 10 cm in intercept diameter (measured perpendicular to the orientation of the piece of debris). To sample fine woody debris we used portions of the 112 line intercept transects ~ 2 m for material 0 cm–2.5 cm in diameter (1-hour and 10-hour fuels), and 4 m for material 2.5 cm–7.6 cm (100-hour fuels). We calculated biomass according to Brown's method [89].

Biomass calculations

We reviewed all allometric equations from the two compendia of equations for North America [43,90] and selected those that best matched the species, geographic location, diameter ranges, and tree densities of the YFDP [44,90–93]. Where no allometric equation existed, we substituted a species (or diameter class within a species) that was a close match for morphology and wood density (see Appendix S1 for details). Because no whole tree biomass equations exist for the largest individuals of the species in the YFDP, we used proxy species. For the largest *Abies concolor* ($n = 112$) we used bole equations for *A. procera*. For *Pinus lambertiana*, we used branch and foliage equations for *Pseudotsuga menziesii*, and for the *Pinus lambertiana* > 179.6 cm dbh ($n = 7$), we used a bole equation for *Pseudotsuga menziesii*. Additionally, no biomass equations exist for branches and foliage of *Abies* > 110 cm dbh or *Pseudotsuga* > 162 cm dbh. For those trees we capped the branch and foliage biomass at the values associated with trees of diameter 110 cm and 162 cm, respectively. All biomass calculations were made within the data ranges of the selected allometric equations (See Appendix S1 for full details of allometric equations). We calculated an error term for tree biomass from the underlying allometric equations. The root mean square error (standard error of estimate) of the allometric equations was transformed from log units to arithmetic units of standard deviation (i.e. Mg/ha) [92]. We defined large diameter structures as pieces ≥ 100 cm in diameter to facilitate comparisons with earlier studies of large-diameter trees in old-growth conifer forests on the Pacific Slope of western North America.

We calculated the biomass of the stems within each 4 m² shrub demography plot based on allometric equations using basal diameter [90]. We used the biomass of the stems within the demography plots and the total area of shrub patches ≥ 2 m² within the YFDP to calculate total shrub biomass. We used the demography plot data for sampled species as proxies for the four species without demography plots (*Corylus cornuta* var. *californica* for *Sambucus racemosa*, *Vaccinium uliginosum* for *Rhododendron occidentale* and *Ribes nevadense*, and one-half the value of *Vaccinium uliginosum* for *Ribes roezlii*). To calculate a stem density equivalent to the standard

Smithsonian CTFS protocol [86], we tallied the number of stems that were ≥ 1 cm dbh in each shrub demography plot and multiplied by the area of each shrub patch ≥ 2 m². Details of allometric equations are in Appendix S1.

We calculated snag biomass using the wood density values of Harmon et al. [15] and a bole volume calculated as a frustum of a cone. We calculated the biomass of litter and duff using the methods of Stephens et al. [94]. For down woody debris larger than 1000-hour fuels (4 inches; ~ 10 cm), we used the large transect protocols of Harmon et al. [15], and we calculated the mass of woody debris using the methods of Harmon and Sexton [87].

To compare actual density and biomass values with the predictions of scaling theory, we used the equations from West et al. [26]. Specifically, we compared the actual diameter (radius) distribution with their predicted distribution, $(r) \propto \frac{1}{r^2}$, where r is tree radius at breast height. We then reconfigured their radius-mass relationship, $r \propto m^{3/8}$, to $m \propto r^{8/3}$, where r is tree radius and m is tree biomass, and combined the mass and frequency equations to develop a relationship for total biomass in terms of tree radius: $(m \propto r^{8/3})(n \propto r^{-2})$ or $biomass \propto r^{2/3}$. We used 5 cm diameter bins (2.5 cm radius bins) to regress curves of these forms to the data.

Quantifying spatial pattern

We quantified global spatial patterns with the univariate and bivariate forms of Ripley's K function, using the square root (L function) transformation in all cases. For a given fully mapped pattern, an estimate of the $L(r)$ function, the statistic $\hat{L}(r)$, is based on the count of neighboring points occurring within a circle of radius r centered on the i th point, summed over all points in the pattern [95,96]. The bivariate form $\hat{L}_{1,2}(r)$ is a straightforward extension of the univariate case: it is the count of type 2 points occurring within a circle of radius r of the i th type 1 point, summed over all type 1 points in the pattern. We characterized patterns at interpoint distances from 0 m to 80 m (one quarter the minimum plot dimension) and used isotropic edge correction to account for points located closer than r to a plot edge [96]. Our study area included enough large-diameter trees to analyze spatial patterns of three tree species: *Abies concolor*, *Calocedrus decurrens* and *Pinus lambertiana*.

Inferential framework for spatial analyses

Univariate tree patterns were compared against a null distribution generated by a completely spatially random (CSR) process. Under CSR the location of each point in the pattern is completely independent of the locations of other points in the pattern. Positive values of $\hat{L}(r)$ indicate spatial clustering (trees have more neighbors than expected under CSR) while negative values of $\hat{L}(r)$ indicate spatial inhibition or uniformity (trees have fewer neighbors than expected under CSR).

Bivariate tree patterns were evaluated against the hypothesis of no interaction between the large-diameter and small-diameter subpopulations. We evaluated this hypothesis using the null model of population independence based on the guidelines of Goreaud & Pélissier [97]. Population independence is evaluated by holding the relative intratype spatial configuration constant (i.e., the relative tree locations within a diameter class are fixed) while subjecting the populations to random toroidal shifts. Under population independence significantly positive values of $\hat{L}_{1,2}(r)$ indicate a spatial attraction between the two types (e.g., originating from a parent-offspring relationship or facilitation) while significantly negative values indicate spatial repulsion between the two

ATTACHMENT D

types (e.g., Janzen-Connell effects or intraspecific competition). Large-diameter trees were ≥ 100 cm dbh; small-diameter trees were < 100 cm dbh.

We used the 9 m radius neighborhood size estimated by Das et al. [24,98] for Sierra Nevada mixed-conifer forests and tested the respective empirical patterns against the corresponding null models over $0 \leq r \leq 9$ m using the goodness-of-fit test developed by Loosmore and Ford [99]. We set $\alpha = 0.05$ and used $n = 999$ simulated patterns in each test ($n = 250$ simulated patterns were used for univariate analyses of small-diameter *A. concolor* and all species pooled, respectively, to mitigate excessively long computation times). To control for multiple tests ($n = 12$) we used the Bonferroni correction, resulting in a threshold P -value of 0.004. Because we had no *a priori* hypotheses about tree patterns at spatial scales > 9 m we investigated patterns at larger scales in an exploratory framework by comparing the empirical $\hat{L}(r)$ curves to the full distribution of $\hat{L}(r)$ curves calculated for the simulated patterns. All analyses were implemented in the statistical program R version 2.14.1 [100]. Spatial analyses were conducted using the spatstat package version 1.25-1 [101].

Supporting Information

Figure S1 Topography of the Yosemite Forest Dynamics Plot. LiDAR-derived ground model at 1 m resolution (5 m contours; 137.2 m vertical relief). Dots indicate corners of each $20 \text{ m} \times 20 \text{ m}$ quadrat of the $800 \text{ m} \times 320 \text{ m}$ plot. Elevation ranges from 1774.1 m in the northeast corner to 1911.3 m along the southern boundary for a vertical relief of 137.2 m. Drainages contain vernal streams. (TIF)

Figure S2 Climatology and water balance of the Yosemite Forest Dynamics Plot. The combination of temperature and precipitation (A) give rise to a pronounced summer drought

(B). Potential evapotranspiration (PET) exceeds available water supply from May through September, decreasing actual evapotranspiration (AET) and producing a climatic water deficit (Deficit) of 197 mm of water. (TIF)

Table S1 Vertebrate species reported in similar forest types within 5 km of the Yosemite Forest Dynamics Plot between 1980 and 2011.

(PDF)

Appendix S1 Allometric equations for total above-ground biomass for trees ≥ 1 cm dbh and shrubs in patches of continuous cover $\geq 2 \text{ m}^2$ in the Yosemite Forest Dynamics Plot.

(PDF)

Acknowledgments

This research was performed under National Park Service research permits YOSE-2008-SCI-0098, YOSE-2010-SCI-0003, and YOSE-2011-SCI-0015. We thank B. Blake of Blake Land Surveys, Buellton, California, for assistance with surveying, GPS location, and geospatial consulting, and J. Knox, K. Blake, J. Bratt, R. Moore, M. Alvarez, R. McMillan, and G. Rice for surveying assistance. We thank S. Roberts for vertebrate data. We thank J. Meyer and the Yosemite National Park Divisions of Resources and Science, Fire and Aviation, Campground Management, and Law Enforcement for logistical support. We thank two anonymous reviewers who helped improve previous versions of this manuscript. This project was made possible by the 115 students and volunteers listed individually at <http://www.yfdp.org>.

Author Contributions

Conceived and designed the experiments: JAL AJL MES JAF. Performed the experiments: JAL AJL MES JAF. Analyzed the data: JAL AJL MES JAF. Wrote the paper: JAL AJL MES.

References

- Brown IF, Martinelli LA, Thomas WW, Moreira MZ, Ferreira CAC, et al. (1995) Uncertainty in the biomass of Amazonian forests: An example from Rondônia, Brazil. *Forest Ecology and Management* 75: 175–189.
- Clark DB, Clark DA (1996) Abundance, growth and mortality of very large trees in Neotropical lowland rain forest. *Forest Ecology and Management* 80: 235–244.
- Martin TA, Brown KJ, Kučera J, Meinzer FC, Sprugel DG, et al. (2001) Control of transpiration in a 220-year old *Abies amabilis* forest. *Forest Ecology and Management* 152: 211–224.
- Rambo T, North M (2009) Canopy microclimate response to pattern and density of thinning in a Sierra Nevada forest. *Forest Ecology and Management* 257: 435–442.
- van Wageningen JW, Moore PE (2010) Fuel deposition rates of montane and subalpine conifers in the central Sierra Nevada, California, USA. *Forest Ecology and Management* 259: 2122–2132.
- Keeton WS, Franklin JF (2005) Do remnant old-growth trees accelerate rates of succession in mature Douglas-fir forests? *Ecological Monographs* 75: 103–118.
- Chao K-J, Phillips OL, Monteagudo A, Torres-Lezama A, Vásquez Martínez R (2009) How do trees die? Mode of death in northern Amazonia. *Journal of Vegetation Science* 20: 260–268.
- Larson AJ, Franklin JF (2010) The tree mortality regime in temperate old-growth coniferous forests: the role of physical damage. *Canadian Journal of Forest Research* 40: 2091–2103.
- Meyer MD, Kelt DA, North MP (2005) Nest trees of northern flying squirrels in the Sierra Nevada. *Journal of Mammalogy* 86: 275–280.
- Van Pelt R, Sillett SC (2008) Crown development of coastal *Pseudotsuga menziesii*, including a conceptual model for tall conifers. *Ecological Monographs* 78: 283–311.
- Hammer TE, Nelson SK (1995) Characteristics of marbled murrelet nest trees and nesting stands. In: Ralph CJ, Hunt GL, Jr., Raphael MG, Piatt JF, eds. *Ecology and conservation of the marbled murrelet*. General Technical Report PSW-152. Department of Agriculture, Forest Service, Pacific Southwest Research Station, Albany, California.
- Nadkarni NM, Matelson TJ (1989) Bird use of epiphyte resources in Neotropical trees. *Condor* 91: 891–907.
- Sillett SC, Van Pelt R (2007) Trunk reiteration promotes epiphytes and water storage in an old-growth redwood forest canopy. *Ecological Monographs* 77: 335–359.
- Harmon ME, Cromack K, Smith BG (1987) Coarse woody debris in mixed-conifer forests, Sequoia National Park, California. *Canadian Journal of Forest Research* 17: 1265–1272.
- Harmon ME, Woodall CW, Fasth B, Sexton J (2008) Woody detritus density and density reduction factors for tree species in the United States: a synthesis. USDA Forest Service General Technical Report NRS-29. Northern Research Station, Newtown Square, Pennsylvania.
- Winter LE, Brubaker LB, Franklin JF, Miller EA, DeWitt DQ (2002) Canopy disturbance over the five-century lifetime of an old-growth Douglas-fir stand in the Pacific Northwest. *Canadian Journal of Forest Research* 32: 1057–1070.
- Swetnam TW (1993) Fire history and climate change in giant sequoia groves. *Science* 262: 885–889.
- Hall CM, James M, Baird T (2011) Forests and trees as charismatic mega-flora: implications for heritage tourism and conservation. *Journal of Heritage Tourism* 6: 309–323.
- Omura H (2004) Trees, forests and religion in Japan. *Mountain Research and Development* 24: 179–182.
- Van Pelt R (2001) *Forest giants of the Pacific coast*. Seattle: University of Washington Press.
- Enquist BJ, West GB, Brown JH (2009) Extensions and evaluations of a general quantitative theory of forest structure and dynamics. *Proc Natl Acad Sci U S A* 106: 7046–7051.
- Knight FR (2003) Stem mapping methodologies and analyses of stem density, plot size, sample size and spatial patterns of large trees in old-growth mixed-conifer and pine forests of the Sierra Nevada and Oregon. Dissertation. University of Washington, Seattle, Washington.
- Busing RT (2005) Tree mortality, canopy turnover, and woody detritus in old cove forests of the southern Appalachians. *Ecology* 86: 73–84.
- Das A, Battles J, Stephenson NL, van Mantgem PJ (2011) The contribution of competition to tree mortality in old-growth coniferous forests. *Forest Ecology and Management* 261: 1203–1213.
- Enquist BJ, Niklas KJ (2001) Invariant scaling relations across tree-dominated communities. *Nature* 410: 655–660.

ATTACHMENT D

26. West GB, Enquist BJ, Brown JH (2009) A general quantitative theory of forest structure and dynamics. *Proc Natl Acad Sci U S A* 106: 7040–7045.
27. Coomes DA, Duncan RP, Allen RB, Truscott J (2003) Disturbances prevent stem size-density distributions in natural forests from following scaling relationships. *Ecology Letters* 6: 980–989.
28. Muller-Landau HC, Condit RS, Harms KE, Marks CO, Thomas SC, et al. (2006) Comparing tropical forest tree size distributions with the predictions of metabolic ecology and equilibrium models. *Ecology Letters* 9: 589–602.
29. Franklin JF, Shugart HH, Harmon ME (1987) Tree death as an ecological process. *BioScience* 37: 550–556.
30. Pielou EC (1962) The use of plant-to-neighbor distances for the detection of competition. *Journal of Ecology* 50: 357–367.
31. Getzin S, Dean C, He F, Trofymow JA, Wiegand K, et al. (2006) Spatial patterns and competition of tree species in a Douglas-fir chronosequence on Vancouver Island. *Ecography* 29: 671–682.
32. Van Pelt R, Franklin JF (2000) Influence of canopy structure on the understory environment in tall, old-growth, conifer forests. *Canadian Journal of Forest Research* 30: 1231–1245.
33. Larson AJ, Franklin JF (2006) Structural segregation and scales of spatial dependency in *Abies amabilis* forests. *Journal of Vegetation Science* 17: 489–498.
34. Taylor AH (2004) Identifying forest reference conditions on early cut-over lands, Lake Tahoe Basin, USA. *Ecological Applications* 14: 1903–1920.
35. North M, Chen J, Oakley B, Song B, Rudnicki M, et al. (2004) Forest stand structure and pattern of old-growth western hemlock/Douglas-fir and mixed-conifer forests. *Forest Science* 50: 299–311.
36. Busing RT, Fujimori T (2002) Dynamics and composition and structure in an old *Sequoia sempervirens* forest. *Journal of Vegetation Science* 13: 785–792.
37. Baishya R, Barik SJ, Upadhyaya K (2009) Distribution pattern of aboveground biomass in natural and plantation forests of humid tropics in northeast India. *Tropical Ecology* 50: 295–304.
38. Gilbert GS, Howard E, Ayala-Orozco B, Bonilla-Moheno M, Cummings J, et al. (2010) Beyond the tropics: forest structure in a temperate forest mapped plot. *Journal of Vegetation Science* 21: 388–405.
39. Chave J, Condit R, Muller-Landau HC, Thomas SC, Ashton PS, et al. (2008) Assessing evidence for a pervasive alteration in tropical tree communities. *PLoS Biology* 6: e45.
40. Makana J-R, Ewango CN, McMahon SM, Thomas SC, Hart TB, et al. (2011) Demography and biomass change in monodominant and mixed old-growth forest of the Congo. *Journal of Tropical Ecology* 27: 447–461.
41. Hao ZQ, Li BH, Zhang J, Wang XG, Ye J, et al. (2008) Broad-leaved Korean pine (*Pinus koraiensis*) mixed forest plot in Changbaishan (CBS) of China: Community composition and structure. *Acta Phytocologica Sinica* 32: 238–250. [In Chinese].
42. Wang X, Wiegand T, Wolf A, Howe R, Davies SJ, et al. (2011) Spatial patterns of tree species richness in two temperate forests. *Journal of Ecology* 99: 1382–1393.
43. Jenkins JC, Chojnacky DC, Heath LS, Birdsey RA (2004) Comprehensive database of diameter-based biomass regressions for North American tree species. USDA Forest Service General Technical Report NE-319. Northeastern Research Station, Newtown Square, Pennsylvania.
44. Keeton WS, Whitman AA, McGee GC, Goodale CL (2011) Late-successional biomass development in northern hardwood-conifer forests of the northeastern United States. *Forest Science* 57: 489–505.
45. Morrison ML, Raphael MG (1993) Modeling the dynamics of snags. *Ecological Applications* 3: 322–330.
46. North M, Innes J, Zald H (2007) Comparison of thinning and prescribed fire restoration treatments to Sierran mixed-conifer historic conditions. *Canadian Journal of Forest Research* 37: 331–342.
47. Bonnicksen TM, Stone EC (1980) The giant sequoia-mixed conifer forest community characterized through pattern analysis as a mosaic of aggregations. *Forest Ecology and Management* 3: 307–328.
48. Das A, Battles J, van Mantgem PJ, Stephenson NL (2008) Spatial elements of mortality risk in old-growth forests. *Ecology* 89: 1744–1756.
49. Lutz JA, van Wagtenonk JW, Franklin JF (2009) Twentieth-century decline of large-diameter trees in Yosemite National Park, California, USA. *Forest Ecology and Management* 257: 2296–2307.
50. Larson AJ, Churchill D (2012) Tree spatial patterns in fire-frequent forests of western North America, including mechanisms of pattern formation and implications for designing fuel reduction and restoration treatments. *Forest Ecology and Management* 267: 74–92.
51. Scholl AE, Taylor AH (2010) Fire regimes, forest change, and self-organization in an old-growth mixed-conifer forest, Yosemite National Park, USA. *Ecological Applications* 20: 362–380.
52. Clark DB, Clark DA (1991) The impact of physical damage on canopy tree regeneration in tropical rain forest. *Journal of Ecology* 72: 447–457.
53. Nesmith JCB, O'Hara KL, van Mantgem PJ, de Valpine P (2010) The effects of raking on sugar pine mortality following prescribed fire in Sequoia and Kings Canyon National Parks, California, USA. *Fire Ecology* 6(3): 97–116.
54. Sánchez Meador AJ, Moore MM, Bakker JD, Parysow PF (2009) 108 years of change in spatial pattern following selective harvest of a *Pinus ponderosa* stand in northern Arizona, USA. *Journal of Vegetation Science* 20: 79–90.
55. Keeler-Wolf T, Moore PE, Reyes ET, Menke JM, Johnson DN, et al. (In press) Yosemite National Park Vegetation Classification and Mapping Project Report. Natural Resource Report NPS/XXXX/NRR-20XX/XXX. National Park Service, Fort Collins, Colorado.
56. Hickman JC, ed. The Jepson Manual: Higher Plants of California. Berkeley: University of California Press.
57. Jennings MD, Faber-Langendoen D, Loucks OL, Peet RK, Roberts D (2009) Standards for associations and alliances of the U.S. National Vegetation Classification. *Ecological Monographs* 79: 173–199.
58. Stephenson NL, van Mantgem PJ (2005) Forest turnover rates follow global and regional patterns of productivity. *Ecology Letters* 8: 524–531.
59. Stephenson NL, van Mantgem PJ, Bunn AG, Bruner H, Harmon ME, et al. (2011) Causes and implications of the correlation between forest productivity and tree mortality rates. *Ecological Monographs* 81: 527–555.
60. Natural Resources Conservation Service (NRCS) (2007) Soil survey geographic (SSURGO) database for Yosemite National Park, California, USA (Soil survey area symbol CA790). <http://soildatamart.nrcs.usda.gov> USDA Natural Resources Conservation Service, Fort Worth, Texas, USA.
61. PRISM (2004) 800-m Climate Normals (1971–2000). PRISM Climate Group, Oregon State University, Corvallis, Oregon, USA.
62. Daly C, Halbleib M, Smith JJ, Gibson WP, Dogett MK, et al. (2008) Physiographically-sensitive mapping of temperature and precipitation across the conterminous United States. *International Journal of Climatology* 28: 2031–2064.
63. Lutz JA, van Wagtenonk JW, Franklin JF (2010) Climatic water deficit, tree species ranges, and climate change in Yosemite National Park. *Journal of Biogeography* 37: 936–950.
64. van Wagtenonk JW, Fites-Kaufman J (2006) Sierra Nevada bioregion. 264–294. In Sugihara NG, van Wagtenonk JW, Shaffer KE, Fites-Kaufman J, Thode AE, eds. *Fire in California's Ecosystems*, University of California Press, Berkeley, California, USA.
65. Tarnay LW, Lutz JA (2011) Sustainable fire: Preserving carbon stocks and protecting air quality as the Sierra Nevada warms. *Park Science* 28(1): 48–55.
66. van Wagtenonk JW, Lutz JA (2007) Fire regime attributes of wildland fires in Yosemite National Park, USA. *Fire Ecology* 3(2): 34–52.
67. Lutz JA, Key CH, Kolden CA, Kane JT, van Wagtenonk JW (2011) Fire frequency, area burned, and severity: a quantitative approach to defining a normal fire year. *Fire Ecology* 7(2): 51–65.
68. Thode AE, van Wagtenonk JW, Miller JD, Quinn JF (2011) Quantifying the fire regime distributions for severity in Yosemite National Park, California, USA. *International Journal of Wildland Fire* 20: 223–239.
69. Lutz JA, Halpern CB (2006) Tree mortality during early forest development: a long-term study of rates, causes, and consequences. *Ecological Monographs* 76: 257–275.
70. Furniss RL, Carolin VM (1977) *Western Forest Insects*. USDA Forest Service Miscellaneous Publication 1339, Washington DC.
71. Edmonds RL, Agee JK, Gara RI (2000) *Forest health and protection*. Boston: McGraw-Hill.
72. Baumgartner K, Rizzo DM (2001) Distribution of *Armillaria* species in California. *Mycologia* 93: 821–830.
73. Rizzo DM, Slaughter GW (2001) Root disease and canopy gaps in developed areas of Yosemite Valley, California. *Forest Ecology and Management* 146: 159–167.
74. van Mantgem PJ, Stephenson NL, Keifer MB, Keeley J (2004) Effects of an introduced pathogen and fire exclusion on the demography of sugar pine. *Ecological Applications* 14: 1590–1602.
75. Hawksworth FG, Wiens D (1996) *Dwarf mistletoes: biology, pathology, and systematics*. USDA Agriculture Handbook 709, USDS Forest Service, Washington DC.
76. Pierson ED, Rainey WE, Chow LS (2006) Bat use of the giant sequoia groves in Yosemite National Park. Yosemite Fund Report, Yosemite National, California.
77. Meyer MD, North MP, Kelt DA (2007) Nest trees of northern flying squirrel in Yosemite National Park, California. *Southwestern Naturalist* 52: 157–161.
78. Roberts SL, van Wagtenonk JW, Kelt DA, Miles AK, Lutz JA (2008) Modeling the effects of fire severity and spatial complexity on small mammals in Yosemite National Park, California. *Fire Ecology* 4(2): 83–104.
79. Roberts SL, van Wagtenonk JW, Miles AK, Kelt DA (2011) Effects of fire on California spotted owl occupancy in a late-successional forest. *Biological Conservation* 144: 610–619.
80. Elsasser AB (1978) Development of regional prehistoric cultures. In: , Heizer RF, volume editor (1978) *Handbook of North American Indians, Volume 8, California*. Washington DC: Smithsonian Institution. pp 37–57.
81. Hiskes G, Hiskes J (2009) The discovery of Yosemite 1833: route of the Walker Expedition through the Yosemite region Red Fox Press.
82. Bunnell LH (1880) *Discovery of the Yosemite and the Indian War of 1851*. Chicago: Flenmin H Revell.
83. Levy R (1978) Eastern Miwok. In: , Heizer RF, volume editor (1978) *Handbook of North American Indians, Volume 8, California*. Washington DC: Smithsonian Institution. pp 398–413.
84. Parker AJ (2002) Fire in Sierra Nevada forests: evaluating the ecological impact of burning by Native Americans. In Vale TR, ed. *Fire, native peoples, and the natural landscape*. Washington DC: Island Press. pp 233–267.
85. Muir J (1911) My first summer in the Sierra. In Cronon W, ed. *John Muir: nature writings*. New York: The Library of America. pp 147–310.

ATTACHMENT D

86. Condit R (1998) Tropical forest census plots. Berlin: Springer-Verlag, Georgetown: R.G. Landes Company. 211 p.
87. Harmon ME, Sexton J (1996) Guidelines for measurements of woody detritus in forest ecosystems. U.S. LTER Network Office: University of Washington, Seattle, WA, USA. 73 p.
88. USDI National Park Service (2003) Fire Monitoring Handbook. Fire Management Program Center, National Interagency Fire Center, Boise, Idaho, USA.
89. Brown JK (1974) Handbook for inventorying downed material. USDA Forest Service Gen Tech Report INT-16. Ogden, Utah, USA.
90. Means JE, Hansen HA, Koerper GJ, Alaback PB, Klopsch MW (1994) Software for computing plant biomass – BIOPAK users guide. USDA Forest Service General Technical Report PNW-GTR-340. Pacific Northwest Research Station, Portland, Oregon, USA.
91. Gholz HL, Grier CC, Campbell AG, Brown AT (1979) Equations for estimating biomass and leaf area of plants of the Pacific Northwest. Research Paper 41. Forest Research Lab, Oregon State University. Corvallis.
92. Westman WE (1998) Aboveground biomass, surface area, and production relations of red fir (*Abies magnifica*) and white fir (*A. concolor*). Canadian Journal of Forest Research 17: 311–319.
93. Jenkins JC, Chojnacky DC, Heath LS, Birdsey RA (2003) National-scale biomass estimators for United States tree species. Forest Science 49: 12–35.
94. Stephens SL, Finney MA, Schantz H (2004) Bulk density and fuel loads of ponderosa pine and white fir forest floors: impacts of leaf morphology. Northwest Science 78: 93–100.
95. Fortin MJ, Dale M (2005) Spatial analysis: a guide for ecologists. Cambridge University Press, Cambridge, UK.
96. Diggle P (2003) Statistical analysis of spatial point patterns. Arnold, London, UK.
97. Goreaud F, Pélissier R (2003) Avoiding misinterpretation of biotic interactions with the intertype K_{12} -function: population independence vs. random labeling hypotheses. Journal of Vegetation Science 14: 681–692.
98. Larson AJ, Churchill D (2008) Spatial patterns of overstory trees in late-successional conifer forests. Canadian Journal of Forest Research 38: 2814–2825.
99. Loosmore NL, Ford ED (2006) Statistical inference using the G or K point pattern spatial statistics. Ecology 87: 1925–1931.
100. R Development Core Team (2011) R: A language and environment for statistical computing. R Foundation for Statistical Computing, Vienna, Austria. <http://www.R-project.org/>.
101. Baddeley A, Turner R (2005) Spatstat: an R package for analyzing spatial point patterns. Journal of Statistical Software 12(6): 1–42.

ATTACHMENT D

EXHIBIT E

ATTACHMENT D

Project Title: Optimizing Spatial and Temporal Treatments to Maintain Effective Fire and Non-fire Fuels Treatments at Landscape Scales

Final Report: JFSP Project: 06-3-3-14

Project Website:

Principal Investigators:

Dr. J. Greg Jones, Research Forester, Human Dimensions Program, Rocky Mountain Research Station, PO Box 7669, 200 East Broadway Missoula, MT 59807; Phone: (406) 329-3396; Fax: (406) 329-3487; Email: jgjones@fs.fed.us

Dr. Woodam Chung, Associate Professor, College of Forestry and Conservation, The University of Montana, Missoula, MT 59812; Phone: (406) 243-6606; Fax: (406) 243-4845; Email: woodam.chung@umontana.edu

Co-Principal Investigator:

Dr. Carl Seielstad, College of Forestry and Conservation, The University of Montana, Missoula, MT 59812; Phone: (406) 532-3283; Email: carl@ntsg.umt.edu

Software Developers:

Janet Sullivan, Human Dimensions Program, Rocky Mountain Research Station, 200 East Broadway, Missoula, MT 59807; Phone: (406) 329-3414; Fax: (406) 329-3487; Email: jsullivan@fs.fed.us

Kurt Krueger, Human Dimensions Program, Rocky Mountain Research Station, 200 East Broadway, Missoula, MT 59807; Phone: (406) 329- 3420; Fax: (406) 329-3487; Email: kkruieger@fs.fed.us

This research was sponsored in part by the Joint Fire Science Program. For further information go to www.firescience.gov



ATTACHMENT D**I. Abstract**

There is a recognized need to apply and maintain fuel treatments to reduce catastrophic wildland fires. A number of models and decision support systems have been developed for addressing different aspects of fuel treatments while considering other important resource management issues and constraints. Although these models address diverse aspects of the fuel treatment-planning problem, no one model adequately handles the strategic maintenance scheduling of fuel treatments while considering 1) the spatial and temporal changes of fuel treatment effects on a landscape, and 2) the economics of maintenance fuel treatments plus other operational constraints.

The objective of this project was to integrate existing fire behavior, vegetation simulation, and land management planning tools into a system that supports long-term fuel management decisions. The system was to build on the existing land management optimization tool MAGIS, while incorporating the Forest Vegetation Simulator and the Fire and Fuels Extension (FVS-FFE) to project vegetation change over planning periods and predict the resulting fuel parameters for fire behavior modeling, and FlamMap to model fire behavior in each planning period. The system was to include automated data transfer interfaces between the models to offer an easier way to use multiple sophisticated models for analyzing alternative fuel management schedules.

The project developed OptFuels, a GIS-based modeling system for spatially scheduling forest fuel treatments over multiple planning periods in the presence of budget and other constraints. OptFuels utilizes FVS-FFE to project stands into the future both with and without fuel treatments and compute the fuel parameters needed for fire behavior modeling in FlamMap, which is conducted for each planning period in each iteration of the OptFuels solver. The OptFuels solver spatially schedules fuel treatments over multiple planning periods (1 – 5 user-defined periods) to minimize the expected loss from potential future wildland fire.

OptFuels has been tested on two fuel treatment planning areas on the Bitterroot National Forest, the 34,000-acre Trapper-Bunkhouse area, and the 103,689-acre Willow-Gird area. Fuel treatment scenarios scheduled over two planning periods were able to substantially reduce the fire arrival time in the wildland urban interface portion of the Trapper-Bunkhouse area, thereby reducing the expected loss from future fires. Smaller reductions in expected loss were found in the Willow-Gird area. Although increases in arrival time were created by the scheduled fuel treatments, these treatments did not increase the arrival times sufficiently in the areas on the landscape having the highest expected loss, such as the wildland urban interface. This occurred primarily because of the relatively close proximity of the ignition points in the wildland urban interface simulating human ignited fires.

II. Background and Purpose

There is a recognized need to apply and maintain fuel treatments to reduce catastrophic wildland fires. The Healthy Forests Restoration Act of 2003 mandates actions to identify and inventory priority areas. Treating all of the 81 million hectares of federal land in the USA considered at risk from fire (Schmidt et al. 2002) would be costly and impractical. Forest managers faced with limited budgets, narrow burning windows, air quality issues, and effects on other critical forest resources must establish priorities for where, when, and how to apply new and maintenance fuel

ATTACHMENT D

treatments. Science-based yet field applicable guidelines to strategically maintain fuel treatments on landscapes should be incorporated into treatment design to reduce catastrophic fire and restore ecosystem health over time. Therefore, decision support systems that can predict the outcomes of fuel treatments are valuable information tools for fuel management decisions. There is a need for the use of such models to be utilized at a national level.

A number of models and decision support systems have been developed for addressing different aspects of fuel treatments while considering other important resource management issues and constraints. These models operate on a variety of geographic scales, varying from an individual stand to an entire landscape comprised of many individual stands. Some models operate only on current conditions, while others span over multiple decades.

A. Fire behavior and fuel hazard modeling

The FARSITE Fire Area Simulator (Finney 1998) was designed to model continuous fire behavior over multiple burning periods at a 30-meter resolution. FARSITE is able to compare the effectiveness of different suppression strategies and treatments for containing fire under varying weather conditions. FARSITE evaluations are based on simulating fires starting at various locations and spreading under varying fuel and weather conditions. There is, however, no temporal component to these analyses that reflects how the effectiveness of treatments changes over time with vegetative growth.

FlamMap (<http://fire.org/>) is a spatial fire area potential calculator for assessing fuel hazard in terms of fire behavior. The purpose of FlamMap is to generate fire behavior data that are comparable across a landscape for a given set of weather and/or fuel moisture data inputs. The fire behavior models in FlamMap are used to make calculations for all cells of a raster landscape, independently of one another (there is no contagious process that accounts for fire movement across the landscape or among adjacent cells). FlamMap calculates the instantaneous behavior of a fire occurring at each pixel in the analysis area based on the same local weather inputs. In this way FlamMap compares potential fire behavior across a landscape by distinguishing different hazardous fuel and topographic combinations.

FlamMap contains an option called Minimum Travel Time (MTT) (Finney 2002) which is a fire growth simulator that uses minimum travel time methods to simulate how fast one fire or a band of multiple fires are expected to move across a landscape. It is used to identify the routes where fire is expected to travel most quickly. Like the main component of FlamMap, these simulations are based on the current fuels, specific locations for fire starts, and weather conditions. If one accepts that fuel treatments should be prioritized on the basis of juxtaposition of high values to hazardous fuels, this program begins to give us the ability to develop a biophysical definition of wildland urban interface based on the distance fire can travel under specified conditions. It does not include endogenous scheduling of treatments, and like the other fire behavior-based models, works only with the current fuels.

The Treatment Optimization Model (TOM) (Finney 2006) is another option on the FlamMap menu. It uses minimum travel time logic to determine effective locations for fuel treatments on a landscape. The treatment locations are based on the fire behavior expected from the current fuels present on the landscape, specific locations for fire starts, and weather conditions. The solutions suggest location, sizes, and orientations of fuel treatments that are efficient and effective at changing large fire growth by reducing the fire spread rate. The treatment locations are selected

ATTACHMENT D

to reduce the rates of fire spread across the landscape, and are not designed to protect specific locations on a landscape, such as designated wildland urban interface. Also, the placement of treatments does not consider feasibility factors associated with location or shape, nor do they address resource effects, or management limitations such as budget. Finally, there is no temporal aspect to TOM, so it cannot analyze alternative timings of fuel maintenance treatments on a landscape.

The Fire and Fuels Extension to the Forest Vegetation Simulator (FVS-FFE) evaluates the effectiveness of proposed fuel treatments in the context of potential fire effects on short- and long-term stand dynamics (Reinhardt and Crookston 2003). In contrast to other fire behavior fuel hazard models, the FVS-FFE has the ability to simulate the dynamics of vegetation, snags, and surface fuels, and the appropriate interactions between these processes at a stand level (Kurz and Beukema 1999). In combination with the Parallel Processing Extension (PPE; Crookston and Stage 1991) the FVS-FFE can be used to simulate the dynamics of landscapes containing several hundred to a few thousand stands. The FVS-FFE does not simulate fire spread between stands, but it has the ability to provide inputs to FARSITE and FlamMap (Hayes and others 2004).

Other fire models include 1) the First Order Fire Effects Model (FOFEM) which models duff and woody fuel consumption, mineral soil exposure, soil heating, smoke production, and tree mortality (Reinhardt and others 1997), 2) FIREHARM which can be used to calculate fire behavior and effects potentials for varying weather percentiles used in fire management planning, and 3) NEXUS (Scott and Reinhardt 2001) which is an Excel(tm) spreadsheet linking surface and crown fire prediction models. All these fire models, however, do not include treatment scheduling or address temporal aspects of fuels management.

B. Landscape simulation and treatment scheduling modeling

SIMPPLLE is a stochastic simulation model for projecting vegetation spatially in the presence of disturbances such as insects, disease, and wildland fire (Chew 1997, Chew and others 2004). Simulations can be made with or without fire suppression, with or without fuel treatments, and under average or extreme fire conditions. Spread logic is included for wildland fire and other disturbance processes. The location and frequencies of disturbance processes quantified from multiple stochastic simulations provide estimates of the location and probabilities of future disturbance processes. These provide a basis for identifying “problem areas,” as well as estimating costs and effects associated with disturbances processes.

MAGIS is an optimization model for spatially scheduling treatments that effectively meet resource and management objectives while satisfying user-imposed resource and operational constraints (Zuuring and others 1995). MAGIS accommodates a wide variety of land management treatment types, and associated costs, revenues, and effects. MAGIS also contains a road-network component for analyzing road construction, re-construction, and closure. The combination of the land management and road-network components provides the capability to include the limitations (for example sediment production) and costs associated with vegetation treatments as well as access and roads in spatially analyzing maintenance of fuel treatments.

SIMPPLLE and MAGIS have been used in a process for spatially scheduling treatments and analyzing the effectiveness of those treatments (Jones and Chew 1999, Chew and others 2003, Jones and others 2004). In this process, SIMPPLLE is used first to run stochastic simulations for the “no action” management alternative. From these simulations the frequency of natural

ATTACHMENT D

disturbances is recorded for each polygon in the landscape, representing the risk of these natural processes occurring over a period of time. These risks are then incorporated into MAGIS and combined with resource and operational objectives and constraints to develop an alternative spatial treatment schedule. These treatments schedules are then simulated in SIMPPLLE and the results compared with the results of the “no action” simulations to measure the effectiveness of the fuel treatment scenario. Key questions, however, remain in the SIMPPLLE/MAGIS approach involving computation of the risk index and the treatment patterns resulting from it, among others.

A past Joint Fire Science project, A Risk-Based Comparison of Potential Fuel Treatment Trade-off Models, compared the SIMPPLLE/MAGIS approach with two non-spatial models FETM (CH2M Hill 1998) and VDDT (Beukema and Kurz 1998) on eight areas representative of major fuel types. The focus was on modeling fuel treatment trade-offs for use in strategic planning. The comparison found significant differences in how information is assembled and used in the models. SIMPPLLE and MAGIS were sensitive to the spatial arrangement of vegetation and treatments, making the data requirements somewhat more stringent, but they also provide as output the spatial arrangement of proposed treatments. Non-spatial solutions may not be either optimal or even operationally feasible.

C. The need for integrating types of models

Although these models address diverse aspects of the fuel treatment-planning problem, no one model adequately handles the strategic maintenance scheduling of fuel treatments while considering 1) the spatial and temporal changes of fuel treatment effects on a landscape, and 2) the economics of maintenance fuel treatments plus other operational constraints. For example, FARSITE and FlamMap are able to compute fire behavior characteristics at a landscape scale, but neither maintenance scheduling nor temporal effects of treatments are included in either model. FVS-FFE has the ability to model stand-level fuel and vegetation dynamics, but it does not simulate the spread of fires between stands. On the contrary, MAGIS has the ability to spatially schedule fire and non-fire maintenance treatments that effectively meet resource and management objectives, but no fire spread logic exists in the system. Fire managers have to use these multiple systems in order to analyze spatial and temporal effects of maintenance fuel treatments, but lack of time and resources to maintain and operate these sophisticated systems has been a hurdle. Consequently, there is a critical need to merge these systems into one easy-to-use decision support system that 1) facilitates automatic linkages among the existing models, 2) streamlines analyses for identifying where, when, and how to treat in order to achieve and maintain desired fuel reduction goals, and 3) bridges the fire sciences and management gap by incorporating given resource and operational constraints (e.g. budgets, treatment acres, and operational feasibility of treatments) into decision-making process.

D. Project objectives

The main objective of this project was to integrate existing fire behavior, vegetation simulation, and land management planning tools into a system that supports long-term fuel management decisions. The system was to build on the existing land management optimization tool MAGIS, while incorporating FVS-FFE to project vegetation change over planning periods and predict the resulting fuel parameters for fire behavior modeling, and FlamMap to model fire behavior in each planning period. The system was to include automated data transfer interfaces between the

ATTACHMENT D

models to offer an easier way to use multiple sophisticated models for analyzing alternative fuel management schedules. The system was to be validated on two landscapes.

III. Study Description and Location

This project developed OptFuels, a GIS-based modeling system for spatially scheduling forest fuel treatments over multiple planning periods in the presence of budget and other constraints. OptFuels utilizes the Forest Vegetation Simulator and the Fire and Fuels Extension (FVS-FFE) to project stands into the future both with and without fuel treatments and compute the fuel parameters needed for fire behavior modeling in FlamMap, which is conducted for each planning period in each iteration of the OptFuels solver. The OptFuels solver spatially schedules fuel treatments over multiple planning periods (1 – 5 user-defined periods) to minimize the expected loss from potential future wildland fire.

The main spatial component of an OptFuels model is a GIS stand polygon coverage. For simplicity, these stand polygons double as treatment unit polygons, thereby avoiding the necessity for a separate treatment unit polygon coverage at this stage in the planning process. Management regimes comprised of one or more treatment activities are assigned to the polygons based on user-specified rules that are tied to spatial zones and stand characteristics. Each management regime is comprised of a sequence of treatment activities that may extend over multiple planning periods to represent scheduled retreatment of the same location, or represent a one-time treatment occurring in a single planning period. Costs for activities are entered as table lookups, allowing costs to vary by conditions where appropriate, while at the same time accommodating a simple average treatment activity cost.

After the management regimes have been assigned to the polygons, OptFuels runs FVS-FFE to simulate the no action landscape. Then treatment options are assigned to the polygons based on the no action output and geographically defined management zones. These treatment options are then simulated with FVS-FFE for the sequence of treatments specified in the management regimes. In this process, FVS-FFE is used to project both treated and untreated stands and compute the resulting fuel parameters for each planning period. Timber and non-merchantable material amounts can be recorded and used for developing recourse management scenarios.

Once an OptFuels model is built, the solver develops alternative treatment schedules for user-specified scenarios. Users specify the fire scenario including the wind direction and speed, the fuel moisture conditions, and ignition points, assign one or more optional constraints on such things as acres to treat, or treatment budget. The OptFuels solver then determines the location and timing of treatment activities to minimize the expected loss from future fire across the planning area.

An OptFuels solution consists of the schedule of treatments selected by the solver, the associated expected loss value, the amounts computed for the constraints, the FlamMap fire behavior summary reports for both the untreated and treated landscapes, and FlamMap-ready landscape files for both the untreated and treated landscapes. These files are useful for additional FlamMap analyses that could be run on the solution results.

ATTACHMENT D

A. System design

Input Data and Model Building Process

Figure 1 presents a flow diagram of the OptFuels data input and model building process. This process can be divided into four components: Framework data, Planning area, Model build, and Fuel treatment scenario specifications.

Framework data – These data are not specific to a fuel treatment planning area, they are expected to apply to multiple planning areas that have similar conditions. The Framework data includes:

- Master list of variables, which become GIS attributes that are used to categorize information in the Framework data. These variables (GIS attributes) include the treatment zones used in assigning management regime options to polygons, the value-at-risk categories present on a polygon, and attributes used in cost table lookups.
- Fuel treatments are defined using FVS keywords for mechanical treatments (such as THINBBA), and prescribed fire. Additional keywords can be used to control fuel calculations (FIRECALC, FUELCALC, and FUELMODL) in FVS. Activity-costs can also be entered to account for administrative and other costs. Costs can be entered as a simple average, or in a table lookup where costs vary by user-defined attributes, such as slope or aspect.

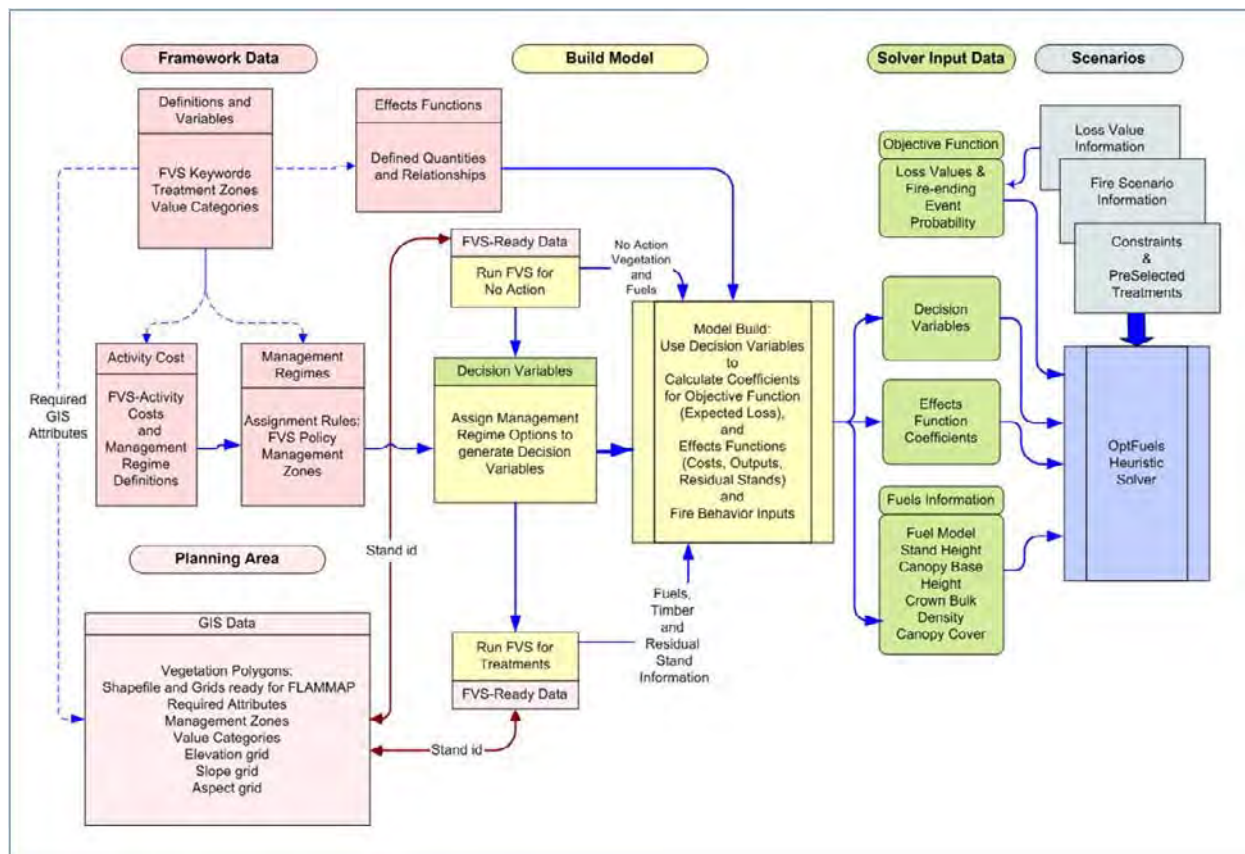


Figure 1. The OptFuels data input and model building process.

ATTACHMENT D

- Management regime definitions. Each management regime is comprised of one or more FVS and non-FVS activities as a sequence (for example: sale preparation cost, followed by mechanical thinning, followed by a broadcast burn) that occurs in a planning period. A given treatment unit polygon may have options for treatment in each planning period.
- Rules for assigning management regimes as options to the GIS polygons. These rules are based on the vegetation and fuel conditions present in the polygon as well as the management zone where the polygon resides. For example, management regimes with mechanical treatment can be limited to a zone where road access exists, or to specific stand conditions (or both). In the same manner, individual (or all) management regimes can be excluded as options in riparian areas or other restrictive land management zones.
- List of the value-at-risk categories for use in the expected loss calculation such as structures, critical wildlife habitat, and so on.

Planning area – These data are comprised of a GIS vegetation polygon coverage that includes the GIS attributes used in the framework data (attributes for management zone, value-at-risk categories and cost table lookups) and an identifier that associates each polygon to FVS-ready stand data. The GIS data goes through validity and completeness checks to ensure all necessary information is present prior to the model building process. The GIS data also include raster grids for elevation, slope, and aspect, and polygon (treatment unit) boundaries.

Model building process – This begins with an OptFuels interface running FVS-FFE for the no action alternative for each unique set of FVS-ready data. One set of FVS-ready data may apply to one or multiple GIS polygons. This design avoids having to run the same FVS-ready data for each polygon to which it applies. The FVS-FFE no action run projects the FVS-ready data through the planning periods (from 1 period to a maximum of 5 periods) and computes the fuels information needed for fire behavior modeling in each planning period.

The management regime assignment rules are applied using results of the no action FVS-FFE runs and the management zone information to assign the management regime options to the polygons. This process creates the decision variables for the OptFuels solver.

Next, the OptFuels interface runs FVS-FFE for the treatments in the management regimes using the FVS-ready data. As with the no action FVS runs, only the unique combinations of management regimes and FVS-ready data are simulated by FVS-FFE. The FVS-FFE simulations project the stands that the FVS-ready data represent through the planning periods, applying the treatment sequences for the management regimes. These simulations compute the fuels information needed for fire behavior modeling in each planning period, as well as the wood product volumes removed by mechanical thinning and statistics describing the residual stands. The fuels data are stored for use by the OptFuels solver.

The last step in the model building process integrates the decision variable information, GIS data, framework data, and results from the FVS-FFE runs to compute the Effects Function Coefficients of each decision variable and stores these results for use by the OptFuels solver. The Effects Functions are computations of model quantities such as acres treated, costs, timber products, and non-monetary resource benefits and impacts as defined by the user. An Effects Function Coefficient measures the contribution of a specific decision variable to a specific Effects Function.

ATTACHMENT D

Fuel treatment scenario specifications – There are three components to specifying a scenario for the OptFuels solver: 1) Loss value information, 2) Fire scenario information, and 3) Constraints and preselected decision variables. The loss value information includes the items of information used in computed expected loss. Loss values for value-at-risk categories are entered by flame length. Following the approach of Calkin and others (2010) we recommend quantifying loss from wildland in terms of percentage loss relative to no fire occurring. This results in an index based on percentage loss that is used by the solver to schedule treatments (the objective is to schedule treatments in the way that minimizes this loss value index). Loss can instead be quantified in dollar terms at user discretion. Users have the ability to apply weights to the value-at-risk categories to reflect their relative importance for guiding fuel treatment decisions. The final item in the loss value information is a table of probabilities for fire duration. These fire duration probabilities could be developed by analyzing the duration of past fires, or through using historical weather data to estimate the probability of fire ending weather patterns at over various numbers of days. We recognize that MTT models fire spread assuming constant fire scenario conditions. However, in the real world, fire spreading weather is not continuous but rather occurs only in blocks of time. Days of fire duration in the real world can be converted to minutes of active fire spread in the fire behavior modeling by estimating the average number of active spread minutes in a 24-hour day.

The fire scenario information for OptFuels is the same information used for MTT. This includes fuel moisture files, custom (optional) fuel model file, fire weather information, and other fuels information (fuel moisture conditioning files, ground fuels etc.). The ignition points for the fire scenario are also specified. In addition, the number of fire spread minutes to run the MTT in the solving process must be specified. This value should be slightly larger than the estimated time needed to spread fire from the ignitions points across the planning area given the specified weather and fuel moisture information.

Constraints and preselected decision variables are optional. Constraints may be imposed on the solution by selecting an effects function and entering limits on its value. This is where limitations on budget, treatment acres, or other such effects function calculations can be specified. The user also has the option to set decision variables (a decision variable is a specific treatment on a specific polygon in a specific period) into the solution. Preselected decision variables occur in the solution schedule regardless of their effect on the objective function or constraints. Preselecting decision variables can be used to test the effects of specific treatments in specific locations, sets of treatments, or use sets of treatments in specific locations as the starting point for a new solution.

Heuristic Solver

The heuristic solver employed in OptFuels is designed to develop a number of alternative fuel treatment schedules (solutions), evaluate the cumulative effects of each alternative treatment schedule, and choose the best fuel treatment schedule that produces maximum treatment effects (minimize overall expected loss) over time while meeting given resource and operational constraints. The solver includes a subroutine to develop FlamMap landscape (LCP) files that represent vegetation and fuels attributes in each time period as treatment effects. Through dynamic link libraries (DLLs), the solver automatically runs the MTT algorithm on each LCP file and stores the outputs (i.e., flame length and fire arrival time in each pixel) for solution evaluation (Figure 2). Each solution is evaluated as the sum of expected loss value of a given

ATTACHMENT D

study landscape over time (Equation 1). Expected loss value in each pixel depends on user-defined relative value of the pixel and burn probability, and estimated flame length and fire arrival time retrieved from the MTT output.

$$\text{Minimize } \sum_{t \in T} \sum_{c \in C} \sum_{f \in F} \text{Loss}_{f,c,t} \times Y_{f,c,t} \times P_{c,t} \quad [\text{Eq.1}]$$

Where

f is an index of flame length category,

c is an index of grid cells (pixels),

t is a time period,

$\text{Loss}_{f,c,t}$ is an expected loss value of grid cell c at flame length category f in time period t ,

$Y_{f,c,t}$ is a binary variable indicating the flame length category of cell c in period t , and

$P_{c,t}$ is a probability of cell c being burn by given fire scenarios (fire ignition locations and durations) in time period t .

A simulated annealing (SA) algorithm is employed in the solver for the optimization engine. Simulated Annealing (SA) is a heuristic search technique that has been widely used to solve large combinatorial problems in various fields (Kirkpatrick and others 1983). The ideas that form the basis for SA were first published by Metropolis and others (1953) in an algorithm to simulate the cooling of materials in a heat bath - a process known as annealing. The approach is a Monte Carlo method that uses a local search in which a subset of solutions is explored by moving from one solution to a neighboring solution. To avoid becoming trapped in a local optimum, the procedure provides for an occasional acceptance of an inferior solution to allow it to move away from a local optimum. The SA algorithm employed in the heuristic solver is briefly explained below and illustrated in Figure 3. Any combinations of budget and acreage constraints can be considered during the optimization process.

Step 1. Develop and evaluate an initial solution. Store the solution as the current solution.

Step 2. Create a new solution by slightly modifying the current solution (randomly select a set of treatment polygons and assign new fuel treatment options including no action).

Step 3. Check the feasibility of the new solution. If the solution violates any of the constraints, discard the solution and go back to Step 2. Evaluate the new solution, otherwise.

Step 4. Accept or discard the new solution based on the SA solution acceptance rule.

Step 5. Go to Step 2 until predefined stopping criterion (i.e., ending temperature) is met.

In order to implement the SA search process, several control parameters need to be set by the user. These include beginning and ending temperatures, repetitions at each temperature level, and temperature cooling rate. The OptFuels interface provides four options for the user to choose from: low intensity, medium intensity, high intensity, and custom option. The higher

ATTACHMENT D

intensity option runs more iterations and thus can likely provide a better solution than the other two lower intensity search options, but requires a larger amount of computation time.

Test runs of the initial version of the solver indicated that the solver required a considerable amount of computation time due to the fire simulation process by MTT and the complexity of spatial and temporal scheduling problems. To improve the efficiency of the solution process, the current version of the heuristic solver was designed for multi-threading and multi-processing using OpenMP with Visual C++. As a result, the solver can now simultaneously run MTT for multiple time periods, and the computation time can be significantly reduced.

System Outputs

A tabular report is created for the schedule of treatments developed by the OptFuels solver. This report includes the expected loss value by planning period and the total expected loss across periods, the values computed for the effects functions, and a listing of the treatments selected by polygon. In addition there are options for spatially displaying various aspects of the treatment schedule solution. GIS maps can show the polygons treated by planning period. The expected loss values computed for the treatment schedule can be mapped for each planning period, showing where loss is expected to occur on the landscape. Finally, the contribution that each polygon makes to individual effects functions can be mapped. This could be used, for example, to see spatial distribution of costs or revenues across the planning area.

OptFuels also outputs selected landscape (LCP) files that were created by the solver to run MTT in the solution process. An LCP is the proprietary format for the fire behavior models FARSITE, FlamMap, and MTT and represents a multi-value spatial grid that includes slope, aspect, elevation, and five fuel characteristics. LCP files are output for each planning period for the treatment schedule developed by the solver and for no action. These LCP files can then be used in FlamMap to develop fire behavior information for the planning area both with and without treatment, including landscape raster grids of fire arrival time and flame length.

B. Test Areas and Test Runs***Trapper-Bunkhouse study area***

This 34,000-acre study area is on the west side of the Bitterroot Valley west of Darby, Montana (Figure 4). Private property and state lands border the project area to the east and the Selway-Bitterroot Wilderness bounds the project area to the west. The wildland urban interface encompasses about 70% of the project area.

Existing fuel loads (including live trees) pose a threat to the public, fire fighters and natural resources. Any large fire (>100 acres), or multiple ignitions in one day on the Bitterroot Face has the potential to overwhelm suppression forces and travel unimpeded to the Forest

ATTACHMENT D

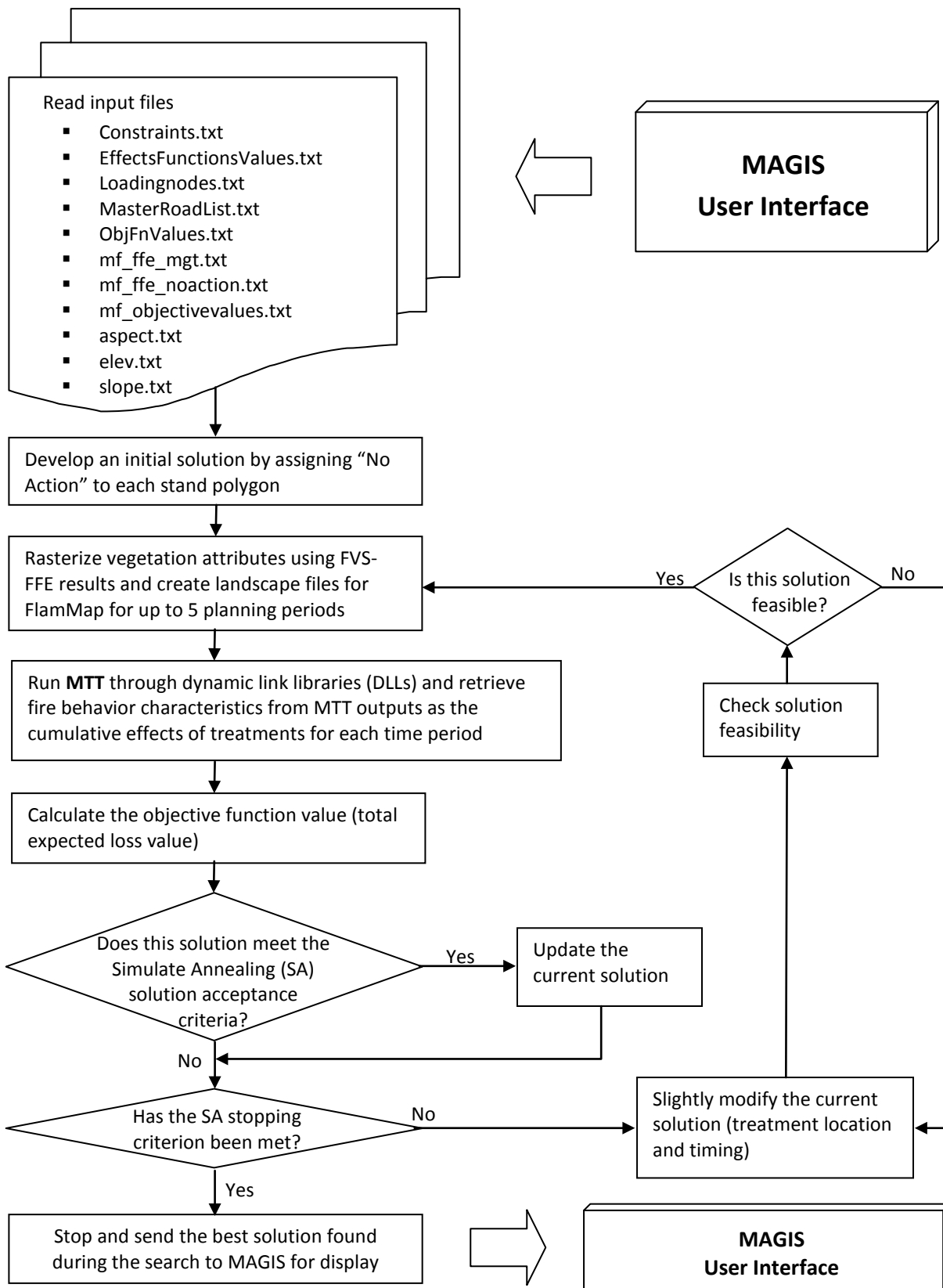


Figure 2. Data flow and analysis employed in the Heuristic Solver to optimize fuel treatment schedules.

ATTACHMENT D

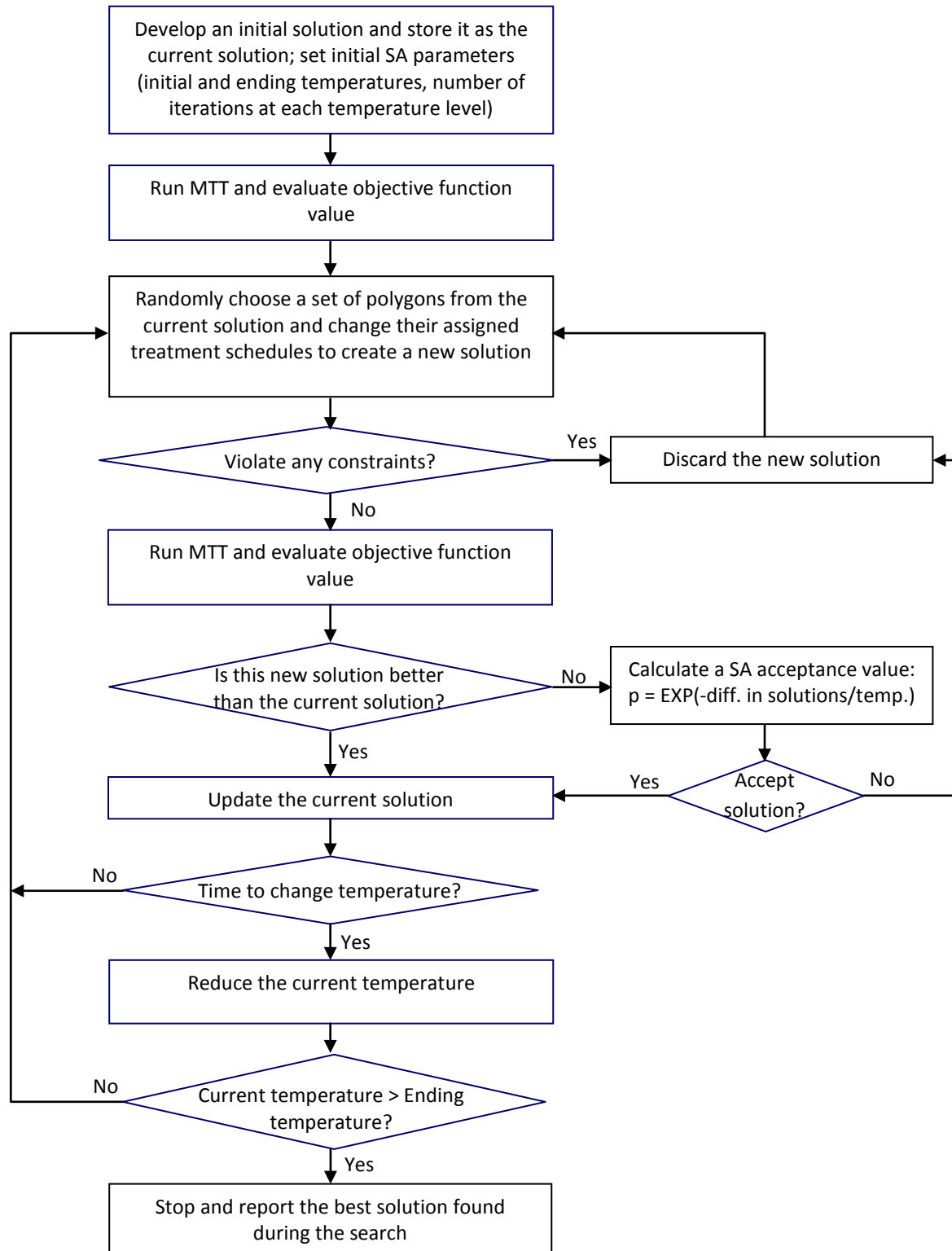


Figure 3. Simulated Annealing algorithm employed in the Heuristic Solver to optimize fuel treatment schedules.

ATTACHMENT D

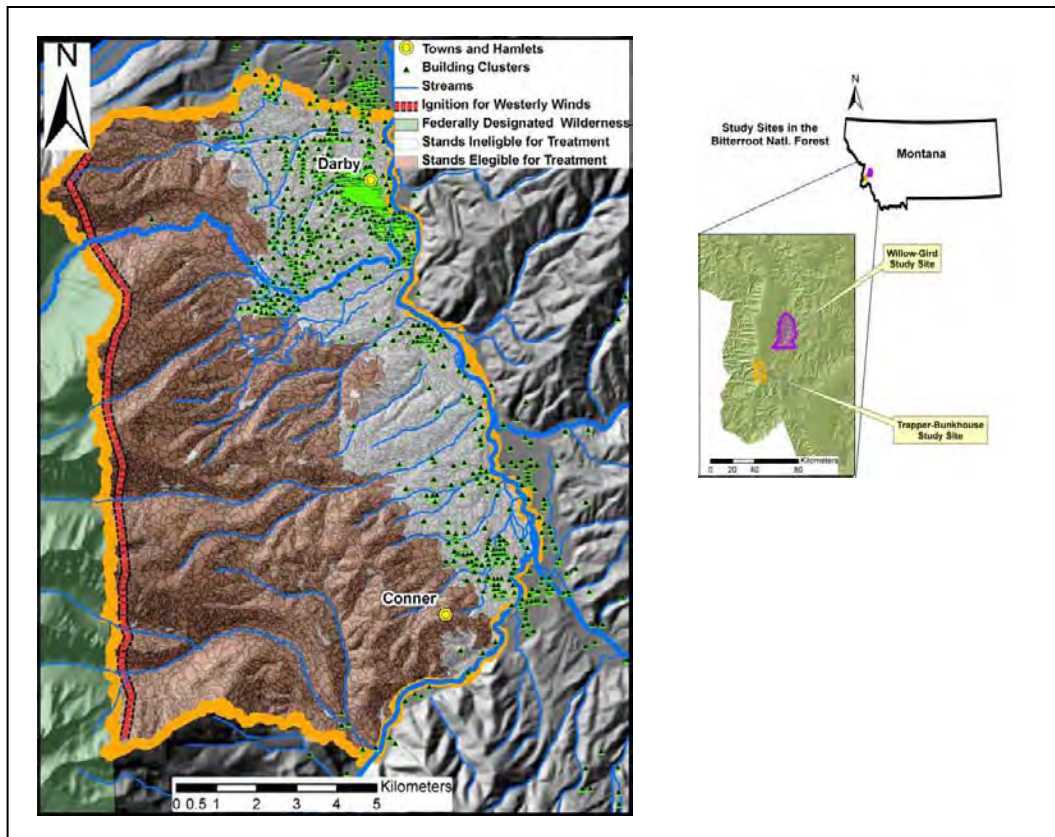


Figure 4. Trapper-Bunkhouse study area.

Service/private boundary and onto private property. This scenario has been demonstrated by the Ward Mountain Fire (1994) and the Blodgett Fire (2000) in which there were homeowner evacuations. The Little Blue Fire (2000) started more than four miles from private property on a remote portion of the West Fork Ranger District, but within 10 hours resulted in home evacuations in the wildland urban interface.

The vegetation structure in the majority of the project area has grown into overstocked, dense stands that are at increased risk of stand-replacing crown fires or intensities that cannot be directly attacked by fire fighters. These dense stands are also susceptible to insect infestations. Eighty-two percent of the project area is highly departed (fire regime condition class 'FRCC' 3) and eighteen percent is moderately departed (FRCC 2) from historical fire frequency and severity, and from historic vegetation structure and fuel loads.

The OptFuels model for this area contained fuel treatment options for 23,957 acres of the 34,000-acre study area. The Restore option was available on 17,014 acres on which prescribed burning could not be accomplished without first reducing ladder fuels. Restore is a mechanical thinning from below designed to remove ladder fuels and reduce stand density to approximately 50-60 ft² of basal area per acre, followed by a broadcast burn to remove activity fuels and small trees. The RxFire option, which applies prescribed fire without mechanical thinning, was available on 6,933 acres.

ATTACHMENT D

Five value-at-risk categories (Figure 5) were used in the expected loss calculation: 1) residential parcels that were stand polygons that contain structures, 2) wildland urban interface (WUI) that was defined as polygons within one-half mile of private structures, and 3) national forest system (NFS) acres not having any other risk category. Loss response functions from Calkin and others (2010) provided the basis for assigning percent loss by flame length categories. Percent loss for residential parcels received an importance weight of 10, wildland urban interface a weight of 8, national forest systems acres not in any other category received a weight of 1.

The fire scenario was a line of ignition on the west boundary of the study area with winds out of the west at 20 mph (Figure 4). Foliar moisture content used the FlamMap default of 100%. Fuel moisture conditioning was used.

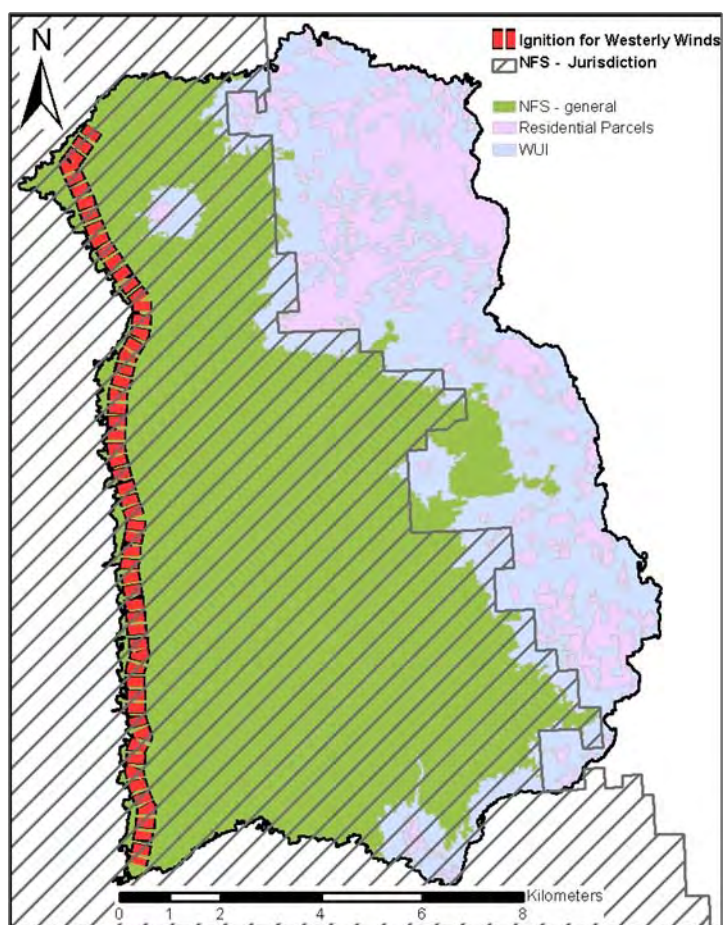


Figure 5. Value-at-risk categories for the Trapper-Bunkhouse study area.

ATTACHMENT D

The fire duration probabilities used were derived from weather station data:

<u>Duration category</u> (minutes of active spread)	<u>Probability of a fire of that duration</u>
< 840	0.9
840 – 1680	0.7
1680 – 2520	0.6
2520 – 3360	0.6
3360 – 4200	0.6
4200 – 5040	0.5
5040 – 5880	0.2
5880 – 6700	0.1
6700<	0

Figure 6 compares the expected loss index for no action with three treatment scenarios with increasing percentages of the 23,957 candidate acres treated per period: 10, 20, and 25 percent. The graphs show the percent of pixels in the entire planning area having each category of loss. In period 1 there is a higher percentage of the area in the 2-6 loss category with increasing percentages of candidate acres treated per period. This result indicates that the acres in the higher loss value categories with no action have moved to the low loss category (2-6) as a result of treatment.

In period 2 the differences with increasing amounts of treatment are much greater, reflecting the residual effects of treatments in period 1 plus the effects of treatments in period 2. Figure 7 compares the loss value index summed across periods for the treatments scenarios with no action and 100% of the area treated in period 1, the lowest possible loss with the treatment options modeled. Treating 20% of the candidate acres per period achieved 28% of the reduction relative to treating the entire landscape in period 1, while treating 25% per period achieved 55% of the reduction.

The flame lengths and arrival times modeled by MTT for the treatment scenario and no action are presented in Figures 8 and 9, respectively. Differences in flame length in period 1 are not pronounced, with somewhat larger differences shown for period 2. Again, the result shows that the acres in the higher flamelength categories with no action have moved to the lower flame length categories (e.g., 0 or 1) as a result of treatment. By comparison, the differences in arrival time across the scenarios were larger, particularly in period 2. The arrival time differences appear to account for the majority of the reductions in expected loss with the higher treatment rates.

Figure 10 shows arrival times across the landscape for the 10% and 25% treatment scenarios compared with no action. Arrival times are most increased in period 2 which includes the effects from both period 1 and 2 treatments. Arrival times are most increased in the wildland urban interface in this fire scenario, resulting in less expected loss in that portion of the study area (Figure 11).

ATTACHMENT D

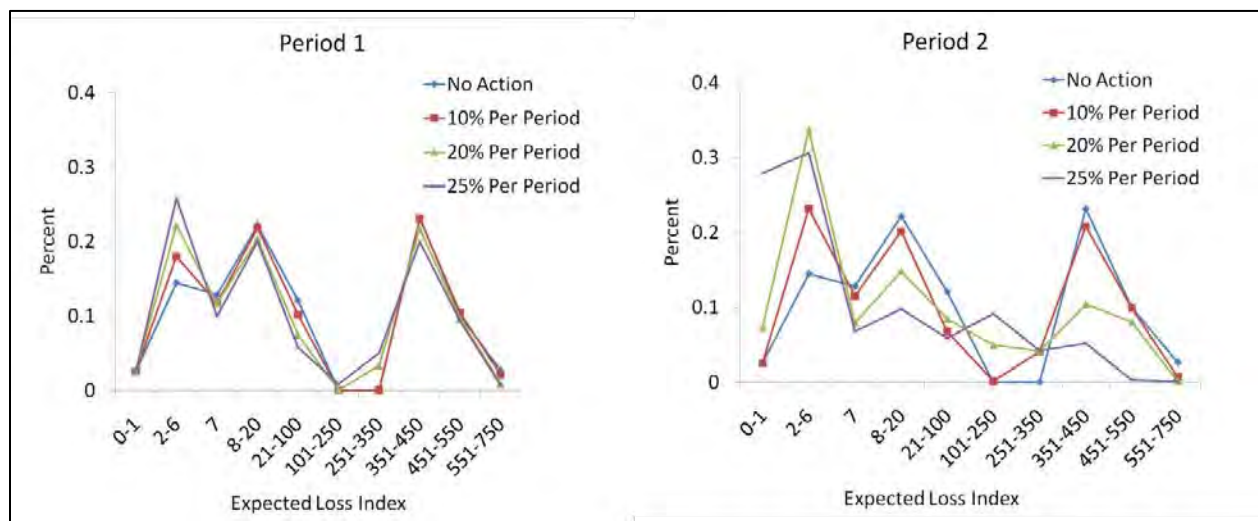


Figure 6. Expected Loss Index by percent of planning area compared across three treatment schedules and no action for periods 1 and 2.

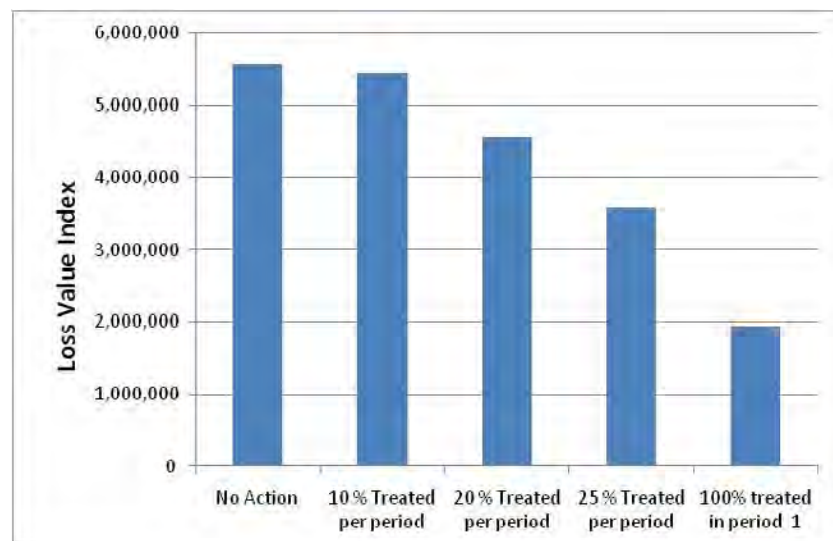


Figure 7. Loss value index summed across periods.

ATTACHMENT D

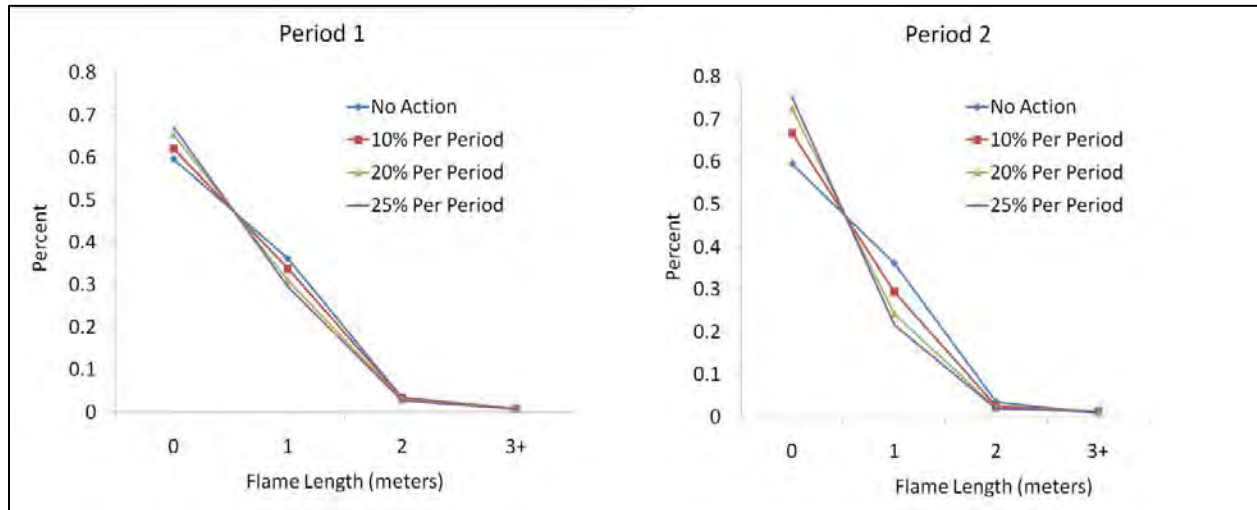


Figure 8. Flame length by percent of planning area compared across three treatment schedules and no action for periods 1 and 2.

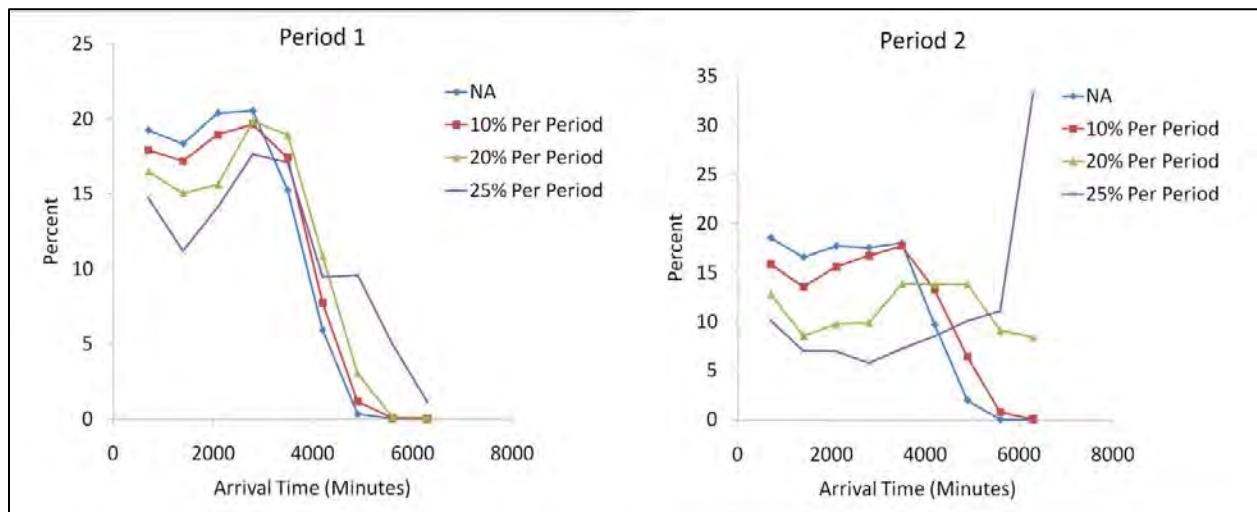


Figure 9. Arrival time by percent of planning area compared across three treatment schedules and no action for periods 1 and 2.

ATTACHMENT D

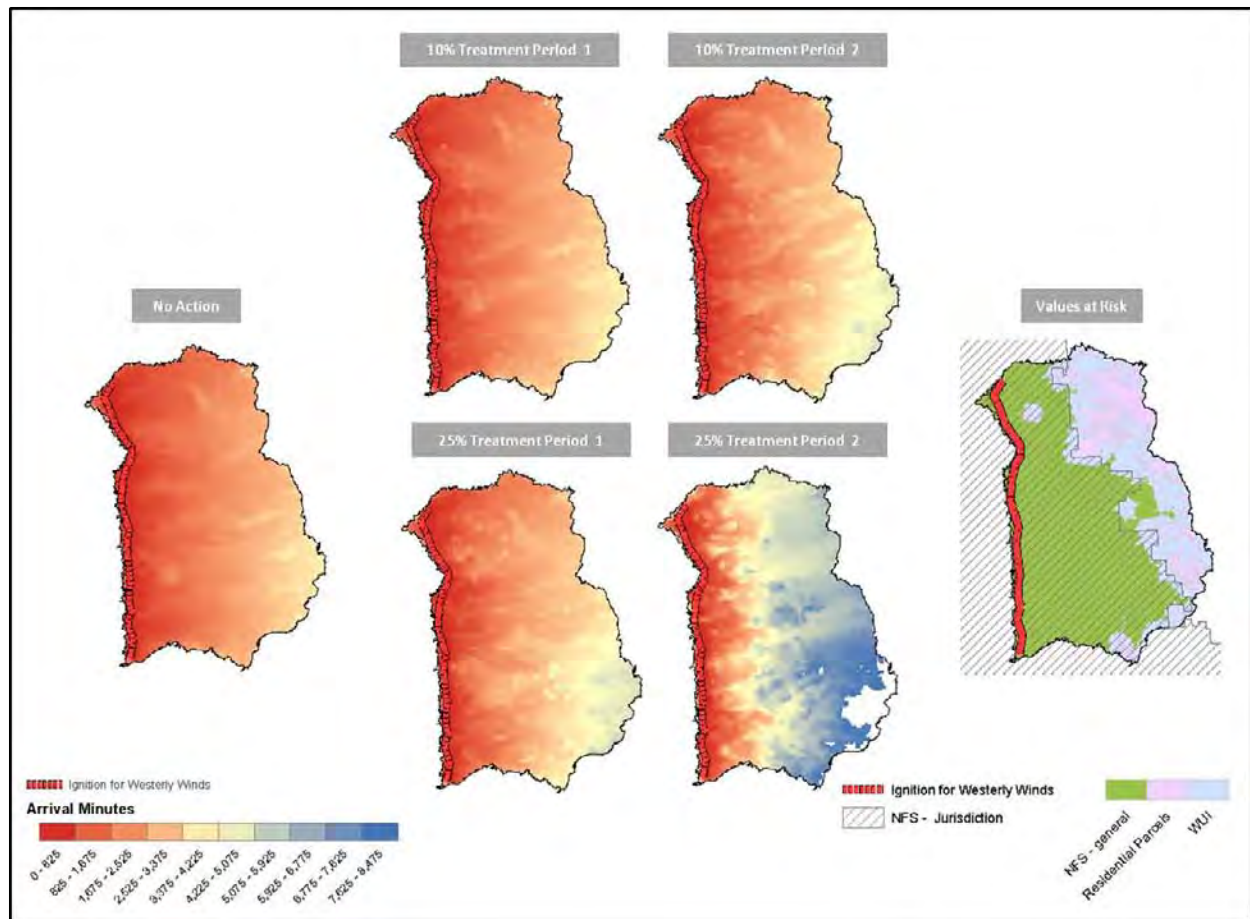


Figure 10. Period 1 and 2 arrival times for the 10% and 25% treatment scenarios compared with no action.

ATTACHMENT D

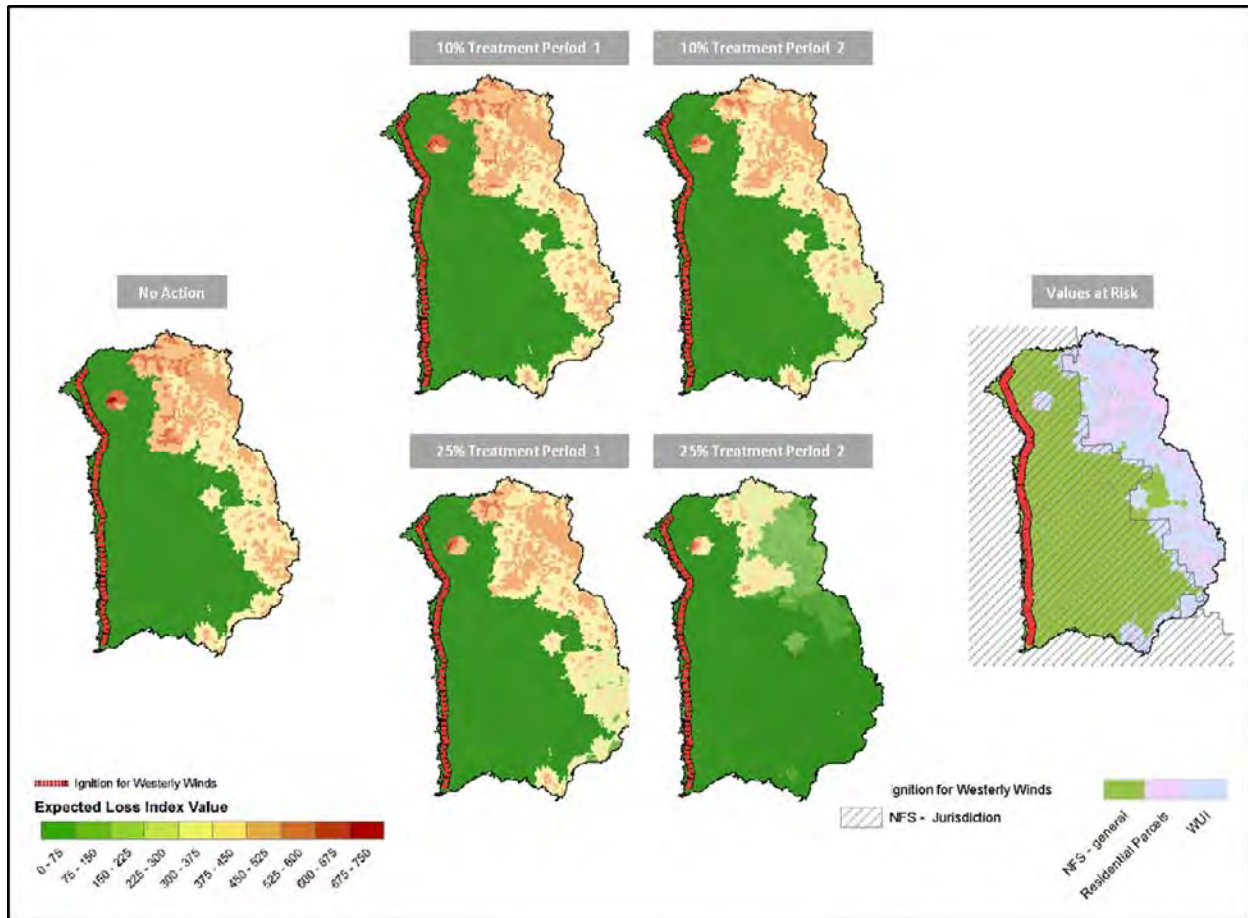


Figure 11. Period 1 and 2 loss values for the 10% and 25% treatment scenarios compared with no action.

Willow-Gird study area

The Willow-Gird study area of 103,689 acres is on the north-east side of the Bitterroot National Forest, straddling the Stevensville and Darby Ranger districts (Figure 12). It is bounded on the west by the Bitterroot Valley and Corvallis, MT, where there is rapid development of residential areas up into the area between Corvallis and the National Forest. To the east are the Sapphire Mountains forming a divide into another developed residential area, Rock Creek, a premier fishing area. The vegetation structure in the majority of the project area has grown into overstocked, dense stands that are at increased risk of insect and disease attack. The area is being considered for restoration treatments to thin dense stands of Ponderosa pine and Douglas-fir at lower elevations, and regenerate native lodgepole pine at higher elevations where it has become decadent and is undergoing active mistletoe infestation, and is therefore at increasing risk for stand-replacing fire.

ATTACHMENT D

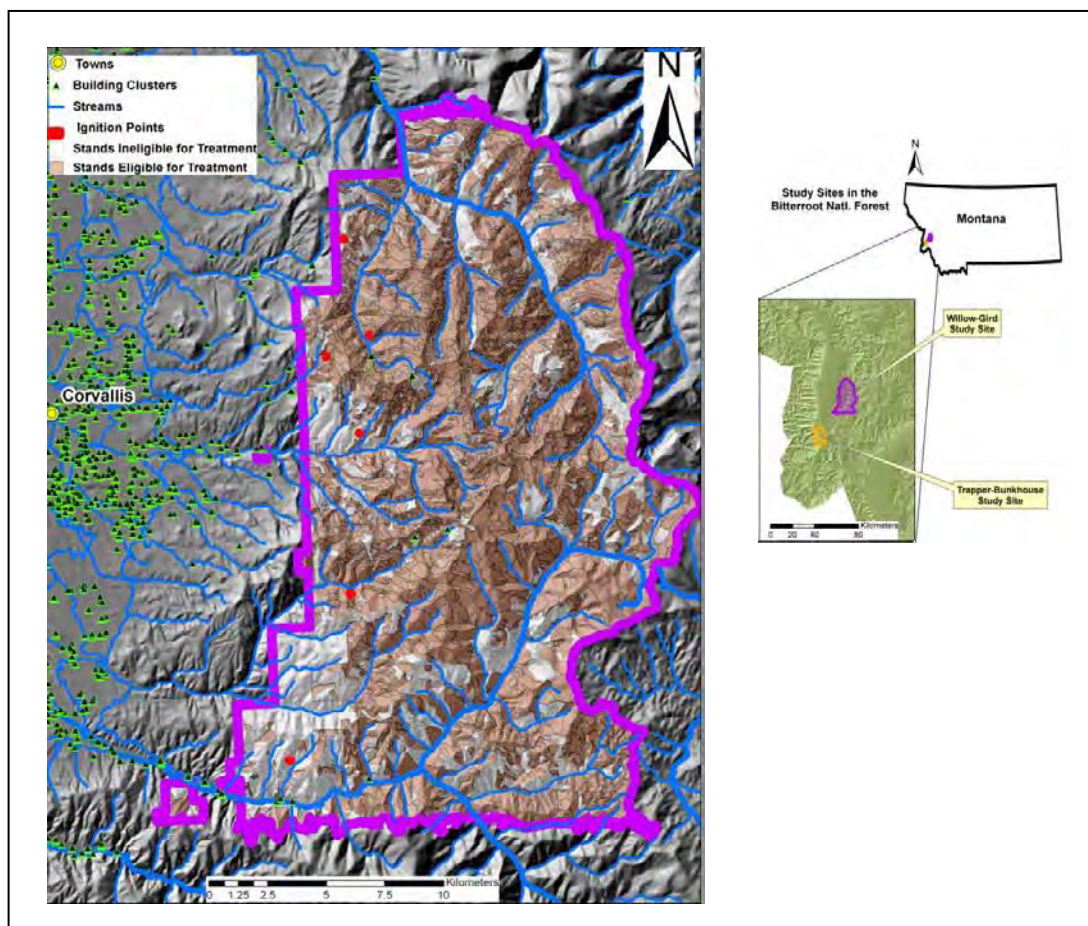


Figure 12. Willow-Gird study area.

The OptFuels model for this area contained fuel treatment options for 78,027 acres. The Restore option (same as described for the Trapper-Bunkhouse Area) was available on 23,354 acres on which prescribed burning could not be accomplished without first reducing ladder fuels. The RxFire option was available on 46,354 acres. The Lodgepole Pine Clear Cut option was available on 8,319 acres.

Five value-at-risk categories (Figure 13) were used in the expected loss calculation: 1) WUII (wildland urban interface) – extends 0.5 mile into the national forest from the forest boundary, 2) State or Private lands, 3) Timber represents national forest acres not having any other risk category, 4) Roadless Timber is designated roadless area in the national forest, and 5) Right of Way is a power-line corridor. Loss response functions from Calkin and others (2010) provided the basis for assigning percent loss by flame length categories. Percent loss in the right-of-way power-line corridor category received an importance weight of 10, wildland urban interface a weight of 5, and all other categories received a weight of 1. The fire duration probabilities were the same as used in the Trapper-Bunkhouse Study Area.

ATTACHMENT D

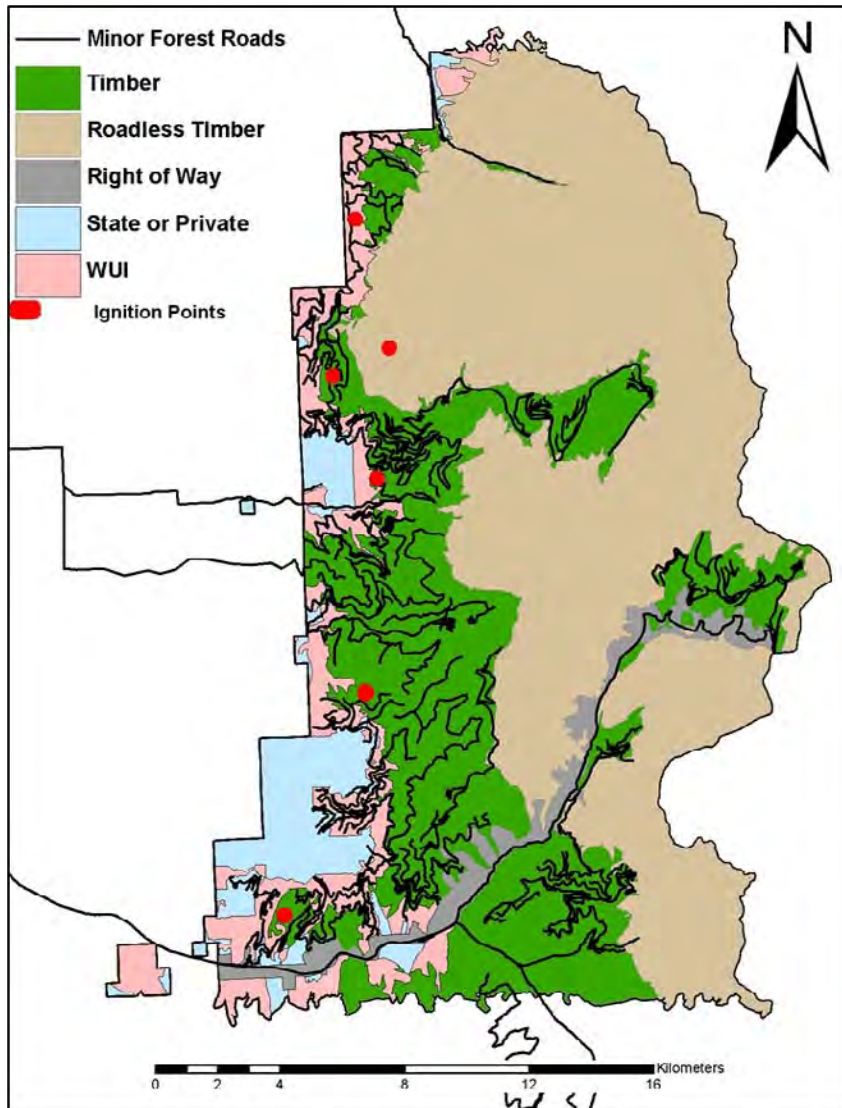


Figure 13. Value-at-risk categories for the Willow-Gird study area.

The fire scenario was the same as used in the Trapper-Bunkhouse Area except in the Willow-Gird area six ignition points were used along the west boundary to represent human-ignited fires in the wildland urban interface.

Figure 14 compares the expected loss index for no action with three treatment scenarios with increasing percentages of the 78,027 candidate acres treated per period: 6.25, 12.5, and 25 percent. While treatments increased the percent of acres in the lowest category of expected loss (drawing acres from higher expected loss categories without treatment) the amount of change was small compared to the Trapper-Bunkhouse area. This is especially true for period 2.

Figure 15 compares arrival times for the treatment scenarios and no action. Much larger differences occurred for arrival time with treatment than were shown for expected loss. Although increases in arrival time were created by the treatments, treatments were unable to

ATTACHMENT D

increase the arrival times sufficiently in the areas on the landscape having the highest expected loss. This occurs because of the relatively close proximity of the ignition points and the WUI which represents the greatest concentration of values at risk (Figure 13). Thus, relatively little reduction in expected loss was achieved by the fuel treatments modeled.

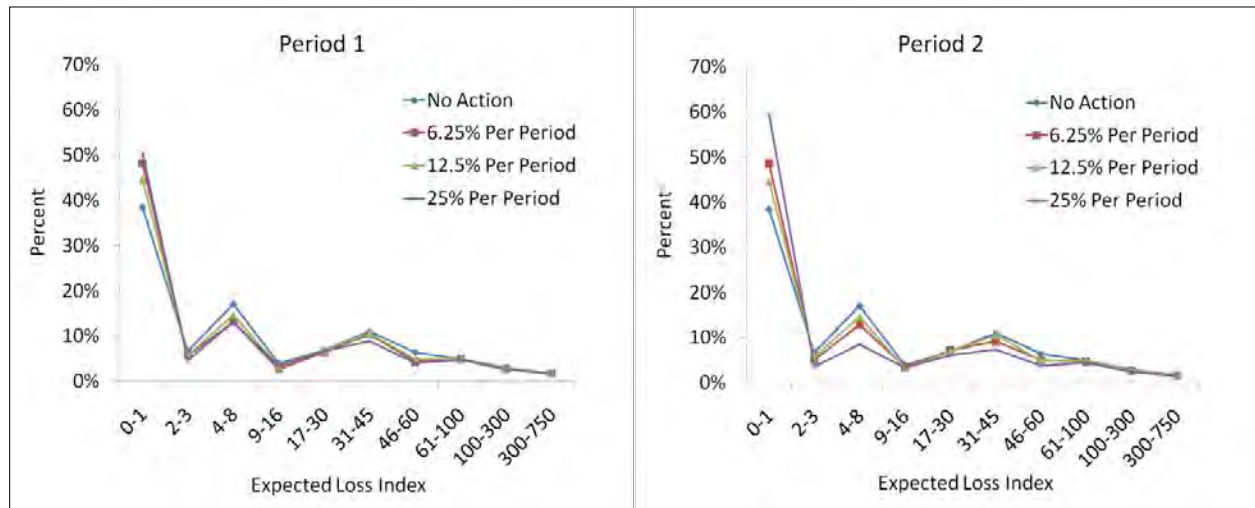


Figure 14. Expected Loss Index by percent of planning area compared across three treatment schedules and no action for periods 1 and 2.

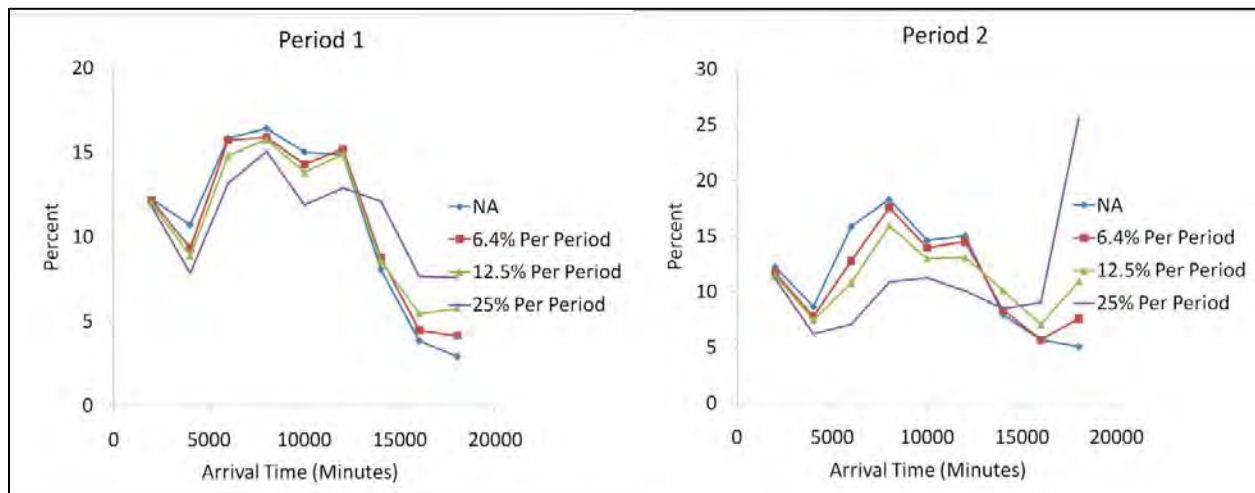


Figure 15. Expected arrival by percent of planning area time compared across three treatment schedules and no action for periods 1 and 2.

ATTACHMENT D

IV. Key Findings

A. Simultaneous multi-period fuel treatment analysis is feasible

This study shows that it is possible to simultaneously schedule fuel treatments across multiple planning periods, which is a computationally challenging problem. This is accomplished by computing and storing all information required by the solving process prior to entering that process. The solver makes spatial fuel treatment selections by period, and updates the landscape fuel grid files for these treatments for each planning period prior to running the minimum travel time fire behavior algorithm for each planning period. The solver also runs on a multi-processor computer to increase the efficiency of the solution process. Earlier approaches to multi-period fuel treatment planning scheduled fuel treatments for one planning period at a time without considering the continuing treatment effects in future periods and whether they can complement the effectiveness of treatments in future periods.

B. Effectiveness of system for scheduling fuel treatments across multiple planning periods

The OptFuels heuristic solver has been able to schedule fuel treatments across multiple planning periods that result in substantial reductions in the expected loss from values at risk across the landscape compared to the untreated landscape given the same fire scenario conditions. These reductions in expected loss with fuel treatment were the result of slower rates of spread (which reduces the probability that the fire duration would be sufficiently long to reach specific locations on the landscape) and lower flame lengths. Continuing effects in period 2 of fuel treatments undertaken in period 1 have been observed by comparing the arrival times and flame lengths predicted for period 2 with another scenario in which only the period 2 treatments were undertaken.

C. Limited availability of inventory data for stand polygons

OptFuels, as well as any planning process that utilizes FVS-FFE to project stand growth and predict fuel parameters for fire behavior modeling, requires FVS-ready inventory data that accurately represent each stand polygon in a planning area. Unfortunately, inventory data needed to produce FVS-ready tree list and stand data are essentially unavailable for stand polygons in forested landscapes. This means that anyone interested in conducting this type of analysis must develop FVS-ready inventory data for each polygon (or grid cell if the analysis is strictly raster-based) if the data does not exist. The best option for accomplishing this appears to be imputation, which in essence matches available inventory plots (such as FIA plots) with stand polygons.

We went through this imputation process numerous times for our two study areas using different combinations of x and y imputation variables with somewhat less than satisfactory results, using a combination of FIA plots and additional plots taken in the project area. In particular, the percent crown closures calculated for the imputed data were consistently much lower across the study area than the crown closure percentages predicted by both R-1 V-Map (Brewer and others 2004) and Landfire, which the study team believed to be a better representation of the study area. These lower density representations of the stand polygons affected the FVS-FFE simulations and the resulting fuel parameters, both with and without treatment. This in turn affected the fire behavior modeling, which even with severe fire conditions consistently predicted less severe fire for the untreated landscape than observed from recent past fires in the same general area.

ATTACHMENT D**D. Importance of selecting effective fuel treatment options**

It is important for obvious reasons to select fuel treatment options that are effective at reducing undesired fire behavior, namely reducing the rate of spread and/or flame length. If the OptFuels solver does not have effective treatments options to select from, it cannot be expected to develop spatial fuel treatment schedules that effectively reduce expected loss from the values-at-risk on the planning landscape. Our experience has been that developing effective fuel treatment options is not as straightforward as one might think. There have been many cases in which thinning to remove ladder fuels followed by a broadcast burn to treat the activity fuels and remove small trees resulted in the same fire behavior as the untreated stand. This highlights the importance of thoroughly testing both the untreated and treated stand fire behavior while selecting treatment options for use in OptFuels.

V. Management Implications**A. Benefits to analyzing spatial fuel treatment schedules over multiple planning periods**

This project has developed and tested OptFuels, an approach for spatially scheduling fuel treatments over time based on minimizing the expected loss of values-at-risk from future wildland fires. OptFuels utilizes FVS-FFE, a well known model for simulating vegetation change, and the Minimum Travel Time option in FlamMap, a well known model for simulating fire spread spatially across landscapes. The OptFuels solver accounts for treatment effects across planning periods in selecting the locations for treatments in each period. Thus the treatments selected for period 1 are not only selected for their effectiveness in modifying fire behavior in period 1, but also for their continuing effect subsequent periods, which is combined with treatments taking place in those subsequent periods.

In addition, OptFuels provides for various types of constraints that can be used to assess trade-offs to better inform decision makers. For example, multiple OptFuels runs with increasing budget constraints can be used to assess the additional fuel treatment benefits that can be achieved over time with increasing fuel treatment costs for a planning area. The effect of increasing budget levels can be measured in terms of change in fire arrival times in specific locations within the planning area, change in flame lengths in specific locations, and change in expected loss from the values-at-risk across the planning area.

Constraints on acres treated can be used to assess trade-offs associated with the amounts of specific types of treatments applied in specific management zones in a planning area. Assume for example, that mechanical fuel treatments are detrimental in a wildlife habitat management zone. Multiple OptFuels runs (in which increasingly limiting constraints are placed on acres of mechanical fuel treatments in that zone) can quantify how much fuel treatment effects are compromised across the landscape by reducing or eliminating mechanical treatments in that zone.

In addition, the connection with FVS provides OptFuels with the ability to estimate wood products and woody biomass that is produced by mechanical fuel treatments. Both the volume and value of wood products can be estimated, as can the net value (revenue minus cost) of mechanical fuel treatments.

ATTACHMENT D

The capability of OptFuels to spatially schedule fuel treatments over multiple planning periods and to constrain those treatment schedules in a variety of ways provides the ability to quantify trade-offs between fuel treatment objectives and other resource management issues and constraints.

B. Important to support development of landscape GIS vegetation coverage with FVS ready data

OptFuels as well as any planning process that utilizes FVS-FFE to simulate stand growth and predict fuel parameters for fire behavior modeling requires FVS-ready data that accurately represent each stand polygon in a planning area. This problem has been addressed in the research community by statistically imputing FIA and other available plot data to either stand polygons or directly to grid cells. This process is quite technical and as of this report has provided less than satisfactory representations of the landscape vegetation on the two study areas in this project (see Key Findings section). We believe it will be difficult for field users to go through the imputation process for each fuel treatment planning area they want to analyze spatially over time. This data issue threatens to hamper the use of this suite of analysis tools. Thus, we believe it is important for management to support development of landscape GIS vegetation coverage with FVS ready data.

C. Important to support development of workforce skills with the models employed by OptFuels

The models employed by OptFuels as well as OptFuels itself require GIS and other computer skills. It is important to support the development of these skills in the workforce for these models to be used effectively. In addition, these models can be run most efficiently by people who work with them on a regular basis. It is difficult for anyone to be proficient at running these models when it is done only once or twice a year. This suggests that the most cost-effective way of organizing work assignments is having a substantial portion of a position devoted to performing analyses with these models, perhaps serving multiple ID team zones or even multiple forests.

VI. Relationship to Other Recent Findings and Ongoing Work

Finney and others (2006) developed a system for spatially placing fuel treatments on a landscape over multiple planning periods to minimize undesired fire behavior. That system stepped through the analysis sequentially, one planning period at a time. After treatments for a period were selected using the TOM (Finney 2006), the post treatment landscape was projected to the next planning period using a custom version of the Parallel Processing extension of FVS (Crookston and Stage 1991). Although their conceptual design for modeling across multiple periods differed from the design we wanted to implement in OptFuels, discussions with the authors of that study were very helpful.

The expected loss computation used by the OptFuels heuristic solver is adapted from the expected net value change calculations in Finney (2005), Ager and others (2007), and Calkin and others (2010). The method of expressing loss as a result of fire as a percentage reduction in value by flame length categories was adapted from Calkin and others (2010).

ATTACHMENT D

This JFSP study provides the basis for a new study centered in the Lake Tahoe Basin. The objective of this new study is to develop an integrated decision support system that optimizes fuel treatment locations in time and space that can also achieve multiple management objectives. Management objectives will be implemented in a flexible manner and can include the reduction of the probability of catastrophic fire, the reduction of sediment inputs into Basin streams, the promotion of species of special concern, among others. The system will identify where, when, and how to treat fuels to maintain desired fuel reduction, forest restoration, and water quality goals at a landscape scale.

The Joint Fire Science Program, the National Wildfire Coordinating Group Fuels Management Committee, and Sonoma Technology, Inc have developed a conceptual design for the Interagency Fuels Treatment - Decision Support System (IFT-DSS). The IFT-DSS organizes fuels-planning software and data into a seamless user environment. OptFuels could provide the process in IFT-DSS for scheduling fuel treatments spatially. OptFuels utilizes FVS-FFE and fire behavior modeling for fuel treatment analyses in the same ways as does IFT-DSS. As a result, the vegetation and fuels data used in OptFuels are the same as well. We will continue to investigate the option of integrating OptFuels into IFT-DSS.

VII. Future Work Needed**A. Modify the heuristic solver to analyze the effectiveness of fuel treatment patterns on two or more fire conditions simultaneously**

The current version of the heuristic solver schedules fuel treatments spatially to minimize the expected loss in values-at-risk for one fire scenario (ignition points, wind direction and speed) at a time. Solving for different fire scenarios separately is likely to schedule fuel treatments in different locations, leaving unanswered the question “What is the best pattern of treatments to minimize expected loss from these two fire scenarios over multiple periods?” In future work we plan to add the capability of developing fuel treatment schedules that minimize expected loss for a small number of fire scenarios of concern. This will involve modeling fire behavior for each of these scenarios (rather than just one scenario) at each iteration in the solution process. Users would weight these alternative fire scenarios based on their relative importance in fuel treatment planning.

B. Develop processes to assist users with preparing input data

OptFuels, as well as any planning process that utilizes FVS-FFE to project stand growth and predict fuel parameters for fire behavior modeling, requires FVS-ready data that accurately represent each stand polygon in a planning area. Unfortunately, FVS-ready data are not generally available for an entire landscape. Associating inventory data (such as FIA plots) to either stand polygons or directly to grid cells is most often accomplished by statistical imputation. This process is quite technical and as described in the Findings section, use of this technique on our study areas provided less than satisfactory representations of the landscape vegetation. Processes are needed to help fuel treatment analysts through the imputation procedures. Alternatively, agencies could supply FVS-ready data to potential users.

ATTACHMENT D**C. Investigate evolutionary optimization algorithms and implement the best choice in OptFuels to run the system in a multi-threading environment to more efficiently solve the large combinatorial optimization problem of fuel treatment scheduling**

OptFuels currently employs a simulated annealing (SA) algorithm for its optimization engine. While SA is known as an efficient neighborhood search algorithm for solving large combinatorial problems, it is not ideal for a multi-threading/multi-processing environment due to its sequential approach to generate and evaluate neighbor solutions. In the future work, we plan to investigate evolutionary optimization algorithms, such as the genetic algorithm (GA) and genetic programming (GP), and implementing the best choice in OptFuels so that the system can be more efficiently run in a multi-threading/multi-processing environment. This modification is expected to largely reduce the system's computation time for developing quality fuel treatment schedules.

D. Integrate FARSITE into OptFuels through dynamic link libraries (DLL) to simulate fire behavior under varying weather and fuel conditions

In the future work, we plan to build a linkage between OptFuels and FARSITE using the FARSITE DLL. OptFuels currently employs FlamMap to estimate changes in fire behavior as the effects of fuels treatments across a landscape. However, FlamMap assumes constant weather and fuel moisture during its run. FARSITE overcomes this limitation and can provide more realistic fire behavior simulation with varying weather and fuel moisture conditions. The FARSITE dynamic link library (DLL) is currently under development by the RMRS Fire Sciences Lab, and will be available soon. We plan to use the DLL to dynamically link FARSITE with OptFuels for automatic data transfer during the program execution.

E. Analyze the effects of treatment polygon size (project area) on solution quality and efficiency

Dealing with individual stand polygons entails a large number of decision variables in the solution process, which increases the size and complexity of scheduling problem. In addition, decisions made on individual polygons that are independent from neighboring polygons makes it difficult for the solver to efficiently converge to the optimal or near-optimal solutions because there is a relatively small chance to simultaneously select adjacent polygons for treatment and thus the synergic effect of treating a larger and contiguous area is not easily evaluated by the solver. To further improve the efficiency of solution process in the solver, we plan to pre-define groups of treatment polygons where treating a larger and contiguous area can generate bigger treatment effects than small, distant polygons of equal total area. Decisions within the heuristic solver will be then be evaluated and made on groups of polygons in the solver as opposed to individual polygons. This will result in much fewer decision variables and narrower solution space to explore.

ATTACHMENT D

VIII. Deliverables Cross-Walk

Proposed	Delivered	Status
Data transfer interfaces between MAGIS, FlamMap and FVS-FFE that automate and integrate model information.	OptFuels application interfaces that include windows data entry forms, program procedures, and a recommended method for using FVS-ready data for landscape-level vegetation and fuels simulation.	Prototypes ready 2008. See Integrated DSS entry below.
Heuristic optimizer that integrates resource issues/economics with fire behavior projections for various treatment options.	C++ executable. Requires multiprocessor machine for reasonably timely results. Prototype FIREMAGIS.exe	1. First version integrated with OptFuels October, 2009. 2. Solver is functional Feb. 2010. 3. In Progress: testing with different data sets.
Integrated decision support system (DSS) with enhanced solution display to optimize fuel management schedules with enhanced GIS-based solution displays for MTT results.	Decision support system that integrates GIS, FVS-FFE, and FlamMap as a single user-driven application (OptFuels). Generates optimal feasible schedule of fuel treatments. Outputs GIS maps and files of solutions. Outputs FlamMap FMP file to allow user to run MTT on solution landscape files.	Complete (beta) version with working interfaces and procedures. Solutions can be analyzed with MTT and ArcGIS. In progress: solution reports and procedures for GIS statistics.
Test models using data from National Forest(s) with input from local management for resource objectives and constraints.	Test models from Bitterroot National Forest analyses: Willow-Gird and Trapper-Bunkhouse.	1. Trapper-Bunkhouse, September 2008. 2. Willow-Gird, May 2009. 3. Maps posted on JFSP website.
Workshops with field managers: 1. Gather feedback on proposed system 2. Present system to potential users	1. 'FIREMAGIS' workshop held September 2008. 2. Workshop scheduled April 2010.	1. Powerpoint presentation on JFSP website.
JFSP reports	Annual and final reports.	Completed, posted on JFSP website.
Publications and Presentations 1. Development. 2. Effects of budget constraints.	1. OptFuels: Optimizing Placement of Fire and Non-fire Fuel Treatments over Time at Landscape Scales.	1. Paper presented at AFE 4 th International Congress on Fire Ecology & Management. Savannah, GA Nov 30- Dec 4, 2009.

ATTACHMENT D

	<p>2. Developing a Decision Support System to Optimize Spatial and Temporal Fuel Treatments at a Landscape Scale.</p> <p>3. OptFuels: A decision support system to optimize spatial and temporal fuel treatments.</p> <p>4. Effects of budget constraints on optimal hazardous fuel reduction treatment scheduling using fire behavior modeling.</p>	<p>2. Paper presented at Council on Forest Engineering, Kings Beach, CA June 15-18 2009.</p> <p>3. Presented at the 13th Symposium on Systems Analysis in Forest Resources, Charleston, SC May 26-29, 2009.</p> <p>4. In progress.</p>
<p>DSS Technology transfer: Website and User Documentation with active tutorials.</p> <p>DSS Distribution System for Software Delivery:</p> <p>Installation package and software delivery system (ftp and website for downloads and updates).</p>	<p>1. Project website: www.fs.fed.us/rm/human-dimensions/optfuels</p> <p>2. Draft user guide and tutorial: www.fs.fed.us/rm/human-dimensions/optfuels/OptFuelsUsersGuide.pdf</p>	<p>1. Project Website live.</p> <p>2. In progress: Userguide (draft manual posted), context-sensitive help, tutorials, installer.</p>
Other Presentations / Posters.	<p>1. Spatial and Temporal Optimization of Fuel Treatments.</p> <p>2. OptFuels: Optimizing Placement of Fire and Non-fire Fuel Treatments over Time at Landscape Scales.</p> <p>3. Fire-MAGIS: A Decision Support System to Optimize Spatial and Temporal Fuel Treatments at Landscape Scales.</p> <p>4. Optimizing Spatial and Temporal Treatments to Maintain Effective Fire and Non-fire Fuels Treatments at Landscape Scales.</p>	<p>1. Poster presented at the 5th Biennial Lake Tahoe Basin Science Conference, Incline Village, NV, March 16-17, 2010.</p> <p>2. Poster presented at AFE 4th International Congress on Fire Ecology & Management. Savannah, GA Nov 30- Dec 4, 2009.</p> <p>3. Poster presented at IUFRO All-D3 Conference, Sapporo Japan, June 15-20, 2008.</p> <p>4. Poster presented at International Mountain Logging and 13th Pacific Northwest Skyline Symposium, Corvallis OR April 1-6 2007.</p>

ATTACHMENT D

	5. Optimizing Spatial and Temporal Treatments to Maintain Effective Fire and Non-fire Fuels Treatments at Landscape Scales	5. Poster presented at 2 nd Fire Behavior and Fuels Conference, Destin, FL March 26-30, 2007
--	--	---

IX. Literature Cited

- Ager, A., Finney, M. 2009. Application of wildfire simulation models for risk analysis. Geophysical Research Abstracts. vol. 11, EGU2009-5489, 2009 EGU General Assembly 2009.
- Brewer, C.K.; Berglund, D.; Barber, J.A.; Bush, R. 2004. Northern region vegetative mapping project summary report and spatial datasets. USDA Forest Service, Northern Region, Missoula, MT.
- Beukema, S.J., Kurz, W.A. 1998. Vegetation dynamics development tool: user's guide (v. 3.0). Available from: ESSA Technologies Ltd., #300-1765 West 8th Avenue, Vancouver, BC V6J 5C6. 104 p.
- CH₂M Hill 1998. Fire emissions tradeoff model (FETM) ver. 3.3 user's guide. CH₂M Hill contract 53-82FT—7-06. Portland, OR: U.S. Department of Agriculture, Forest Service, Pacific Northwest Region. 52 p.
- Calkin, David E.; Ager, Alan A.; Gilbertson-Day, Julie 2010. Wildfire risk and hazard: procedures for the first approximation. Gen. Tech. Rep. RMRS-GTR-235. Fort Collins, CO: U.S. Department of Agriculture, Forest Service, Rocky Mountain Research Station. 62 p.
- Chew, J.D. 1997. Simulating Vegetation Patterns and Processes at Landscape Scales. In Proceedings of Eleventh Annual Symposium on Geographic Information Systems, Integrating Spatial Information Technologies for Tomorrow. 1997 Feb 17-20; Vancouver, British Columbia, Canada. p. 287-290.
- Chew, J.D., Jones, J.G., Stalling, C., Sullivan, J., Slack, S. 2003. Combining simulation and optimization for evaluating the effectiveness of fuel treatments for four different fuel conditions at landscape scales. In Arthaud, G.J., Barret, T.M., (Tech. Comp.) Systems Analysis in Forest Resources: Proceedings of the Eighth Symposium, held September 27-30, 2000, Snowmass Village, Colorado, USA. Dordrecht: Kluwer Academic Publishers. p.35-46.
- Chew, J.D., Stalling, C., Moeller, K. 2004. Integrating knowledge for simulating vegetation change at landscape scales. Western Journal of Applied Forestry 19(2):102-108
- Crookston, N.L. and A.R. Stage. 1991. User's Guide to the Parallel Processing Extension of the Prognosis Model. Gen. Tech. Rep.-INT-281. Ogden, UT: USDA Forest Service, Intermountain Research Station. 93p.
- Finney, M.A. 1998. FARSITE: Fire Area Simulator--model development and evaluation. USDA Forest Service Res. Pap. RMRS-RP-4.
- Finney, M.A. 2002. Fire growth using minimum travel time methods. Can. J. For. Res. 32:1420-1424.

ATTACHMENT D

- Finney, M.A. 2005. The challenge of quantitative risk analysis for wildland fire. *Forest Ecology and Management*. 211:97-108.
- Finney, Mark A. 2006. A computational method for optimizing fuel treatment locations. In: Andrews, Patricia L.; Butler, Bret W., comps. 2006. *Fuels Management-How to Measure Success: Conference Proceedings*. 28-30 March 2006; Portland, OR. *Proceedings RMRS-P-41*. Fort Collins, CO: U.S. Department of Agriculture, Forest Service, Rocky Mountain Research Station. p. 107-123.
- Finney, Mark A.; Seli, Rob C.; McHugh, Charles W.; Ager, Alan A.; Bahro, Berni; Agee, James K. 2006. Simulation of Long-Term Landscape-Level Fuel Treatment Effects on Large Wildfires. In: Andrews, Patricia L.; Butler, Bret W., comps. 2006. *Fuels Management-How to Measure Success: Conference Proceedings*. 28-30 March 2006; Portland, OR. *Proceedings RMRS-P-41*. Fort Collins, CO: U.S. Department of Agriculture, Forest Service, Rocky Mountain Research Station. p. 125-147.
- Hayes, Jane L.; Ager, Alan. A.; Barbour, R. James, tech. eds. 2004. *Methods for integrated modeling of landscape change: Interior Northwest Landscape Analysis System* Gen. Tech. Rep. PNW-GTR-610. Portland, OR: U.S. Department of Agriculture, Forest Service, Pacific Northwest Research Station. 218 p.
- Jones, J.G., Chew, J.D. 1999. Applying simulation and optimization to evaluate the effectiveness of fuel treatments for different fuel conditions at landscape scales. In Neuenschwander, L. F., Ryan, K. C., Gollberg, G. E., and Greer, J. D., editors. *Crossing the millennium: integrating spatial technologies and ecological principles for a new age in fire management*. University of Idaho and International Association of Wildland Fire. Moscow, Idaho. Vol. 2, p. 89-96.
- Jones, G., Chew, J., Silverstein, R., Stalling, C., Sullivan, J., Troutwine, J., Weise, D., Garwood, D. 2004. Spatial analysis of fuel treatment options for chaparral on the Angeles National Forest. In: USDA Forest Service Gen. Tech. Rep. PSW-GTR (in press).
- Kirkpatrick, S., C.D. Gelatt, and M.P. Vecchi. 1983. Optimization by simulated annealing. *Science* 220: 671-680.
- Kurz, W.A. and S.J. Beukema. 1999. Decision support needs of JFSP stakeholders and the role of the fire and fuel extension to FVS. ESSA Technologies Ltd., Vancouver, BC CANADA. 57pp.
- Metropolis, N., A. Rosenbluth, M. Rosenbluth, A. Teller, and E. Teller. 1953. Equation of state calculations by fast computing machines. *Journal of Chemical Physics* 21: 1087-1101.
- Reinhardt, E.D., Crookston, N.L. (Tech. Ed.) 2003. *The Fire and Fuels Extension to the Forest Vegetation Simulator*. USDA Forest Service Gen. Tech. Rep. RMRS-GTR-116.
- Reinhardt, E.D., Keane, R.E. and Brown, J. K. 1997. *First Order Fire Effects Model: FOFEM 4.0 user's guide*. USDA Forest Service Gen. Tech. Rep. INT-GTR-344.
- Schmidt, K.M., Menakis, J.P., Hardy, C.C., Hann, W.J., Bunnell, D.L. 2002. Development of coarse-scale spatial data for wildland fire and fuel management . General Technical Report, RMRS-GRR-87, U.S. Department of Agriculture, Forest Service, Rocky Mountain Research Station, Fort Collins, CO.

ATTACHMENT D

- Scott, J.H., Reinhardt, E.D. 2001. Assessing crown fire potential by linking models of surface and crown fire behavior. USDA Forest Service Res. Pap. RMRS-29.
- Zuuring, H.R., Wood, W.L., Jones, J.G. 1995. Overview of MAGIS: a multi-resource analysis and geographic information system. USDA Forest Service Res. Note INT-427.

ATTACHMENT D

EXHIBIT F

Effects of fuel spatial distribution on wildland fire behaviour

Adam L. Atchley^{id A,E}, Rodman Linn^A, Alex Jonko^{id A}, Chad Hoffman^{id B},
Jeffrey D. Hyman^{id A}, Francois Pimont^{id C}, Carolyn Sieg^D and
Richard S. Middleton^{id A}

^ALos Alamos National Laboratory, Earth and Environmental Sciences, PO Box 1663 Los Alamos,
NM 87545, USA.

^BColorado State University, Warner College of Natural Resources, 1472 Campus Delivery Fort
Collins, CO 80523-1472, USA.

^CINRAE, URFM, Site Agroparc Domaine Saint Paul F-84914 Avignon, France.

^DUSDA Forest Service, Rocky Mountain Research Station, 2500 S, Pine Knoll Dr. Flagstaff,
AZ 86001, USA.

^ECorresponding author. Email: aatchley@lanl.gov

Abstract. The distribution of fuels is recognised as a key driver of wildland fire behaviour. However, our understanding of how fuel density heterogeneity affects fire behaviour is limited because of the challenges associated with experiments that isolate fuel heterogeneity from other factors. Advances in fire behaviour modelling and computational resources provide a means to explore fire behaviour responses to fuel heterogeneity. Using an ensemble approach to simulate fire behaviour in a coupled fire–atmosphere model, we systematically tested how fuel density fidelity and heterogeneity shape effective wind characteristics that ultimately affect fire behaviour. Results showed that with increased fuel density fidelity and heterogeneity, fire spread and area burned decreased owing to a combination of fuel discontinuities and increased fine-scale turbulent wind structures that blocked forward fire spread. However, at large characteristic length scales of spatial fuel density, the fire spread and area burned increased because local fuel discontinuity decreased, and wind entrainment into the forest canopy maintained near-surface wind speeds that drove forward fire spread. These results demonstrate the importance of incorporating high-resolution fuel fidelity and heterogeneity information to capture effective wind conditions that improve fire behaviour forecasts.

Keywords: fire behaviour modelling, fuel classification, fuel representation, wind response.

Received 20 June 2020, accepted 14 December 2020, published online 27 January 2021

Introduction

It is exceedingly difficult to know *a priori* if a wildland fire will extinguish, or spread and contribute to the annual 36 to 46 million km² burned globally (Doerr and Santin 2016). Nevertheless, this knowledge is critical for forecasting if a wildland fire will meet management targets or for guiding management response to fires that endanger lives and property. A combination of environmental factors – including wind, topography, fuel moisture, and the amount and arrangement of fuel – determine wildland fire behaviour. For example, the spatial distribution of fuel heterogeneity, which determines the arrangement of combustible material and local wind flows, significantly influences fire behaviour (Turner and Romme 1994; Finney 2001; Knapp and Keeley 2006; Parsons *et al.* 2017). Simulated wind conditions, coupled to fire interacting with heterogeneous forest canopies, show that fire behaviour is affected by fuel structure (Pimont *et al.* 2011; Linn *et al.* 2013; Hoffman *et al.* 2015; Parsons *et al.* 2017; Ziegler *et al.* 2017). However, studies that systematically characterise the sensitivity of fire behaviour to fuel heterogeneity are

absent owing to poorly described fuel conditions and computational or experimental costs. Therefore, the response of fire behaviour to fuel arrangement remains poorly quantified, which limits estimates of fire outcomes.

Over the past two decades, a growing breadth of fire scenarios – ranging from prescribed fires in marginal conditions to high-intensity wildfires – and the increasing availability of computational resources have motivated the development of coupled fire–atmosphere models, such as WFDS (Mell *et al.* 2007, 2009; Bova *et al.* 2016), FIRESTAR3D (Frangieh *et al.* 2018; Morvan *et al.* 2018), FIRETEC (Linn 1997; Linn *et al.* 2002) and QUIC-Fire (Linn *et al.* 2020). These models resolve wind fields that are consistent with local heterogeneous vegetation structure and respond to dynamic two-way feedbacks between the fire and surrounding winds that compare well with observations (Linn and Cunningham 2005; Linn *et al.* 2012; Hoffman *et al.* 2016). By simulating wind flows and explicitly accounting for shear stress through canopy structures, including intermittent gusts and lulls that result from gaps between groups of trees (Pimont *et al.* 2009), fire

ATTACHMENT D

B *Int. J. Wildland Fire*A. L. Atchley *et al.*

behaviour simulations respond to the aerodynamic influences of canopy structure and the spatial heterogeneity of vegetation and buoyant heat from combustion. Although many of these models are too computationally expensive for operational use, they allow a fully three-dimensional description of the forest. The development of this class of models now lets us test how sensitive simulated fire behaviour is to representation of fuel and the characterisations of fuel heterogeneity, especially for low-intensity fires that are more sensitive to fuel arrangement compared with high-intensity fires (Clements *et al.* 2016).

Discontinuities in the horizontal distribution of canopy fuels associated with large-scale heterogeneities create wind patterns (Dupont and Brunet 2007) that influence fire behaviour. Forest structure affects the fire environment by determining: (1) the distribution of combustible material; (2) the ambient flow patterns through and around vegetation (Gao and Shaw 1989; Finnigan 2000; Pimont *et al.* 2011); and (3) the response of winds to the heat released during the fire (Kiefer *et al.* 2018). Canopy heterogeneity increases the spatial and temporal variation in the wind field within and just above the canopy, with the intermittent sweeping of fast-moving air down into the canopy and the ejection of slow-moving air upward out of the canopy (Kiefer *et al.* 2016; Kiefer *et al.* 2018; Moon *et al.* 2019). The aggregated effects of this turbulence alter the mean wind shear above (Dupont and Brunet 2008), within and below the canopy. Likewise, the distribution of fuels influences the spatial patterns of winds that can be drawn in by the fire and fire-influenced winds that feed back to fire behaviour (Kiefer *et al.* 2018).

Variability in wind conditions associated with boundary-layer turbulence and wind–canopy interaction is recognised as a chief contributor to uncertainty in fire behaviour (Burrows *et al.* 2000; Sun *et al.* 2009; Linn *et al.* 2012; Pinto *et al.* 2016; Benali *et al.* 2017). Atmospheric turbulence is amplified when winds interact with fire (Clements *et al.* 2008), increasing uncertainties in fire behaviour simulations, especially under marginal fire conditions (Hiers *et al.* 2020) when fire-influenced winds are significantly stronger than ambient winds. This complicates the ability to measure how forest heterogeneity interacts with fire-influenced winds to affect fire behaviour.

Given the influence of canopy structure on ambient and fire-induced winds, it is essential to explicitly account for the effects of canopy structure when exploring the interaction between forest structure and fire behaviour (Hilton *et al.* 2015). Nevertheless, the effects of forest heterogeneity on the variability of fire behaviour have not been quantified adequately (Parsons *et al.* 2017) because few studies systematically account for increasing levels of fuel variability. Therefore, a generalised understanding of how spatial fuel characterisation determines fire behaviour is lacking. By identifying how fuel heterogeneity influences fire behaviour and describing essential aspects of fuel heterogeneity, simulated uncertainty and fire behaviour variability can be constrained.

To determine the influence of vegetation structure on fire behaviour, an analysis of ensembles of simulations is required to avoid confounding mean behaviour with the influences of site and moment-specific conditions (Parsons *et al.* 2017). Fire behaviour at a specific location in time and space is a function of the site and moment-specific environmental conditions, including the local arrangement of fuels and timing of gusts

relative to the fire's arrival at that location. The absence of precise knowledge of fuel locations or relative timing of fires and wind events limits predictability (Pimont *et al.* 2017). Ensembles of vegetation scenarios with the same macro-scale characteristics (e.g. canopy bulk density) but different fine-scale characteristics (e.g. the position of individual trees) can help (1) determine the sensitivity of fire behaviour to fine-scale fuel characteristics, and (2) quantify the uncertainty associated with fire behaviour forecasts. By performing ensemble simulations with a physics-based model of combined dynamic winds and fire behaviour, we can quantify both the mean and variability in fire behaviour associated with macro-scale fuel heterogeneity. Likewise, an ensemble approach provides a measure of fire behaviour uncertainty within constrained conditions (Pinto *et al.* 2016) that can inform fuel management planning and risk assessment frameworks for operational use (Ager *et al.* 2011; Finney *et al.* 2011). Increasingly, probabilistic ensemble methods have also been shown to elicit fundamental behaviour within complex fire models that account for non-linear processes (Cruz and Alexander 2017). To discern fire behaviour sensitivity to details of fuel heterogeneity, ensembles of multiple fuel beds that have the same domain fuel load and spatial characterisation of the variance of fuel density are required. Here, we investigated the sensitivity of fire behaviour simulations in FIRETEC to spatial characterisation of fuel arrangement. Virtual canopies with the same macro-scale characteristics but different degrees of detail in representation were developed to perform ensemble fire behaviour simulations.

Methodology

We used FIRETEC, a mechanistic fire–atmosphere model, to investigate how the representation and heterogeneity of fuel influence simulated fire behaviour. We generated ensembles of virtual forest canopies based on field measurements from a 50 × 20-m ponderosa pine (*Pinus ponderosa*)-dominated plot near Flagstaff, AZ, with 860 trees ha⁻¹, a mean diameter at breast height (DBH) of 23 cm and a mean tree height of 14 m (Linn *et al.* 2005). Each ensemble features identical macro-scale characteristics, including domain average and vertical profiles of fuel density (0.083 kg m⁻³) (Fig. 1, plot (a)), average tree height, and average height to live crown, but with different variance and spatial characterisation of fuel conditions. We conducted a total of 101 simulations, including 20 replicates each of five different heterogeneous fuel distributions, and an unreplicated simulation with a homogeneous fuel distribution (Average Fuel). We explored the spectrum of fuel fidelity starting with the low-fidelity homogeneous or Average Fuel case. The five heterogeneous fuel scenarios represent a stepwise increase in fuel fidelity and length scales of fuel heterogeneity representation. They are: (1) Average Tree, with one representative tree randomly replicated across the domain (no difference between trees); (2) Forest Data, with variable trees, whose attributes match field data, randomly placed across the domain; (3) 15-m Gaps, with the same fuel fidelity as Forest Data, but with trees aggregated to create 15-m gaps; (4) 30-m Gaps, same as Forest Data, with trees aggregated to create 30-m gaps, and (5) 45-m Gaps, same as Forest Data, with trees aggregated to create 45-m gaps. In each simulation, the total fuel load was held constant, and only the

ATTACHMENT D

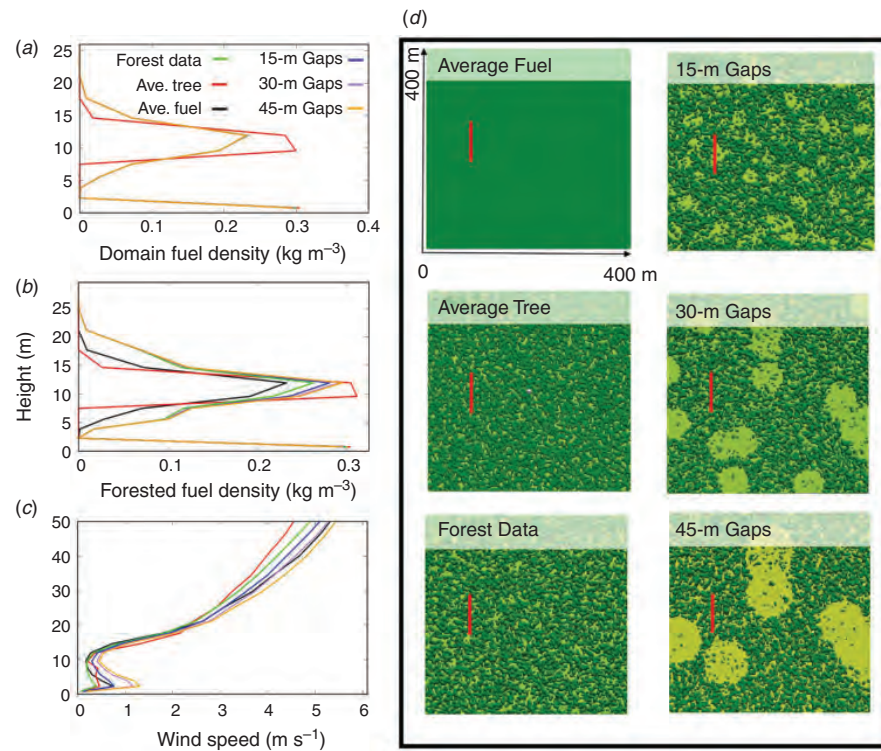


Fig. 1. (a) Domain-average vertical fuel density profiles for each ensemble; note that all ensembles except Ave. Tree overlap. (b) Vertical fuel density profiles averaged over areas with canopy fuel densities above zero. Note that excluding areas where vertical fuel density equalled zero resulted in a gradation of fuel density with increased fuel variance. Domain fuel density equalled 0.083 kg m^{-3} for all ensembles, and variation of canopy fuel density plotted was due to differences in tree density for the areas with trees. (c) Ensemble-average u wind (streamwise velocity) profiles to 50 m above the surface before ignition. (d) Example fuel domains for each of the six ensembles. Red lines denote the fire ignition locations.

Table 1. Domain fuel load characteristics

Representation class (Ensemble)	Fuel density variance	Fuel density correlation length (m)
Average Fuel	0	0
Average Tree (1)	0.188	1
Forest Data (2)	0.299	2
15-m Gaps (3)	0.359	10
30-m Gaps (4)	0.364	27
45-m Gaps (5)	0.377	40

arrangement of the trees was altered. The 20 replicates were developed by rerandomising tree and gap locations. All simulations were performed in 400×400 -m domains with 2-m horizontal discretisation to a height of 600 m. Domain fuel density was defined as the total mass of fuel within the $160\,000\text{-m}^2$ domain between the ground and 22.9 m, top of the highest cell containing fuel. We established a gradient of fuel density variability between the ensembles, starting with $0 (\text{kg m}^{-3})^2$ for the Average Fuel ensemble and increasing to $0.377 (\text{kg m}^{-3})^2$ for the

45-m Gap ensemble (Table 1). Likewise, there was a gradient of increasing lengths at which deviations from the local fuel load were no longer similar (correlation lengths).

We developed a different 3D fuel density arrangement for each replicate within each ensemble using values for tree height, crown radius and height to live crown obtained from data. For the Forest Data ensemble, the distribution of fine fuel in the canopy was parameterised following the methods outlined by Linn *et al.* (2005), where sampled trees and their dimensions were randomly placed throughout the domain to maintain observed stem density and forest characteristics. We developed the Average Tree virtual forest realisations by first estimating the mean tree height, height to live crown and crown circumference, and then randomly populating the domain with trees that had these properties. Note that populating the domain with a single-tree representation resulted in slightly different vertical profiles of fuel density (Fig. 1a). To develop the Average Fuel realisation, we computed the vertical distribution of fuel by horizontally averaging every vertical layer in the Forest Data domains. This vertical distribution was then applied to every x and y location to establish a horizontally homogeneous forest with the same vertical distribution of fuel density as for the

ATTACHMENT D

D *Int. J. Wildland Fire*A. L. Atchley *et al.*

Forest Data cases. Because there was no spatial variation in the Average Fuel realisation, only one ensemble member was used. For the 15-, 30- and 45-m Gap ensembles, we randomly selected locations for gap creation. All trees within the gap were then moved to a new random location, which might be placed back in the gaps, thus ensuring that the overall fuel load and canopy density was maintained among ensembles. This approach effectively decreased the fuel density within the designated patches and increased the fuel density in other areas (Fig. 1b), which mimics the structure found in forests with natural disturbances (Lindenmayer and Franklin 2002; Mitchell *et al.* 2006).

We parameterised surface fuels assuming that grass dominates in the spaces between trees, and litter accumulates and diminishes grass loads beneath trees. We used a grass fuel density of 0.35 kg m^{-3} , which had a height of 0.7 m, and a litter fuel density of 0.5 kg m^{-3} , which had a maximum litter depth of 10 cm under dense trees. The spatial distribution of grass and litter contributed to the overall domain fuel density variance and spatial gradients of fuel density variance. As described in Linn *et al.* (2005), the total fuel loads in surface cells included contributions from grass, litter, and short trees that reached into the lowest computational cell. The aggregated fuel properties of the combined surface fuels (e.g. moisture and height) were determined via a mass-weighted average. We observed no difference in domain surface fuel density between ensembles (Fig. 1a; all lines overlap below 2 m).

Fire simulations

To represent wind conditions characteristic of a given ensemble, turbulent structures need to develop in response to the simulated forest structure from an initial inflow boundary condition, which generally requires simulations to include a long fetch area. To reduce the size of the computational domain, we used the methodology described in Pimont *et al.* (2020). A large-scale pressure gradient force and cyclic boundary conditions, where winds exiting the domain are cycled back as inflow into the domain, create the long fetch necessary for turbulence to adjust to the ensemble fuel structure. This results in turbulent structures evolving within the model domain to be spun up and used as inflow boundary conditions during the fire simulation. We developed ensemble-specific wind fields using a single representative fuel arrangement for each ensemble. A 3-m s^{-1} streamwise wind speed (u) was specified at 25 m above the ground, ~ 10 m above the canopy that accompanied an initial log profile wind speed with height. This fairly low wind speed was chosen to represent marginal fire spread conditions. The winds and turbulence were spun up in this manner for 500 s, at which time the mean vertical velocity profile and the turbulence profiles ceased to change with time. Using the cyclic boundary condition mode, we simulated turbulent winds for each ensemble type for an additional 20 min as forcing conditions for the combustion simulations.

Each realisation within a given ensemble used the same representative forcing conditions but resulted in different wind profiles, as determined by the specific drag imparted by the characteristic spatial fuel arrangement of that ensemble (Fig. 1). These forcing conditions were applied for an additional 400 s before the time of ignition so that the flow field could adjust to the specific vegetation distribution. Ignition in each simulation

was achieved by bringing surface and canopy fuels up to combustion temperatures (1000 K) for 3 s in a 100-m-long and 4-m-deep rectangular area located 100 m from the upwind domain boundary. The idealised ignition method is intended to ensure each realisation starts with a similar region of combustion. Not including the model spin up, each realisation required 64 processors and 16 h of wall-clock time to simulate combustion, resulting in 103 524 CPU hours for all combustion simulations. Spinning up wind fields for all ensembles required an additional 12 288 CPU hours.

Fire and wind behaviour metrics

For each ensemble and realisation, we calculated the forward rate of fire spread, heat release per unit area and the total area burned. We calculated the spread distance for each fire to be the farthest distance of the fire front from the ignition line along the streamwise wind direction (u) and plotted it against time to evaluate the forward rate of fire spread. Heat release per unit area is the total amount of energy released by combustion per second divided by the area of the fire, and therefore has units of kilowatts per metre squared. The area burned was estimated as the total area of the domain where combustion (i.e. loss of fuel mass) occurred projected onto a 2D plane. We quantified domain wind conditions in terms of turbulence kinetic energy (TKE), which is a measure of the energy associated with fluctuations in the wind field shear stress. TKE was calculated by summing the variances of the directional wind component:

$$\text{TKE} = \frac{1}{2} ((u'u') + (v'v') + (w'w')) \quad (1)$$

where:

$$\begin{aligned} u'u' &= \frac{1}{t} \int_0^t (u_{(t,i,j)} - \bar{u}_{(i,j)})^2 dt \\ v'v' &= \frac{1}{t} \int_0^t (v_{(t,i,j)} - \bar{v}_{(i,j)})^2 dt \\ w'w' &= \frac{1}{t} \int_0^t (w_{(t,i,j)} - \bar{w}_{(i,j)})^2 dt \end{aligned} \quad (2)$$

Here, u is the streamwise horizontal wind component, v is the cross-stream horizontal wind component, w is the vertical wind component, i and j are the indices of specific cells, and t is the time index.

Results and discussion

The Average Fuel simulation had the greatest forward spread, heat release rate per unit area and area burned (Fig. 2). The Average Tree ensemble with randomly placed trees slowed the forward spread and decreased fire intensity compared with the Average Fuel simulation. Increasing the level of detail in the representation of fuels resulted in added variations in fuel density, such as small gaps between trees that caused the fire to slow and reduced heat per unit area. Likewise,

ATTACHMENT D

Effects of fuel spatial distribution

Int. J. Wildland Fire E

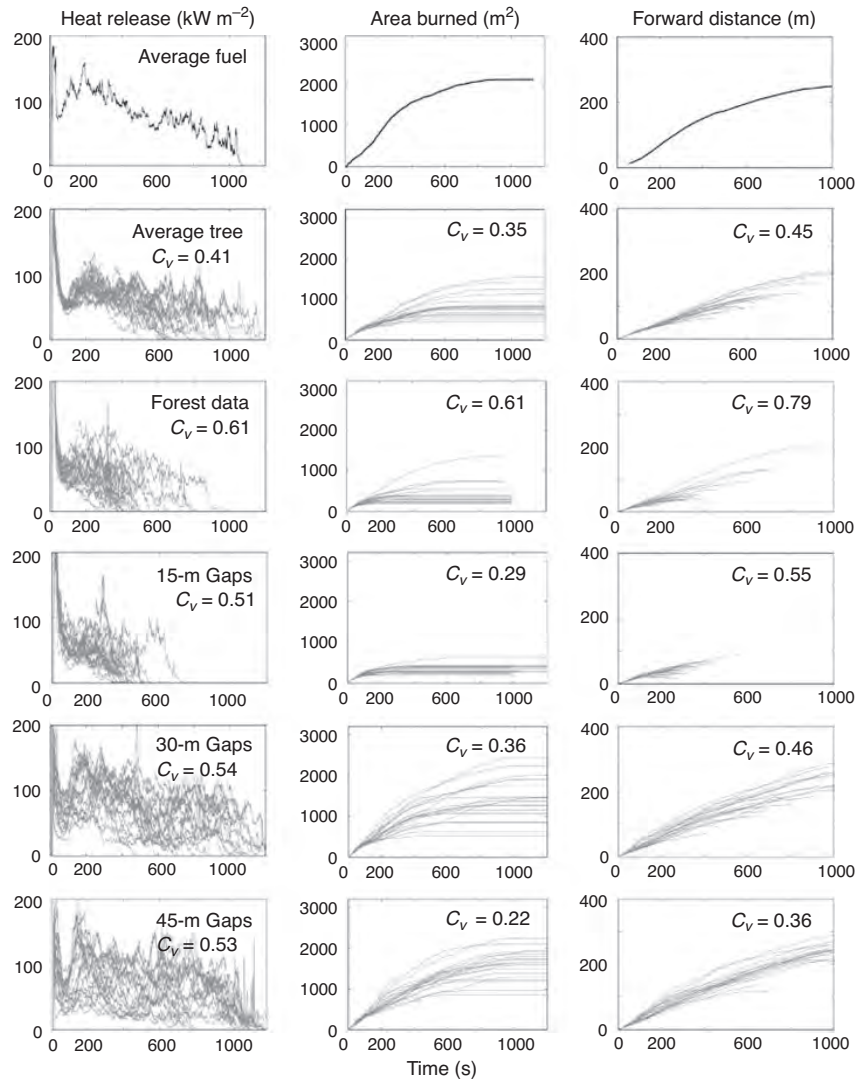


Fig. 2. Time series of fire intensity (left), area burned (centre), and forward progress of fire (right) highlight variability in fire metrics for all ensembles except for Average Fuel, which only has one ensemble member. The coefficient of variation, $C_v = \frac{\sigma}{\bar{X}}$ (σ is the standard deviation and \bar{X} is the mean), is also provided for each ensemble.

increasing the variation of sizes and shapes of trees to that of the Forest Data and 15-m Gap ensembles further reduced heat released, rate of spread and area burned. Conversely, increasing local canopy density and the length scale of sparse forest gaps from the 15-m to the 30- and 45-m ensembles resulted in simulated fire behaviour metrics to rebound compared with the simulated results of the Average Tree, Forest Data and 15-m Gap ensembles. The increase in fire behaviour metrics for the 30- and 45-m Gap ensembles demonstrates that increasing variability in spatial fuel density does not necessarily act to slow fire progression and that fire behaviour is a result of complex interactions with fuel structure.

Ensemble results (Fig. 2) show a range of fire outcomes within each characteristic fuel representation, except for the Average Fuel simulation, which did not have any replicates. The range in fire behaviour outcomes for each ensemble was determined by the variation between details of specific fuel representations, fuel arrangement for given realisations and the associated wind variability. Interestingly, the range in fire behaviour metrics did not increase along the gradient of fuel density variability because the Forest Data and the 15-m Gap ensembles generally did not propagate fire and extinguished quickly. However, when scaled by the mean fire behaviour, the coefficient of variability for the Forest Data remained high.

ATTACHMENT D

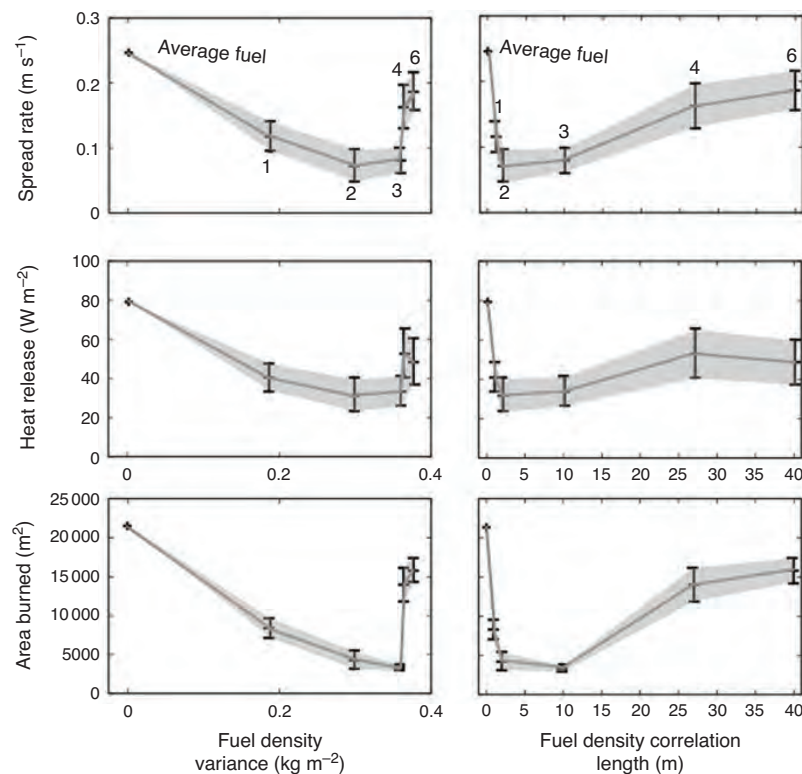
F *Int. J. Wildland Fire*A. L. Atchley *et al.*

Fig. 3. Mean and the 95th confidence interval of spread rate, heat release rate, and area burned for each ensemble plotted against variation in fuel density and correlation length of fuel density. Numbered ensembles are cross-referenced in Table 1.

Furthermore, one Forest Data realisation carried 200 m, which contributed to the observed variability in that ensemble (Fig. 2). This suggested that while there is a high probability that fires in the Forest Data ensemble will not spread under the conditions simulated, there is also the possibility that some fires will act outside the ensemble characteristic. Similarly, the large fuel density correlation lengths in the large-gap ensembles also contributed to variability in fire size and behaviour, similar to what Parsons *et al.* (2017) observed.

Emergent fire behaviour from characteristic fuel variability

Differences between ensembles indicated that both the representation and heterogeneity of fuel density influenced fire behaviour. How fuel arrangement characteristics influenced probable fire behaviour in these marginal conditions was shown by plotting summarised fire behaviour metrics for each ensemble against the domain variance of fuel density and the correlation length of that variability (Fig. 3). As fuel density variability increased, all fire behaviour metrics (forward spread, heat released and area burned) decreased linearly for correlation lengths less than 10 m. However, as the correlation length of fuel density increased beyond 10 m, the fire behaviour metrics rebounded (Fig. 3). In the 30- and 45-m Gap ensembles, which correspond to correlation lengths of 27 and 40 m respectively, all fire behaviour metrics increased compared with the other

ensembles except for the Average Fuel case. The 45-m Gap ensemble had slightly greater spread rates and area burned than the 30-m Gap ensemble, whereas the 30-m Gap ensemble had a slightly greater heat release. However, these changes were also associated with an increased variance for both the 30- and 45-m Gap ensembles, and distinguishing ensemble trends from each other was difficult.

These results have three implications for simulating fires in a forest with heterogeneous fuels using process-based modelling: (1) there can be significant differences associated with representing the canopy and surface fuels as a homogeneous layer for ecosystems that naturally include gaps between trees; (2) the variability between sizes and shapes of trees in the forest can have significant impacts on fire behaviour by slowing spread; and (3) the length scales of heterogeneity in fuel density also influenced fire behaviour, where length scales greater than 10 m increased rate of spread and area burned. The sensitivity of fire behaviour to fuel fidelity and variability highlighted in these results suggests the need for increased fuel description detail. Historically, fuels were characterised using stand-scale spatially averaged descriptors (i.e. canopy bulk density, canopy base height), often without considering the within-stand variability (Hoffman *et al.* 2016). However, rapidly evolving remote sensing and machine learning techniques can now characterise three-dimensional fuel structure, including tree-scale spatial

ATTACHMENT D

Effects of fuel spatial distribution

Int. J. Wildland Fire G

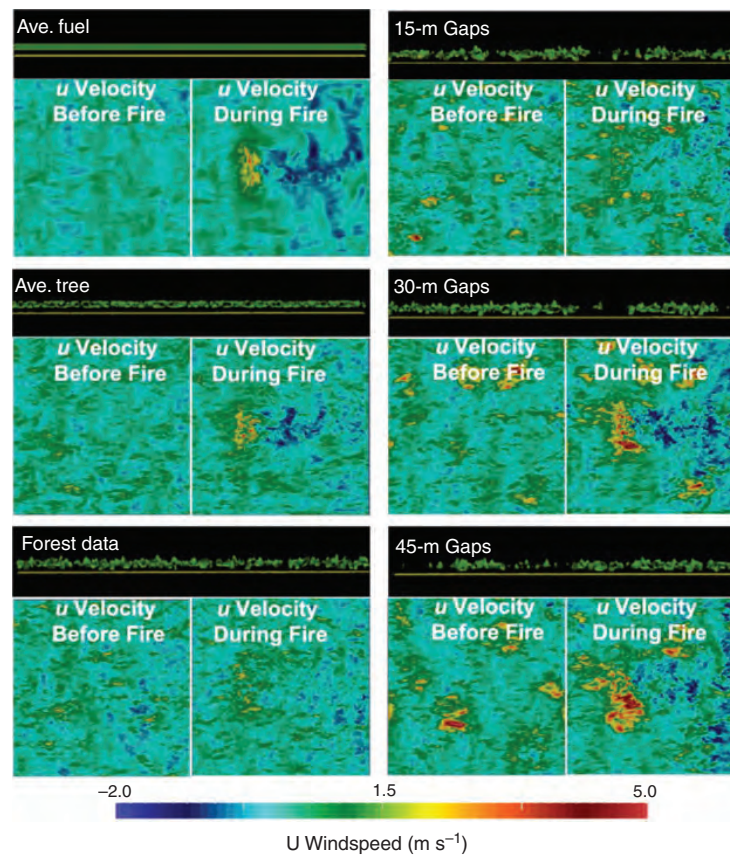


Fig. 4. Horizontal fuel profiles from a sample realisation of each ensemble, a u velocity snapshot at mid-canopy height (11 m) before ignition and after ignition showing the interaction of wind flow with the fire. Note the disaggregated u velocities in the Forest Data and 15-m Gaps ensembles.

heterogeneity (Liao *et al.* 2018; Massetti *et al.* 2019; Narine *et al.* 2019) and three-dimensional below-canopy fuel density (Hudak *et al.* 2020). Furthermore, the ability to quantify fuel structure and model physically based fire dynamics motivates an in-depth understanding of the three-dimensional wind and fuel interactions that influence fire behaviour. Combining three-dimensional wind and fuel interactions with quickly assessed remote sensing and machine learning techniques could increase the application and accuracy of data-driven wildfire models (Coen and Schroeder 2013; Coen *et al.* 2013).

Influence of changing the level of detail in fuels descriptions

The Average Fuel realisation had the least amount of fuel detail, where the horizontal fuel mass was spread evenly, creating a continuous layer of low-density fuel rather than individual trees. Conversely, when representing individual trees, the same amount of canopy mass was concentrated into localised areas – ‘trees’ – leaving gaps in the canopy. Similarly, surface fuel also shifted to denser litter under trees and less dense grass in spaces between trees. Gaps between trees acted as barriers to crown fire spread, which required stronger and more consistent local winds

to bridge the gaps. Additionally, the representation of individual trees and litter, in which the fuel density was higher than in the homogenised Average Fuel, slowed fire spread because it took longer to consume fuels of higher densities and push forward spread, behaviour previously observed by Pimont *et al.* (2006). Areas with higher fuel densities also released more heat, resulting in a stronger local vertical motion, which, coupled with longer combustion residence time, resulted in longer periods of updrafts that impeded the forward propagation due to winds in the along-stream direction.

Canopy structure impacted winds because randomly arranged trees imposed variable aerodynamic drag. It is not surprising that winds would be slower within or right behind dense vegetation compared with lower-density vegetation. Although there were gaps in the Average Tree canopy, those gaps were not large enough for the wind to efficiently penetrate and reestablish, and thus the average wind speeds within the canopy were lower (Fig. 1). The lower wind speed within the canopy combined with canopy gaps and higher localised fuel densities of trees all worked to slow or stop canopy fire spread because the weak winds could not push the simulated fire across

ATTACHMENT D

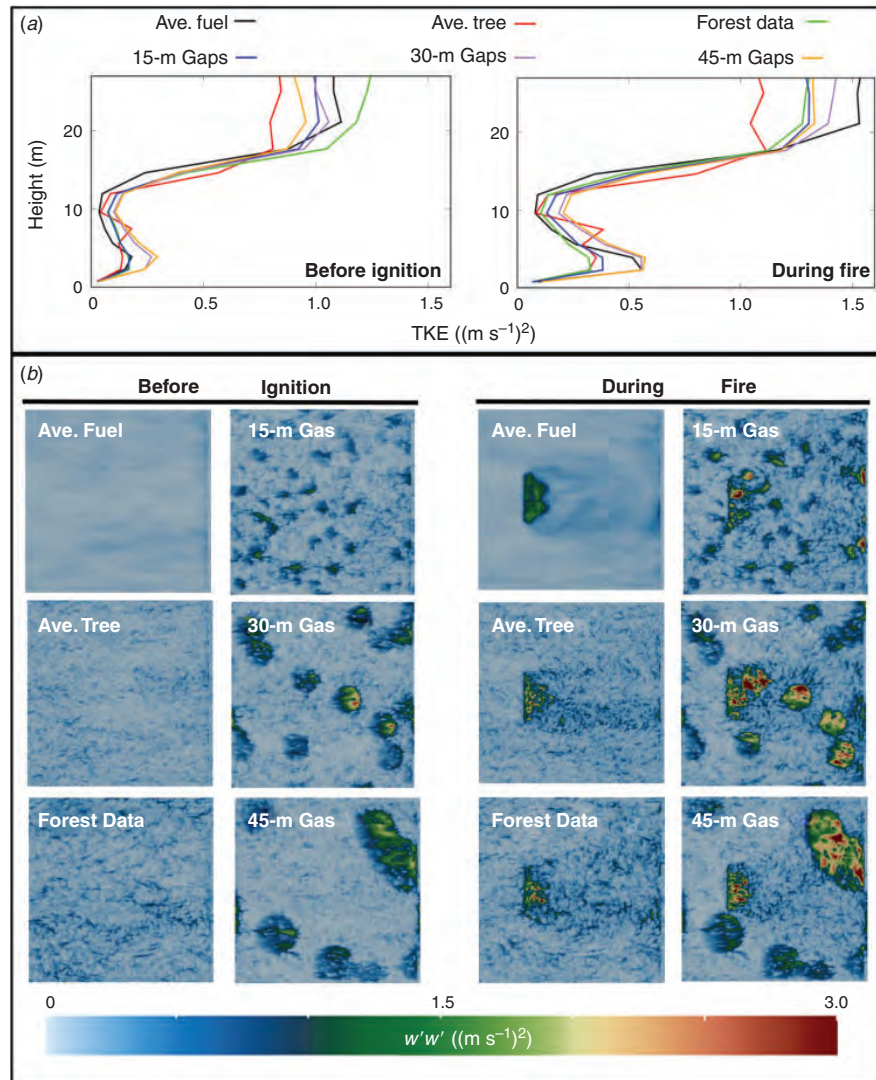
H *Int. J. Wildland Fire*A. L. Atchley *et al.*

Fig. 5. Average turbulent kinetic energy (TKE) for the 2.5 min before the time of ignition is plotted on the left in panel (a) and the average TKE for the 2.5 min after ignition on the right of panel (a). Panel (b) shows the average $w'w'$ magnitude for the 2.5 min before ignition (left) compared with the 2.5 min following ignition (right) at the mean canopy height of 10 m for a sample realisation from each ensemble.

the gaps and the buoyancy-induced flow was less likely to lean enough to the side to ignite a neighbouring tree.

Describing the variation among the trees

When considering differences between the Forest Data and Average Tree ensembles, the additional representation of fuel fidelity and therefore variation among trees resulted in a further decrease in fire spread, heat release per unit area and area burned. Using heterogeneous tree sizes and shapes meant trees were interacting with the wind field over a larger vertical extent than an averaged canopy or as a characteristic tree. This essentially broke up the larger-scale wind patterns into tree and

gap-scale patterns. The level of explicit detail related to the canopy structure influenced simulated winds and turbulence; similarly to Boudreault *et al.* (2014), greater canopy representation resulted in a higher level of fine-scale turbulence (Fig. 4). For example, the presence of low hanging branches or smaller trees in the forest data ensemble disrupted dominant winds, especially near the surface, resulting in the lowest subcanopy wind speeds (Fig. 1b). Low wind speeds below the canopy hindered both surface and crown fire spread. Interestingly, complex canopy-driven disruptions to dominant wind flow were noticeable without fire as well as with fire when buoyant wind dynamics caused high-speed horizontal winds to feed the fire

ATTACHMENT D

from multiple directions (Fig. 4). These findings contrast with earlier studies that reported little change in overall turbulent kinetic energy associated with small-scale heterogeneity because vertical shear instabilities typically dominated (Patton 1997; Pimont *et al.* 2011). Our results suggest that even if the fine-scale turbulence was only a marginal contribution to the total kinetic energy budget, the turbulent features associated with small-scale heterogeneity can impact fire behaviour through their influence on both instantaneous local flows and reaction rates.

Influences of fuel density heterogeneity

The wind and fire behaviour also responded to a heterogeneous density of canopy fuel, suggesting that including canopy fuel heterogeneity in forest inventory databases or fuel class descriptions may help fire behaviour forecasts. The increased continuity of canopy fuel in densely forested regions and the increased surface and canopy wind speeds generated by the large gaps resulted in increased forward spread and area burned. The small distance between adjacent trees in aggregated canopies reduced the barriers to active crown fire spread. Likewise, surface fuel continuity increased with less-dense and faster-burning grasses. In addition, as canopy gap size increased, winds could penetrate through the canopy, resulting in increased wind velocity and fire spread.

Our results show that large openings in the canopy allow large-scale wind entrainment below the canopy, similarly to Dupont *et al.* (2011) and Pimont *et al.* (2011), and push the fire front along despite the increased fuel heterogeneity. To visualise how these openings allowed wind turbulence to pass vertically through the canopy, we examined the magnitude of the vertical variance of velocity ($w'w'$) 2.5 min before the fire was ignited and 2.5 min after ignition (Fig. 5). Using $w'w'$ allowed us to visualise the persistence of positive and negative vertical fluctuations from the mean and to identify areas of strong variations. The areas of large $w'w'$ corresponded to large canopy openings. Moreover, there was a larger increase of $w'w'$ and TKE during the fire (Fig. 5) for the 30- and 45-m Gap ensembles. Corresponding increases in $u'u$ and $v'v'$ (not shown) accompanied increases in $w'w'$. Large gaps in the canopy acted to increase wind entrainment, shear stress above the canopy shown as increased windspeed in Fig. 1c, and therefore TKE before and especially during combustion, thus allowing larger and consistent wind structures to interact with the fire (Fig. 5). This ability to move air in and out of the openings and an increase in the cross-stream wind turbulence ($v'v'$) also helped to maintain a larger fire line width (Hilton *et al.* 2015).

The non-monotonic relationship between correlation length of fuel variability and fire behaviour metrics, which rebounded at large length scales, illustrated that below a certain gap size, changes to canopy and subcanopy winds were not strong enough to change fire behaviour. Studies of wind interaction with forest canopies suggest that for winds to re-equilibrate to the absence of trees, a length of ~ 22 to 30 times the average canopy height is needed (Lee 2000; Pimont *et al.* 2018). To induce canopy and subcanopy turbulent wind structures, a length of 1 to 5 times the canopy height appears to be necessary (Pimont *et al.* 2011; Parsons *et al.* 2017). At 1.8 to 2.6 times the average canopy height, the 30- and 45-m Gap ensembles resulted in the canopy

and subcanopy wind turbulence structures that influenced fire behaviour. In contrast, the ratio between gap length and canopy height for the 15-m Gap ensemble was not enough for the canopy and subcanopy turbulent winds to develop.

We note that we have focused on a ponderosa pine forest with circular canopy gaps of different sizes under low-velocity wind conditions, which demonstrated the dominant role that forest canopy heterogeneity has on effective wind conditions driving fire behaviour. However, many different forest types and conditions will likely impart unique signatures on fire behaviour such as the level of surface fuel homogenisation. A supplementary analysis (see supplementary material) comparing a homogenised surface fuel configuration with our heterogeneous grass and litter surface fuel conditions demonstrates a strong influence of surface fuel conditions. Yet for our simulations, surface fuel homogeneity or heterogeneity does not significantly affect the relationship between fire behaviour metrics and fuel density variability or the length scales of that variability. We therefore hypothesise that fuel variability and the spatial length scales of that variability will influence fire behaviour in predictable ways. For example, greater wind velocities associated with more extreme burning conditions would dampen the effects of spatial variability on fire behaviour (e.g. Sieg *et al.* 2017). In contrast, increased canopy height could strengthen the relationship. Additionally, the overall domain canopy density could play a role in the strength of this relationship, where lower forest densities could weaken the effects of spatial fuel variability on fire behaviour.

Conclusions

We demonstrated that fuel variability and spatial characterisation of fuel density influenced simulated fire behaviour. Greater detail in fuel representation resulted in increasingly fine-scale wind discontinuities, which reduced fire spread and area burned. Likewise, when introducing variability in tree size and shape, the strength of fire behaviour metrics decreased. Spatial scales of fuel variability were also instrumental in the interaction of wind and fuel variability in determining fire spread. We observed a non-monotonic relationship between correlation length of fuel variability and fire metrics, all of which decreased with increasing correlation length up to 10 m but increased with correlation lengths above 10 m. Wind entrainment associated with large, sparse canopy patches resulted in both mean and localised wind speeds and faster fire spread. Furthermore, the turbulent wind conditions in large openings resulted in a disproportional increase in TKE and crosswinds that maintain fire line width.

The use of ensembles with equally probable spatial fuel distributions to characterise fire behaviour was necessary given the range of outcomes. Although mean behaviour for each ensemble was identified, significant overlap existed among individual realisations from different ensembles, highlighting the limitation of drawing conclusions from a single model realisation. Nevertheless, this research clearly shows how both the level of detail used to represent fuels and the inherent aggregation in canopy fuels influenced potential fire behaviour. Fuel characterisation that moves beyond spatially averaged descriptions to include increased spatial fidelity and effective wind description associated with characteristic fuel heterogeneity will better constrain fire behaviour uncertainty.

ATTACHMENT D

J Int. J. Wildland Fire

A. L. Atchley et al.

Conflicts of interest

The authors declare no conflicts of interest.

Acknowledgements

Sources of funding for this research included USDA Forest Service Research (both Rocky Mountain Research Station and Washington Office) National Fire Plan through Interagency Agreements 13-IA-11221633–103 and 17-IA-11221633–164 with Los Alamos National Laboratory. Los Alamos National Laboratory's Institutional Computing Program provided computational resources and Los Alamos National Laboratory's Laboratory Directed Research and Development (LDRD) program provided model development support. We also extend a special thanks to Stephanie Zeller for her aid in developing visualisations and the valuable contributions from four anonymous reviewers.

References

- Ager AA, Vaillant NM, Finney MA (2011) Integrating fire behavior models and geospatial analysis for wildland fire risk assessment and fuel management planning. *Journal of Combustion* **2011**, 1–19. doi:10.1155/2011/572452
- Benali A, Sá ACL, Ervilha AR, Trigo RM, Fernandes PM, Pereira JMC (2017) Fire spread predictions: sweeping uncertainty under the rug. *The Science of the Total Environment* **592**, 187–196. doi:10.1016/j.scitotenv.2017.03.106
- Boudreault LE, Bechmann A, Sørensen NN, Sogachev A, Dellwik E (2014) Canopy structure effects on the wind at a complex forested site. *The Science of the Total Environment* **524**, 012112. doi:10.1088/1742-6596/524/1/012112
- Bova AS, Mell WE, Hoffman CM (2016) A comparison of level set and marker methods for the simulation of wildland fire front propagation. *International Journal of Wildland Fire* **25**, 229–241. doi:10.1071/WF13178
- Burrows N, Ward B, Robinson A (2000) Behaviour and some impacts of a large wildfire in the Gnaragana maritime pine (*Pinus pinaster*) plantation, Western Australia. *CALMscience* **3**, 251–260.
- Clements CB, Zhong S, Bian X, Heilman WE, Byun DW (2008) First observations of turbulence generated by grass fires. *Journal of Geophysical Research* **113**, D22102. doi:10.1029/2008JD010014
- Clements CB, Lareau NP, Seto D, Contezac J, Davis B, Teske C, Zajkowski TJ, Hudak AT, Bright BC, Dickinson MB, Butler BW, Jimenez D, Hiers JK (2016) Fire weather conditions and fire-atmosphere interactions observed during low-intensity prescribed fires – RxCADRE 2012. *International Journal of Wildland Fire* **25**, 90–101. doi:10.1071/WF14173
- Coen JL, Schroeder W (2013) Use of spatially refined satellite remote sensing fire detection data to initialize and evaluate coupled weather–wildfire growth model simulations. *Geophysical Research Letters* **40**, 5536–5541. doi:10.1002/2013GL057868
- Coen JL, Cameron M, Michalakos J, Patton EG, Riggan PJ, Yedinak KM (2013) WRF-Fire: coupled weather–wildland fire modeling with the weather research and forecasting model. *Journal of Applied Meteorology and Climatology* **52**, 16–38. doi:10.1175/JAMC-D-12-023.1
- Cruz MG, Alexander ME (2017) Modelling the rate of fire spread and uncertainty associated with the onset and propagation of crown fires in conifer forest stands. *International Journal of Wildland Fire* **26**, 413–426. doi:10.1071/WF16218
- Doerr SH, Santin C (2016) Global trends in wildfire and its impacts: perceptions versus realities in a changing world. *Philosophical Transactions of the Royal Society B: Biological Sciences* **371**, 20150345. doi:10.1098/RSTB.2015.0345
- Dupont S, Brunet Y (2007) Edge flow and canopy structure: a large-eddy simulation study. *Boundary-Layer Meteorology* **126**, 51–71. doi:10.1007/S10546-007-9216-3
- Dupont S, Brunet Y (2008) Influence of foliar density profile on canopy flow: a large-eddy simulation study. *Agricultural and Forest Meteorology* **148**, 976–990. doi:10.1016/j.agrformet.2008.01.014
- Dupont S, Bonnefond J-M, Irvine MR, Lamaud E, Brunet Y (2011) Long-distance edge effects in a pine forest with a deep and sparse trunk space: *in situ* and numerical experiments. *Agricultural and Forest Meteorology* **151**, 328–344. doi:10.1016/j.agrformet.2010.11.007
- Finney MA (2001) Design of regular landscape fuel treatment patterns for modifying fire growth and behavior. *Forest Science* **47**, 219–228.
- Finney MA, Grenfell IC, McHugh CW, Seli RC, Trethewey D, Stratton RD, Brittain S (2011) A method for ensemble wildland fire simulation. *Environmental Modeling and Assessment* **16**, 153–167. doi:10.1007/S10666-010-9241-3
- Finnigan J (2000) Turbulence in plant canopies. *Annual Review of Fluid Mechanics* **32**, 519–571. doi:10.1146/ANNUREV.FLUID.32.1.519
- Frangieh N, Morvan D, Meradi S, Accary G, Bessonov O (2018) Numerical simulation of grassland fires behavior using an implicit physical multiphase model. *Fire Safety Journal* **102**, 37–47. doi:10.1016/j.firesaf.2018.06.004
- Gao W, Shaw R (1989) Observation of organized structure in turbulent flow within and above a forest canopy. In 'Boundary layer studies and applications'. (Ed. RE Munn) pp. 349–377. (Springer: Berlin, Germany)
- Hiers JK, O'Brien JJ, Varner JM, Butler BW, Dickinson M, Furman J, Gallagher M, Goodwin D, Goodrick SL, Hood SM, Hudak A, Kobziar LN, Linn R, Loudermilk EL, McCaffrey S, Robertson K, Rowell EM, Skowronski N, Watts AC, Yedinak KM (2020) Prescribed fire science: the case for a refined research agenda. *Fire Ecology* **16**, 11. doi:10.1186/S42408-020-0070-8
- Hilton JE, Miller C, Sullivan AL, Rucinski C (2015) Effects of spatial and temporal variation in environmental conditions on simulation of wildfire spread. *Environmental Modelling & Software* **67**, 118–127. doi:10.1016/j.envsoft.2015.01.015
- Hoffman CM, Linn R, Parsons R, Sieg C, Winterkamp J (2015) Modeling spatial and temporal dynamics of wind flow and potential fire behavior following a mountain pine beetle outbreak in a lodgepole pine forest. *Agricultural and Forest Meteorology* **204**, 79–93. doi:10.1016/j.agrformet.2015.01.018
- Hoffman C, Canfield J, Linn R, Mell W, Sieg C, Pimont F, Ziegler J (2016) Evaluating crown fire rate of spread predictions from physics-based models. *Fire Technology* **52**, 221–237. doi:10.1007/S10694-015-0500-3
- Hudak AT, Kato A, Bright BC, Loudermilk EL, Hawley C, Restaino JC, Ottmar RD, Prata GA, Cabo C, Prichard SJ, Rowell EM (2020) Towards spatially explicit quantification of pre-and postfire fuels and fuel consumption from traditional and point cloud measurements. *Forest Science* **66**, 428–442. doi:10.1093/FORSCI/FXZ085
- Kiefer MT, Heilman WE, Zhong S, Charney JJ, Bian X (2016) A study of the influence of forest gaps on fire-atmosphere interactions. *Atmospheric Chemistry and Physics* **16**, 8499–8509. doi:10.5194/ACP-16-8499-2016
- Kiefer MT, Zhong S, Heilman WE, Charney JJ, Bian X (2018) A numerical study of atmospheric perturbations induced by heat from a wildland fire: sensitivity to vertical canopy structure and heat source strength. *Journal of Geophysical Research, D, Atmospheres* **123**, 2555–2572. doi:10.1002/2017JD027904
- Knapp EE, Keeley JE (2006) Heterogeneity in fire severity within early season and late season prescribed burns in a mixed-conifer forest. *International Journal of Wildland Fire* **15**, 37–45. doi:10.1071/WF04068
- Lee X (2000) Air motion within and above forest vegetation in non-ideal conditions. *Forest Ecology and Management* **135**, 3–18. doi:10.1016/S0378-1127(00)00294-2
- Liao W, Van Coillie F, Gao L, Li L, Zhang B, Chanussot J (2018) Deep learning for fusion of APEX hyperspectral and full-waveform LiDAR remote sensing data for tree species mapping. *IEEE Access: Practical*

ATTACHMENT D

Effects of fuel spatial distribution

Int. J. Wildland Fire K

- Innovations, Open Solutions* **6**, 68716–68729. doi:10.1109/ACCESS.2018.2880083
- Lindenmayer DB, Franklin JF (2002) 'Conserving forest biodiversity: a comprehensive multiscaled approach.' (Island press: Washington, DC, USA).
- Linn R, Cunningham P (2005) Numerical simulations of grass fires using a coupled atmosphere–fire model: basic fire behavior and dependence on wind speed. *Journal of Geophysical Research, D, Atmospheres* **110**, D13107. doi:10.1029/2004JD005597
- Linn R, Reisner J, Colman JJ, Winterkamp J (2002) Studying wildfire behavior using FIRETEC. *International Journal of Wildland Fire* **11**, 233–246. doi:10.1071/WF02007
- Linn R, Winterkamp J, Colman JJ, Edminster C, Bailey JD (2005) Modeling interactions between fire and atmosphere in discrete element fuel beds. *International Journal of Wildland Fire* **14**, 37–48. doi:10.1071/WF04043
- Linn R, Anderson K, Winterkamp J, Brooks A, Wotton M, Dupuy J-L, Pimont F, Edminster C (2012) Incorporating field wind data into FIRETEC simulations of the International Crown Fire Modeling Experiment (ICFME): preliminary lessons learned. *Canadian Journal of Forest Research* **42**, 879–898. doi:10.1139/X2012-038
- Linn RR (1997) A transport model for prediction of wildfire behavior. Los Alamos National Laboratory. Report number: LA-13334-T (Los Alamos, NM, USA).
- Linn RR, Sieg CH, Hoffman CM, Winterkamp JL, McMillin JD (2013) Modeling wind fields and fire propagation following bark beetle outbreaks in spatially heterogeneous pinyon–juniper woodland fuel complexes. *Agricultural and Forest Meteorology* **173**, 139–153. doi:10.1016/J.AGRFORMET.2012.11.007
- Linn RR, Goodrick SL, Brambilla S, Brown MJ, Middleton RS, O'Brien JJ, Hiers JK (2020) QUIC-fire: a fast-running simulation tool for prescribed fire planning. *Environmental Modelling & Software* **125**, 104616. doi:10.1016/J.ENVSOFT.2019.104616
- Massetti A, Rüdiger C, Yebrá M, Hilton J (2019) The Vegetation Structure Perpendicular Index (VSPi): a forest condition index for wildfire predictions. *Remote Sensing of Environment* **224**, 167–181. doi:10.1016/J.RSE.2019.02.004
- Mell W, Jenkins MA, Gould J, Cheney P (2007) A physics-based approach to modelling grassland fires. *International Journal of Wildland Fire* **16**, 1–22. doi:10.1071/WF06002
- Mell W, Maranghides A, McDermott R, Manzano SL (2009) Numerical simulation and experiments of burning Douglas fir trees. *Combustion and Flame* **156**, 2023–2041. doi:10.1016/J.COMBUSTFLAME.2009.06.015
- Mitchell RJ, Hiers JK, O'Brien JJ, Jack SB, Engstrom RT (2006) Silviculture that sustains: the nexus between silviculture, frequent prescribed fire, and conservation of biodiversity in longleaf pine forests of the south-eastern United States. *Canadian Journal of Forest Research* **36**, 2724–2736. doi:10.1139/X06-100
- Moon K, Duff TJ, Tolhurst KG (2019) Sub-canopy forest winds: understanding wind profiles for fire behaviour simulation. *Fire Safety Journal* **105**, 320–329. doi:10.1016/J.FIRESAF.2016.02.005
- Morvan D, Accary G, Meradji S, Frangieh N, Bessonov O (2018) A 3D physical model to study the behavior of vegetation fires at laboratory scale. *Fire Safety Journal* **101**, 39–52. doi:10.1016/J.FIRESAF.2018.08.011
- Narine LL, Popescu SC, Malambo L (2019) Synergy of ICESat-2 and Landsat for mapping forest aboveground biomass with deep learning. *Remote Sensing* **11**, 1503. doi:10.3390/RS11121503
- Parsons R, Linn R, Pimont F, Hoffman C, Sauer J, Winterkamp J, Sieg C, Jolly W (2017) Numerical investigation of aggregated fuel spatial pattern impacts on fire behavior. *Land* **6**, 43. doi:10.3390/LAND6020043
- Patton EG (1997) Large-eddy simulation of turbulent flow above and within a plant canopy. PhD dissertation, University of California, Davis, CA, USA.
- Pimont F, Linn RR, Dupuy J-L, Morvan D (2006) Effects of vegetation description parameters on forest fire behavior with FIRETEC. *Forest Ecology and Management* **234**, S120. doi:10.1016/J.FORECO.2006.08.161
- Pimont F, Dupuy JL, Linn RR, Dupont S (2009) Validation of FIRETEC wind-flows over a canopy and a fuel-break. *International Journal of Wildland Fire* **18**, 775–790. doi:10.1071/WF07130
- Pimont F, Dupuy J-L, Linn RR, Dupont S (2011) Impacts of tree canopy structure on wind flows and fire propagation simulated with FIRETEC. *Annals of Forest Science* **68**, 523–530. doi:10.1007/S13595-011-0061-7
- Pimont F, Dupuy J-L, Linn RR, Parsons R, Martin-StPaul N (2017) Representativeness of wind measurements in fire experiments: lessons learned from large-eddy simulations in a homogeneous forest. *Agricultural and Forest Meteorology* **232**, 479–488. doi:10.1016/J.AGRFORMET.2016.10.002
- Pimont F, Dupuy J-L, Linn RR, Parsons RA (2018) Wind measurement accuracy in fire experiments. In 'Advances in forest fire research'. (Ed. DX Viegas) pp. 716–724. (Imprensa da Universidade de Coimbra: Coimbra, Portugal). doi:10.14195/978-989-26-16-506_78
- Pimont F, Dupuy J-L, Linn RR, Sauer JA, Muñoz-Esparza D (2020) Pressure-gradient forcing methods for large-eddy simulations of flows in the lower atmospheric boundary layer. *Atmosphere* **11**, 1343. doi:10.3390/ATMOS11121343
- Pinto RMS, Benali A, Sá ACL, Fernandes PM, Soares PMM, Cardoso RM, Trigo RM, Pereira JMC (2016) Probabilistic fire spread forecast as a management tool in an operational setting. *SpringerPlus* **5**, 1205. doi:10.1186/S40064-016-2842-9
- Sieg CH, Linn RR, Pimont F, Hoffman CM, McMillin JD, Winterkamp J, Baggett LS (2017) Fires following bark beetles: factors controlling severity and disturbance interactions in ponderosa pine. *Fire Ecology* **13**, 1–23. doi:10.4996/FIREECOLOGY.130300123
- Sun R, Krueger SK, Jenkins MA, Zulauf MA, Charney JJ (2009) The importance of fire–atmosphere coupling and boundary-layer turbulence to wildfire spread. *International Journal of Wildland Fire* **18**, 50–60. doi:10.1071/WF07072
- Turner MG, Romme WH (1994) Landscape dynamics in crown fire ecosystems. *Landscape Ecology* **9**, 59–77. doi:10.1007/BF00135079
- Ziegler JP, Hoffman C, Battaglia M, Mell W (2017) Spatially explicit measurements of forest structure and fire behavior following restoration treatments in dry forests. *Forest Ecology and Management* **386**, 1–12. doi:10.1016/J.FORECO.2016.12.002

ATTACHMENT D

EXHIBIT G



OPEN

Effects of canopy midstory management and fuel moisture on wildfire behavior

Tirtha Banerjee^{1✉}, Warren Heilman^{2,6}, Scott Goodrick^{3,6}, J. Kevin Hiers^{4,6} & Rod Linn^{5,6}

Increasing trends in wildfire severity can partly be attributed to fire exclusion in the past century which led to higher fuel accumulation. Mechanical thinning and prescribed burns are effective techniques to manage fuel loads and to establish a higher degree of control over future fire risk, while restoring fire prone landscapes to their natural states of succession. However, given the complexity of interactions between fine scale fuel heterogeneity and wind, it is difficult to assess the success of thinning operations and prescribed burns. The present work addresses this issue systematically by simulating a simple fire line and propagating through a vegetative environment where the midstory has been cleared in different degrees, leading to a canopy with almost no midstory, another with a sparse midstory and another with a dense midstory. The simulations are conducted for these three canopies under two different conditions, where the fuel moisture is high and where it is low. These six sets of simulations show widely different fire behavior, in terms of fire intensity, spread rate and consumption. To understand the physical mechanisms that lead to these differences, detailed analyses are conducted to look at wind patterns, mean flow and turbulent fluxes of momentum and energy. The analyses also lead to improved understanding of processes leading to high intensity crowning behavior in presence of a dense midstory. Moreover, this work highlights the importance of considering fine scale fuel heterogeneity, seasonality, wind effects and the associated fire-canopy-atmosphere interactions while considering prescribed burns and forest management operations.

Increasing wildfire impacts has been documented over the past decades^{1,2} and is projected to increase under climate change in the United States (US) and other parts of the world^{1–8}. Apart from the changing patterns of precipitation, vapor pressure deficit and longer drought periods^{7,9}, an increasing trend of human habitation at the wildland-urban interface (WUI) has rendered the problem of wildfire management particularly complex. The WUI is the fastest growing land-use type in the US¹⁰ and also poses significant wildfire threat in other countries such as Portugal. In the western US, about 50% of residential households are situated at the WUI, and flammable vegetation can come into close contact with infrastructure. This situation enhances the impact of wildfires, particularly with fast moving wildfires that escape efforts at containment during initial attack¹¹.

Successful suppression of small fires, called initial attack, is critical to limiting fire size, but successful suppression is increasingly difficult in the growing WUI. Mechanical thinning and prescribed burns are offered as effective techniques to decrease fuel loads and limit fire spread into communities^{12,13}. However, given the complexity of interactions between fine scale fuel heterogeneity and wind, it has been difficult to assess the success of such management operations. Thinning forests may decrease fire intensity but also increase rates of spread during critical phases of initial attack under certain conditions^{14–18}. Under extreme wind events such as those experienced in Paradise, California during the Camp Fire in 2018¹⁹ or the south eastern Australian fires in 2019²⁰, fire behaviour in fuel treatments can be affected by fire-atmosphere interactions, affecting fire suppression outcomes.

The main factors that control the rapid expansion of small wildfires are the response times of fire crew, size of fire upon initiation of suppression action²¹, and weather condition for that day. The removal of midstory and understory vegetation is targeted by managers to reduce wildfire intensity and decrease the probability of surface fire transitions to crown fire^{22–25}. Thus, fuel treatment strategies focus on reduction of surface fuels, increasing the height to the live crown, decreasing crown density and a species-selective approach¹². However, in order to assess the impact of fuel reduction treatments on fire behavior outcomes, one must consider the types of fuels,

¹Department of Civil and Environmental Engineering, University of California, Irvine, CA 92697, USA. ²Northern Research Station, U.S. Forest Service, Lansing, MI 48910, USA. ³Southern Research Station, U.S. Forest Service, Athens, GA 30602, USA. ⁴Tall Timbers Research Station, Tallahassee, FL 32312, USA. ⁵Earth and Environmental Sciences Division, Los Alamos National Laboratory, Los Alamos, NM 87545, USA. ⁶These authors contributed equally: Warren Heilman, Scott Goodrick, J. Kevin Hiers and Rod Linn. ✉email: tirthab@uci.edu

ATTACHMENT D

such as dead and live fuels, litter, ladder (midstory) fuels and canopy fuels associated with larger trees and their effects on fire behavior under different conditions of moisture levels²⁶.

The reduction of midstory and understory vegetation does not drive fire behavior in isolation. Depending upon the seasonality and fuel conditions, midstory vegetation can increase wind drag lowering wind speeds or increase fuel moisture, which each can slow fire spread or reduce intensity. Thus, to evaluate the efficacy of fuel treatments, fuel structure alone is insufficient to understand how treatments will alter future wildfire spread and suppression success^{18,27–39}. To this effect, Bessie and Johnson⁴⁰ determined that local weather conditions, especially factors governing fuel moisture and wind speed are stronger indicators to determine fire behavior in vegetative fuel beds compared to stand age or species composition^{41,42}. Keyes and Varner⁴³ recognized that higher wind speeds and turbulence in the sub canopy after thinning treatment might lead to higher mid-flame wind speeds, enhanced rates of spread and erratic fire behavior. Varner and Keyes²⁶ highlighted the importance of variations of fuel moisture and wind adjustment factors post fuel treatment in influencing fire spread and intensity. Moon et al.⁴⁴ studied sub canopy wind variations under a variety of fuel structures and called for further research into fire behavior under fuel treatment scenarios which incorporates the changes in wind among other factors post treatment. A broader discussion into sub-canopy changes under fuel treatment and associated fire behavior is beyond the scope of the current paper and the interested reader is referred to Banerjee¹⁸ for a detailed review.

Beer⁴⁵ identified several mechanisms through which a fire propagates within a fuel bed. He also discussed the potential influence of coherent structures such as sweeps and ejections in a vegetation canopy where a surface fire burns the understory but the canopy crown remains unburnt. The fluctuations in vertical wind velocity generated by the fire can interact with these motions and help disperse heat to the unburnt fuel elements downstream of the flame sheet. Moreover, Cheney et al.⁴⁶ determined that while wind and dead moisture are important for grass fires, fuel load is the primary determinant of fire intensity. On the other hand, closed canopy forests with a higher moisture content and lower wind speeds can lead to lower intensity and slow moving fires⁴⁷. Additionally, changing stand structure by thinning can lead to reduced torching and crowning potential^{48,49}. Contreras et al.⁵⁰ used light detection and ranging (LiDAR) mapped forest structure data to characterize the role of vegetation connectivity and thinning operations (that reduce connectivity) in the context of crown fire potential. White et al.⁵¹ and Davies et al.⁵² determined that the flammability of surface fuels are also important in governing fire severity. The type of ignition is another factor that sets up the initial condition for fire propagation. Keeley and Syphard⁵³ identified the major wildfires in California from 2003 to 2018 and deduced that the fire regimes can be either identified as fuel dominated or wind dominated. In either case, the complex fire-fuel-atmosphere interaction is of critical importance.

Fuel moisture patterns in humid environments are more complex than previously assumed⁵⁴, and environmental conditions during a wildfire event may have non-linear treatment effectiveness outcomes. Finney et al.⁵⁵ identified the importance of studying turbulent flows associated with fuel structures and fuel moisture, especially how they contribute to buoyancy production and flow instabilities, but as yet, these complex coupled fire-atmospheric dynamics have not been applied to the question of fuel treatment effectiveness on initial attack success.

Computational fluid dynamic (CFD) modeling approaches are capable of representing the non-linear feedback between changes in forest structure, complex in stand flows, and fire behavior outcomes^{56–64}. Pimont et al.⁶⁵ used FIRETEC to study the effect of different fuel treatments in the landscape on fire behavior. Linn et al.⁶⁶ used FIRETEC to model wind fields and fire propagation following bark beetle outbreaks. Kiefer et al.⁶⁷ studied the detailed budget of turbulent kinetic energy during a low intensity fire and investigated the sensitivity of mean and turbulent flows to canopy density as well as atmospheric stability using the ARPS-CANOPY model. Another series of studies^{68–72} conducted detailed turbulence measurements during grass fires and surface understory fires using high frequency micrometeorological measurements from the FIREFLUX campaigns and two New Jersey Pine Barrens fire experiments.

However, there remains uncertainty regarding the complicated fire-atmosphere interaction in the canopy sub layer in presence of midstory vegetation of different densities, which governs fire spread in treated vs. untreated fuels. In this work, simulations using FIRETEC are used to address the following questions:

- What are the driving factors governing fire behavior under different levels of midstory management and fuel moisture?
- What are important factors leading to torching and crowning?
- How to characterize turbulent transport of momentum and energy to explain fundamental differences in fire behavior?

To answer these questions, specifically six sets of simulations are conducted. The cases are described in more detail in the methods section. The simulation cases are called dry no midstory (DN), dry sparse midstory (DS), dry dense midstory (DD), moist no midstory (MN), moist sparse midstory (MS) and moist dense midstory (MD), respectively. For brevity, these abbreviated forms will be used for further discussion. It is also important to note that the vegetation phenology in this study is driven by seasonality rather than atmospheric conditions.

Results

Burnt area. Figure 1 shows the burnt area after 520 s of fire propagation. Since the initial and boundary conditions are same for all the simulations, the differences in fire spread are entirely due to differences in canopy structure among the different cases. For the dry scenario, the DN case and the DD case have burnt areas of similar sizes, although the burn scar shapes are slightly different. The DS case has a smaller and thinner burn area. For the moist scenario, the MN case has the largest burn area. The size of the burn area is smaller for the MS and smallest for the MD case. Figure 1 highlights a crucial factor—namely the competing influences of fuel avail-

ATTACHMENT D

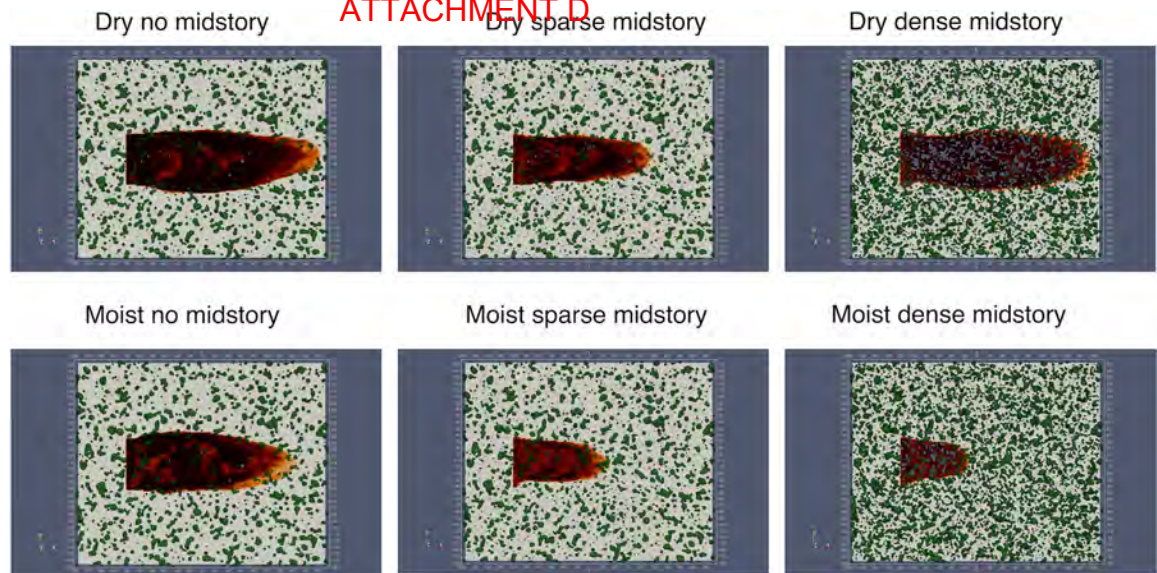


Figure 1. Burnt area after 520 s for different cases. Green depicts midstory vegetation, the light yellow shade depicts the ground surface covered with grass and litter and the dark color depicts burned area.

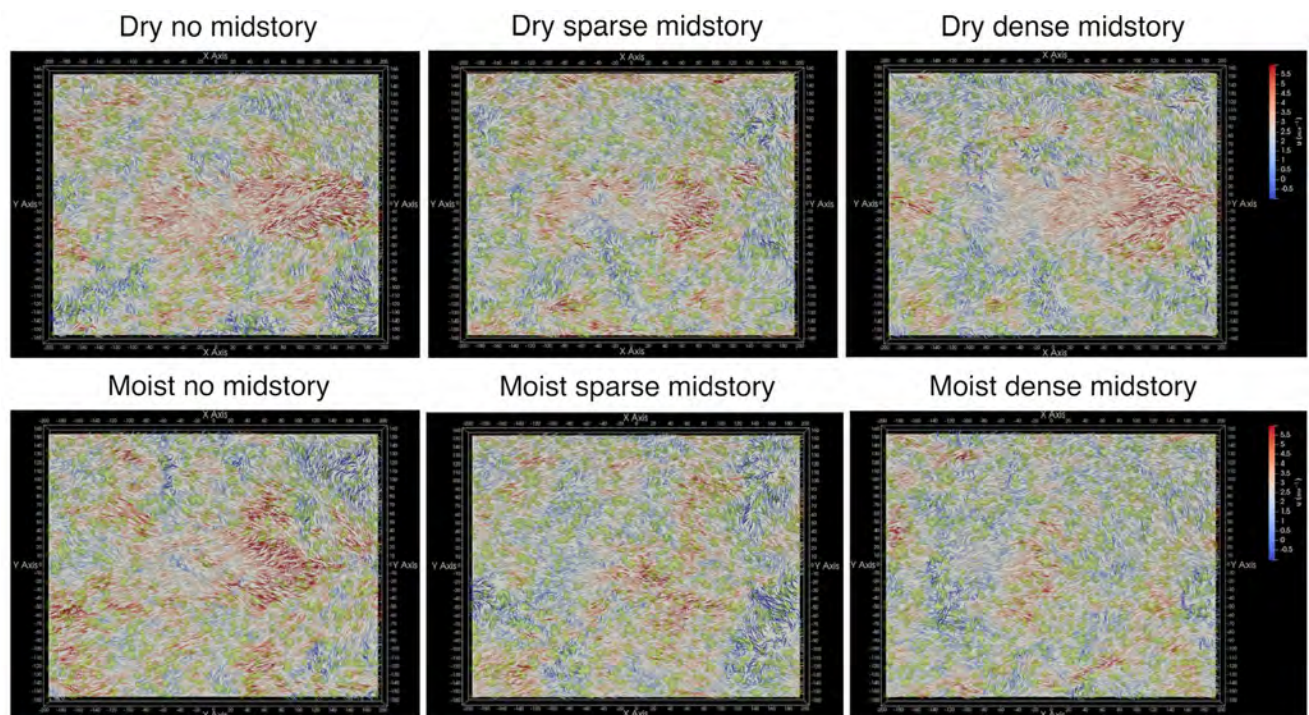


Figure 2. Sub canopy wind field ($x - y$ plane at 7 m height) with arrows colored by instantaneous streamwise velocity component (u) after 520 s for the six scenarios.

ability, fuel moisture and wind effects. Under dry conditions, the availability of dry fuels in the DD case creates a strong head fire. However, the DN case is characterized by a stronger wind field inside the canopy due to lower vegetative drag. This indicates that there is likely a threshold effect, where either the fuel availability or the wind effects dominate. The DS case falls in the intermediate regime, and consequently has a smaller burn scar. Under moist conditions, the higher fuel moisture dampens the effect of fuel availability on fire propagation, and thus the wind effect dominates. This fact is highlighted in Fig. 2, which plots the horizontal ($x - y$) wind field at 7 m height, with velocity vectors colored by the streamwise velocity component (u). As observed, the no midstory case has higher wind speeds compared to the other cases due to lower vegetative drag. A more quantitative understanding of the role of turbulence will be discussed in a subsequent section.

ATTACHMENT D

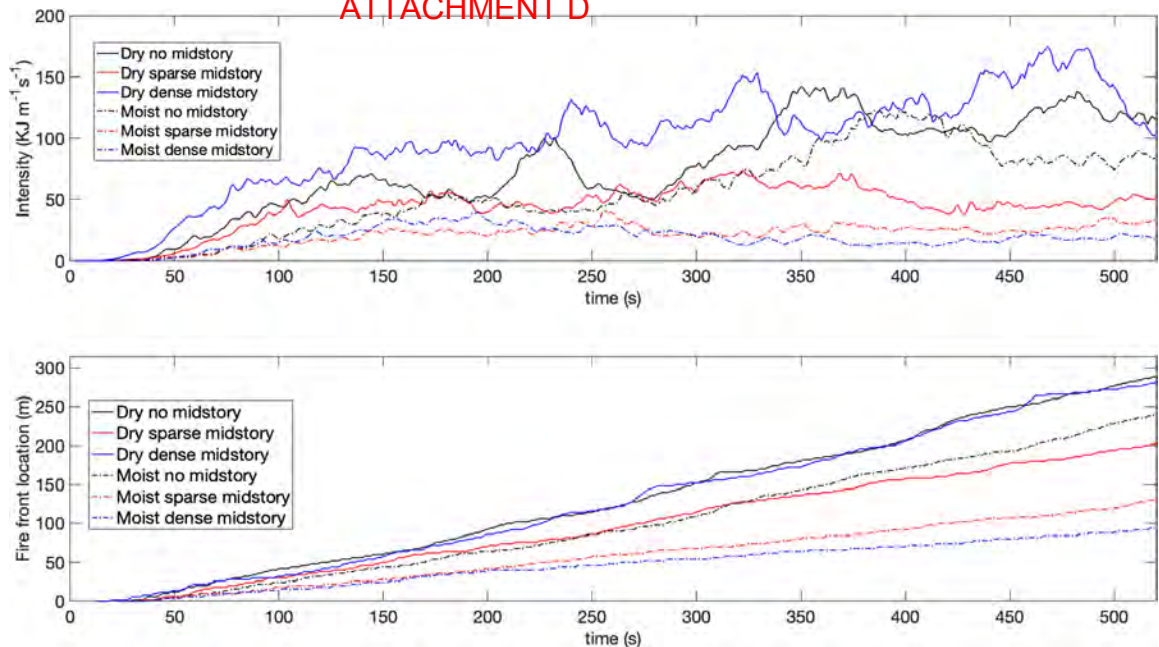


Figure 3. Burning intensity (top) and fire front location with respect to time (bottom) for different cases. The black lines indicate non midstory cases, the red lines indicate the sparse midstory cases and the blue lines indicate the dense midstory cases. The solid lines indicate dry scenarios and the dash dotted lines indicate moist scenarios.

Fire intensity, fire spread and fuel consumption. Figure 3 shows burning intensity (top panel) and the location of the fire front (bottom panel) with respect to time. As observed, the DD case has the highest intensity because of elevated fuel availability among all cases. Interestingly the DN case burns more intensely compared to the DS case, highlighting the critical interaction between fuel availability and wind effects. The moist cases generally showed reduced fire intensity than the dry cases as expected. The differences among the fire intensities observed within the moist cases are smaller than those among the dry cases. This implies the absence of any critical behavior feedback for the moist cases with respect to the competition between wind effects and fuel availability and the dominance of wind effects for the moist scenarios.

Interestingly the fire front propagation spread rate follows the trend of the intensities. However the difference between the cases do not follow the trend in differences of fire intensity. The DN and DD cases have similar spread rates and these two cases show the fastest fire front propagation, although the DN case is slightly faster. The reason for this behavior is likely the same—one dominated by dry fuel availability and the other by strong winds. The effect of the wind prevails for the moist cases as well and the MN case is faster than the MS and MD cases. To summarize, it can be stated that fire intensity is strongly governed by fuel availability and fire propagation speed is governed by wind effects. However, fuel moisture significantly reduces both fire intensity and rate of spread. This is partly because fire induces its own wind environment as well. However, under drier scenarios the effect of vegetative drag becomes more evident.

Figure 4 shows the consumption of canopy overstory fuels (top panels) and canopy midstory and understory fuels (bottom panels) after 520 s. The left panels show the actual amount of fuel remaining over time in metric tons (kg multiplied by 1000) for the entire domain (12.8 ha), the middle panels show the percentage consumption and the right panels show the rate of consumption per second. Any vegetation below 5 m height is considered midstory and understory vegetation. Note that all cases start with the same amount of overstory fuel (35 metric tons). As the leftmost bottom panel shows, the dense midstory cases have about 35 metric tons of midstory and understory fuels, although the moist case has slightly more fuel, as expected, since the deciduous midstory seasonally loses leaf biomass. The sparse midstory case has about 27 metric tons midstory and understory fuels in the moist season and about 26 metric tons in the dry season. The no midstory case has about 22 metric tons of understory fuels, and that amount does not vary in the dry and moist seasons.

A few observations can be made from Fig. 4:

- **Net consumption** The net consumption for the overstory is highest for the DD case, about 40%. The DN case has a similar consumption rate—about 30%. Interestingly, both the dry dense and DN cases have about 45% consumption for the mid and understory fuels. This indicates that while crowning happens for both these cases, driven by the dry fuels and higher winds, the presence of midstory and understory fuels influence how much overstory fuel the crown fire consumes. Moreover, the MN case has about 25% consumption for the overstory fuel and 35% consumption for the mid and understory fuels. The fact that the MN case has more consumption than the DS case is also highlights that wind effects can dominate over moisture effects.

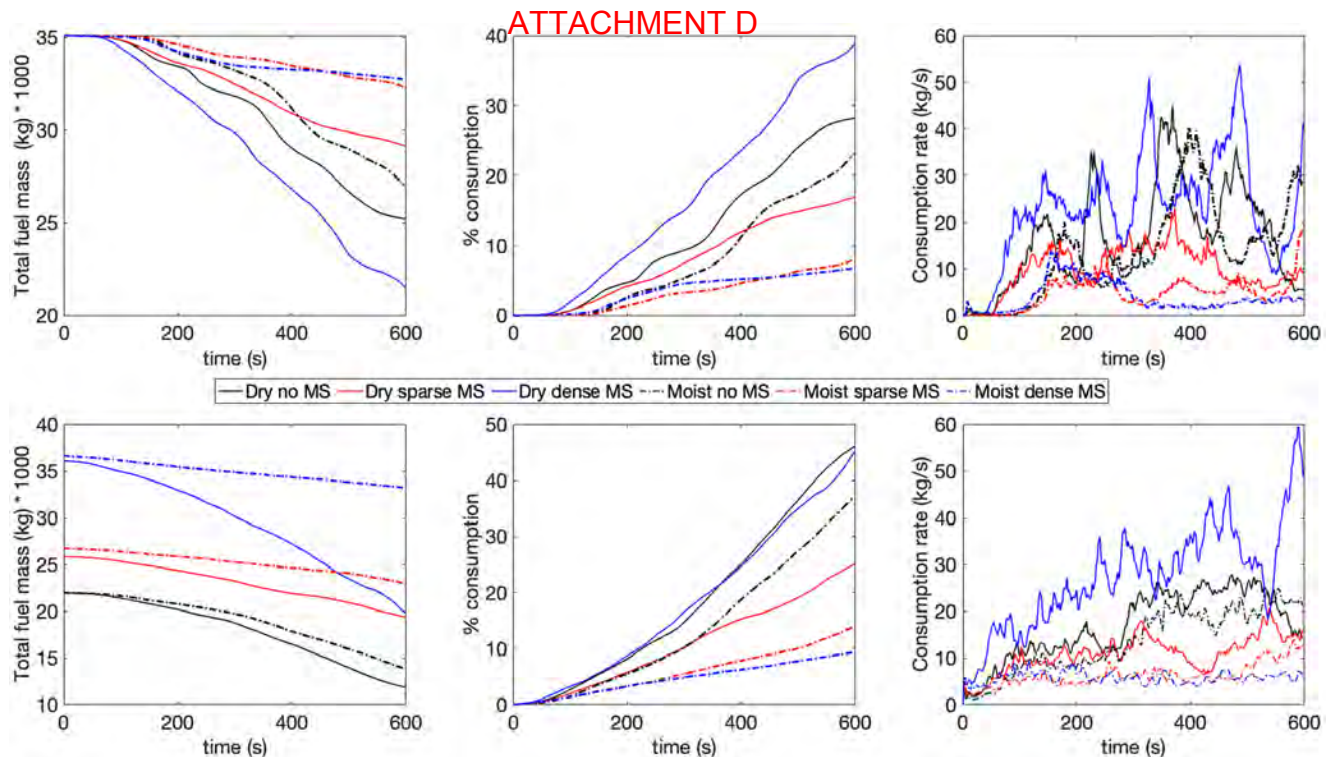


Figure 4. Actual fuel amount remaining over time (left), percentage consumption (middle) and rate of consumption (right) of fuel elements with respect to time for different cases. Line styles are same as Fig. 3. The top row shows the quantities for the overstory and the bottom row for the midstory and understory combined.

- Difference based on fuel moisture** The dry fuels are always consumed more than moist fuels, as expected, both for overstory and understory vegetation. The difference between dry and moist scenarios is most prominent for the dense midstory cases—about 35% more overstory and about 40% more mid and understory fuels are consumed in the dry condition compared to the moist condition, highlighting the importance of fuel moisture and seasonality in fire behavior. This difference is strikingly lower for the no midstory cases—about 5% for both overstory and mid/understory fuels. This indicates that when wind effects are more prominent, seasonal changes in moisture are less important. For the sparse midstory cases, this difference is about 10% for both overstory and mid/understory fuels, highlighting the fact that fire behavior is partially dominated by both wind and moisture effects.
- Rate of consumption** The rate of consumption with respect to time closely follows the trends of actual consumption. However it is important to note that the rate curve is not uniform and is highly variable in time. This non uniformity is more conspicuous for the overstory fuel compared to the midstory and understory fuels. This is due to the complex nature of the turbulence and combustion phenomena across a strongly heterogeneous canopy fuel complex.

To understand the role of turbulence inside the canopy in more detail, virtual sensors were placed at different locations on the domain, so turbulent statistics could be calculated. In section, time series of such turbulence statistics are presented.

Characterization of wind and turbulence. Figure 5a shows 1 min moving average means of several quantities at 3 m height at the domain center. Figure 5b shows the same at 7 m and Fig. 5c shows the same for 15 m height. These three locations are chosen so the variations in turbulent quantities and fluxes can be shown with time as the fire approaches the domain and with height so the dynamics inside the canopy can be probed in a much more detailed and quantitative way. Several observations can be made from Fig. 5a–c:

- Mean streamwise velocity (U)** Because of higher vegetative drag, the U velocities are higher for the cases with no midstory and sparse midstory compared to the dense midstory case before the fire reaches the center of the domain. The DD case also records negative U velocities at 3m height before the fire starts influencing the velocity field. The velocities for all cases are centered around $1\text{--}3\text{ ms}^{-1}$ before the influence of the fire, with the dense midstory cases (dry and moist) recording the lowest U velocities. Once the fire starts influencing the velocity field, the U velocities for the six different cases diverge widely. Still, the no midstory cases report the highest U velocities—about $6\text{--}8\text{ ms}^{-1}$. However, when the fire reaches the domain center, the DN case records a strong U velocity even at 7 m height (7 ms^{-1}). This is likely due to also the loss of vegetation due to burning, which reduces the drag force when the fire passes a particular region. The DN case also records

ATTACHMENT D

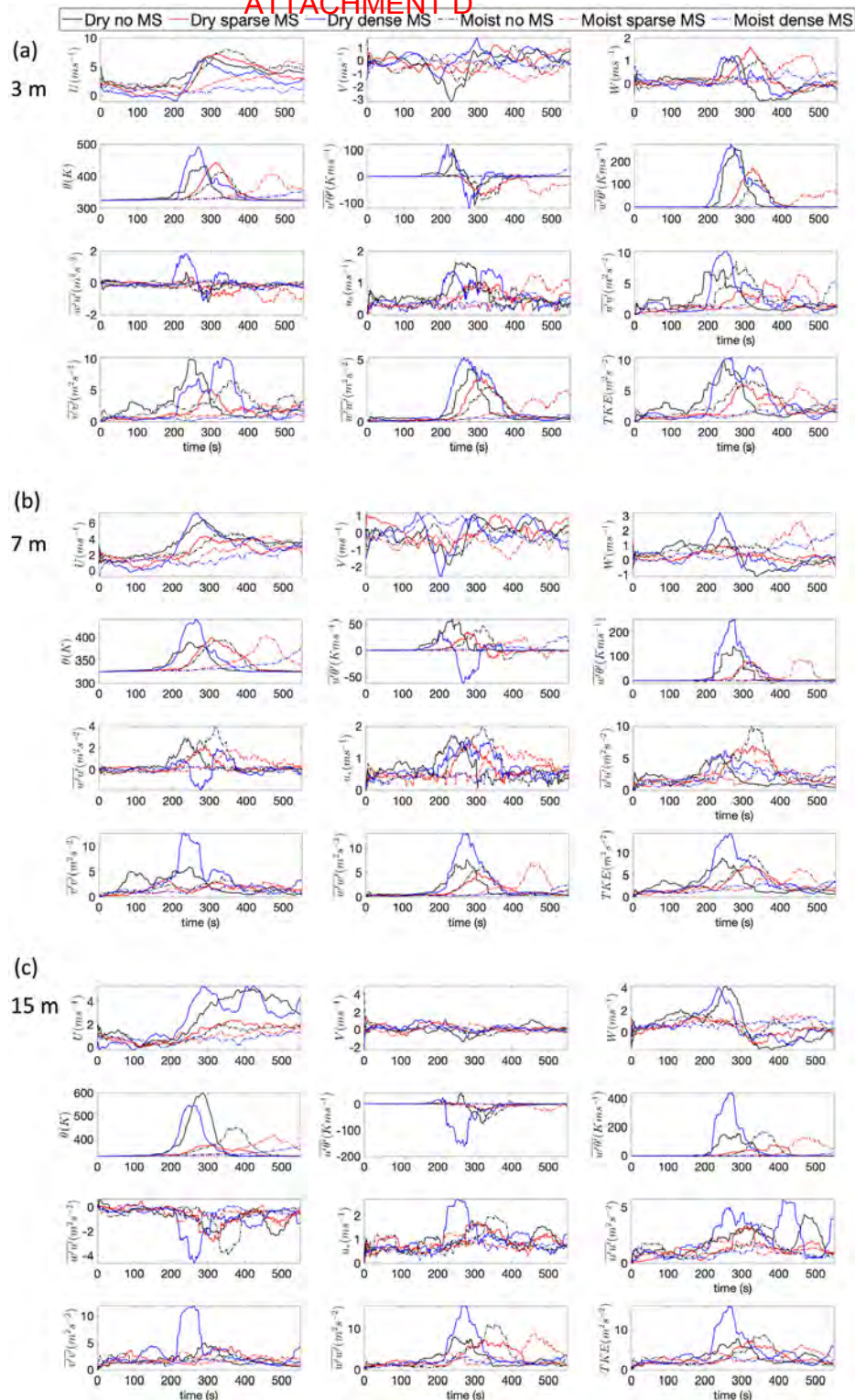


Figure 5. Moving average of turbulence statistics at (a) 3 m height, (b) 7 m height and (c) 15 m height at the domain center. Line styles are same as Fig. 3. U is the mean streamwise velocity, V is the mean cross stream velocity, W is the mean vertical velocity, θ is potential temperature, $u'w'$ and $w'w'$ are sensible heat flux along the streamwise (u) and vertical (w) directions (the primed quantities are fluctuations from the mean). $w'u'$ is the vertical momentum flux, $u'u'$, $v'v'$ and $w'w'$ are velocity variances in u , v and w directions respectively. TKE is turbulent kinetic energy and defined by one half of the summation of $u'u'$, $v'v'$ and $w'w'$.

ATTACHMENT D

strong U velocities at 7 m height, both before and during the fire front passage. At 15 m, the high canopy drag results in lower velocities for all the cases except for the DD case and the DN case. The high velocity for the DD case is partly due to loss of fuel by burning and partly due to high turbulence due to buoyancy. Note that U is generally higher for all cases the canopy mid-story and understory compared to the canopy crown region where the drag is much higher.

- **Mean cross stream velocity (V)** Although the inflow boundary conditions prescribe a zero V component, it becomes finite as the flow field is influenced by the fire. Before the fire influences the domain, the V velocities are centered around zero. However they start to diverge as the fire gains strength. As noticed in Fig. 2, there is a significant cross flow component as the cold wind wraps around the fire and entrains the burnt area behind the top flank of the fire. This V component also experiences drag and thus the no midstory case has the highest (-3 ms^{-1}) V velocity at 3 m height. Interestingly, the DD case also picks up a strong V component, probably influenced by cold air entrainment due to high intensity burning. At 7 m height, the finite V component still persists. However, at 15 m, the V velocity component is almost zero, due to the strong drag effects of the vegetation crown.
- **Mean vertical velocity (W)** At 3 m height, the cases with no and sparse midstory has strong vertical updrafts ($1.5\text{--}2 \text{ ms}^{-1}$). This can be attributed to lower drag forces, as dry and moist scenarios for these two cases record similar W components as well. Interestingly, the DD has strong updrafts but the MN case does not. This indicates that the buoyancy generated due to intense burning of dry fuels is responsible for the updrafts. Note that the strong updrafts are followed by downdrafts (order of 0.5 ms^{-1}), as the cold air entrains the burnt area behind the fire front. At 7 m, the DD case reports even higher updrafts (3 ms^{-1}) and a stronger downdraft (-1 ms^{-1}) after the fire front moves past the virtual sensor. This is likely due to the presence of dense dry midstory which burns vigorously, and supported by the fact that under moist conditions, the dense midstory case has lowest W components. This effect is dominated by stronger drag forces. Interestingly, the sparse moist midstory case also has strong updrafts (2.5 ms^{-1}), likely due the nonlinear combination of drag and buoyancy effects. At the crown level (15 m height), both the dry dense and DN cases record strong updrafts (4 ms^{-1}), due to effects described previously.
- **Potential temperature (θ)** at 3 m height, the air temperature reaches the highest level (500 K) for the DD case. The no midstory and sparse midstory cases reach slightly lower temperature (about 375 K). The dry cases reach higher temperatures than the moist cases, as expected. The only exception is the MS case (about 300 K). This also explains the previous observations regarding the high updrafts for the dry midstory cases. At 7 m height, the difference among the cases become more prominent. The DD case reaches a peak temperature of about 450 K and the other cases reaches around 400 K when the fire reaches the sensor. At the crown level of 15 m, the dry dense and DN cases reach high temperatures of about 550–600 K. The other cases still record about 400 K.
- **Streamwise sensible heat flux ($\overline{u'\theta'}$)** This term can also be called the kinematic advective heat flux along the streamwise (x) direction and is a measure of horizontal heat transfer along the mean flow direction at any level. A positive heat flux should indicate advective heating of the fuel elements in the direction of the fire spread. This is why the peaks for $\overline{u'\theta'}$ occur before the spike in temperature as the fire approaches the sensor. The DD case records the highest $\overline{u'\theta'}$ at 3 m height (about 110 K ms^{-1}), followed by the DN case. After the fire passes, the $\overline{u'\theta'}$ becomes negative, indicating that the fuel elements are cooling down. At 7 m height, the DN case records more advective heating compared to the DD case. However, the magnitude of $\overline{u'\theta'}$ is lower at 7 m, about 50 K ms^{-1} for the DN case. This can be attributed to higher amount of fuel availability at this level. Interestingly, the moist cases record $\overline{u'\theta'}$ of a similar order of magnitude. This indicates that advective heating at the midstory level in the model is dominated by wind and drag, not moisture. At the crown height of 15 m, the heating effects are even smaller than the midstory and understory levels. However, there is strong cooling effect, probably attributed to the crowning behavior at this level.
- **Vertical sensible heat flux ($\overline{w'\theta'}$)** A positive value of $\overline{w'\theta'}$ represents an upward flux of warm air due to buoyancy and should be interpreted as a measure of the strength of the buoyant flame dynamics. The presence of a fire generates buoyancy driven turbulence, which should result in a strongly positive $\overline{w'\theta'}$. The dry cases register higher values of vertical sensible heat flux compared to the moist cases. At 3 m, both the DD and DN cases record similar $\overline{w'\theta'}$, about 250 K ms^{-1} . The DS case records about 175 K ms^{-1} . At 7 m, the trends remain similar, although the DD case $\overline{w'\theta'}$ values (about 250 K ms^{-1}) are nearly twice as large as the the DN case. This behavior is an indicator of laddering as the fire climbs up towards the crown. The MN case has lower $\overline{w'\theta'}$ at 7 m height (about 70 K ms^{-1}) which indicates that the sensible heat flux is definitely impacted strongly by fuel moisture. However, the dry sparse and moist sparse cases record similar $\overline{w'\theta'}$ at 7 m, which means that under sparse conditions, moisture effects are less prominent. At the crown height of 15 m, the DD case records a much stronger $\overline{w'\theta'}$ of about 400 K ms^{-1} , while the other cases remain similar to the 7 m level. This increasing $\overline{w'\theta'}$ with height for the DD case is an indicator of crown fire behavior.
- **Vertical momentum flux ($\overline{w'u'}$)** The parameter $\overline{w'u'}$ represents the vertical flux of horizontal momentum and its value should be negative inside the vegetation canopy in regular atmospheric boundary layer flow as the canopy absorbs momentum from the flow and acts as a momentum sink. The value of $\overline{w'u'}$ should also change as the canopy is consumed by the fire, which changes canopy drag. However, as the presence of fire create a strong buoyancy driven updraft, it can create a positive momentum flux in the canopy sublayer. At the 3 m height, all the cases record negative $\overline{w'u'}$. However, as the fire passes the virtual sensor, the DD case records a strong positive $\overline{w'u'}$. However, as the fire passes the sensor, cool air rushes in a negative $\overline{w'u'}$ is recorded because of strong drag effects. The DN case also shows a similar behavior although the peak values are much lower. At 7 m height, the no midstory and sparse midstory cases, (both dry and moist) records strong positive $\overline{w'u'}$. Higher drag at this level reduces $\overline{w'u'}$ for the DD case. Interestingly, at 7 m level, the burning of midstory fuels still generate upward fluxes of momentum. At the 15 m level, the upward flux of

ATTACHMENT D

momentum is small, indicating that the crown region absorbs the locally generated upward momentum flux and the fire does not 'leak' additional momentum into the atmospheric surface layer above the canopy. Moreover, at the crown height of 15 m, the canopy also absorbs momentum from the overlying air mass perturbed by the fire and the DD case absorbs most of it even when the fire is burning strongly. Another interesting fact is that the momentum flux is not very sensitive to moisture effects.

- **Friction velocity (u_*):** The friction velocity is computed as

$$u_* = (\overline{u'w'^2} + \overline{v'w'^2})^{1/4}, \quad (1)$$

where v' denotes cross stream velocity fluctuations and u_* represents the net magnitude of wind shear stress at a particular height. In regular atmospheric turbulence, u_* can range between 0.1 ms^{-1} to 0.5 ms^{-1} . At the 3 m height, u_* is indeed at that range for all cases, until the fire enhances the magnitude of the turbulence locally. This increase of u_* is observed for all cases during fire front propagation, which is associated with strong vertical motions close to the flame associated with a 'chimney effect'⁶⁹, resulting in higher turbulent stress. At 3 m height, the DN case records u_* around 1.6 ms^{-1} as the fire passes the sensor. The DD case records a slightly lower u_* but of similar order of magnitude during fire passage. The sparse cases also report a u_* about 1.2 ms^{-1} . At 7 m level, u_* is higher for all the cases, while the no midstory cases reach magnitudes around 2 ms^{-1} . The amount of moisture does not have much impact in the magnitude of shear stress and potentially is more strongly driven by the amount of fuel present and at the rate fuel is removed by fire. u_* returns to pre-fire magnitudes after the fire passes, in spite of ongoing smoldering. Interestingly, at crown height, the DD case has the highest magnitude of u_* (around 2.6 ms^{-1}), likely due to buoyancy generated turbulence during the fire. Before and after the fire passage, the dense midstory case has much lower magnitudes of u_* .

- **Turbulent kinetic energy (TKE):** The turbulent kinetic energy is computed as

$$TKE = \frac{1}{2} (\overline{u'u'^2} + \overline{v'v'^2} + \overline{w'w'^2}), \quad (2)$$

where u' , v' and w' are fluctuations from the 1 min moving averaged mean. Figure 5 shows the individual components of TKE as well as the net TKE for the three heights and for the six different cases. At 3 m height, before the fire, the DN case has higher magnitudes of TKE, about $2.5 \text{ m}^2\text{s}^{-2}$, while the DD case has slightly lower TKE close to the surface. This indicates the effect of fuel drag. As the fire passes, the TKE for all cases increases significantly, from 0.5 – $2.5 \text{ m}^2\text{s}^{-2}$ to about $10 \text{ m}^2\text{s}^{-2}$. The DD case records the highest TKE in this range. Interestingly, this TKE rise has two components. First, the large rise is contributed by $\overline{u'u'}$, during intense burning between 200 and 300 s. Next, a strong rise is recorded for $\overline{v'v'}$, between 300 and 400 s, which leads to the net TKE peak that lasts between 200 and 400 s. This rise is associated with strong crosswind flows that wrap around the fire. The $\overline{w'w'}$ component shows the contribution from buoyancy driven turbulence, which is vertical in direction. The DD case records the highest $\overline{w'w'}$ as well due to most intense burning, followed by the DN and DS cases. The moist cases record lower $\overline{w'w'}$ which is expected, as the intensity of burning is less. However, the patterns of $\overline{u'u'}$ and $\overline{v'v'}$ are more complicated as they are dependent of vegetative drag and how fuel is removed with burning, which also dictates the nature of the wind as it rushes to the upstream of the fire flank as the fire passes the area. The net TKE contains all these combined effects. After fire front passage, TKE values return to their pre-fire-front-passage values. Another interesting observation is that even during fire front passage, the relative contributions of $\overline{u'u'}$, $\overline{v'v'}$ and $\overline{w'w'}$ remain similar, i.e. $\overline{w'w'} \approx 0.5\overline{u'u'}$ and $TKE \approx \overline{u'u'} \approx \overline{v'v'}$ in terms of magnitude, which is also observed in regular atmospheric turbulence⁷³. At 7 m height, the net TKE follows similar patterns, although the DD case records about $15 \text{ m}^2\text{s}^{-2}$ during fire passage, while the DN case is still at $10 \text{ m}^2\text{s}^{-2}$. This contribution is mainly due to buoyancy effects and cross stream velocity components, as the $\overline{w'w'}$ increases significantly at this height, about $15 \text{ m}^2\text{s}^{-2}$, due to higher fuel availability. At this height, the contribution to TKE from $\overline{u'u'}$ is rather small, because of higher fuel drag. The no midstory and sparse midstory cases have higher $\overline{u'u'}$ at this height. At the crown height of 15 m, the trends are similar to the midstory level. Another point to note here that the level of vertical turbulence can also set the boundary conditions for spotting potential, which can launch firebrands aloft. These embers and other burning particles can get transported by the turbulent wind aloft the canopy sub layer and create spot fires ahead of the fire front.

- **Isotropy** Another factor associated with TKE is isotropy. Figure 6 shows the time variation of $\overline{w'w'}/(2 * TKE)$ for all 6 cases, for the three heights 3 m, 7 m and 15 m. For isotropic turbulence, this value should be $0.33^{71,74}$. If this value is < 0.33 , it indicates that the horizontal component of the TKE ($\overline{u'u'} + \overline{v'v'}$) strongly dominates over the vertical component $\overline{w'w'}$. Before the fire front passage, all cases exhibit strong anisotropy, however, the anisotropy is stronger (further away from 0.33) close to the ground surface and is more isotropic at crown height. During fire front passage, the strong buoyancy effects enhance $\overline{w'w'}$ and increases isotropy for all cases and all levels, especially for the DD case.

There are few instances in the literature that have reported fine-scale turbulent quantities in such detail as discussed above, especially in the context of wildfires spreading in a vegetative environment. However, Clements et al.⁶⁹ had conducted field experiments (FIREFLUX) which collected high frequency turbulent data on a micro-meteorological tower at four heights (2 m, 10 m, 28 m, 42 m) in the path of a grass fire. This allowed the authors to examine mean and turbulent quantities before, during and after fire front propagation. Clements et al.⁶⁹ used 1 min moving averages to look at the evolution of flow statistics as the fire passed the tower, which is the strategy used in this work as well. They observed friction velocities (u_*) in the range of 2.5 – 3 ms^{-1} at 2 m height and 3 – 3.5 ms^{-1} during fire front passage. The u_* observed in this study has a similar order of magnitude.

ATTACHMENT D

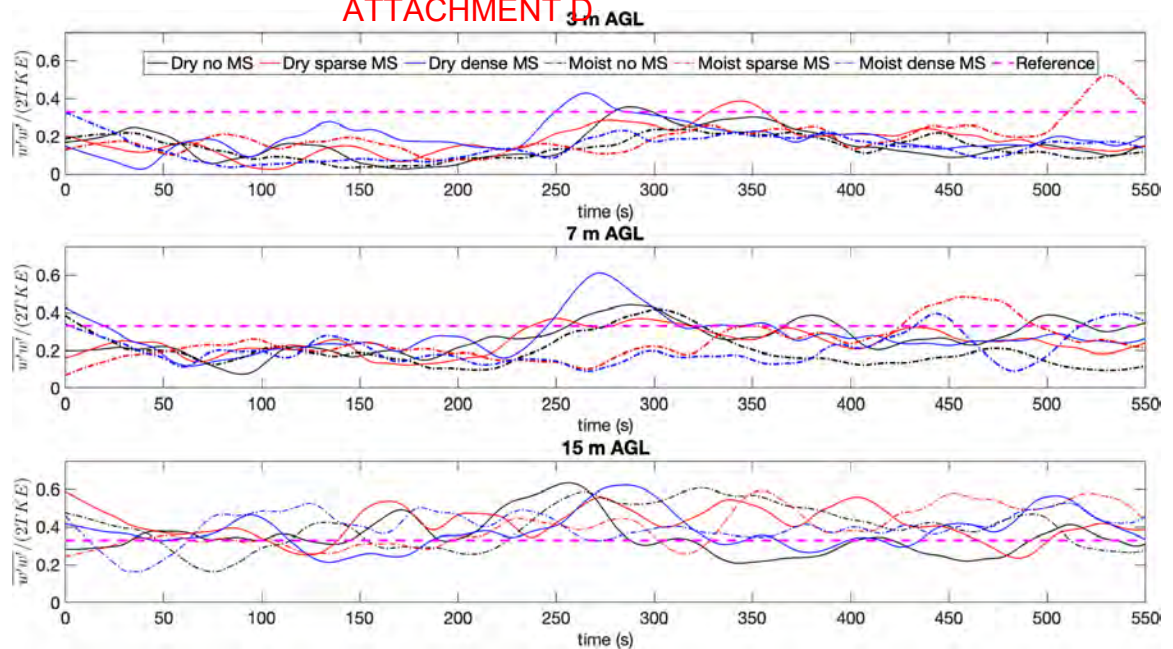


Figure 6. Time variation of 1 min averaged values of $\overline{w'w'}/(2 * TKE)$ showing turbulent anisotropy. Line styles are same as Fig. 3. Dashed magenta line shows the value of 0.33 for isotropic turbulence.

Moreover, they observed TKE in the range of $6\text{--}12 \text{ m}^2\text{s}^{-2}$ which is also the range observed in this study. Heilman et al.⁷⁴ reported peak TKE values of $5\text{--}20 \text{ m}^2\text{s}^{-2}$ during two burns at the New Jersey Pine Barrens (forest environment). Heilman et al.⁷¹ reported similar trends of turbulence anisotropy (0.10–0.20) during these burn operations. The buoyancy flux, defined as $B_f = g/\theta * w'\theta'$ are also on the order of $0.5\text{--}1 \text{ m}^2\text{s}^{-3}$ similar to the magnitudes reported by⁶⁹. However, the difference between fuel characteristics (grass in the case of⁶⁹, forest vegetation in this case) precludes further one to one comparisons.

Discussion

In this work, we investigated the drivers of wildfire spread following linear ignition in the context of active fuel reduction treatments. We further examined how clearing midstory vegetation alters fire behavior through changes in canopy drag and the interdependence on fuel moisture. A line ignition was used to investigate the fundamental processes in fire behavior, with the application of these simulations addressing potential fire size on initial attack success. Simulations in this study were conducted using HIGRAD/FIRETEC to observe bulk fire behavior indicators such as fire intensity, fire spread rate and fuel consumption.

The generally expected trend was found with the DD case, which produced the highest fire intensity. Interestingly, under dry conditions, the gradual lowering of midstory density did not yield monotonically decreasing trends of fire intensity. Up to a level of midstory thinning, termed sparse midstory in this study, the fire intensity and rate of spread were reduced. However, under the DN case, where most of the midstory and understory vegetation was thinned, the wind speed and turbulence levels were enhanced such that the rate of spread increased and was often higher than the DD case. More interestingly, the fire intensity actually increased compared to the DS case with the absence of midstory but lower than the DD case. The enhanced wind speed, turbulence and the resulting augmented sensible heat flux were partly responsible for this behavior, which is seemingly counter intuitive as the DS case was characterized by more fuels.

This behavior further highlight the trade off between fuel availability and wind effects. Under the DN case, the wind effects dominated as the canopy drag was low. Under the DD case, the fuel effect dominated as there is simply too much dry fuel. In the sparse case where both the fuel effects and wind effects were moderated, both fire spread and fire intensity were reduced. This trade off offers another perspective on the practice of fuel treatments with prescribed fires. Under dry conditions, both no thinning and excessive thinning can lead to high amount of fuel consumption. Whereas a moderate degree of thinning can lead to lowered consumption for both overstory and understory vegetation. Hence burn managers might consider this trade-off on consumption as well as the consequences on fire intensity and rate of spread when conducting cost-benefit analyses of a prescribed fire.

Under seasonably moist conditions, these trade-offs were absent and wind effects dominated the fire, with the fire being slower and less intense with higher fuel moisture. Higher winds drove the fire faster under moist conditions. To understand the physical mechanisms behind this behavior, detailed analyses were conducted by collecting data on virtual towers at different locations. Time series of flow quantities such as mean velocities, potential temperature and turbulent statistics such as sensible advective and buoyant turbulent heat fluxes, turbulent stress (momentum flux), friction velocity (a measure of shear stress) and turbulent kinetic energy and its components were plotted at the domain center, at three different heights, close to the surface, at midstory height and at crown height.

ATTACHMENT D

These emergent picture of the consequences of nonlinear fire atmosphere interaction in the fine scales on fire behavior is also consistent with new insights coming out the analyses of a large number of recent fires in California⁵³, which were identified to be either fuel dominated or wind dominated. Consequences of long term fire suppression policy, silvicultural practices, grazing and timber harvesting practices can alter the fire regime in either directions. For the fuel driven fires, altering fuels can offer bottom up controls as hypothesized by Keeley and Syphard⁵³ and clearly demonstrated in this work. It is also important to recognize that when extreme synoptic scale wind events (such as Santa Ana winds) dominate fire behavior, fuel treatments are hardly a limiting factor and those cases are beyond the scope of the current manuscript. However, mastication and thinning operations can establish a higher degree of control even on fires on shrub type ecosystems under lower wind events^{75,76}. Future research will attempt to establish the limits of these top down and bottom up controls on wildland and prescribed fires, as well as their interaction with complex terrain.

Nevertheless, a physical understanding of canopy-fire atmosphere in such detail as explored in this work can help burn managers design treatments to alter fire behavior. Moreover, the patterns of fire spread within treatment zones during initial attack will depend heavily on interacting factors of canopy-induced winds, fuels moisture, and loading. The suite of conditions under which desired fire behavior can increase suppression success can only be fully understood in the context of complex feedbacks. The details provided in the current analyses offers an unprecedented level of insight into mechanisms that govern momentum and energy exchange in the the complex heterogeneous canopy environment, which are relevant for fire behavior assessments. Moreover, the analyses also shed light on the potential indicators of high intensity crowning behavior. To conclude, this work highlights the importance of accounting for the effects of vegetation management, fine-scale vegetation heterogeneity, winds, and turbulence on fire behavior when conducting prescribed burn operations and the success of initial attacks on wildland fires.

Methods

Fuel data. The fuel data were collected at the Eglin Air Force Base in Florida. Based on tree inventory data, three major species of trees were present, namely longleaf pines (*Pinus palustris*), common persimmon (*Diospyros virginiana* L.) and turkey oaks (*Quercus cerris*). Further details about the fuel data collection methods are described in⁷⁷. The average tree canopy density (fine fuel) was 0.3 kg m^{-3} for longleaf pines and persimmons. For turkey oaks, this value was 0.4 kg m^{-3} . The density of grass was 1.573 kg m^{-3} , with an average grass height of 0.5 m. The average litter height was 0.1 m and the litter load was 5.0 kg m^{-3} . Moreover, the density of grass was reduced and the litter density was increased below the trees due to canopy shading, using an exponential attenuation factor 5.0. Under the moist condition, the nominal fuel moisture was 133% for longleaf pines, 170% for persimmons, 200% for turkey oaks and 8% for grass and litter. The nominal fuel size was 0.0005 m for longleaf pines and persimmons and 0.0002 m for turkey oaks. Note that the persimmons and the turkey oaks usually comprised the midstory. In the dry season, the moisture for the turkey oaks were 15% and the persimmons were killed (omitted from the fuel complex in the model). Tree data were collected in three stages of management—‘no midstory’ where there are only 408 pines per hectares (1 hectare is equal to 10,000 square meters), ‘well managed or sparse midstory’ where there are 408 pines, 551 persimmons and 44 turkey oaks per hectare; ‘unmanaged or dense midstory’ where there are 408 pines, 551 persimmons and 983 turkey oaks per hectare. The average height for the longleaf pines was 18 m and the average height for the midstory vegetation was about 11 m. It is also important to note that the fuel loading values (2.0–2.5 metric tons per hectare for midstory + understory) and 2.7–3.0 metric tons per hectare for overstory) are consistent with those observed both in the US Southeast (Longleaf and Loblolly pines)⁷⁸ and the Southwest (Ponderosa pine and mixed conifer stands)⁷⁹. So the observations in this work are deemed to reflect a wide range of conditions. Another important point to note is that the moist or dry conditions in fuel moisture are entirely driven by seasonality and not by other management efforts.

Since the purpose of these simulations was to isolate the effects of midstory fuel management on wildland fire behavior, surface fuel conditions were held unchanged. Varying the surface fuel moisture would impose additional variations in fire behavior unrelated to treatment evaluations—and it would further complicate the interpretation of the results. In addition, whether this level of midstory fuel treatment would be sufficient to make the surface fuel drier is not clear and the literature poses contrasting evidences. Whitehead et al.¹⁵ noted that forest thinning might lead to enhanced solar radiation, wind speed and near-surface temperature but did not find any significant changes in relative humidity or surface fuel moisture. Kalias and Kent¹⁷ lists several studies which reported fuel treatment effects on fuel moisture and fire behavior. Banerjee¹⁸ also offers a detailed review on this topic and summarizes these contrasting evidences. Some field experimental studies such as Bigelow and North⁸⁰, Faiella and Bailey⁸¹ and Estes et al.⁸² have reported no appreciable changes in the surface fuel moisture post thinning. Bigelow and North⁸⁰ argued that micrometeorological changes in the sub canopy environment post thinning can counter each other. An increase in wind speed after thinning could increase the turbulence driven mixing of the air above and below the canopy sub layer, thereby not allowing air temperature to increase or surface fuel moisture to decrease. On the other hand, some other studies such as Pook and Gill⁸³, Weatherspoon et al.⁸⁴ and Countryman⁸⁵ noted that thinning could lead to a drier surface fuel layer, which could enhance fire intensity. Given these uncertainties, it is unclear at this stage if changes in the midstory fuel (without removing the entire crown) would lead to any appreciable changes in the surface fuel moisture. While more research is needed to address this topic, the surface fuel properties were held fixed in this study while the midstory fuel was varied across the six simulation cases in this study based on available data.

Model description. Simulations are conducted using the HIGRAD/FIRETEC code developed at Los Alamos National Laboratory^{86–88}. FIRETEC is a large-eddy simulation (LES) tool that can resolve atmospheric tur-

ATTACHMENT D

bulence over three dimensional heterogeneous fuel distributions at spatial resolutions on the order of 2 m and can capture the spread, intensity and extent of burn area under different ignition conditions. FIRETEC simulates the movement of a wildfire by accounting for a few processes, such as the convective heating of fuel elements in front of a flame, the entrainment of cold air from the surroundings atmosphere, radiative heating and cooling of fuels and the drag experienced by the wind over vegetation canopy. The combustion of solids, which leads to chemical products and heat, is handled using a single compartment model without regards to chemical composition of the fuels. More specifically, it includes an evolution equation for the density of dry fuel as well as the density of water separately. A budget equation for the internal energy of the fuel that includes radiation, advection and energy exchange due to chemical reactions and evaporation of water tracks the temperature of the solid fuel elements. The evolution of the density and momentum of the gas phase are governed by the mass and momentum budgets of a fully compressible Navier Stokes equation. There is another budget equation for the internal energy of the gas phase which results in the potential temperature of the gas phase. It includes turbulent advection, turbulent diffusion as well as radiation effects and the energy exchange with the burning solids. Last but not the least, an advection diffusion equation tracks the evolution of oxygen. It is important to note that fine scale (below 2 m) processes are treated as sub grid scale processes. The sub grid scale variations of temperature, velocity and fine scale fuel features are parameterized.

Simulations. Each simulation is conducted over a 400 m by 320 m (12.8 ha) domain with a grid resolution of 2 m by 2 m. The vertical extent of the domain is 550 m. The vertical grid resolution is non uniform and uses a grid stretching function in order to accommodate more grid points close to the surface within the vegetation canopy. There are 49 grid points in the vertical direction, 12 of which are within the canopy layer. The average grid spacing within the canopy layer is 1.8 m. The time step of each simulation is 0.02 s. Each simulation is spun up with a wind run for 3100 s (about 52 min) so that sufficient turbulence is generated and the wind field develops a steady state. Periodic boundary conditions are used on both sides of the domain. 80 processors are used in parallel for each set of simulations. An inlet wind profile with a value of 8 ms^{-1} at 30 m above ground level (AGL) is prescribed, which adjusts to the vegetation for the corresponding simulation during the wind run and follows a logarithmic profile above the zero plane displacement height. A free slip boundary condition is used at the top of the domain. The fire simulations start after the wind runs, with an ignition line, 4 m wide, 80 m long and offset by 80 m from the left edge of the domain along the wind direction (x axis) and centered perpendicular to the wind direction (y axis). Note that line ignitions are standard while investigating fundamental aspects of wildland fire behavior both in terms of experiments and simulations^{46,87}. The target temperature of ignition is 1000 K and a ramp rate of 350 K s^{-1} is used. Each fire simulation is run for 600 s (10 min).

Received: 7 March 2020; Accepted: 29 September 2020

Published online: 14 October 2020

References

1. Westerling, A. L. Increasing western us forest wildfire activity: sensitivity to changes in the timing of spring. *Philos. Trans. R. Soc. B* **371**, 20150178 (2016).
2. Dennison, P. E., Brewer, S. C., Arnold, J. D. & Moritz, M. A. Large wildfire trends in the western united states, 1984–2011. *Geophys. Res. Lett.* **41**, 2928–2933 (2014).
3. Kasischke, E. S. & Turetsky, M. R. Recent changes in the fire regime across the North American boreal region—spatial and temporal patterns of burning across Canada and Alaska. *Geophys. Res. Lett.* **33** (2006).
4. Littell, J. S., McKenzie, D., Peterson, D. L. & Westerling, A. L. Climate and wildfire area burned in western US ecoprovinces, 1916–2003. *Ecol. Appl.* **19**, 1003–1021 (2009).
5. Abatzoglou, J. T. & Kolden, C. A. Relationships between climate and macroscale area burned in the western United States. *Int. J. Wildland Fire* **22**, 1003–1020 (2013).
6. Kelly, R. *et al.* Recent burning of boreal forests exceeds fire regime limits of the past 10,000 years. *Proc. Natl. Acad. Sci.* **110**, 13055–13060 (2013).
7. Abatzoglou, J. T. & Williams, A. P. Impact of anthropogenic climate change on wildfire across western US forests. *Proc. Natl. Acad. Sci.* **113**, 11770–11775 (2016).
8. Williams, A. P. & Abatzoglou, J. T. Recent advances and remaining uncertainties in resolving past and future climate effects on global fire activity. *Curr. Clim. Change Rep.* **2**, 1–14 (2016).
9. Seager, R. *et al.* Climatology, variability, and trends in the us vapor pressure deficit, an important fire-related meteorological quantity. *J. Appl. Meteorol. Climatol.* **54**, 1121–1141 (2015).
10. Radeloff, V. C. *et al.* Rapid growth of the us wildland–urban interface raises wildfire risk. *Proc. Natl. Acad. Sci.* **115**, 3314–3319 (2018).
11. Fried, J. S. *et al.* Predicting the effect of climate change on wildfire behavior and initial attack success. *Clim. Change* **87**, 251–264 (2008).
12. Agee, J. K. & Skinner, C. N. Basic principles of forest fuel reduction treatments. *For. Ecol. Manag.* **211**, 83–96 (2005).
13. Schwilk, D. W. *et al.* The national fire and fire surrogate study: effects of fuel reduction methods on forest vegetation structure and fuels. *Ecol. Appl.* **19**, 285–304 (2009).
14. Whitehead, R. *et al.* Effect of a spaced thinning in mature lodgepole pine on within-stand microclimate and fine fuel moisture content. In Andrews, P. L., & Butler, B. W., comps. *Fuels Management-How to Measure Success: Conference Proceedings*. 28–30 March 2006; Portland, OR. *Proceedings RMRS-P-41*. Fort Collins, CO: US Department of Agriculture, Forest Service, Rocky Mountain Research Station, vol. 41, 523–536 (2006).
15. Whitehead, R. J. *et al.* *Effect of commercial thinning on within-stand microclimate and fine fuel moisture conditions in a mature lodgepole pine stand in southeastern British Columbia*. Canadian Forest Service, Canadian Wood Fibre Centre. British Columbia, Information Report, FI-X-004 (2008).
16. Parsons, R. A. *et al.* Modeling thinning effects on fire behavior with standfire. *Ann. For. Sci.* **75**, 7 (2018).
17. Kalies, E. L. & Kent, L. L. Y. Tamm review: Are fuel treatments effective at achieving ecological and social objectives? A systematic review. *For. Ecol. Manag.* **375**, 84–95 (2016).
18. Banerjee, T. Impacts of forest thinning on wildland fire behavior. *Forests* **11**, 918 (2020).

ATTACHMENT D

19. Syifa, M., Panahi, M. & Lee, C.-W. Mapping of post-wildfire burned area using a hybrid algorithm and satellite data: the case of the camp fire wildfire in California, USA. *Remote Sensing* **12**, 623 (2020).
20. Storey, M. A., Price, O. F., Sharples, J. J. & Bradstock, R. A. Drivers of long-distance spotting during wildfires in south-eastern Australia. *Int. J. Wildland Fire* (2020).
21. Arienti, M. C., Cumming, S. G. & Boutin, S. Empirical models of forest fire initial attack success probabilities: the effects of fuels, anthropogenic linear features, fire weather, and management. *Can. J. For. Res.* **36**, 3155–3166 (2006).
22. Van Wagner, C. E. *Fire Behaviour Mechanisms in a Red Pine Plantation: Field and Laboratory Evidence*, vol. 1229 (Ministry of Forestry and Rural Development, 1968).
23. Wagner, C. V. Conditions for the start and spread of crown fire. *Can. J. For. Res.* **7**, 23–34 (1977).
24. Graham, R. T., Harvey, A. E., Jain, T. B. & Tonn, J. R. Effects of thinning and similar stand treatments on fire behavior in western forests. *USDA Forest Service, Pacific Northwest Research Station, General Technical Report PNW-GTR-463* (1999).
25. Graham, R. T., McCaffrey, S. & Jain, T. B. Science basis for changing forest structure to modify wildfire behavior and severity. *The Bark Beetles, Fuels, and Fire Bibliography* 167 (2004).
26. Varner, M. & Keyes, C. R. Fuels treatments and fire models: errors and corrections. *Fire Manag. Today* **69**, 47–50 (2009).
27. Amiro, B., Stocks, B., Alexander, M., Ana, F. & Wotton, B. Fire, climate change, carbon and fuel management in the Canadian boreal forest. *Int. J. Wildland Fire* **10**, 405–4 (2001).
28. Pollet, J. & Omi, P. N. Effect of thinning and prescribed burning on crown fire severity in ponderosa pine forests. *Int. J. Wildland Fire* **11**, 1–10 (2002).
29. Peterson, D. L. *et al.* *Forest structure and fire hazard in dry forests of the western United States*. Gen. Tech. Rep. PNW-GTR-628. Portland, OR: US Department of Agriculture, Forest Service, Pacific Northwest Research Station. 30 p 628 (2005).
30. Stephens, S. L. & Moghaddas, J. J. Experimental fuel treatment impacts on forest structure, potential fire behavior, and predicted tree mortality in a California mixed conifer forest. *For. Ecol. Manag.* **215**, 21–36 (2005).
31. Safford, H. D., Schmidt, D. A. & Carlson, C. H. Effects of fuel treatments on fire severity in an area of wildland-urban interface, angora fire, lake Tahoe basin, California. *For. Ecol. Manag.* **258**, 773–787 (2009).
32. Stephens, S. L. *et al.* Fire treatment effects on vegetation structure, fuels, and potential fire severity in western us forests. *Ecol. Appl.* **19**, 305–320 (2009).
33. Hudak, A. *et al.* *Review of fuel treatment effectiveness in forests and rangelands and a case study from the 2007 megafires in central Idaho USA* (no. rmrs-gtr-252). Fort Collins, CO: Rocky Mountain Research Station Publishing Services (2011).
34. Waldrop, T. A. & Goodrick, S. L. *Introduction to prescribed fires in southern ecosystems*. Science Update SRS-054. Asheville, NC: US Department of Agriculture Forest Service, Southern Research Station. 80 p. 54, 1–80 (2012).
35. Martinson, E. J. & Omi, P. N. *Fuel treatments and fire severity: a meta-analysis*. Res. Pap. RMRS-RP-103WWW. Fort Collins, CO: US Department of Agriculture, Forest Service, Rocky Mountain Research Station. 38, p. 103 (2013).
36. Kennedy, M. C. & Johnson, M. C. Fuel treatment prescriptions alter spatial patterns of fire severity around the wildland-urban interface during the Wallow Fire, Arizona, USA. *For. Ecol. Manag.* **318**, 122–132 (2014).
37. Barnett, K., Parks, S. A., Miller, C. & Naughton, H. T. Beyond fuel treatment effectiveness: characterizing interactions between fire and treatments in the US. *Forests* **7**, 237 (2016).
38. Just, M. G., Hohmann, M. G. & Hoffmann, W. A. Where fire stops: vegetation structure and microclimate influence fire spread along an ecotonal gradient. *Plant Ecol.* **217**, 631–644 (2016).
39. Veenendaal, E. M. *et al.* On the relationship between fire regime and vegetation structure in the tropics. *New Phytol.* **218**, 153–166 (2018).
40. Bessie, W. & Johnson, E. The relative importance of fuels and weather on fire behavior in subalpine forests. *Ecology* **76**, 747–762 (1995).
41. Rothermel, R. C. *A mathematical model for predicting fire spread in wildland fuels*. Res. Pap. INT-115. Ogden, UT: US Department of Agriculture, Intermountain Forest and Range Experiment Station. 40 p. 115 (1972).
42. Hoffman, C. M. *et al.* Surface fire intensity influences simulated crown fire behavior in lodgepole pine forests with recent mountain pine beetle-caused tree mortality. *For. Sci.* **59**, 390–399 (2012).
43. Keyes, C. & Varner, J. Pitfalls in the silvicultural treatment of canopy fuels. *Fire Management Today* (2006).
44. Moon, K., Duff, T. & Tolhurst, K. Sub-canopy forest winds: understanding wind profiles for fire behaviour simulation. *Fire Saf. J.* **105**, 320–329 (2016).
45. Beer, T. The interaction of wind and fire. *Boundary-Layer Meteorol.* <https://doi.org/10.1007/BF00183958> (1991).
46. Cheney, N., Gould, J. & Catchpole, W. The influence of fuel, weather and fire shape variables on fire-spread in grasslands. *Int. J. Wildland Fire* **3**, 31–44 (1993).
47. Cochrane, M. A. Fire science for rainforests. *Nature* **421**, 913 (2003).
48. Fulé, P. Z., McHugh, C., Heinlein, T. A. & Covington, W. W. *Potential fire behavior is reduced following forest restoration treatments* (Technical Report 2001).
49. Fulé, P. Z., Crouse, J. E., Roccaforte, J. P. & Kalies, E. L. Do thinning and/or burning treatments in western USA ponderosa or Jeffrey pine-dominated forests help restore natural fire behavior? *For. Ecol. Manag.* **269**, 68–81 (2012).
50. Contreras, M. A., Parsons, R. A. & Chung, W. Modeling tree-level fuel connectivity to evaluate the effectiveness of thinning treatments for reducing crown fire potential. *For. Ecol. Manag.* **264**, 134–149 (2012).
51. White, D. L., Waldrop, T. A. & Jones, S. M. *Forty years of prescribed burning on the santee fire plots: effects on understory vegetation*. Gen. Tech. Rep. SE-69. Asheville, NC: US Department of Agriculture, Forest Service, Southeastern Forest Experiment Station. pp. 51–59 (1990).
52. Davies, G., Domenech-Jardi, R., Gray, A. & Johnson, P. Vegetation structure and fire weather influence variation in burn severity and fuel consumption during peatland wildfires. *Biogeosciences* **12**, 15737–15762 (2016).
53. Keeley, J. E. & Syphard, A. D. Twenty-first century California, USA, wildfires: fuel-dominated vs. wind-dominated fires. *Fire Ecol.* **15**, 24 (2019).
54. Hiers, J. K. *et al.* Fine dead fuel moisture shows complex lagged responses to environmental conditions in a saw palmetto (*Serenoa repens*) flatwoods. *Agric. For. Meteorol.* **266**, 20–28 (2019).
55. Finney, M. A. *et al.* Role of buoyant flame dynamics in wildfire spread. *Proc. Natl. Acad. Sci.* **112**, 9833–9838 (2015).
56. Reisner, J., Wynne, S., Margolin, L. & Linn, R. Coupled atmospheric-fire modeling employing the method of averages. *Mon. Weather Rev.* **128**, 3683–3691 (2000).
57. Mell, W., Maranghides, A., McDermott, R. & Manzello, S. L. Numerical simulation and experiments of burning douglas fir trees. *Combust. Flame* **156**, 2023–2041 (2009).
58. Morvan, D. Physical phenomena and length scales governing the behaviour of wildfires: a case for physical modelling. *Fire Technol.* **47**, 437–460 (2011).
59. Parsons, R. A., Mell, W. E. & McCauley, P. Linking 3d spatial models of fuels and fire: effects of spatial heterogeneity on fire behavior. *Ecol. Model.* **222**, 679–691 (2011).
60. Parsons, R. *et al.* *STANDFIRE: An IFT-DSS module for spatially explicit, 3d fuel treatment analysis* (Technical Report 2015).
61. Hoffman, C. M., Linn, R., Parsons, R., Sieg, C. & Winterkamp, J. Modeling spatial and temporal dynamics of wind flow and potential fire behavior following a mountain pine beetle outbreak in a lodgepole pine forest. *Agric. For. Meteorol.* **204**, 79–93 (2015).
62. Hoffman, C. *et al.* Evaluating crown fire rate of spread predictions from physics-based models. *Fire Technol.* **52**, 221–237 (2016).

ATTACHMENT D

63. Pimont, F. *et al.* Modeling fuels and fire effects in 3d: model description and applications. *Environ. Model. Softw.* **80**, 225–244 (2016).
64. Pimont, F., Dupuy, J.-L., Linn, R. R., Parsons, R. & Martin-StPaul, N. Representativeness of wind measurements in fire experiments: lessons learned from large-eddy simulations in a homogeneous forest. *Agric. For. Meteorol.* **232**, 479–488 (2017).
65. Pimont, F., Dupuy, J.-L., Linn, R. R. & Dupont, S. Impacts of tree canopy structure on wind flows and fire propagation simulated with FIRETEC. *Ann. For. Sci.* **68**, 523 (2011).
66. Linn, R. R., Sieg, C. H., Hoffman, C. M., Winterkamp, J. L. & McMillin, J. D. Modeling wind fields and fire propagation following bark beetle outbreaks in spatially-heterogeneous Pinyon–Juniper woodland fuel complexes. *Agric. For. Meteorol.* **173**, 139–153 (2013).
67. Kiefer, M. T., Heilman, W. E., Zhong, S., Charney, J. J. & Bian, X. Mean and turbulent flow downstream of a low-intensity fire: influence of canopy and background atmospheric conditions. *J. Appl. Meteorol. Climatol.* **54**, 42–57 (2015).
68. Clements, C. B. *et al.* Observing the dynamics of wildland grass fires: fireflux—a field validation experiment. *Bull. Am. Meteorol. Soc.* **88**, 1369–1382 (2007).
69. Clements, C. B., Zhong, S., Bian, X., Heilman, W. E. & Byun, D. W. First observations of turbulence generated by grass fires. *J. Geophys. Res. Atmos.* **113**, D22 (2008).
70. Seto, D., Clements, C. B. & Heilman, W. E. Turbulence spectra measured during fire front passage. *Agric. For. Meteorol.* **169**, 195–210. <https://doi.org/10.1016/j.agrformet.2012.09.015> (2013).
71. Heilman, W. E. *et al.* Observations of fire-induced turbulence regimes during low-intensity wildland fires in forested environments: implications for smoke dispersion. *Atmos. Sci. Lett.* **16**, 453–460 (2015).
72. Clements, C. B. *et al.* The fireflux II experiment: a model-guided field experiment to improve understanding of fire–atmosphere interactions and fire spread. *Int. J. Wildland Fire* **28**, 308–326 (2019).
73. Banerjee, T. & Katul, G. Logarithmic scaling in the longitudinal velocity variance explained by a spectral budget. *Phys. Fluids* **25**, 125106 (2013).
74. Heilman, W. E. *et al.* Atmospheric turbulence observations in the vicinity of surface fires in forested environments. *J. Appl. Meteorol. Climatol.* **56**, 3133–3150 (2017).
75. Keeley, J. E. & Zedler, P. H. Large, high-intensity fire events in southern California shrublands: debunking the fine-grain age patch model. *Ecol. Appl.* **19**, 69–94 (2009).
76. Jin, Y. *et al.* Contrasting controls on wildland fires in southern California during periods with and without Santa Ana winds. *J. Geophys. Res. Biogeosciences* **119**, 432–450 (2014).
77. Hiers, J. K., O'Brien, J. J., Will, R. E. & Mitchell, R. J. Forest floor depth mediates understory vigor in xeric pinus palustris ecosystems. *Ecol. Appl.* **17**, 806–814 (2007).
78. Parresol, B. R., Shea, D. & Ottmar, R. Creating a fuels baseline and establishing fire frequency relationships to develop a landscape management strategy at the savannah river site. In Andrews, P. L. & Butler, B. W., comps *Fuels Management-How to Measure Success: Conference Proceedings. 28–30 March 2006; Portland, OR. Proceedings RMRS-P-41. Fort Collins, CO: US Department of Agriculture, Forest Service, Rocky Mountain Research Station*, vol. 41, pp 351–366 (2006).
79. Sackett, S. S. & Haase, S. M. *Fuel loadings in southwestern ecosystems of the United States*. United States Department of Agriculture, Forest Service General Technical Report 187–192 (1996).
80. Bigelow, S. W. & North, M. P. Microclimate effects of fuels-reduction and group-selection silviculture: implications for fire behavior in Sierran mixed-conifer forests. *For. Ecol. Manag.* **264**, 51–59 (2012).
81. Faiella, S. M. & Bailey, J. D. Fluctuations in fuel moisture across restoration treatments in semi-arid ponderosa pine forests of northern Arizona, USA. *Int. J. Wildland Fire* **16**, 119–127 (2007).
82. Estes, B. L., Knapp, E. E., Skinner, C. N. & Uzoh, F. C. Seasonal variation in surface fuel moisture between unthinned and thinned mixed conifer forest, northern California, USA. *Int. J. Wildland Fire* **21**, 428–435 (2012).
83. Pook, E. & Gill, A. Variation of live and dead fine fuel moisture in pinus radiata plantations of the Australian-capital-territory. *Int. J. Wildland Fire* **3**, 155–168 (1993).
84. Weatherspoon, C. P. & Skinner, C. Fire-silviculture relationships in sierra forests. *Sierra nevada ecosystem project: final report to congress* **2**, 1167–1176 (1996).
85. Countryman, C. Old-growth conversion also converts fire climate. *US Forest Service Fire Control Notes* **17**, 15–19 (1955).
86. Linn, R. R. A transport model for prediction of wildfire behavior. Technical Report, Los Alamos National Lab., NM (United States) (1997).
87. Linn, R., Winterkamp, J., Colman, J. J., Edminster, C. & Bailey, J. D. Modeling interactions between fire and atmosphere in discrete element fuel beds. *Int. J. Wildland Fire* **14**, 37–48 (2005).
88. Linn, R. R. & Cunningham, P. Numerical simulations of grass fires using a coupled atmosphere-fire model: basic fire behavior and dependence on wind speed. *J. Geophys. Res. Atmos.* **110**, D13 (2005).

Acknowledgements

T. Banerjee acknowledges a Director's fellowship from Los Alamos National Laboratory, which helped initiate this work. The Los Alamos National Laboratory Institutional Computing Program provided critical computing resources for this work. This work has been assigned LA-UR-19-23583. Los Alamos National Laboratory is operated by Triad National Security, LLC for the National Nuclear Security Administration of U.S. Department of Energy under contract 89233218CNA000001. Additionally, T. Banerjee acknowledges the funding support from the University of California Laboratory Fees Research Program funded by the UC Office of the President (UCOP), grant ID LFR-20-653572. Additional support was provided by the new faculty start up grant provided by the Department of Civil and Environmental Engineering, and the Henry Samueli School of Engineering, University of California, Irvine.

Author contributions

T.B. planned and designed the project, conducted the analysis and wrote the paper. R.L. and K.H. collected the fuel data used in the paper. K.H., S.G. and W.H. provided comments and suggestions.

Competing interests

The authors declare no competing interests. The founding sponsors had no role in the design of the study; in the collection, analyses, or interpretation of data; in the writing of the manuscript, and in the decision to publish the results.

Additional information ATTACHMENT D

Correspondence and requests for materials should be addressed to T.B.

Reprints and permissions information is available at www.nature.com/reprints.

Publisher's note Springer Nature remains neutral with regard to jurisdictional claims in published maps and institutional affiliations.



Open Access This article is licensed under a Creative Commons Attribution 4.0 International License, which permits use, sharing, adaptation, distribution and reproduction in any medium or format, as long as you give appropriate credit to the original author(s) and the source, provide a link to the Creative Commons licence, and indicate if changes were made. The images or other third party material in this article are included in the article's Creative Commons licence, unless indicated otherwise in a credit line to the material. If material is not included in the article's Creative Commons licence and your intended use is not permitted by statutory regulation or exceeds the permitted use, you will need to obtain permission directly from the copyright holder. To view a copy of this licence, visit <http://creativecommons.org/licenses/by/4.0/>.

© The Author(s) 2020

ATTACHMENT D

EXHIBIT H

ATTACHMENT D

Deconstructing the King megafire

JANICE L. COEN ^{1,4}, E. NATASHA STAVROS,² AND JOSEPHINE A. FITES-KAUFMAN³

¹National Center for Atmospheric Research, P.O. Box 3000, Boulder, Colorado 80307 USA

²California Institute of Technology, Jet Propulsion Laboratory, 4800 Oak Grove Drive, MS 233-300, Pasadena, California 91109 USA

³Pacific Southwest Region, USDA Forest Service, 1323 Club Drive, Vallejo, California 94592 USA

Abstract. Hypotheses that megafires, very large, high-impact fires, are caused by either climate effects such as drought or fuel accumulation due to fire exclusion with accompanying changes to forest structure have long been alleged and guided policy, but their physical basis remains untested. Here, unique airborne observations and microscale simulations using a coupled weather–wildland-fire-behavior model allowed a recent megafire, the King Fire, to be deconstructed and the relative impacts of forest structure, fuel load, weather, and drought on fire size, behavior, and duration to be separated. Simulations reproduced observed details including the arrival at an inclined canyon, a 25-km run, and later slower growth and features. Analysis revealed that fire-induced winds that equaled or exceeded ambient winds and fine-scale airflow undetected by surface weather networks were primarily responsible for the fire’s rapid growth and size. Sensitivity tests varied fuel moisture and amount across wide ranges and showed that both drought and fuel accumulation effects were secondary, limited to sloped terrain where they compounded each other, and, in this case, unable to significantly impact the final extent. Compared to standard data, fuel models derived solely from remote sensing of vegetation type and forest structure improved simulated fire progression, notably in disturbed areas, and the distribution of burn severity. These results point to self-reinforcing internal dynamics rather than external forces as a means of generating this and possibly other outlier fire events. Hence, extreme fires need not arise from extreme fire environment conditions. Kinematic models used in operations do not capture fire-induced winds and dynamic feedbacks so can underestimate megafire events. The outcomes provided a nuanced view of weather, forest structure, fuel accumulation, and drought impacts on landscape-scale fire behavior—roles that can be misconstrued using correlational analyses between area burned and macroscale climate data or other exogenous factors. A practical outcome is that fuel treatments should be focused on sloped terrain, where factors multiply, for highest impact.

Key words: coupled atmosphere–fire model; fire behavior; fire model; LiDAR; multiple plumes; numerical weather prediction; pyrocumulus; wildfire; wildland fire.

INTRODUCTION

Wildfire is a major force in the western United States and globally and has the potential to reshape forested landscapes into new and possibly novel configurations (Bond and Keeley 2005, Turner 2010). For years, concern has been rising that long-term fire exclusion (Keane et al. 2002) and, increasingly, climate change may be changing fire behavior and increasing the risk of very large, severe fires (Westerling et al. 2006, Williams 2013), yielding a new category of wildfires, “megafires,” that are becoming more common in the western United States and perhaps worldwide. The term became widespread in 2002 when five western U.S. states experienced their worst fires on record (Williams 2013), the magnitude and impacts of which stood out even in regions frequented by fire. The term has since been applied to describe outbreaks of large, intense fires in other fire-prone locations such as Australia (Bartlett et al. 2007), Canada (Stocks et al. 2003), Greece (Dimitrakopoulos et al. 2011), and Europe overall (Tedim et al. 2014). Criteria identifying a megafire vary; fires may be notable in terms of size, severity, cost, resources required, or human, economic, or environmental impacts.

Analysis of historical data suggests that climatic factors have become more favorable for wildfires in general (Westerling et al. 2006, Barbero et al. 2014, Dennison et al. 2014, Stavros et al. 2014), and very large fires in particular (Dennison et al. 2014), increasing their frequency and extent (Dennison et al. 2014) over recent decades in some regions. Though still an infrequent event—only a small percentage of fires exceed 100 ha in size—very large fires have a disproportionate impact on overall area burned (Littell et al. 2009), 80–96% of which is due to the largest 1% of fires (Strauss et al. 1989). The hypotheses that megafires in general, or individual megafires in particular, are directly attributable to either climate change effects such as drought or long-term fuel accumulation due to fire exclusion with accompanying changes to forest structure have been widely asserted but are not directly experimentally testable; most evidence supporting either thesis is correlational, integrated over broad scales, and circumstantial. The climate hypothesis (Dale et al. 2001, Flannigan et al. 2009) has generated debate amid the broader climate change controversy while the “century of suppression” hypothesis (Williams 2013) has led to second-guessing of well-intentioned and strongly supported fire management programs and intense criticism of land management agencies. The debate has raged with significant consequences on forest policy issues, conservation, healthy forest initiatives, and public passion. The debate in the United States is paralleled by debates elsewhere in countries with fire-prone ecosystems.

Manuscript received 1 September 2017; revised 25 January 2018; accepted 29 March 2018. Corresponding Editor: Bradford P. Wilcox.

⁴E-mail: janicec@ucar.edu

ATTACHMENT D

Similarly, debates have contested the relative importance of climate-scale factors such as drought vs. day-to-day weather in creating very large fires (Abatzoglou and Kolden 2011, Riley et al. 2013). Fire growth is episodic, and even during sustained drought, most growth occurs on a small proportion of days—not always consecutive—during a wildfire’s active period (Wang et al. 2014). Anecdotal firefighter reports from recent megafires describe unprecedented fire behavior that could not be reproduced with standard fire behavior modeling systems. Further complicating understanding, observational data on megafires, which may behave differently than less extreme events (Alvarado et al. 1998, Pyne 2015), have been limited. Reproducibility that is possible with repeatable laboratory experiments and more common occurrences is often not possible when the subject is an extreme or unusual unplanned natural event. Thus, broad regional statistical analyses have been recommended (Schoennagel et al. 2004), either time series or spatial correlations, to draw out the causal factors. Inferences about the atmospheric factors causing these events, for example, have relied upon statistical correlations between megafire occurrence and macroscale monthly weather data (Bowman et al. 2017) and been specified to speculate on the cause of individual megafires or megafires in general. Brotak and Reifsnnyder (1977) identify synoptic conditions associated with large fires, chiefly strong prefrontal surface winds preceding a trough, while Peterson et al. (2015a) draw similar conclusions in the context of the Rim Fire, concluding strong prefrontal surface winds aligned with terrain drove some periods of extreme fire spread. Similarly, studies have used statistical analyses to identify environmental factors related to observed degrees of severity, such as the severity of previous burns and topographic slope (Harris and Taylor 2017) and, for the Rim Fire, the influence of forest structure, fire history, topographic, and weather conditions (Lydersen et al. 2014). The latter study indicated that on days characterized by strong plume activity, severity was moderate to severe regardless of forest conditions. While these approaches identify general associations, they may overlook important factors for which data are not available. Thus, the mechanisms causing the emergence of one of these rare events are still not well understood and have not yet been scrutinized with complementary methods such as physically based process studies, either observational studies or contemporary dynamic models that simulate fire behavior—methods that, of necessity, examine individual events.

This study decomposes the factors leading to the size, behavior, and duration of a megafire of a type increasingly common in the United States and similar to fires in Mediterranean Europe, Australia, Canada, and Israel. The 2014 King Fire, which occurred in California’s northern Sierra Nevada mountains, stood out due to its size, rapid spread, and severity. It provides a unique opportunity for hypothesis testing and separation of the effects of climate, short-term weather, and forest condition because airborne remote sensing provided preburn forest structure and vegetation type data, thermal imagery during the fire, and quantitative characterization of impacts to vegetation postfire. Before the King Fire, in the summer of 2014, NASA’s preHypIRI preparatory program (Lee et al. 2015) imaged the entire region containing the fire with high-resolution airborne spectroscopic and thermal sensors. Additionally, much of

the area was surveyed with LiDAR by the U.S. Department of Agriculture Forest Service, providing direct information on forest structure. Thermal imagery was acquired during active burning, and comprehensive LiDAR, thermal, and spectroscopic data were acquired over the burn scar shortly after the fire. These data sets, taken together, allow fire behavior during the event to be related to prior forest structure and field condition, enable energy release during the fire to be estimated from contemporaneous thermal imagery, and further constrain modeled fire behavior by comprehensively surveying residual forest structure postburn. By combining these data with a fully mechanistic coupled atmosphere–wildland–fire model, we could estimate the separate effects of the antecedent drought, fuel, forest structure, topography, and weather on a single fire. By doing so, we could connect cause and effect as in a process study and uncover the dependency of fire behavior on these contributing factors in a way that is currently unique and a countercheck to conclusions garnered from the previously mentioned broad statistical analyses. This more clearly refines how climate change impacts might be distributed locally and how climate change, disturbances, and land management practices might cumulatively shape future fires. While the King Fire is only a single example and inherently unreplicable and this data set is unique and likely to remain so until and unless spectroscopic and LiDAR coverage becomes ubiquitous, this study provides a paradigm for interpreting the factors that lead to extreme fires.

We seek to disentangle the influence of weather, fuels, and climate factors on the King Fire and provide insights into megafire behavior. We ask (1) Does current understanding, as encapsulated in a state-of-the-art modeling system, explain the megafire’s behavior? (2) Does better representing the spatial variability of forest structure, derived solely from airborne remote sensing observations of pre- and postfire forest structure and composition, improve simulation and understanding of fire behavior and effects? We examine attributable factors to answer (3) What role did fire-induced winds play in its rapid growth? (4) Did drought contribute to the fire’s rapid growth and extent? (5) How would this fire have behaved if fuel had not accumulated? This uniquely observed case study provided an opportunity to gain insight that can inform science and wildfire management more generally, as well as raising hypotheses that can be tested in other settings. Because, while these factors may have differing importance in other fires occurring in different terrain, forest type, and weather, the physical relationships presented in this study, as well as identification of the conditions under which drought and fuel load can and cannot affect fire behavior, are ubiquitous. This work suggests how megafire behavior may be better interpreted, predicted, and mitigated.

Study context

During the study period, a trough of low pressure was approaching the California coast, preceded by weak southwesterly surface winds, where they generally ascended the west slopes of the Sierra Nevada Mountain Range. The King Fire was ignited at 18:37 (all times Pacific Daylight Time [PDT], Coordinated Universal Time [UTC] –7 h) on 13 September 2014 near Pollock Pines, California, USA (ignition location

38.782° N, 120.604° W). It spread during a severe drought (Griffin and Anchukaitis 2014) in the central Sierra Nevada mountain range in complex terrain covered by mixed conifer forests (shown in Appendix S1: Fig. S1), which generates complex fuel beds shaped by drought, land management practices (e.g., forest cultivation and harvesting, fire suppression, and fuel mitigation), and burn scars from numerous prior fires. The King fire grew 7 km to the northeast through the evening of 16 September as nearby surface weather stations recorded weak-to-moderate south-southwesterly winds (Fig. 1a) upon which weak diurnal circulations (e.g., 0–3 m/s at Bald Mountain) and gusts of 2–10 m/s were superimposed (Fig. 1b). From 21:49 on 16 September, when the fire was mapped by the National Infrared Operations (NIROPs) airborne imager, until 13:06 on 17 September, when satellite active fire detection data from the Visible and Infrared Imaging Radiometer Suite (VIIRS; Schroeder et al. 2014) detected the fire entering the Rubicon Canyon, the fire traveled north over rolling hills. In an afternoon run that was unanticipated in light of weak-to-moderate ambient winds, the fire grew over 16,200 ha

(40,000 acres), racing approximately 25 km to the northeast over the next 11 h, an average spread rate of 2.3 km/h, following the canyon to its crest at Hell Hole Reservoir, where growth stalled. Operational fire behavior models largely failed to capture this run, instead predicting slower expansion similar to previous days (J. A. Fites-Kaufman, *personal observations*). Beginning at 16:00 on 17 September, humidity increased and area winds weakened and changed to easterlies, redirecting and slowing growth (Fig. 1c). Progression was mapped nightly by NIROPs (Fig. 1d) and twice daily (early afternoon and midnight) by VIIRS. The fire was contained at 39,545 ha (97,717 acres) on 10 October.

Based on how the fire environment (fuel properties and moisture content, terrain slope, and weather, notably wind) affects fire behavior, primary factors that could have shaped this event are winds, which may have included fire-induced winds; the Rubicon Canyon's inclined, concave shape; and fuel properties including amount, vegetation type and structure, and fuel moisture content. Appendix S1 reviews key dependencies. In summary, (1) fire spread rate is only weakly

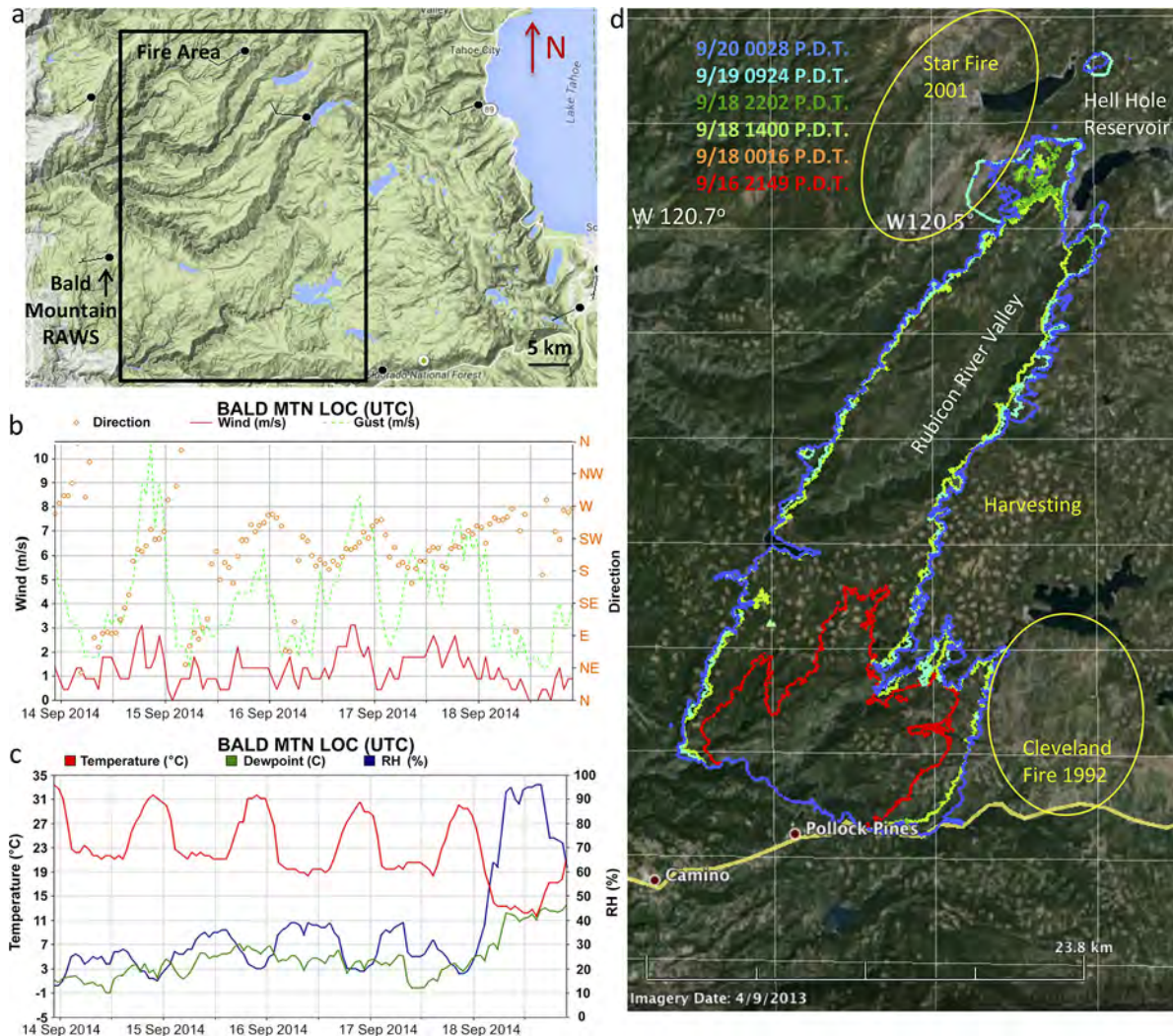


FIG. 1. Overview of the King Fire (California, USA) environment and progression. (a) Weather station wind data near the King Fire at 14:00 17 September. The boxed area is shown in (d). (b) Winds at Bald Mountain weather station. Wind directions are N, north; NW, northwest; W, west; SW, southwest; S, south; SE, southeast; E, east; NE, northeast. (c) Temperature and humidity at the Bald Mountain weather station. (d) NIROPs airborne fire mapping data collected during periods 1 and 2. Yellow annotations indicate disturbance areas.

ATTACHMENT D

influenced by fuel load, (2) spread rate is directly influenced by the dead fuel moisture content, which responds rapidly to weather changes, rather than the fuel moisture content of live canopy fuels, which reflects longer term conditions such as drought, and (3) spread rate is indirectly sensitive to conditions that cause faster heat release on inclined terrain through production of an along-slope component of fire-induced winds.

MATERIALS AND METHODS

Model description

The CAWFE modeling system (derived from coupled atmosphere–wildland–fire environment) integrates a numerical weather prediction (NWP) model (Clark and Hall 1991, Clark et al. 1996, 1997) designed for simulations in complex terrain with a wildland fire behavior module (Clark et al. 2004, Coen 2005, 2013). Fig. 2 shows a schematic of the system. Gridded atmospheric states from model analyses (distributed by the National Oceanic and Atmospheric Administration) are used to initialize and update the boundary conditions of the outermost of several interactive, nested modeling domains (analyses *available online*).⁵ Regional weather is simulated at horizontal grid spacing of tens of kilometers while horizontal and vertical grid refinement allows simulations to telescope into tens to hundreds of meters near the fire.

CAWFE operates at resolutions that are extremely fine for weather models yet too coarse to resolve combustion. Instead, the fire module parameterizes fire processes with semiempirical relationships. A semiempirical spread rate formula (Rothermel 1972) is used to parameterize surface fire spread in terms of terrain, fuel properties, and wind at the fire line, although in CAWFE, the latter includes fire-induced winds. Another relationship (Albini 1994) estimates the rate at which fuels of various sizes are consumed once passed by the flaming front. The model calculates the sensible (thermal) and latent (water vapor) heat releases and the smoke particulate release via an emission factor. The surface fire heats and dries the tree canopy, if present. If the remaining heat flux exceeds a threshold (Van Wagner 1977), a crown fire is ignited and travels through the canopy at a semiempirically determined rate (Rothermel 1991), consumes the tree biomass, and releases more sensible and latent heat. A simple radiation treatment distributes sensible and latent heat fluxes and particulates from the fire into the lower atmosphere. The NWP model and fire module are coupled such that heat and water vapor fluxes from the fire alter the atmospheric state, notably producing fire winds, and the evolving atmospheric state affects fire behavior.

CAWFE's fire behavior module is similar to the standard fire behavior models used as operational tools. However, key differences are that CAWFE simulates three-dimensional airflow at fine resolution (hundreds of meters) as it varies in time and space over the fire, capturing intricate mountain airflows, whereas standard fire models project fire extent by ingesting weather data (either a single time or a time series) from a single weather station that may be kilometers from the

fire or, more recently, a coarse surface weather-gridded forecast product. In addition, CAWFE is a dynamic modeling system that allows two-way feedback between the weather and the fire, allowing the heat released by the fire to alter the atmospheric state, which, in turn, directs the fire. These “fire-induced winds” (discussed in Appendix S1: Section “Winds”) may greatly exceed background winds. CAWFE has been applied to wildland fires that span a wide range of terrain, weather, and fuel conditions (e.g., a windstorm in the Colorado Front Range [Coen and Schroeder 2015], solar heating-driven mountain valley circulations [Coen 2005], a southern California Santa Ana [Coen and Riggan 2014], and a thunderstorm gust front in the desert southwest [Coen and Schroeder 2017]). The weather model has been applied and validated over 30 yr to simulate many meteorological phenomena, including precipitation formation, terrain-induced turbulence, and windstorms. CAWFE simulations of over 15 fire events have been tested against in situ measurements and incident team maps, fires mapped by airborne infrared instruments, and VIIRS satellite active fire detection data (Coen and Schroeder 2013, 2015, 2017, Coen and Riggan 2014).

Experimental design

The objectives of the study were to reproduce the unfolding of the King megafire and then analyze sensitivity experiments to disentangle how factors contributed to its exceptional and unanticipated behavior. The factors include terrain-shaped airflows, fire-induced winds, drought as it affects fire behavior, fuel accumulation as it affects fuel loads, and forest structure as revealed in a separate study by analyses of airborne remote sensing measurements.

CAWFE was applied to two periods during the King Fire, separated because model error growth precludes a single fine-scale simulation from retaining sufficient skill throughout the entire event. First, a four-nested-domain simulation (finest atmospheric spatial resolution, 370 m; fuel grids, 74.1 m) modeled the period 17:00 16 September to 19:45 18 September, initializing a fire in progress using the 21:49 16 September NIROPs airborne fire mapping data.

In the second period, a five-nested domain simulation (finest atmospheric spatial resolution, 185 m; fuel grids, 37.0 m) spanned 21:00 18 September to 20:51 19 September, during which time the fire was initialized in progress with the 01:03 19 September VIIRS active fire detection data (Schroeder et al. 2014). National Centers for Environmental Prediction (NCEP) Final Operational Global Analysis-gridded atmospheric data were used to initialize the atmospheric state and provide boundary conditions to a Weather Research and Forecasting (WRF) Model (Skamarock et al. 2005) simulation. WRF dynamically downscaled the analyses to provide initial conditions and hourly lateral boundary gradients of atmospheric state variables for the outermost domain (10-km horizontal grid resolution) of CAWFE simulations. Inner CAWFE domains were refined to 3.33, 1.11, 0.370, and (for period 2) 0.185 km. Simulations ingested fuel data categorized into fuel models, a stylized categorical classification of fuel type, amount, and physical arrangement, using the 13-category Albini (1976) classification system as restated by Anderson (1982). Based on weather station data, dead fuel moisture content was set 5% and 12% for periods 1 and 2,

⁵ <http://nomads.ncdc.noaa.gov>

ATTACHMENT D

1569

CAWFE® Modeling System

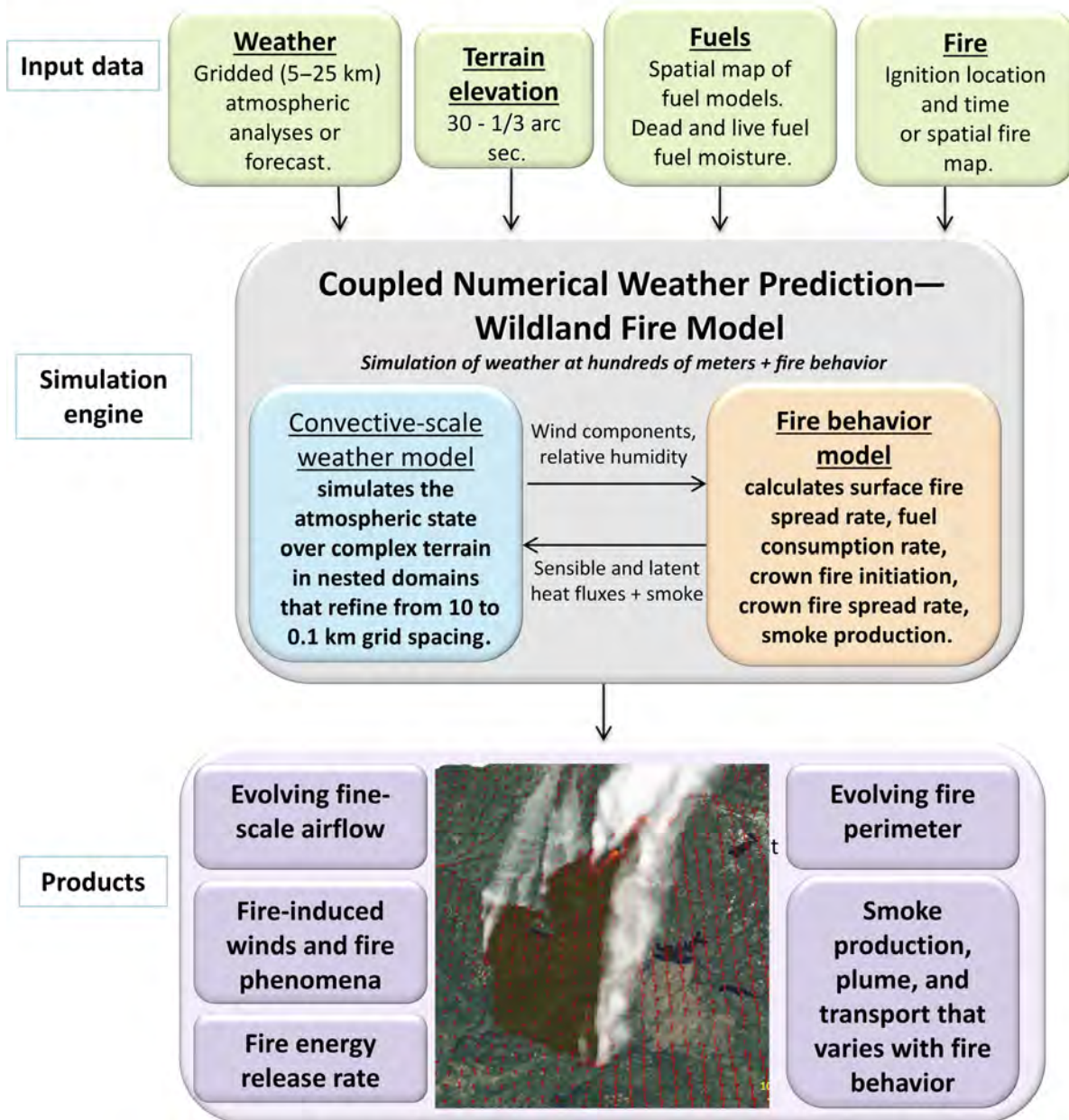


FIG. 2. Overview of the CAWFE modeling system.

respectively, each experiencing a diurnal increase and decrease of 1% (data available online).⁶ Sensitivity experiments to test the effect of drought during period 1 varied the dead fuel moisture content (DFMC) from the measured 5% to its historical low (3%) and high (8%) and the live fuel moisture content (LFMC) from 120% in the control experiment to 90% and 150%, values that bracket the natural range from extreme drought to spring moisture values. Experiments to test the effect of fuel accumulation simultaneously halved the fuel load and depth, thus keeping the packing ratio constant, to represent preaccumulation surface fuel load. Other tests

varied the canopy fuel load from the control experiment value of 1.11 to 3.33 kg/m². This was the most direct approach to test fuel accumulation; other effects on forest structure such as the accumulation of ladder fuels may also have occurred but are much more difficult to credibly implement and test.

Fuel data

Fuel models establish properties needed for the fire module algorithms including fuel load, fuel bed depth, surface area to volume ratio, and moisture of extinction. Two sources provided data mapping how fuel models varied in space. The

⁶<http://mesowest.utah.edu>

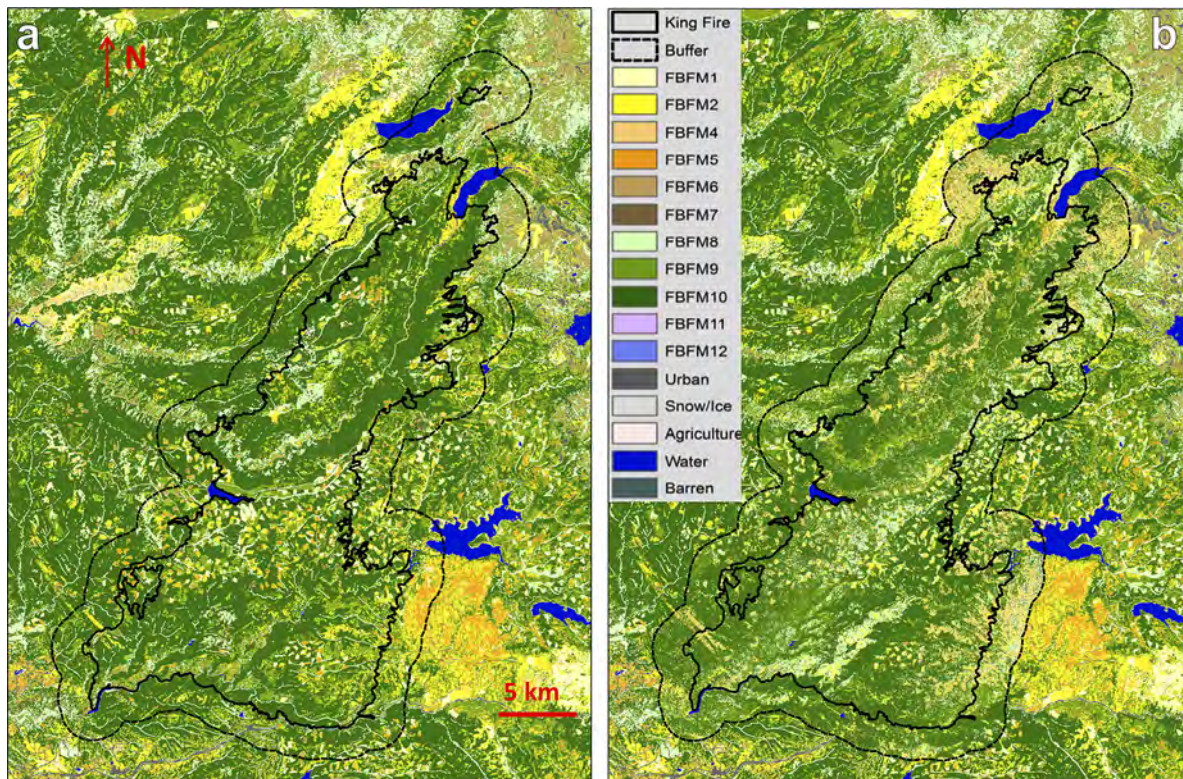


FIG. 3. Spatial variability in fuel models from LANDFIRE and remote sensing data. Fuel models classified according to the Anderson 13-category Fire Behavior Fuel Models (FBFM) system (Anderson 1982; FBFM1-FBFM3 are types of grasses, FBFM4-FBFM7 are shrubs, FBFM8-FBFM10 are forest litter from light to heavy, and FBFM11-FBFM13 are slash piles) from (a) LANDFIRE and (b) MapFUELS data (both reproduced from Stavros et al. (2018)). The heavy solid line indicates the King fire outline, and the thin black line indicates the area over which the analysis for defining MapFUELS fuel models was performed.

control experiment used 2012 fuel model data from the Landscape Fire and Resource Management Planning Tools Project (LANDFIRE) database available from the U.S. Department of Agriculture Forest Service and U.S. Department of Interior (Fig. 3a; data *available online*).⁷ An alternative method (Stavros et al. 2018) called MapFUELS established maps of these fuel models using only remote sensing observations from the Airborne Visible Infrared Imaging Spectrometer (AVIRIS) to create a dominant vegetation map and clusters of structural metrics (Fig. 3b) from the Airborne Snow Observatory (ASO) light detection and ranging (LiDAR; Painter et al. 2016). MapFUELS data were derived from pre- and postfire airborne data (Stavros et al. 2016) and evaluated against forest inventory analysis field data. That analysis covered actual fire area plus a 2-km buffer. Differences were most apparent in areas varying from a natural state such as in dense plantation, harvested and replanted areas, and areas in transition such as the 1992 Cleveland burn scar in the southeast and the 2001 Star Fire west of Hell Hole Reservoir (Fig. 4). For both sources, data were resampled to model fuel cells (5×5 cells are within each atmospheric grid cell) using nearest-neighbor resampling. Standard fuel loads and other properties from (Anderson 1982) were used. In simulations using data from both sources, where a forest fuel type was indicated, the canopy fuel load uses the control experiment value of 1.11 kg/m^2 .

⁷ <http://www.landfire.gov>

RESULTS

Fire progression

We simulated two periods during the King Fire with the CAWFE coupled weather-wildland-fire model. Period 1 spanned 17:00 16 September to 19:45 18 September. During this time, the CAWFE simulation reproduced notable features of the fire event (Appendix S1: Video S1). These included weak-to-moderate southerly winds (Fig. 4a), multiple heading regions along the fire front (Appendix S1: Fig. S2), each pulling a section of the fire up a draw through fire-induced winds and creating a distinct smoke plume, the fire entering the Rubicon Canyon at approximately 13:00 (Fig. 4b), and the fire's 25 km run up canyon on the afternoon of 17 September (Fig. 4c) to Hell Hole Reservoir where growth diminished due to reaching the canyon's top, rockier terrain, and weaker ambient winds (Fig. 4d). VIIRS data (Fig. 5a) supported this sequence of events but indicated the flanks' simulated lateral growth was overestimated (Fig. 5b). This variance from actual outcomes may have occurred because the model neglected fire suppression, which was heavily applied to the western flank south of the Rubicon Canyon, because of deficiencies in identifying forest structure in prior disturbances (later discussed in *Sensitivity to spatial distribution of fuel models*), and inherent model error. Within the Rubicon Canyon, a narrow band of wind (Fig. 4b, c) channeled by the upward, concave valley shape contributed to the run. The heat released by the fire

ATTACHMENT D

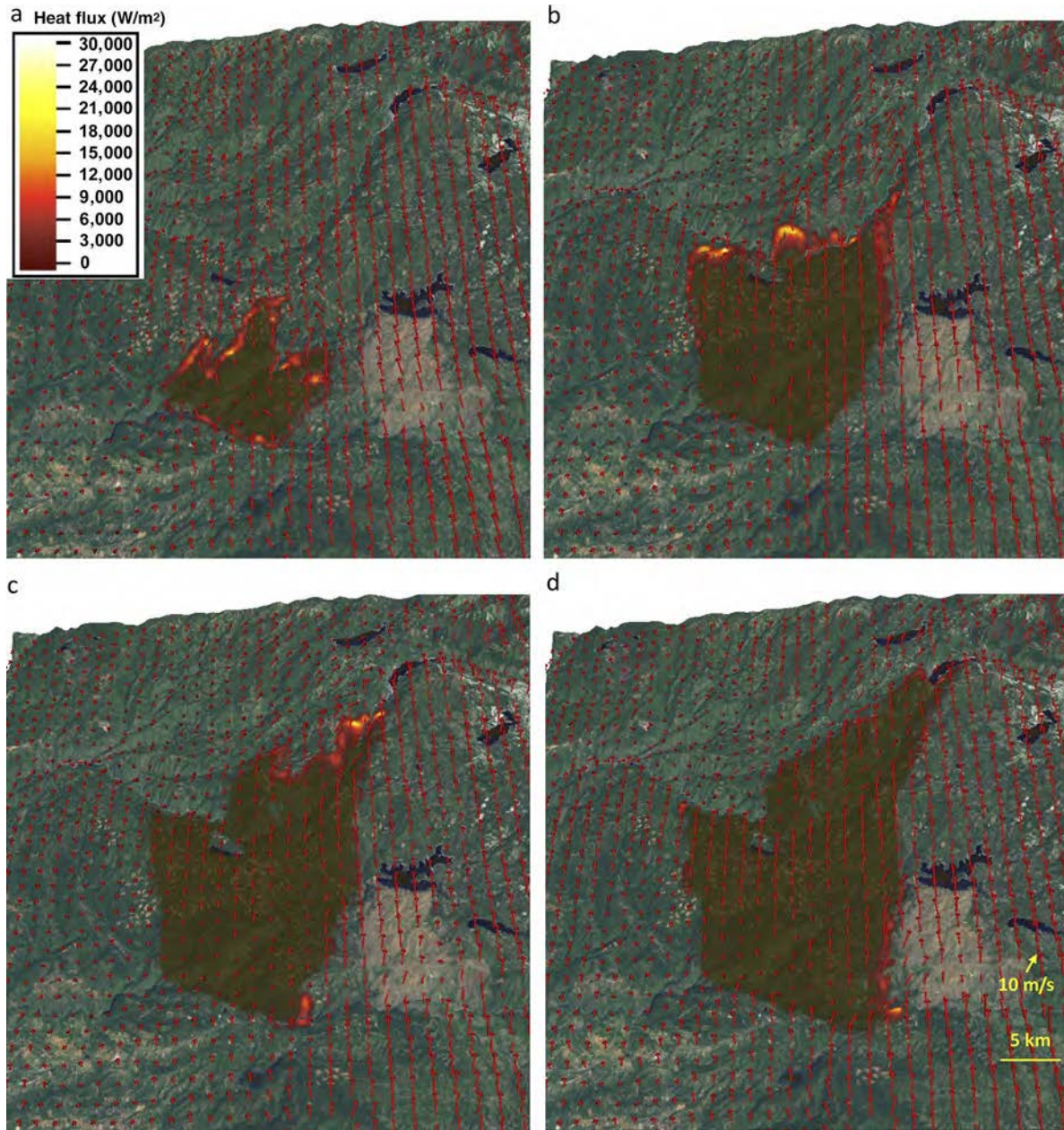


FIG. 4. Snapshots throughout the control simulation of the King Fire. Simulated total heat flux in domain 4 (colored according to key at right) with wind vectors (every fourth grid point) near the surface, at (a) 22:00 on 16 September, (b) 13:00 on 17 September, (c) 18:00 on 17 September, and (d) 23:00 on 17 September.

created a single, strong, downwind-leaning plume that drew air faster over the fire front, further accelerating the fire (later discussed in *Fire-induced winds*).

A pyrocumulus cloud was produced in the simulation for under 1 h at approximately 19:00 on 18 September (Appendix S1: Fig. S3), as the leading edge of the fire was approaching the top of the canyon. It occurred near the base of a moist layer that extended from 3 to 6 km above ground level. The fire plume increased the ambient relative humidity of approximately 60% at that height to saturation, forming trace amounts of cloud and rainwater. As the amount of liquid produced was small and this occurred late in the fire's run, it contributed little to simulated fire growth.

During period 2, from 21:00 on 18 September to 20:51 on 19 September, the fire was less active and spread slowly under moist easterlies. It crept outward along its flanks with active burning at the northern edge toward the west and higher intensity burning within 0.3 to 1 km wide lobes that were aligned with small drainages. These lobes lay under fire-produced convective cells that drew the fire up the drainages, which served as topographic "chimneys." The simulation (Fig. 6a) contained features seen in concurrent high spatial resolution (35-m pixel) thermal infrared data from MASTER (Moderate Resolution Imaging Spectroradiometer [MODIS]/Advanced Spaceborne Thermal Emission and Reflection Radiometer [ASTER] airborne prototype; Hook et al. 2001; Fig. 6b).

ATTACHMENT D

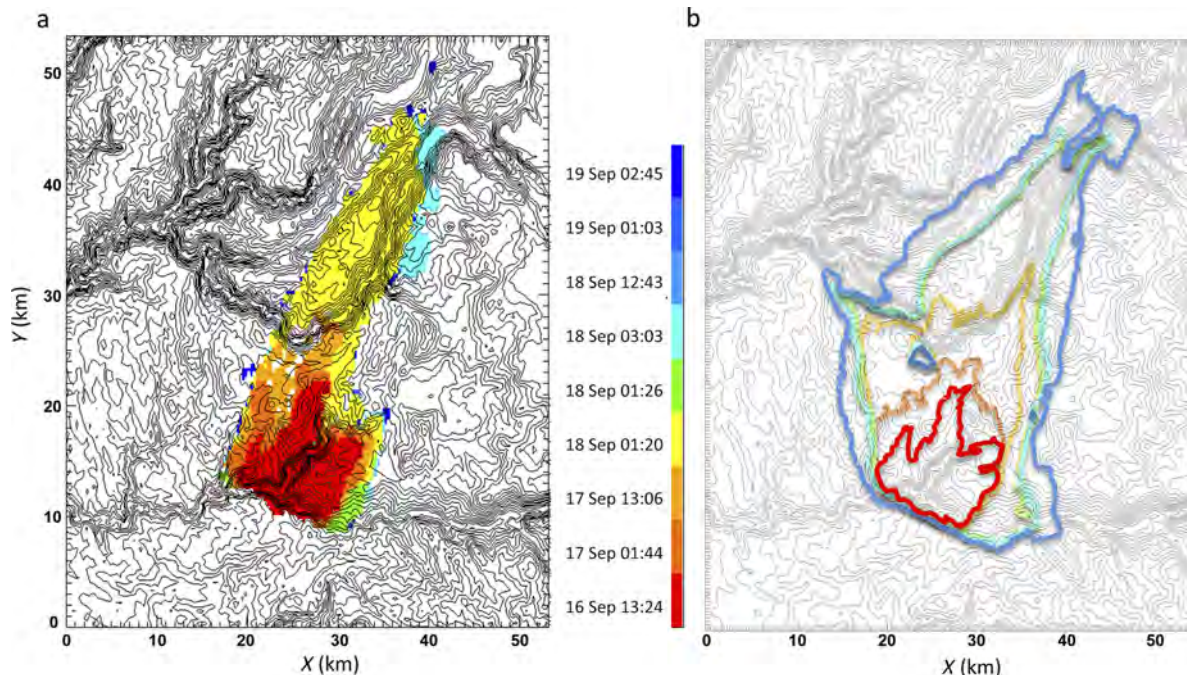


FIG. 5. Observed and simulated fire progression. (a) NIROPs extent used to initialize fire in progress (red) (21:49 on 16 September) and later VIIRS fire detections through 02:45 on 19 September. NIROPs data are distributed by the National Interagency Fire Center (<https://ftp.nifc.gov>). (b) Simulated fire extents at VIIRS detection times to 12:43 on 18 September, plotted with corresponding colors. Historical active fire detection data are distributed by the USDA Forest Service Active Fire Mapping Program (<https://fsapps.nwcg.gov/afm/>).

Fire-induced winds

Fire-induced winds were calculated using the difference between the west-east, south-north, and vertical wind components in the control simulation and corresponding fields in a simulation without a fire. At 22:00 on 16 September, as the fire drew itself up drainages in the rolling hills south of the Rubicon Canyon, the horizontal component of the fire-induced winds was 0–11.1 m/s, (Fig. 7a) on the order of the ambient winds, and the impact on the vertical wind component was –3.4 to 8.7 m/s (Fig. 7b). These perturbations appear as individual updraft plumes along the fire line, compensating downdrafts and inflow into the plumes, and outflow accelerated downwind to the north-northeast. Fire-induced winds were arranged differently at 16:20 on 17 September as the fire raced up canyon, when the horizontal winds in the fire's leading edges, those driving it up canyon, reached 12–13.7 m/s (Fig. 7c) and fire-induced vertical winds, located primarily in the plume leading the fire, ranged from –5.1 to 14.5 m/s (Fig. 7d), both exceeding ambient winds.

Sensitivity to drought

The control simulation used the 10 h DFMC at the Bald Mountain Remote Automated Weather Station (RAWS), which was measured at its historical average of 5% during the fire, similar to other nearby stations. The 10 h DFMC reflected the response of smaller fuel elements that spread a fire front to varying weather. Concurrently, exceptionally low moisture content was measured in larger dead fuel elements that respond over longer timescales that reflect the drought but these do not influence spread rate. Sensitivity experiments

varied the DFMC using the historical low and high extremes of 3% and 8%, respectively. Fires in all three simulations traveled rolling hills to reach the Rubicon Canyon in the early morning of 18 September. The simulated fire for the observed DFMC arrived in 12 h at 17:00, while simulations with historical high (low) DFMC experiments arrived at the same time (1 h earlier), respectively (Fig. 8). Both the control and historical high DFMC simulations took 6.3 h to cross the Rubicon Canyon and begin their runs, while the historically low DFMC simulation crossed and began to climb at once. After each simulated fire began to climb, the race up canyon of experiments with 8%, 5%, and 3% DFMC took 16.7, 15.0, and 11.7 h, respectively. Faster moving simulated fires reached waypoints sooner but did not lead to a larger ultimate fire extent, the growth of which was restricted by rocky terrain at the top and slowed by deteriorating weather conditions as winds changed direction and weakened, humidity increased, and rain occurred over the area.

LFMC had the potential to influence fire behavior. Energy rising from a surface fire is used to heat and dry the canopy, and if the remaining energy flux exceeds a threshold, the canopy ignited. Thus, the barrier to igniting canopies with higher LFMC is higher. Contrarily, once ignited, the latent heat flux is higher, per kilogram fuel consumed, for higher LFMC, as water vapor contributes to the air's buoyancy, fueling stronger fire-induced winds, although the canopy fuel consumed may be lower. The difference in evolving fire extent or rate of spread, as expressed through CAWFE simulations, between experiments with LFMC of 90%, 120%, and 150%, effectively the natural range of values, was negligible (not shown). Differences in fire effects such as burn severity were not tested.

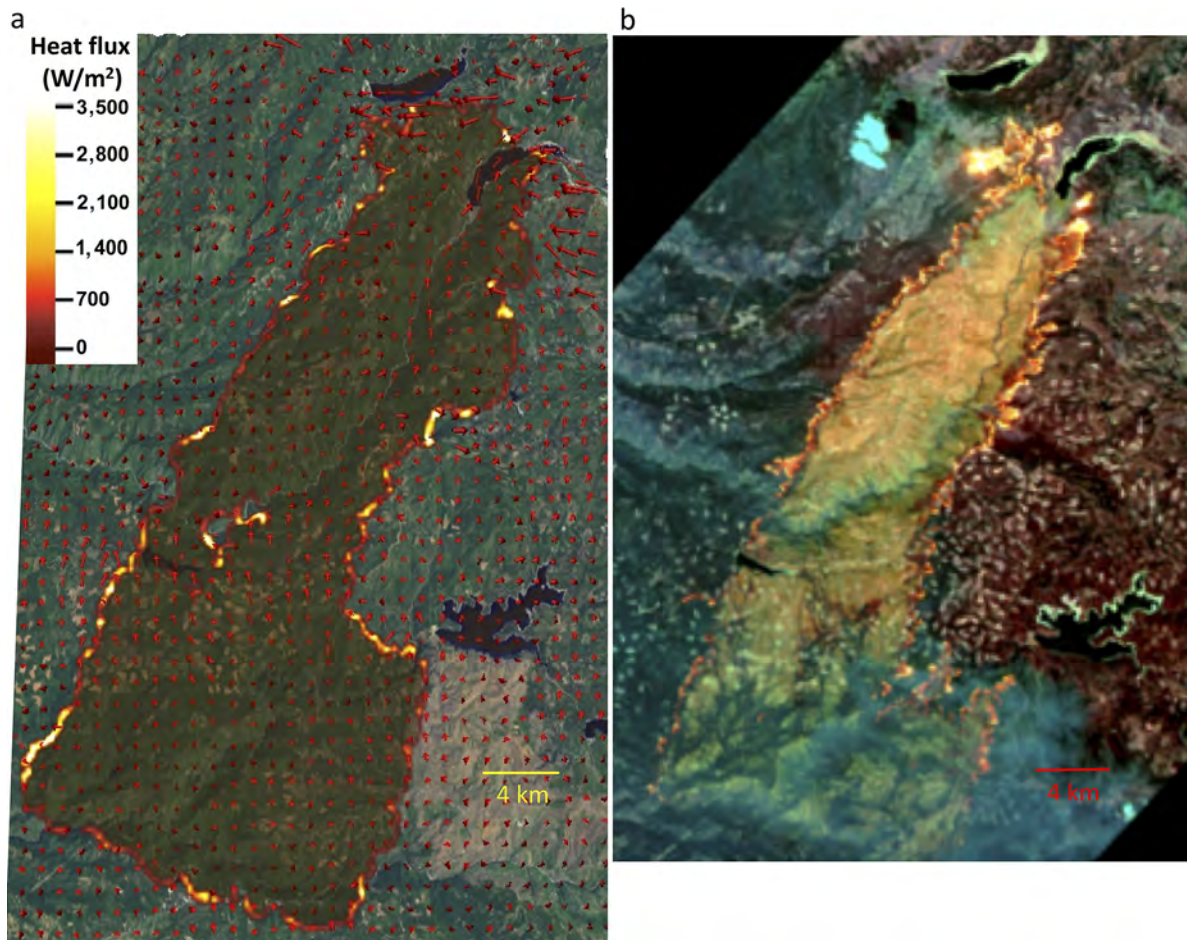


FIG. 6. Simulation and MASTER imagery of King Fire at 12:00 on 19 September. (a) Model simulation of King Fire at 12:00 on 19 September using LANDFIRE fuels at the time of (b) MODIS-ASTER (MASTER) airborne infrared imagery of the King Fire. Reproduced from Lee et al. (2015).

Sensitivity to fuel accumulation

We tested the effect of surface fuel accumulation due to fire suppression by comparing a simulation with standard conditions (the control) to a simulation with one-half the surface fuel load in one-half the depth (thereby keeping the packing ratio constant) to approximate fuels before accumulation. Increased fuel during the early growth period on rolling terrain extended the fire perimeter by up to 3 km. Fuel accumulation had much greater impact on inclined terrain, increasing fire extent by 16 km during the up-canyon run (Fig. 9), but although it accelerated fire spread, ultimately did not increase the final extent due to the topographic and weather constraints.

Unlike surface fuel load, which is input into the spread rate formula, the canopy fuel load does not directly affect the spread rate. However, the sensible and latent heat released by its consumption contribute to vertical motion as, when climbing sloped terrain, a component of the fire plume updraft lies along the surface in the direction of fire propagation; that is, the canopy fuel load can impact fire spread rate through fire-induced winds. Consistent with this rationale, increasing the canopy fuel load by a factor of three had little effect on early growth over rolling hills before reaching the Rubicon Canyon,

but had more effect later on growth up the canyon, increasing fire extent by 12 km over the control by 24 h (Fig. 10). Again, this ultimately did not lead to a greater fire extent.

Sensitivity to spatial distribution of fuel models

To evaluate the effect of limitations with spatial maps of fuel models, we compared periods 1 and 2 of the control simulation, which used fuel models classified into the Anderson (1982) 13 fuel models from the fire management standard LANDFIRE database, against simulations using a fuel model map also classified into the Anderson 13 fuel models that was developed from a technique called MapFUELS (Stavros et al. 2018), which employs only remote sensing observations. Applied to the King Fire data set, MapFUELS fuel maps varied from LANDFIRE most clearly in areas with harvesting and replanting, recovering burn scars, or dense plantation (Fig. 3). CAWFE simulations using MapFUELS data experienced different fire behavior producing a narrower fire by correctly not spreading through harvested patches or into the Cleveland Fire scar, the successional recovery of which appears faster than indicated in LANDFIRE, and better predicting the fire's passage north to the Rubicon Canyon through harvested areas (Fig. 11). However, the MapFUELS simulation

ATTACHMENT D

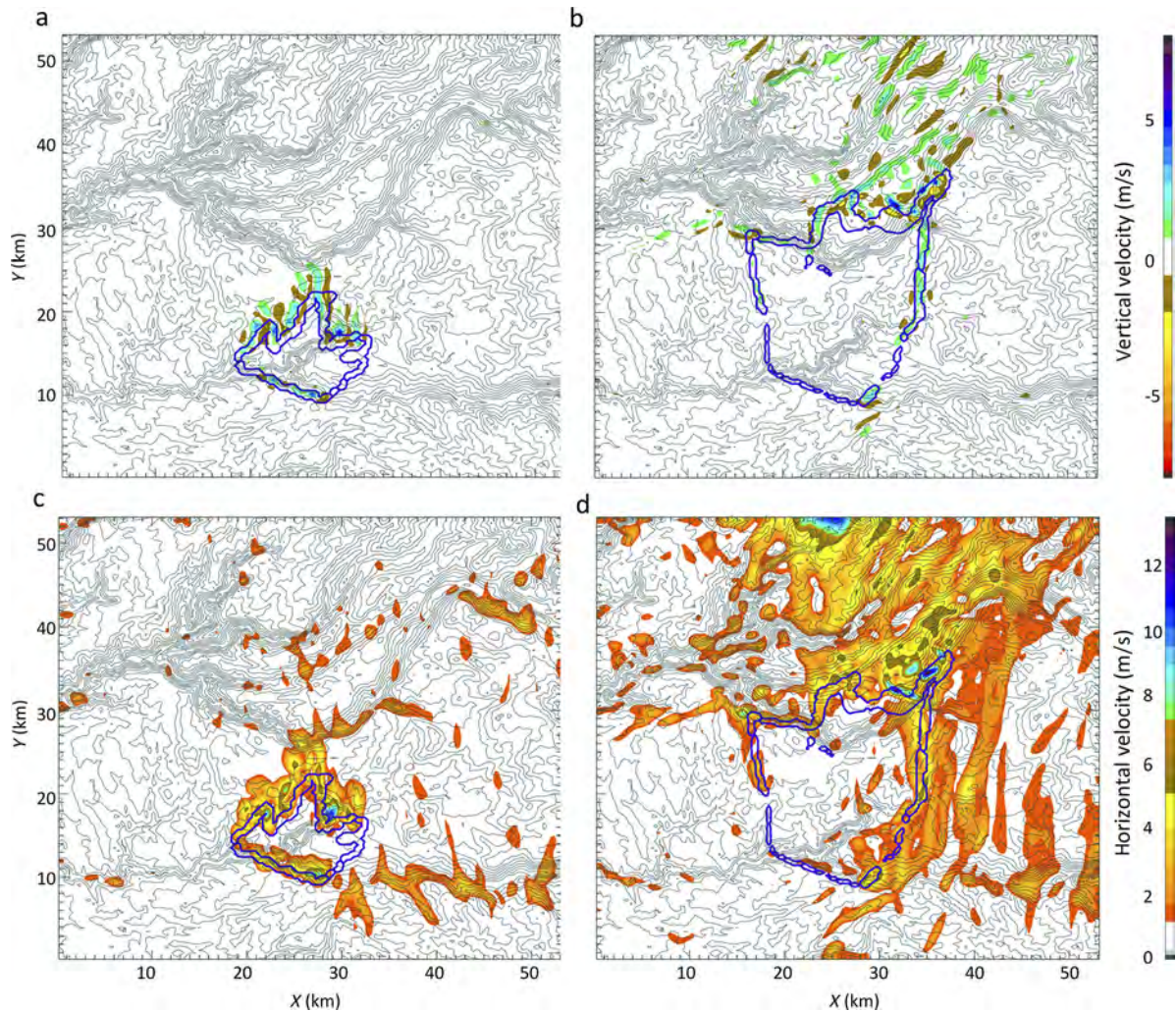


FIG. 7. Fire-induced winds. Fire-induced vertical (a, b) and horizontal (c, d) winds in m/s at 22:00 on 16 September (a, c) and 16:40 on 17 September (b, d).

produced too slow a run up the Rubicon Canyon and slightly exaggerated fire spread into the 2001 Star Fire scar, erroneously extending the fire by an additional 1–2 km. (Fig. 12).

Burn severity

Burn severity is distinct from instantaneous fire intensity (Keeley 2009) and is broadly defined as the degree to which fire has affected a site, a combined effect of fire intensity and residence time. Different severity metrics exist and depend on the medium being affected, for example, tree and shrub mortality, organic matter loss, or soil hydrologic impacts. The postfire Rapid Assessment of Vegetation Condition (RAVG) Composite Burn Index (CBI) severity assessment (distributed by the USDA Forest Service) represents the magnitude of fire-caused changes to the understory (grass and shrub layers), mid-story, and overstory (data available online).⁸ The RAVG CBI showed that much of the Rubicon Canyon experienced high burn severity (Fig. 13a).

⁸ https://apps.fs.usda.gov/arcx/rest/services/RDW_Wildfire/RAVG_CompositeBurnIndex/MapServer

Because CAWFE simulates a fire's intensity and heat flux to the atmosphere, we used total heat flux released over time at each point (related to the intensity of burning and integrated consumption over the residence time) as a proxy for severity for comparison with CBI. A visual comparison with results using LANDFIRE fuels (Fig. 13b) showed the simulated burn severity using MapFUELS fuels (Fig. 13c) better represented the extent and location of high severity areas.

DISCUSSION

Recent large, high-impact fires around the world have stimulated discussions that fire behavior has entered a new regime. Changing climate conditions that may create long-term drought and land management policies that emphasize fire exclusion leading to fuel accumulation are frequently cited as causes of large, severe fires. This is an intuitively obvious conclusion that is apparently supported by statistical studies that interpret correlations between atmospheric state variables or live fuel moistures and regional or national area burned as evidence of a causal relationship that can be repurposed to explain individual megafires. However, our work

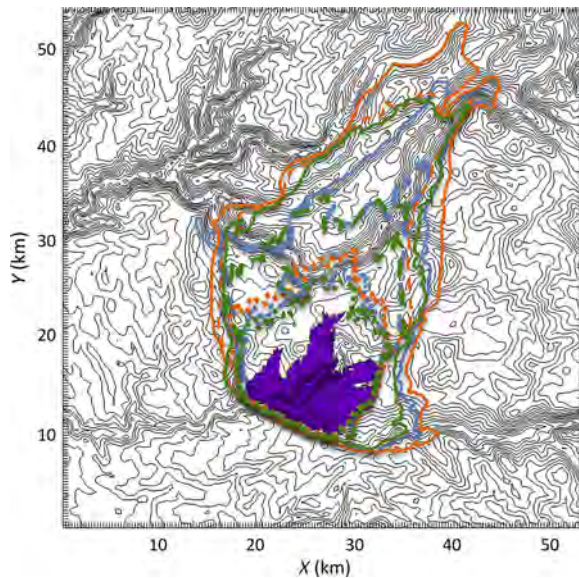


FIG. 8. Effect of dead fuel moisture content on fire evolution. The simulated evolution of fires with historical high (8%; green), low (3%; orange), and measured (5%; blue) dead fuel moisture content at 12 h (dotted line), 24 h (dashed line), and 36 h (solid line). The fire perimeter detected by NIROPs (purple) was introduced at 21:49 on 16 September.

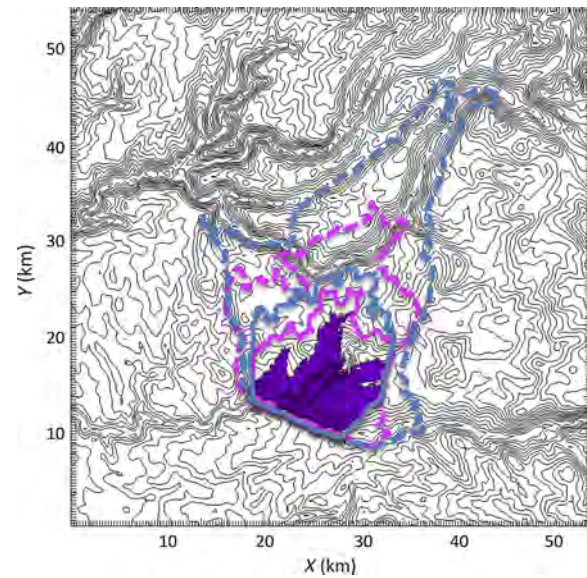


FIG. 9. Effect of surface fuel amount on fire evolution. The simulated evolution of fires with current surface fuel load and depth (blue) and with one-half the load and one-half the depth (pink), representative of conditions before fuel accumulation due to fire suppression, at 12 h (solid line) and 36 h (dashed line) into the simulation. The fire perimeter detected by NIROPs (purple) was introduced at 21:49 on 16 September.

suggests that the issue of what causes megafires and how future conditions will shape their frequency is not settled and should be critically re-examined from other perspectives.

Taking a different approach—that of a process study—this work used a physically based coupled NWP–wildland fire behavior model to reveal and examine the key processes underpinning the rapid growth and ultimate size of a specific megafire, the 2014 King Fire. More broadly, this study drew from fire behavior science to show the mechanisms through which both external and internally generated factors, with varying relative degrees of importance, drive any wildfire. Sensitivity experiments quantified how and to what degree drought and fuel accumulation contributed to this fire’s behavior and how sensitive the results were to the type of fuel by using fuel maps derived solely from a unique set of remote sensing data, which, if applied in other settings, offer the potential to better monitor vegetation structure and composition.

We found that the CAWFE coupled weather–wildland–fire model reproduced the expanding fire extent and features documented by airborne and satellite observations, including an afternoon run during which the fire grew over 16,200 ha (40,000 acres) and other distinctive features. Results showed that the King Fire’s growth primarily resulted from submesoscale winds within the Rubicon Canyon, beneath the resolution of sparse meteorological surface observation networks characteristic of remote areas or standard weather forecast models, and fire-induced winds that were on the order of or greater than ambient winds and enhanced by the convex canyon’s upward tilt. While the fine-scale winds and fire-induced circulations were not detectable in widely spaced weather station data, the data used by macroscale statistical studies, nor were they captured in current operational fire growth tools that underestimated the growth, both were captured by CAWFE. Thus,

while this megafire’s behavior was not outside current understanding of fire behavior, it required a newer, coupled model to capture fire–atmosphere feedbacks and how the impacts of contributing factors can multiply through dynamic interactions—effects missing from all kinematic operational tools, including the different fire spread models used in the United States, Canada, and Australia. The perceived unpredictability of fires, which may merely reflect the limitations of current models, and notion that fire behavior is entering a new regime may reflect an increasingly dominant role of internal dynamics in driving fire behavior, supporting Alvarado et al.’s (1998) observation that megafires may behave differently than less extreme events.

There are broader implications. Fire behavior modeling is performed not only for fire management but also to support decision-making for preserving ecological resources, managing carbon emissions, establishing policy promoting forest resilience, and protecting endangered species habitat. So, rather than dismissing this underestimate by current operational tools of an extreme event as an anomaly, it is important to recall that the largest 1% of fires account for 80–96% of area burned (Strauss et al. 1989) and a disproportionately large portion of impacts. Understanding the mechanisms and actual contributing factors leading to megafires, and being able to model the full extent of outliers, is vital for shaping policy recommendations aimed at mitigating a disturbance dominated by extreme events.

Additional simulations isolated the contribution from fuel moisture—the primary path through which drought impacts fire behavior—and fuel amount, which is the most direct way to indicate how preventing fuel accumulation might have created a different outcome. We found that varying the surface dead fuel moisture content across its historical range had little impact on the rate of fire progression in the growth

ATTACHMENT D

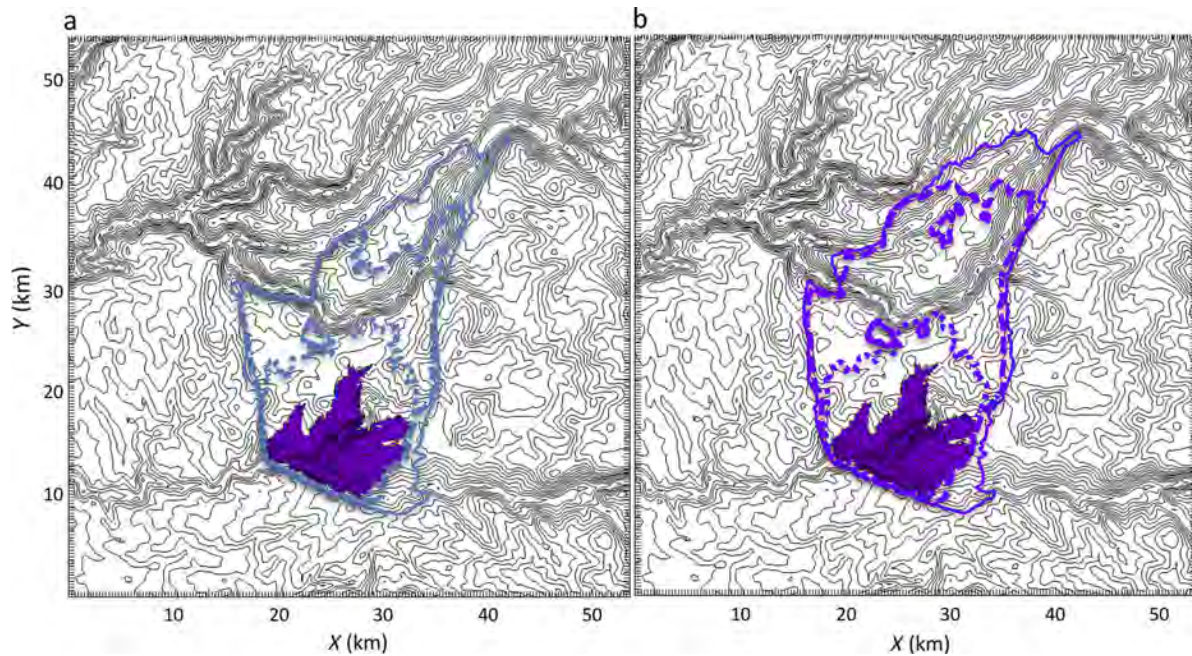


FIG. 10. Effect of canopy fuel load on fire evolution. The simulated evolution of fires with (a) current canopy fuel load and depth (blue) and with (b) three times the canopy fuel load (purple) at 12 h (dotted line), 24 h (dashed line), and 36 h (solid line). The fire perimeter detected by NIROPs (solid purple fill) was introduced at 21:49 on 16 September.

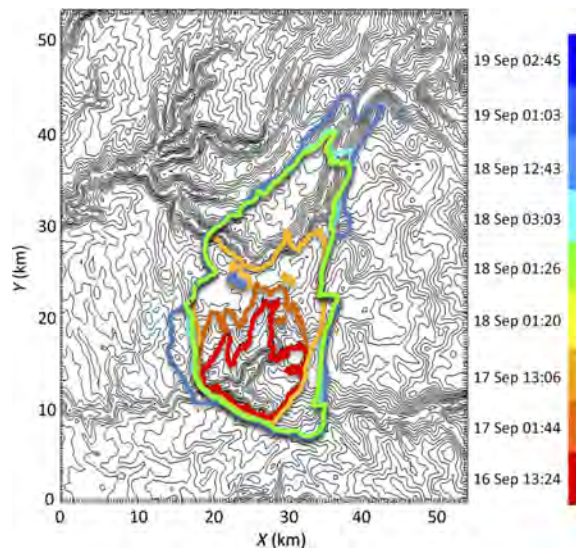


FIG. 11. Simulated fire evolution using remotely sensed fuel data. NIROPs extent used to initialize fire in progress at 21:49 on 16 September and simulated perimeters at later VIIRS fire detection times using MapFUELS-derived fuel type.

toward the Rubicon Canyon, where terrain was essentially flat. And, despite a prolonged drought reflected in live canopy fuel moisture and larger surface fuels, the dead fuel moisture content that impacts spread rate was measured as average from a historical perspective. In addition, it caused little difference, and in the case of live fuel moisture content, effectively no difference, in how fast the fire would have traveled up the Rubicon Canyon compared to historically high

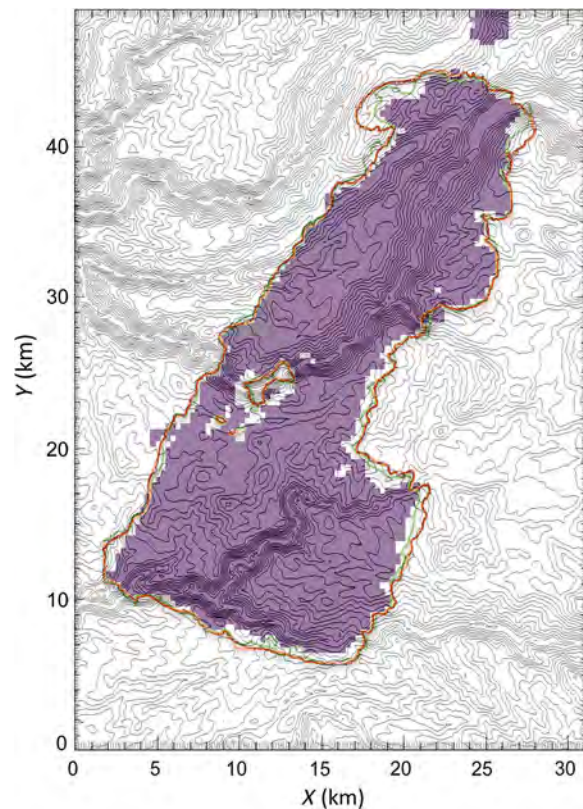


FIG. 12. Simulated fire evolution using two fuel sources and comparison to satellite active fire detection data. The VIIRS active fire map near the end of period 2 (purple), at 14:08 on 19 September. CAWFE simulated extent at the same time using LANDFIRE fuel model data (green) and MapFUELS-derived data (orange).

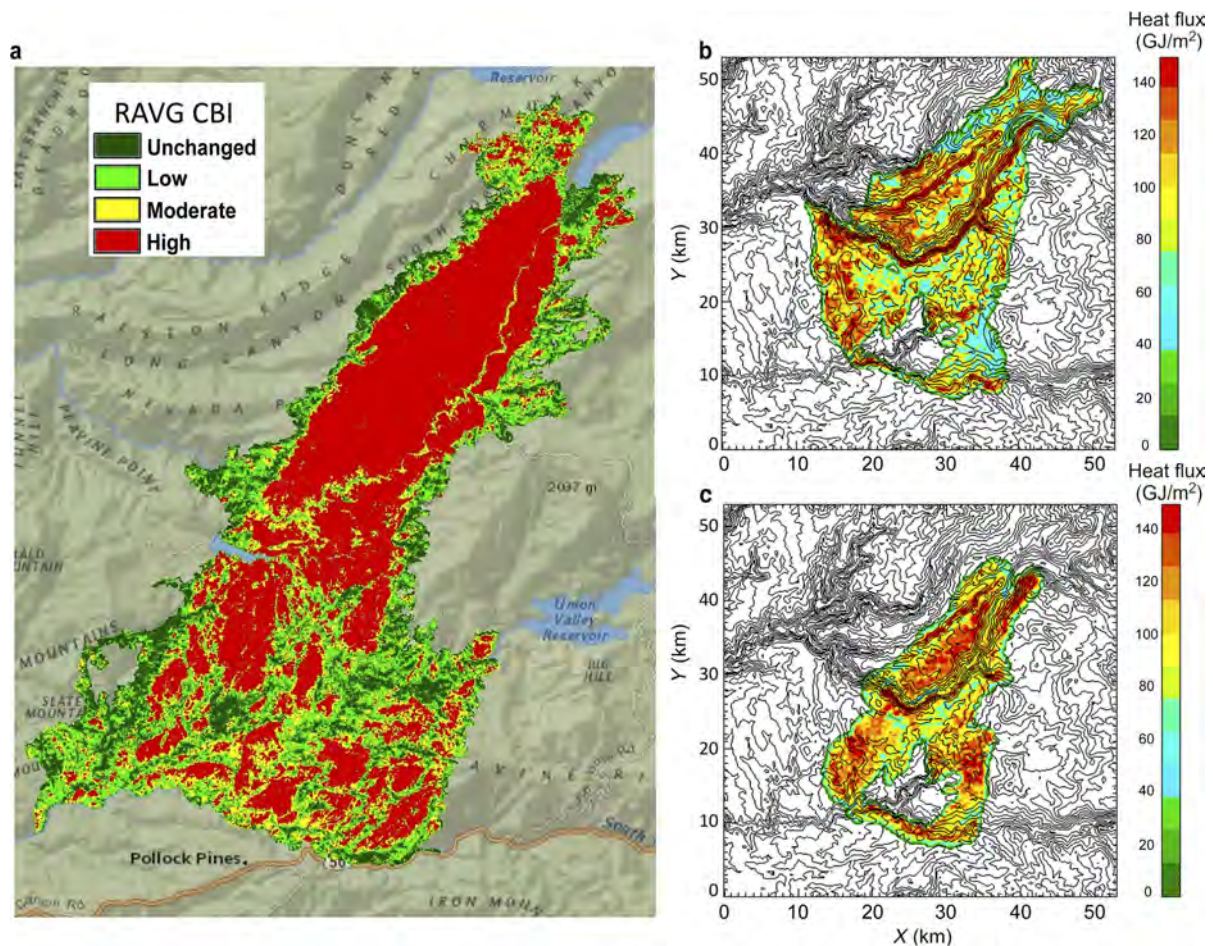


FIG. 13. Observed soil burn severity and simulated severity using fuel data from two sources. (a) Rapid Assessment of Vegetation Condition (RAVG) Composite Burn Index (CBI) severity product from the USDA Forest Service Geospatial Technology and Applications Center. Simulated sensible and latent heat flux summed over time at each point using (b) LANDFIRE and (c) MapFUELS fuel models.

fuel moisture conditions, suggesting drought contributed little to this fire's behavior throughout the event on its own. However, had dead fuel moisture content been at its historical low, the fire would have arrived at the canyon's top 3 h earlier—a change in behavior that could have had implications for suppression activity and personnel safety. Interestingly, although a faster moving simulated fire would have reached waypoints sooner, results suggested it would not have ultimately become a larger fire because growth was slowed by terrain at the canyon's top and constrained by weakening and shifting winds and increasing humidity and rain, a reflection of the complex terrain and episodic nature of weather periods that shape wildfire growth.

Intuitively, it seems that drought should increase fire rate of spread, a belief bolstered by regional or national correlations between drought indices and areas burned and indications of fuel moisture thresholds that trigger fire behavior (Dennison and Moritz 2009), but our outcomes and the limited mechanisms through which drought may influence a fire's spread rate (Appendix S1) show that drought's effect on surface and canopy fuels as represented in landscape-scale fire behavior models is secondary. The effect of drought on fuel moisture, which can have high spatial variability, may instead be more nuanced than directly

influencing the rate of spread. For example, drought may sustain more ignitions or may assure the spatial continuity of sufficiently dry fuels to maintain fire spread across the landscape (M. Gill, *public communication*) and dehydrate fuel on sheltered, moister facets of terrain (Bradstock 2010).

The impact of fuel accumulation was also modulated by topography. Specifically, less fuel accumulation would have had little impact on the rate at which the King Fire spread across rolling terrain toward the Rubicon Canyon but would have slowed fire spread up the canyon. The fire would have consumed less fuel, produced lower heat fluxes and weaker updrafts, and thus caused weaker fire-induced winds. Likewise, experiments with greater canopy fuel load, which solely impact fire spread indirectly through additional heat fluxes that generate stronger fire-induced winds, increased fire spread rate only on inclined terrain. Because increased fuel amounts only accelerated the fire when climbing sloped terrain, fuel reduction efforts aimed at reducing some metrics of fire behavior could be focused on inclined terrain for maximum impact on fire behavior. This work complements studies (LaCroix et al. 2006, Finney 2007, Syphard et al. 2011, Dicus and Osborne 2015) that indicate how treatment patterns may be optimized at the landscape scale to obstruct wildfire growth. However, those conclusions should be re-examined

ATTACHMENT D

with very-high-resolution coupled weather–fire models such as CAWFE that capture the fine-scale weather and fire-induced winds that can dominate extreme behavior and create outlier events that cause disproportionate impact.

This work found that both drought and fuel accumulation's impacts on the King Fire occurred primarily when the fire was burning in inclined terrain, where fuel amount and moisture dynamically compounded each other through the medium of fire-induced winds. That fire growth frequently occurs in complex terrain suggests this reinforcement effect on fire behavior by terrain could be widespread, and because of the implications, warrants further study and highlights the need to investigate climate and fuel impacts on fire behavior and effects jointly. In investigating a specific case, this work supports findings from statistical regression models relating climate factors to wildfire, for example, (Riley et al. 2013), that emphasize short-term indicators of drought (the rapidly responding dead fuel moisture content) more than long-term factors (such as live fuel moisture content). Simulations support studies that show short-term fire weather to be a significant predictor (Barbero et al. 2014), as weather windows enable and curtail fire growth. This suggests the cautionary point that in some conditions, for example, when a fire's expansion is limited by topography or the duration of a weather window favorable for growth, as in the King Fire, conditions can create instantaneously rapid spread rates and affect when a fire reaches its ultimate extent yet not have an opportunity to create a bigger fire.

We found that dead fuel moisture was a less significant factor in this case than winds and fire-induced winds, reinforcing previous conclusions (Coen and Schroeder 2015), that the degree to which changing fuel properties (either amount or dead fuel moisture) affect fire behavior is secondary to the spread rate's sensitivity to winds, when winds are significant. We suggest caution in interpreting studies that use statistical regression on variables such as wind measured at surface weather stations as this may misinterpret fire weather influence. This is because significant contributions come from wind patterns that occur at spatial scales finer than resolved by station data and from fire-induced winds, neither of which are reflected in meteorological data. However, these results do not contradict the macroscale statistical correlations between burned area and climate factors such as drought, because the macroscale correlations represent how these locally heterogeneous climate impacts would appear when summed over all fires over large areas.

In totality, this work—event simulations, sensitivity experiments, and synthesis of fire behavior studies—indicates that the events distinguishing the King fire in particular, and perhaps other megafires more generally, can be interpreted as arising through self-reinforcing, internal system dynamics (e.g., fire-generated winds) rather than from the direct effect imposed by individual external factors (e.g., drought, fuel accumulation, ambient wind). In both interpretations, the factors, various measures of fuel moisture and amount, wind, etc., affect the fire to varying degrees through their individual direct impacts on fire behavior. However, the escalation to another level of intensity, becoming a megafire, is possible in fires where factors fortuitously align and their effects amplify one another, manifesting as and feeding back on each other through dynamic effects such as fire-induced winds and

airflow acceleration from topographic channeling or thermodynamics. But importantly, this interpretation allows that extreme behavior/high-impact fires need not arise from an extreme fire environment condition (either winds or fuels), as in the King fire, no individual environmental factor foretold megafire behavior. Further, varying individual fire behavior input parameters across their observed natural range did not make or break the megafire. This finding contradicts a widespread belief within the forestry community, partially generated by longtime use of kinematic fire spread models that omit dynamic feedbacks, that the energy needed to drive extreme fires requires exceptional amounts of burnable biomass, amounts exceeding those given by the Albini (1976) and Anderson (1982) surface fuel models and canopy fuel loads used here. In addition, this work casts doubt on the effectiveness of using predicted broad climate variables to explain and predict future megafire occurrence.

Fuel type and structure derived solely from an unprecedented set of airborne remote sensing data provided a more physically based representation of fuel models, and in conjunction with a physically based model, allowed attribution of various aspects of this fire's behavior to specific controls. Since this analysis depended on serendipitous collection of prefire data, this opportunity is not easily repeated, and so provides unique insights. Remote-sensing-derived fuel models generally improved simulations, notably in disturbed areas, which is important because megafires frequently encounter previous burn scars and managed lands that may impede or accelerate fire progression. The remote sensing-based fuels visually improved the simulated spatial distribution of burn severity, supporting studies that assert the importance of forest successional state on fire impacts (Lyons-Tinsley and Peterson 2012). Current analyses are limited to areas mapped by airborne missions and depend on availability of preburn data and resources to collect post-fire observations. Data from similar instrumentation, LiDAR and spectroscopy, on upcoming satellite remote sensing missions may expand the opportunity for such analyses (Dubayah et al. 2014, Jetz et al. 2016).

This approach and the different perspective it provides on the origin of the King megafire, and possibly megafires more generally, suggests several steps as part of a broad-based community path forward. These include broader use of coupled models to investigate fire behavior and revisiting conclusions made based on uncoupled models. A second step is developing widespread and regularly updated remote-sensing-based fuel mapping products, culminating in inclusion in community databases, as in Peterson et al. (2015b). Improved global forest structural, compositional, and moisture data could enable megafire growth and effects to be better predicted in the future. While progress has been made, as noted in Appendix S1, a third need is better understanding of crown fires, notably, collecting large enough samples to make stronger conclusions about how fuel properties and condition affect crown fire initiation, growth, and fire effects and continuing progress toward mapping canopy fuel moisture accurately with remote sensing data. Further pre-, during, and post-megafire observations, including unsaturated thermal infrared airborne observations, and coupled modeling studies are needed to better understand the internal dynamics of these events and their effects. Fourth, studies

on the potential for future megafires in particular should perhaps be focused on the degree to which weather will be more episodic and have more frequent or longer multiday fire weather periods and how this coincides with changing ignition patterns rather than on broad climate variables and fire season length. Regional climate simulations are now being run at approximately 10 km grid spacing (Prein et al. 2013), and although these still do not explicitly resolve convective precipitation, they may indicate changing patterns. The scales influencing fires range over several orders of magnitude and it is not feasible to test all factors or all fires with one approach. Diverse methods, arising from different areas of expertise, each of which providing a unique, partial insight, are needed to unravel this important problem.

ACKNOWLEDGMENTS

We thank Van Kane, Robert McGaughey, Carlos Ramirez, Harshvardhan Singh, Zachary Tane, Wilfrid Schroeder, Patricia Oliva, Bob Eisele, Philip Riggan, Scott Conway, James Done, and two anonymous reviewers for their contributions, helpful discussions, or suggestions for improving the manuscript. We thank Tom Painter and Megan Richardson for supporting the ASO data collection and processing. This work was supported by the National Aeronautics and Space Administration (NASA) under awards NNX12AQ87G and NNN12AA01C, the Federal Emergency Management Agency under award EMW-2011-FP-01124, and the U.S. Department of Agriculture Forest Service. The National Center for Atmospheric Research is sponsored by the National Science Foundation (NSF). Any opinions, findings, and conclusions or recommendations expressed in this material are the authors' and do not reflect the views of NSF. Part of the research described in this paper was carried out at the Jet Propulsion Laboratory, California Institute of Technology, under a contract with NASA. Government sponsorship is acknowledged.

LITERATURE CITED

- Abatzoglou, J. T., and C. A. Kolden. 2011. Relative importance of weather and climate on wildfire growth in interior Alaska. *International Journal of Wildland Fire* 20:479–486.
- Albini, F. A. 1976. Estimating wildfire behavior and effects. General Technical Report INT-30. USDA Forest Service Intermountain Forest and Range Experiment Station, Ogden, Utah, USA.
- Albini, F. A. 1994. PROGRAM BURNUP: a simulation model of the burning of large woody natural fuels. Final Report on Research Grant INT-92754-GR by USDA Forest Service to Montana State University, Mechanical Engineering Department, Bozeman, Montana, USA.
- Alvarado, E., D. V. Sandberg, and S. G. Pickford. 1998. Modeling large forest fires as extreme events. *Northwest Science* 72:66–75.
- Anderson, H. E. 1982. Aids to determining fuel models for estimating fire behavior. General Technical Report INT-122. USDA Forest Service Intermountain Forest and Range Experiment Station, Ogden, Utah, USA.
- Barbero, R., J. T. Abatzoglou, E. A. Steel, and N. K. Larkin. 2014. Modeling very large-fire occurrences over the continental United States from weather and climate forcing. *Environmental Research Letters* 9:124009.
- Bartlett, T., M. Leonard, and G. Morgan. 2007. The megafire phenomenon: some Australian perspectives. In *The 2007 Institute of Foresters of Australia and New Zealand Institute of Forestry Conference: Programme, Abstracts and Papers*. Institute of Foresters of Australia, Canberra, Australian Capital Territory, Australia. <http://www.forestry.org.au/pdf/pdf-public/conference2007/papers/Bartlett%20Megafire-final%20Draft27%202003.pdf>
- Bond, W. J., and J. E. Keeley. 2005. Fire as a global 'herbivore': the ecology and evolution of flammable ecosystems. *Trends in Ecology and Evolution* 20:387–394.
- Bowman, D. M. J. S., G. J. Williamson, J. T. Abatzoglou, C. A. Kolden, M. A. Cochrane, and A. M. S. Smith. 2017. *Nature Ecology & Evolution* 1:0058.
- Bradstock, R. A. 2010. A biogeographic model of fire regimes in Australia: current and future implications. *Global Ecology and Biogeography* 19:145–158.
- Brotak, E. A., and W. E. Reifsnnyder. 1977. An investigation of the synoptic situations associated with major wildland fires. *Journal of Applied Meteorology* 16:867–870.
- Clark, T. L., J. Coen, and D. Latham. 2004. Description of a coupled atmosphere-fire model. *International Journal of Wildland Fire* 13:49–64.
- Clark, T. L., and W. D. Hall. 1991. Multi-domain simulations of the time dependent Navier Stokes equations: benchmark error analyses of nesting procedures. *Journal of Computational Physics* 92:456–481.
- Clark, T. L., W. D. Hall, and J. L. Coen. 1996. Source code documentation for the Clark-Hall Cloud-scale model: Code version G3CH01. The National Center for Atmospheric Research (NCAR) Technical Note. NCAR/TN-426+STR. The National Center for Atmospheric Research, Boulder, Colorado, USA.
- Clark, T. L., T. Keller, J. Coen, P. Neilley, H. Hsu, and W. D. Hall. 1997. Terrain-induced turbulence over Lantau Island: 7 June 1994 tropical storm Russ case study. *Journal of Atmospheric Science* 54:1795–1814.
- Coen, J. L. 2005. Simulation of the Big Elk Fire using coupled atmosphere-fire modeling. *International Journal of Wildland Fire* 14:49–59.
- Coen, J. L. 2013. Modeling wildland fires: a description of the coupled atmosphere-wildland fire environment model (CAWFE). NCAR Technical Note NCAR/TN-500+STR. The National Center for Atmospheric Research, Boulder, Colorado, USA.
- Coen, J. L., and P. J. Riggan. 2014. Simulation and thermal imaging of the 2006 Esperanza wildfire in southern California: application of a coupled weather-wildland fire model. *International Journal of Wildland Fire* 23:755–770.
- Coen, J. L., and W. Schroeder. 2013. Use of spatially refined remote sensing fire detection data to initialize and evaluate coupled weather-wildfire growth model simulations. *Geophysical Research Letters* 40:5536–5541.
- Coen, J. L., and W. Schroeder. 2015. The High Park Fire: coupled weather-wildland fire model simulation of a windstorm-driven wildfire in Colorado's Front Range. *Journal of Geophysical Research*. Atmospheres 120:131–146.
- Coen, J. L., and W. Schroeder. 2017. Coupled weather-fire modeling: from research to operational forecasting. *Fire Management Today* 75:39–45.
- Dale, V. H., et al. 2001. Climate change and forest disturbances. *BioScience* 51:723–734.
- Dennison, P. E., S. C. Brewer, J. D. Arnold, and M. A. Moritz. 2014. Large wildfire trends in the western United States, 1984–2011. *Geophysical Research Letters* 41:2928–2933.
- Dennison, P. E., and M. A. Moritz. 2009. Critical live fuel moisture in chaparral ecosystems: a threshold for fire activity and its relationship to antecedent precipitation. *International Journal of Wildland Fire* 18:1021–1027.
- Dicus, C., and K. J. Osborne. 2015. How fuel treatment types, locations, and amounts impact landscape-scale fire behavior and carbon dynamics. Pages 50–59 in *Proceedings of the Large Wildland Fires Conference*, 19 to 23 May 2014, Missoula, Montana, USA. http://www.fs.fed.us/rm/pubs/rmrs_p073.pdf.
- Dimitrakopoulos, A., C. Gogi, G. Stamatelos, and I. Mitsopoulos. 2011. Statistical analysis of the fire environment of large forest fires (>1000 ha) in Greece. *Polish Journal of Environmental Studies* 20:327–332.
- Dubayah, R., et al. 2014. The global ecosystem dynamics investigation (GEDi) lidar. In *Proceedings of ForestSAT2014*, 4–7 November 2014, Riva del Garda, Italy. Edmund Mach Foundation, San Michele All'adige, Trentino, Italy.

ATTACHMENT D

- Finney, M. A. 2007. A computational method for optimising fuel treatment locations. *International Journal of Wildland Fire* 16:702–711.
- Flannigan, M. D., M. A. Krawchuk, W. J. de Groot, B. Mike Wotton, and L. M. Cowman. 2009. Implications of changing climate for global wildland fire. *International Journal of Wildland Fire* 18:483–507.
- Griffin, D., and K. J. Anchukaitis. 2014. How unusual is the 2012–2014 California drought? *Geophysical Research Letters* 41:9017–9023.
- Harris, L., and A. H. Taylor. 2017. Previous burns and topography limit and reinforce fire severity in a large wildfire. *Ecosphere* 8:e02019.
- Hook, S. J., J. J. Myers, K. J. Thorne, M. Fitzgerald, and A. B. Kahle. 2001. The MODIS/ASTER airborne simulator (MASTER)—a new instrument for earth science studies. *Canadian Journal of Forest Research* 76:93–102.
- Jetz, W., et al. 2016. Monitoring plant functional diversity from space. *Nature Plants* 2:16024.
- Keane, R. E., K. C. Ryan, T. T. Veblen, C. D. Allen, J. Logan, and B. Hawkes. 2002. Cascading effects of fire exclusion in the Rocky Mountain ecosystems: a literature review. General Technical Report RMRS-GTR-91. USDA Forest Service Rocky Mountain Research Station, Fort Collins, Colorado, USA.
- Keeley, J. E. 2009. Fire intensity, fire severity and burn severity: a brief review and suggested usage. *International Journal of Wildland Fire* 18:116–126.
- LaCroix, J. J., S.-R. Ryu, D. Zheng, and J. Chen. 2006. Simulating fire spread with landscape management scenarios. *Forest Science* 52:522–529.
- Lee, C. M., M. L. Cable, S. J. Hook, R. O. Green, S. L. Ustin, D. J. Mandl, and E. M. Middleton. 2015. An introduction to the NASA Hyperspectral InfraRed Imager (HyspIRI) mission and preparatory activities. *Remote Sensing of Environment* 167:6–19.
- Littell, J. S., D. McKenzie, D. L. Peterson, and A. L. Westerling. 2009. Climate and wildfire area burned in western US eco-provinces, 1916–2003. *Ecological Applications* 19:1003–1021.
- Lydersen, J. M., M. P. North, and B. M. Collins. 2014. Severity of an uncharacteristically large wildfire, the Rim Fire, in forests with relatively restored frequent fire regimes. *Forest Ecology and Management* 328:326–334.
- Lyons-Tinsley, C., and D. L. Peterson. 2012. Surface fuel treatments in young, regenerating stands affect wildfire severity in a mixed conifer forest, eastside Cascade Range, Washington, USA. *Forest Ecology and Management* 270:117–125.
- Painter, T. H., et al. 2016. The Airborne Snow Observatory: fusion of lidar, imaging spectrometer, and physically-based modeling for mapping snow water equivalent and snow albedo. *Remote Sensing of Environment* 184:139–152.
- Peterson, D. A., E. J. Hyer, J. R. Campbell, M. D. Fromm, J. W. Hair, C. F. Butler, and M. A. Fenn. 2015a. The 2013 Rim FIRE implications for predicting extreme fire spread, pyroconvection, and smoke emissions. *Bulletin of the American Meteorological Society* 96:229–247.
- Peterson, B., K. J. Nelson, C. Seielstad, J. Stoker, W. M. Jolly, and R. Parsons. 2015b. Automated integration of lidar into the LANDFIRE product suite. *Remote Sensing Letters* 6:247–256.
- Prein, A. F., G. H. Holland, R. M. Rasmussen, J. Done, K. Ikeda, M. P. Clark, and C. H. Liu. 2013. Importance of regional climate model grid spacing for the simulation of heavy precipitation in the Colorado headwaters. *Journal of Climate* 26:4848–4857.
- Pyne, S. J. 2015. Between two fires: a fire history of contemporary America. University of Arizona Press, Tucson, Arizona, USA.
- Riley, K. L., J. T. Abatzoglou, I. C. Grenfell, A. E. Klene, and F. A. Heinsch. 2013. The relationship of large-fires occurrence with drought and fire danger indices in the Western USA, 1984–2008: the role of temporal scale. *International Journal of Wildland Fire* 22:894–909.
- Rothermel, R. C. 1972. A mathematical model for predicting fire spread in wildland fuels. Research Paper INT-115, USDA Forest Service, Intermountain Forest and Range Experiment Station, Ogden, Utah, USA.
- Rothermel, R. C. 1991. Predicting behavior and size of crown fires in the Northern Rocky Mountains. Research Paper INT-438. USDA Forest Service, Ogden, Utah, USA.
- Schoennagel, T., T. Veblen, and W. Romme. 2004. Interaction of fire, fuels, and climate across Rocky Mountain forests. *BioScience* 54:661–676.
- Schroeder, W., P. Oliva, L. Giglio, and I. A. Csizsar. 2014. The new VIIRS 375 m active fire detection data product: algorithm description and initial assessment. *Remote Sensing of Environment* 143:85–96.
- Skamarock, W. C., J. B. Klemp, J. Dudhia, D. O. Gill, D. M. Barker, W. Wang, and J. G. Powers. 2005. A description of the advanced research WRF version 2. Technical Note. NCAR/TN- 4681STR. The National Center for Atmospheric Research (NCAR), Boulder, Colorado, USA.
- Stavros, E. N., J. T. Abatzoglou, N. K. Larkin, D. McKenzie, and E. A. Steel. 2014. Climate and very large wildland fires in the contiguous western USA. *International Journal of Wildland Fire* 23:899–914.
- Stavros, E. N., J. Coen, B. Peterson, H. Singh, K. Kennedy, C. Ramirez, and D. Schimel. 2018. Use of imaging spectroscopy and LIDAR to characterize fuels for fire behavior prediction. *Remote Sensing Applications: Society and Environment* 11:41–50.
- Stavros, E. N., Z. Tane, V. Kane, S. Veraverbeke, R. McGaughey, J. Lutz, C. Ramirez, and D. Schimel. 2016. Unprecedented remote sensing data over the King and Rim Megafires in the Sierra Nevada Mountains of California. *Ecology* 97:3334.
- Stocks, B. J., et al. 2003. Large forest fires in Canada, 1959–1997. *Journal of Geophysical Research* 108:8149.
- Strauss, D., L. Bednar, and R. Mees. 1989. Do one percent of forest fires cause ninety-nine percent of the damage? *Forest Science* 35:319–328.
- Syphard, A. D., R. M. Scheller, B. C. Ward, W. D. Spencer, and J. R. Strittholt. 2011. Simulation landscape-scale effects of fuels treatments in the Sierra Nevada, California, USA. *International Journal of Wildland Fire* 20:364–383.
- Tedim, F., G. Xanthopoulos, and V. Leone. 2014. Forest fires in Europe: facts and challenges. Ch. 5. Pages 77–99 in D. Paton, editor. *Wildfire. Hazards, risks, and disasters*. Elsevier, Philadelphia, Pennsylvania, USA.
- Turner, M. G. 2010. Disturbance and landscape dynamics in a changing world. *Ecology* 91:2833–2849.
- Van Wagner, C. E. 1977. Conditions for the start and spread of crown fire. *Canadian Journal of Forest Research* 7:23–34.
- Wang, X., M. Parisien, M. D. Flannigan, S. A. Parks, K. R. Anderson, J. M. Little, and S. W. Taylor. 2014. The potential and realized spread of wildfires across Canada. *Global Change Biology* 20:2518–2530.
- Westerling, A. L., H. G. Hidalgo, D. R. Cayan, and T. W. Swetnam. 2006. Warming and earlier spring increase western US forest wildfire activity. *Science* 313:940–943.
- Williams, J. 2013. Exploring the onset of high-impact mega-fires through a forest land management prism. *Forest Ecology and Management* 294:4–10.

SUPPORTING INFORMATION

Additional supporting information may be found online at: <http://onlinelibrary.wiley.com/doi/10.1002/eap.1752/full>

DATA AVAILABILITY

Data available from NASA ORNL DAAC: <https://doi.org/10.3334/ornldaac/1288>

ATTACHMENT D

EXHIBIT I

Does increased forest protection correspond to higher fire severity in frequent-fire forests of the western United States?

CURTIS M. BRADLEY,^{1,†} CHAD T. HANSON,² AND DOMINICK A. DELLA SALA³

¹Center for Biological Diversity, PO Box 710, Tucson, Arizona 85701 USA

²Earth Island Institute, 2150 Allston Way, Suite 460, Berkeley, California 94704 USA

³Geos Institute, 84-4th Street, Ashland, Oregon 97520 USA

Citation: Bradley, C. M., C. T. Hanson, and D. A. DellaSala. 2016. Does increased forest protection correspond to higher fire severity in frequent-fire forests of the western United States? *Ecosphere* 7(10):e01492. 10.1002/ecs2.1492

Abstract. There is a widespread view among land managers and others that the protected status of many forestlands in the western United States corresponds with higher fire severity levels due to historical restrictions on logging that contribute to greater amounts of biomass and fuel loading in less intensively managed areas, particularly after decades of fire suppression. This view has led to recent proposals—both administrative and legislative—to reduce or eliminate forest protections and increase some forms of logging based on the belief that restrictions on active management have increased fire severity. We investigated the relationship between protected status and fire severity using the Random Forests algorithm applied to 1500 fires affecting 9.5 million hectares between 1984 and 2014 in pine (*Pinus ponderosa*, *Pinus jeffreyi*) and mixed-conifer forests of western United States, accounting for key topographic and climate variables. We found forests with higher levels of protection had lower severity values even though they are generally identified as having the highest overall levels of biomass and fuel loading. Our results suggest a need to reconsider current overly simplistic assumptions about the relationship between forest protection and fire severity in fire management and policy.

Key words: biodiversity; climate; fire frequency; fire severity; fire suppression; Gap Analysis Program levels; logging; protected areas.

Received 4 May 2016; revised 28 June 2016; accepted 5 July 2016. Corresponding Editor: Debra P. C. Peters.

Copyright: © 2016 Bradley et al. This is an open access article under the terms of the Creative Commons Attribution License, which permits use, distribution and reproduction in any medium, provided the original work is properly cited.

† **E-mail:** cbradley@biologicaldiversity.org

INTRODUCTION

It is a widely held assumption among federal land management agencies and others that a lack of active forest management of some federal forestlands—especially within relatively frequent-fire forest types such as ponderosa pine (*Pinus ponderosa*) and mixed conifers—is associated with higher levels of fire severity when wildland fires occur (USDA Forest Service 2004, 2014, 2015, 2016). This prevailing forest/fire management hypothesis assumes that forests with higher levels of protection, and therefore less logging, will burn more intensely due to higher fuel loads and forest density. Recommendations have been made to increase logging as fuel

reduction and decrease forest protections before wildland fire can be more extensively reintroduced on the landscape after decades of fire suppression (USDA Forest Service 2004, 2014, 2015, 2016). The concern follows that, in the absence of such a shift in forest management, fires are burning too severely and may adversely affect forest resilience (North et al. 2009, 2015, Stephens et al. 2013, 2015, Hessburg 2016). Nearly every fire season, the United States Congress introduces forest management legislation based on this view and aimed at increasing mechanical fuel treatments via intensive logging and weakened forest protections.

However, the fundamental premise for this fire management strategy has not been rigorously

tested across broad regions. We broadly assessed the influence of forest protection levels on fire severity in pine and mixed-conifer forests of the western United States with relatively frequent-fire regimes to test this assumption. We used vegetation burn severity data from all fires >405 ha over a three-decade period, 1984–2014, in forests with varying levels of protection.

Study area

Pine and mixed-conifer forests at low/mid-elevations, where historical fires were relatively frequent, are broadly distributed across several ecoregions in the western United States (Fig. 1; Appendix S1: Table S1). Although ponderosa pine often dominates these forests, they can also include Jeffrey pine (*Pinus jeffreyi*), which in places intermix with, and are similar to, ponderosa pine forests, and Madroñal pine-oak (*Quercus* spp.) forests with a diversity of pines. Mixed-conifer forests at low/mid-elevations are also broadly distributed across multiple ecoregions (Fig. 1). They can include additional pines (e.g., lodgepole pine, *Pinus contorta*; sugar pine, *Pinus lambertiana*), true firs (*Abies* spp.), Douglas-fir (*Pseudotsuga menziesii*), and incense-cedar (*Calocedrus decurrens*).

METHODS

We used Gap Analysis Program (GAP) protection classes (USGS 2012), as described below, to determine whether areas with the most protection (i.e., GAP1 and GAP2) had a tendency to burn more severely than areas where intensive management is allowed (i.e., GAP3 and GAP4). We compared satellite-derived burn severity data for 1500 fires affecting 9.5 million hectares from years for which there were available data (1984–2014) among four different forest protection levels (Fig. 1), accounting for variation in topography and climate. We analyzed fires within relatively frequent-fire forest types comprised of pine and mixed-conifer forests mainly because these are the predominant forest types at low to mid-elevations in the western United States, there is a large data set on fire occurrence, and they have been a major concern of land managers for some time due to decades of fire suppression. We defined geographic extent of forest types from the Biophysical Settings data set (BpS) (Rollins 2009; *public communication*, <http://www.landfire.gov>)

that derived forest maps from satellite imagery and represents plant communities based on NatureServe's Ecological Systems classification. Baker (2015) noted that some previous work found ~65% classification accuracy of this system with regard to specific forest types and, accordingly, he analyzed groups of related forest types in order to improve accuracy. We followed his approach (see Appendix S1: Table S1). The categories selected from the Biophysical Settings map were ponderosa/Jeffrey pine and mixed-conifer forest types with relatively frequent-fire regimes (e.g., Swetnam and Baisan 1996, Taylor and Skinner 1998, Schoennagel et al. 2004, Stephens and Collins 2004, Sherriff et al. 2014), compared to other forest types with different fire regimes such as high-elevation forests and many coastal forests not studied herein. Forest types in our study totaled 29.2 million hectares (Fig. 1; Appendix S1: Table S1). We used the BpS data to capture areas that were classified as forests before fire, because postfire vegetation maps can potentially show these same areas as temporarily changed to other vegetation types. We sampled our response and predictor variables on an evenly spaced 90 × 90 m grid within these forest types using ArcMap 10.3 (ESRI 2014). This created a data set of 5,580,435 independent observations from which we drew our random samples to create our models. The 90-m spacing was chosen because it was the smallest spacing of points that was computationally practical with which to operate.

Fires

The Monitoring Trends in Burn Severity project (MTBS, *public communication*, <http://www.mtbs.gov>) is a U.S. Department of Interior and Department of Agriculture-sponsored program that has compiled burn severity data from satellite imagery, which became available in 1984, for fires >405 ha, and was current up to 2014 (Eidenshink et al. 2007). The MTBS Web site allows bulk download of spatial products that include two closely related indices of burn severity: differenced normalized burn ratio (dNBR) (Key and Benson 2006) and relative differenced normalized burn ratio (RdNBR) (Miller and Thode 2007). Both indices are calculated from Landsat TM and ETM satellite imagery of reflected light from the earth's surface at infrared wavelengths from before and after fire to



Fig. 1. Pine and mixed-conifer forests, fires, and ecoregions analyzed in this study.

measure associated changes in vegetation cover and soil characteristics. We defined burn severity with the RdNBR index because it adjusts for pre-fire conditions at each pixel and provides a more consistent measure of burn severity than dNBR when studying broad geographic regions with many different vegetation types (Miller et al.

2009a, Norton et al. 2009). RdNBR values typically range from negative 500 to 1500 with values further away from zero representing greater change from prefire conditions. Negative values represent vegetation growth and positive values increasing levels of overstory vegetation mortality. The RdNBR values could be used to classify

fires into discrete burn severity classes of low, medium, and high but this was not performed in our study, as we desired to have a continuous response variable in our models.

We intersected forest sampling points with fire perimeters downloaded from MTBS to determine fires that occurred in our analysis area, and censored fires with <100 sampling points (81 ha). The remaining points represented sampling locations from 2069 fires (Fig. 1). We extracted RdNBR values at each sampling point as our response variable as well as predictor variables that included topography, geography, climate, and GAP status. These sampling points were used to investigate the relationship between forest protection levels and burn severity (Appendix S1: Tables S2 and S3). We chose topographic and climatic variables based on previous studies that quantified the relationship between burn severity, topography, and climate (Dillon et al. 2011, Kane et al. 2015).

Topographic and climatic data

To account for the effects of topographic and climatic variability, we derived several topographic indices (Appendix S1: Table S2) from seamless elevation data (*public communication*, <http://www.landfire.gov/topographic.php>) downscaled to 90-m² spatial resolution due to computational limits when intersecting sampling points. These indices capture categories of topography, including percentage slope, surface complexity, slope position, and several temperature and moisture metrics derived from aspect and slope position. We used the Geomorphometry and Gradient Metrics Toolbox version 2.0 (*public communication*, <http://evansmurphy.wix.com/evansspatial>) to compute these metrics. We also computed several temperature and precipitation variables (Appendix S1: Table S3) by downloading climatic conditions for each month from 1984 to 2014 from the PRISM climate group (*public communication*, <http://prism.oregonstate.edu>). Climate grids record precipitation and minimum, mean, and maximum temperature at a 4-km grid scale created by interpolating data from over 10,000 weather stations. To determine the departure from average conditions, we subtracted each climate grid by its 30-yr mean monthly value. These “30-yr Normals” data sets were also downloaded from the PRISM Web site and reflected the mean values from the most recent full decades (1981–2010). We

determined mean seasonal values with summer defined as the mean of July, August, and September of the year before a given fire; fall being the mean of October, November, and December of the previous year; winter the mean of January, February, and March of the current year of a given fire; and spring the mean of April, May, and June of the current year.

Protected area status and ecoregion classification

We used the Protected Areas Database of the United States (PAD-US; USGS 2012) to determine forest protection status, which is the U.S. official inventory of protected open space. The PAD-US includes all federal and most State conservation lands and classifies these areas with a GAP ranking code (see map at: <http://gis1.usgs.gov/csas/gap/viewer/padus/Map.aspx>). The GAP status code (herein referred to interchangeably as GAP class or protection status) is a metric of management to conserve biodiversity with four relative categories. GAP1 is protected lands managed for biodiversity where disturbance events (e.g., fires) are generally allowed to proceed naturally. These lands include national parks, wilderness areas, and national wildlife refuges. GAP2 is protected lands managed for biodiversity where disturbance events are often suppressed. They include state parks and national monuments, as well as a small number of wilderness areas and national parks with different management from GAP1. GAP3 is lands managed for multiple uses and are subjected to logging. Most of these areas consist of non-wilderness USDA Forest Service and U.S. Department of Interior Bureau of Land Management lands as well as state trust lands. GAP4 is lands with no mandate for protection such as tribal, military, and private lands. GAP status is relevant to the intensity of both current and past managements.

We made one modification to GAP levels by converting Inventoried Roadless Areas (IRAs) from the 2001 Roadless Area Conservation Rule (S_USA.RoadlessArea_2001, *public communication*, <http://data.fs.usda.gov/geodata/edw/dataset.php>) to GAP2 unless these areas already were defined as GAP1. We considered most IRAs as GAP2 given they are prone to policy changes and because they allow for certain limited types of logging (e.g., removal of predominately small trees for fuel reduction in some circumstances).

However, we note that very little logging has occurred within IRAs since the Roadless Rule, although there occasionally have been proposals to log portions of some IRAs pre- and postfire, and fire suppression often occurs.

We modified level III ecoregions (U.S. Environmental Protection Agency (EPA) 2013) to create areas of similar climate and geography (Fig. 1). We did this by extracting ecoregions and combining adjacent provinces in our study region.

Random Forests analysis

We investigated the relationship between protection status and burn severity using the data-mining algorithm Random Forests (RF) (Breiman 2001) with the “randomForestSRC” add-in package (Ishwaran and Kogalur 2016) in R (R Core Team 2013). This algorithm is an extension of classification and regression trees (CART) (Breiman et al. 1984) that recursively partitions observations into groups based on binary rule splits of the predictor variables. The main advantage of using RF in our study is that it can work with spatially autocorrelated data (Cutler et al. 2007). It can also model complex, nonlinear relationships among variables, makes no assumption of variable distributions (Kane et al. 2015), and produces accurate predictions without overfitting the available data (Breiman 2001).

Our independent observations were a random subset of our 5.5 million points, from which we drew three random samples of 25,000 points each. Each sample consisted of 500 fires randomly selected without replacement from the pool of 2069 fires. Fifty points were then randomly selected within each of the 500 fires. Our dependent variables were all continuous (Appendix S1: Tables S2 and S3) except for the main variable of interest, protected area status, which included the four GAP levels. The three observation samples were used to create three RF model runs, each consisting of 1000 regression trees. We conducted three RF model runs to assess whether our random samples of 25,000 points produced fairly consistent results.

The RF algorithm samples approximately 66% of the data to build the regression trees, and the remaining data are used for validation and to assess variable importance. We used this validation sample to determine the amount of variance explained and variable importance.

The algorithm also produces individual variable importance measures by calculating differences in prediction mean-square-error before and after randomly permuting each dependent variable's values. Variable importance is a measure of how much each variable contributes to the model's overall predictive accuracy.

Unlike linear models, RF does not produce regression coefficients to examine how a change in a predictor variable affects the response variable. The analogy to this in RF is the partial dependence plot which is a graphical depiction of how the response will change with a single predictor while averaging out the effects of the other predictors, such as the climatic and topographic variables (Cutler et al. 2007). We used this approach, in addition to using RF to determine overall variable importance as described above, in order to determine the effect of GAP status, in particular, on fire severity, while averaging out effects of climate and topography.

Mixed-effects analysis

We performed a linear mixed-effects analysis using the “nlme” add-on package in R (Pinheiro et al. 2015). We used a random intercept model and identified year of fire ($n = 31$) and ecoregion ($n = 10$) as random effects. Similar to our RF models, our independent observations were a random subset of our 5.5 million points but for these models we drew three random samples of 50,000 points each. Each sample consisted of 500 fires randomly selected without replacement, and within each of those fires, 100 points were randomly selected. Our dependent variables were the same used in our RF models, and we log-transformed the non-normal variables of slope, surface roughness, and topographic radiation aspect index. We removed dependent variables that were correlated with each other (Pearson's $r > 0.5$), retaining 21 of 45 candidate dependent variables, and centered these on their means. Model reduction was performed in a stepwise process using bidirectional elimination with Bayesian information criterion selection criterion.

Spatial autocorrelation analysis

Spatial autocorrelation (SA) is the measure of similarity between pairs of observations in relationship to the distance between them. Ecological variables are inherently autocorrelated because

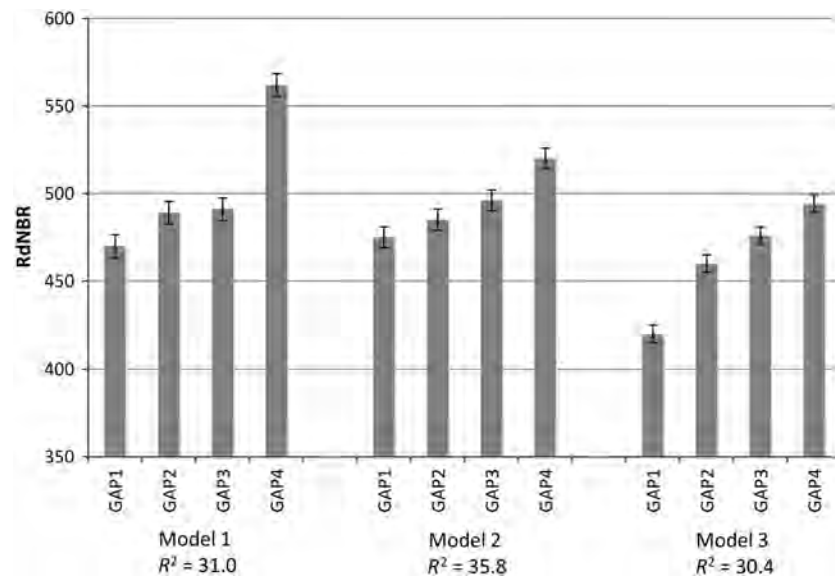


Fig. 2. Random Forests partial dependence of protection status vs. RdNBR burn severity for each model ($n = 25,000$). The variance explained is shown as pseudo R^2 .

landscape attributes that are closer together are often more similar than those that are far apart.

We assessed the SA in the Pearson residuals with inspection of Moran's I autocorrelation index using the "APE" package add-in in R (Paradis et al. 2004) after removing points that shared the same x and y coordinates. Moran's I is an index that ranges from -1 to 1 with the sign of the values indicating strength and direction of SA. Values close to zero are considered to have a random spatial pattern. Our mixed-effects models all had a Moran's I values statistically different from 0 at the 95% confidence level ($P < 0.001$) so we included a spatial correlation structure in our model using the "nlme" package in R. Of Gaussian, exponential, linear, and spherical spatial correlation structures, we determined that the exponential structure produced the lowest Akaike's information criterion (AIC). Despite these additions, our second measurements still found relatively small, but significant, autocorrelation (Moran's I for model runs 1, 2, 3 = 0.10, 0.08, 0.10, all $P < 0.001$).

RESULTS

With regard to ranking of variables in the model runs, variable importance plots from the three RF model runs show that protection status

was consistently ranked as one of the 10 most important of the 45 variables in explaining burn severity (Appendix S1: Table S4). The most important variable explaining burn severity was ecoregion for models 1 and 2 and maximum temperature from the previous fall for model 3.

With regard to the GAP status variable in particular, after averaging out the effects of climatic and topographic variables, the RF partial dependence plots show an increasing trend of fire severity with decreasing protection status (Fig. 2). Fires in GAP4 had mean RdNBR values greater than two standard errors higher than all other GAP levels. Fires in GAP3 had mean RdNBR values two standard errors higher than GAP1 in all model runs. GAP3 differences with GAP2 were less pronounced with only one model showing differences greater than two standard errors. Fires in GAP1 were consistently the least severe, being two standard errors less than GAP3 in all model runs and two standard errors less than GAP2 in two of three model runs.

Our mixed-effects models validated these findings with similar results (Fig. 3, Appendix S1: Table S5). Like our RF models, our linear mixed-effects models showed GAP4 fires to have significantly higher RdNBR values and GAP1 fires to have significantly lower RdNBR values when compared to all other GAP classes. Fires in GAP

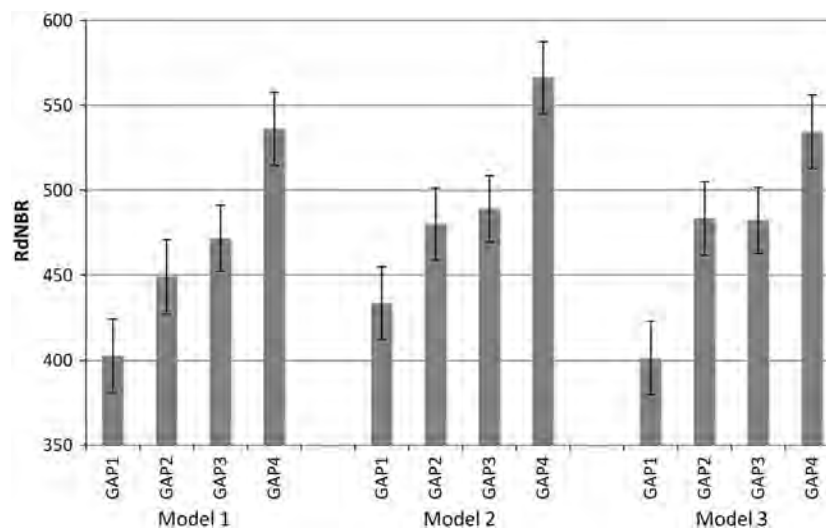


Fig. 3. Linear mixed effects models of protection status vs. RdNBR burn severity ($n = 50,000$).

status levels 2 and 3 were not significantly different in the mixed-effects models. Although the level of autocorrelation was significant, it was small in our model (Moran's $I \sim 0.1$) and not enough to account for such a substantial difference in burn severity among protection classes.

DISCUSSION

Protected forests burn at lower severities

We found no evidence to support the prevailing forest/fire management hypothesis that higher levels of forest protections are associated with more severe fires based on the RF and linear mixed-effects modeling approaches. On the contrary, using over three decades of fire severity data from relatively frequent-fire pine and mixed-conifer forests throughout the western United States, we found support for the opposite conclusion—burn severity tended to be higher in areas with lower levels of protection status (more intense management), after accounting for topographic and climatic conditions in all three model runs. Thus, we rejected the prevailing forest management view that areas with higher protection levels burn most severely during wildfires.

Protection classes are relevant not only to recent or current forest management practices but also to past management. Millions of hectares of land have been protected from logging since the 1964 Wilderness Act and the 2001 Roadless Rule, but these areas are typically categorized

as such due to a lack of historical road building and associated logging across patches >2000 ha, while GAP3 lands, for instance, such as National Forests lands under “multiple use management,” have generally experienced some form of logging activity over the last 80 yr.

We expect that the effects of historic logging from nearly a century ago to gradually lessen over time, as succession and natural disturbance processes reestablish structural and compositional complexity, but it was beyond the scope of this study to attempt to assess the relative role of recent vs. historical logging. Similarly, industrial fire suppression programs that intensified in the 1940s influenced fire extent across forest protection classes. While more recent let-burn policies have been applied in GAP1 and GAP2 forests in some circumstances, evidence indicates that protected forests nevertheless remain in a substantial fire deficit, relative to the prefire suppression era (Odion et al. 2014, 2016, Parks et al. 2015). Thus, we believe it is unlikely that recent decisions to allow some backcountry fires to burn, largely unimpeded, account for much of the differences in fire severity among protection classes that we found, simply because such let-burn policies have not been extensive enough to remedy the ongoing fire deficit.

While forests in different protection classes can vary in elevation, with protected forests often occupying higher elevations, our results indicate that protection class itself produced notable

differences in fire severity after averaging out the effects of elevation and climate (see Fig. 2 and *Results* above). In our study, GAP1 forests were 284 m on average higher in elevation than GAP4 forests, while GAP1 forests experienced lower fire severity. This is the opposite of expectations if elevation was a key influence because higher elevation forests are associated with higher fire severity (see, e.g., Schoennagel et al. 2004, Sherriff et al. 2014). We note that we are not the first to determine that increased fire severity often occurs in forests with an active logging history (Countryman 1956, Odion et al. 2004).

Prevailing forest–fire management perspectives vs. alternative views

An extension of the prevailing forest/fire management hypothesis is that biomass and fuels increase with increasing time after fire (due to suppression), leading to such intense fires that the most long-unburned forests will experience predominantly severe fire behavior (e.g., see USDA Forest Service 2004, Agee and Skinner 2005, Spies et al. 2006, Miller et al. 2009b, Miller and Safford 2012, Stephens et al. 2013, Lydersen et al. 2014, Dennison et al. 2014, Hessburg 2016). However, this was not the case for the most long-unburned forests in two ecoregions in which this question has been previously investigated—the Sierra Nevada of California and the Klamath-Siskiyou of northern California and southwest Oregon. In these ecoregions, the most long-unburned forests experienced mostly low/moderate-severity fire (Odion et al. 2004, Odion and Hanson 2006, Miller et al. 2012, van Wagendonk et al. 2012). Some of these researchers have hypothesized that as forests mature, the overstory canopy results in cooling shade that allows surface fuels to stay moister longer into fire season (Odion and Hanson 2006, 2008). This effect may also lead to a reduction in pyrogenic native shrubs and other understory vegetation that can carry fire, due to insufficient sunlight reaching the understory (Odion et al. 2004, 2010).

Another fundamental assumption is that current fires are becoming too large and severe compared to recent historical time lines (Agee and Skinner 2005, Spies et al. 2006, Miller et al. 2009b, Miller and Safford 2012, Stephens et al. 2013, Lydersen et al. 2014, Dennison et al. 2014, Hessburg 2016). However, others have shown

that this is not the case for most western forest types. For instance, using the MTBS (www.mtbs.gov) data set, Picotte et al. (2016) found that most vegetation groups in the conterminous United States exhibited no detectable change in area burned or fire severity from 1984 to 2010. Similarly, Hanson et al. (2009) found no increase in rates of high-severity fire from 1984 to 2005 in dry forests within the range of the northern spotted owl (*Strix occidentalis caurina*) based on the MTBS data set. Using reference data and records of high-severity fire, Baker (2015) found no significant upward trends in fire severity from 1984 to 2012 across all dry western forest regions (25.5 million ha), nearly all of which instead were too low or were within the range of historical rates. Parks et al. (2015) modeled area burned as a function of climatic variables in western forests and non-forest types, documenting most forested areas had experienced a fire deficit (observed vs. expected) during 1984 to 2012 that was likely due to fire suppression.

Whether fires are increasing or not depends to a large extent on the baseline chosen for comparisons (i.e., shifting baseline perspective, Whitlock et al. 2015). For instance, using time lines predating the fire suppression era, researchers have documented no significant increases in high-severity fire for dry forests across the West (Williams and Baker 2012a, Odion et al. 2014) or for specific regions (Williams and Baker 2012b, Sherriff et al. 2014, Tepley and Veblen 2015). Future trends, with climate change and increasing temperatures, may be less simple than previously believed, due to shifts in pyrogenic understory vegetation (Parks et al. 2016).

This is more than just a matter of academic debate, as most forest management policies assume that fire, particularly high-severity fire, is increasing, is in excess of recent historical baselines, and needs to be reduced in size, intensity, and occurrence over large landscapes to prevent widespread ecosystem damages (policy examples include USDA Forest Service 2002, Healthy Forests Restoration Act 2003, USDA Forest Service 2009, HR 167: Wildfire Disaster Funding Act 2015). However, large fires (landscape scale or the so-called megafires) produce myriad ecosystem benefits underappreciated by most land managers and decision-makers (DellaSala and Hanson 2015a, DellaSala et al. 2015). High-severity fire

patches, in particular, provide a pulse of “biological legacies” (e.g., snags, down logs, and native shrub patches) essential for complex early seral associates (e.g., many bird species) that link seral stages from new forest to old growth (Swanson et al. 2011, Donato et al. 2012, DellaSala et al. 2014, Hanson 2014, 2015, DellaSala and Hanson 2015a). Complex early seral forests are most often logged after fire, which, along with aggressive fire suppression, exacerbates their rarity and heightens their conservation importance (Swanson et al. 2011, DellaSala et al. 2014, 2015, Hanson 2014).

Limitations

One limitation of our study is that, due to the coarseness of the management intensity variables that we used (i.e., GAP status), we cannot rule out whether low intensities of management decreased the occurrence of high-severity fire in some circumstances. However, the relationship between forest density/fuel, mechanical fuel treatment, and fire severity is complex. For instance, thinning without subsequent prescribed fire has little effect on fire severity (see Kalies and Yocum Kent 2016) and, in some cases, can increase fire severity (Raymond and Peterson 2005, Ager et al. 2007, Wimberly et al. 2009) and tree mortality (see, e.g., Stephens and Moghaddas 2005, Stephens 2009: Figure 6)—the effects depend on the improbable co-occurrence of reduced fuels (generally a short time line, within a decade or so) and wildfire activity (Rhodes and Baker 2008) and can be over-ridden by extreme fire weather (Bessie and Johnson 1995, Hély et al. 2001, Schoennagel et al. 2004, Lydersen et al. 2014). Empirical data from actual fires also indicate that postfire logging can increase fire severity in reburns (Thompson et al. 2007), despite removal of woody biomass (tree trunks) described by land managers as forest fuels (Peterson et al. 2015). While our study did not specifically test for these effects, such active forest management practices are common on GAP3 and GAP4 lands. Recognizing these limitations, researchers have stressed the need for managers to strive for coexistence with fire by prioritizing fuel reduction nearest homes and allowing more fires to occur unimpeded in the backcountry (Moritz 2014, DellaSala et al. 2015, Dunn and Bailey 2016, Moritz and Knowles 2016).

Follow-up research at finer scales is needed to determine management emphasis and history in relation to fire severity. However, we believe our findings are robust at the subcontinental and ecoregional scales.

CONCLUSIONS

In general, our findings—that forests with the highest levels of protection from logging tend to burn least severely—suggest a need for managers and policymakers to rethink current forest and fire management direction, particularly proposals that seek to weaken forest protections or suspend environmental laws ostensibly to facilitate a more extensive and industrial forest–fire management regime. Such approaches would likely achieve the opposite of their intended consequences and would degrade complex early seral forests (DellaSala et al. 2015). We suggest that the results of our study counsel in favor of increased protection for federal forestlands without the concern that this may lead to more severe fires.

Allowing wildfires to burn under safe conditions is an effective restoration tool for achieving landscape heterogeneity and biodiversity conservation objectives in regions where high levels of biodiversity are associated with mixed-intensity fires (i.e., “pyrodiversity begets biodiversity,” see DellaSala and Hanson 2015b). Managers concerned about fires can close and decommission roads that contribute to human-caused fire ignitions and treat fire-prone tree plantations where fires have been shown to burn uncharacteristically severe (Odion et al. 2004). Prioritizing fuel treatments to flammable vegetation adjacent to homes along with specific measures that reduce fire risks to home structures are precautionary steps for allowing more fires to proceed safely in the backcountry (Moritz 2014, DellaSala et al. 2015, Moritz and Knowles 2016).

Managing for wildfire benefits as we suggest is also consistent with recent national forest policies such as 2012 National Forest Management Act planning rule that emphasizes maintaining and restoring ecological integrity across the national forest system and because complex early forests can only be produced by natural disturbance events not mimicked by mechanical fuel reduction or clear-cut logging (Swanson et al. 2011, DellaSala et al. 2014). Thus, managers

wishing to maintain biodiversity in fire-adapted forests should appropriately weigh the benefits of wildfires against the ecological costs of mechanical fuel reduction and fire suppression (Ingalsbee and Raja 2015) and should consider expansion of protected forest areas as a means of maintaining natural ecosystem processes like wildland fire.

ACKNOWLEDGMENTS

We would like to thank Monica Bond and Derek Lee for statistical advice and Randi Spivak and Jay Lininger for providing helpful comments on this manuscript. We also thank the reviewers for suggestions, which improved the manuscript.

LITERATURE CITED

- Agee, J. K., and C. N. Skinner. 2005. Basic principles of forest fuel reduction treatments. *Forest Ecology and Management* 211:83–96.
- Ager, A. A., A. J. McMahan, J. J. Barrett, and C. W. McHugh. 2007. A simulation study of thinning and fuel treatments on a wildland-urban interface in eastern Oregon, USA. *Landscape and Urban Planning* 80:292–300.
- Baker, W. L. 2015. Are high-severity fires burning at much higher rates recently than historically in dry-forest landscapes of the Western USA? *PLoS ONE* 10:e0141936.
- Bessie, W. C., and E. A. Johnson. 1995. The relative importance of fuels and weather on fire behavior in subalpine forests. *Ecology* 76:747–762.
- Breiman, L. 2001. Random forests. *Machine Learning* 45:5–32.
- Breiman, L., J. Friedman, R. Olshen, and C. Stone. 1984. *Classification and regression trees*. Wadsworth, Belmont, California, USA.
- Countryman, C. M. 1956. Old growth conversion also converts fire climate. *Fire Control Notes* 17: 15–19.
- Cutler, D. R., T. C. Edwards, K. H. Beard, A. Cutler, K. T. Hess, J. Gibson, and J. J. Lawler. 2007. Random forests for classification in ecology. *Ecology* 88:2783–2792.
- DellaSala, D. A., M. L. Bond, C. T. Hanson, R. L. Hutto, and D. C. Odion. 2014. Complex early seral forests of the Sierra Nevada: What are they and how can they be managed for ecological integrity? *Natural Areas Journal* 34:310–324.
- DellaSala, D. A., and C. T. Hanson. 2015a. Ecological and biodiversity benefits of megafires. Pages 23–54 in D. A. DellaSala and C. T. Hanson, editors. *The ecological importance of mixed-severity fires: nature's phoenix*. Elsevier, Waltham, Massachusetts, USA.
- DellaSala, D. A., and C. T. Hanson, editors. 2015b. *The ecological importance of mixed-severity fires: nature's phoenix*. Elsevier, Waltham, Massachusetts, USA.
- DellaSala, D. A., D. B. Lindenmayer, C. T. Hanson, and J. Furnish. 2015. In the aftermath of fire: Logging and related actions degrade mixed- and high-severity burn areas. Pages 313–347 in D. A. DellaSala and C. T. Hanson, editors. *The ecological importance of mixed-severity fires: nature's phoenix*. Elsevier, Waltham, Massachusetts, USA.
- Dennison, P. E., S. C. Brewer, J. D. Arnold, and M. A. Moritz. 2014. Large wildfire trends in the western United States, 1984–2011. *Geophysical Research Letters* 41:2928–2933.
- Dillon, G. K., Z. A. Holden, P. Morgan, M. A. Crimmins, E. K. Heyerdahl, and C. H. Luce. 2011. Both topography and climate affected forest and woodland burn severity in two regions of the western US, 1984 to 2006. *Ecosphere* 2:130.
- Donato, D. C., J. L. Campbell, and J. F. Franklin. 2012. Multiple successional pathways and precocity in forest development: Can some forests be born complex? *Journal of Vegetation Science* 23:576–584.
- Dunn, C. J., and J. D. Bailey. 2016. Tree mortality and structural change following mixed-severity fire in *Pseudotsuga* forests of Oregon's western Cascades, USA. *Forest Ecology and Management* 365: 107–118.
- Eidenshink, J., B. Schwind, K. Brewer, Z. Zhu, B. Quayle, and S. Howard. 2007. A project for monitoring trends in burn severity. *Fire Ecology* 3:3–21.
- ESRI. 2014. ArcGIS desktop: release 10.3. Environmental Systems Research Institute, Redlands, California, USA.
- Hanson, C. T. 2014. Conservation concerns for Sierra Nevada birds associated with high-severity fire. *Western Birds* 45:204–212.
- Hanson, C. T. 2015. Use of higher-severity fire areas by female Pacific fishers on the Kern Plateau, Sierra Nevada, California, USA. *Wildlife Society Bulletin* 39:497–502.
- Hanson, C. T., and D. C. Odion. 2016. Historical forest conditions within the range of the Pacific Fisher and Spotted Owl in the central and southern Sierra Nevada, California, USA. *Natural Areas Journal* 36:8–19.
- Hanson, C. T., D. C. Odion, D. A. DellaSala, and W. L. Baker. 2009. Overestimation of fire risk in the Northern Spotted Owl recovery plan. *Conservation Biology* 23:1314–1319.

- Healthy Forest Restoration Act. 2003. P.L. 108-148. <https://www.congress.gov/bill/108th-congress/house-bill/1904>
- Hély, C., M. Flannigan, Y. Bergeron, and D. McRae. 2001. Role of vegetation and weather on fire behavior in the Canadian mixedwood boreal forest using two fire behavior prediction systems. *Canadian Journal of Forest Research* 31:430–441.
- Hessburg, P. F., et al. 2016. Tamm review: management of mixed-severity fire regime forests in Oregon, Washington, and northern California. *Forest Ecology and Management* 366:221–250.
- HR 167: Wildfire Disaster Funding Act. 2015. S.235. <https://www.congress.gov/bill/114th-congress/senate-bill/235>
- Ingalsbee, T., and U. Raja. 2015. The rising costs of wildfire suppression and the case for ecological fire use. Pages 348–371 in D. A. DellaSala and C. T. Hanson, editors. *The ecological importance of mixed-severity fires: nature's phoenix*. Elsevier, Waltham, Massachusetts, USA.
- Ishwaran, H., and U. B. Kogalur. 2016. Random forests for survival, regression and classification (RF-SRC). R package version 2.0.7. <https://cran.r-project.org/package=randomForestSRC>
- Kalies, E. L., and L. L. Yocum Kent. 2016. Tamm review: Are fuel treatments effective at achieving ecological and social objectives? A systematic review. *Forest Ecology and Management* 375:84–95.
- Kane, V. A., C. A. Cansler, N. A. Povak, J. T. Kane, R. J. McGaughey, J. A. Lutz, D. J. Churchill, and M. P. North. 2015. Mixed severity fire effects within the Rim fire: relative importance of local climate, fire weather, topography, and forest structure. *Forest Ecology and Management* 358:62–79.
- Key, C. H., and N. C. Benson. 2006. Landscape assessment: sampling and analysis methods. Pages 1–55 in D. C. Lutes, R. E. Keane, J. F. Caratti, C. H. Key, N. C. Benson, S. Sutherland, and L. J. Gangi, editors. *FIREMON: fire effects monitoring and inventory system*. General Technical Report RMRS-GTR-164-CD. USDA Forest Service, Rocky Mountain Research Station, Fort Collins, Colorado, USA.
- Lydersen, J. M., M. P. North, and B. M. Collins. 2014. Severity of an uncharacteristically large wildfire, the Rim Fire, in forests with relatively restored frequent fire regimes. *Forest Ecology and Management* 328:326–334.
- Miller, J. D., E. E. Knapp, C. H. Key, C. N. Skinner, C. J. Isbell, R. M. Creasy, and J. W. Sherlock. 2009a. Calibration and validation of the relative differenced normalized burn ratio (RdNBR) to three measures of fire severity in the Sierra Nevada and Klamath Mountains, California, USA. *Remote Sensing of Environment* 113:645–656.
- Miller, J. D., and H. Safford. 2012. Trends in wildfire severity: 1984 to 2010 in the Sierra Nevada, Modoc Plateau, and southern Cascades, California, USA. *Fire Ecology* 8:41–57.
- Miller, J. D., H. D. Safford, M. Crimmins, and A. E. Thode. 2009b. Quantitative evidence for increasing forest fire severity in the Sierra Nevada and Southern Cascade Mountains, California and Nevada, USA. *Ecosystems* 12:16–32.
- Miller, J. D., C. N. Skinner, H. D. Safford, E. E. Knapp, and C. M. Ramirez. 2012. Trends and causes of severity, size, and number of fires in northwestern California, USA. *Ecological Applications* 22: 184–203.
- Miller, J. D., and A. E. Thode. 2007. Quantifying burn severity in a heterogeneous landscape with a relative version of the delta normalized burn ratio (dNBR). *Remote Sensing of Environment* 109: 66–80.
- Moritz, M. A., et al. 2014. Learning to coexist with wildfire. *Nature* 515:58–66.
- Moritz, M. A., and S. G. Knowles. 2016. Coexisting with wildfire. *American Scientist* 104:220–227.
- North, M., A. Brough, J. Long, B. Collins, P. Bowden, D. Yasuda, J. Miller, and N. Sugihara. 2015. Constraints on mechanized treatment significantly limits mechanical fuels reduction extent in the Sierra Nevada. *Journal of Forestry* 113:40–48.
- North, M., P. Stine, K. O'Hara, W. Zielinski, and S. Stephens. 2009. An ecosystem management strategy for Sierran mixed-conifer forests. General Technical Report PSW-GTR-220, USDA Forest Service, Pacific Southwest Research Station, Albany, California, USA.
- Norton, J., N. Glenn, M. Germino, K. Weber, and S. Seefeldt. 2009. Relative suitability of indices derived from Landsat ETM+ and SPOT 5 for detecting fire severity in sagebrush steppe. *International Journal of Applied Earth Observation and Geo-information* 11:360–367.
- Odion, D. C., E. J. Frost, J. R. Strittholt, H. Jiang, D. A. DellaSala, and M. A. Moritz. 2004. Patterns of fire severity and forest conditions in the Klamath Mountains, northwestern California. *Conservation Biology* 18:927–936.
- Odion, D. C., and C. T. Hanson. 2006. Fire severity in conifer forests of the Sierra Nevada, California. *Ecosystems* 9:1177–1189.
- Odion, D. C., and C. T. Hanson. 2008. Fire severity in the Sierra Nevada revisited: conclusions robust to further analysis. *Ecosystems* 11:12–15.
- Odion, D. C., M. A. Moritz, and D. A. DellaSala. 2010. Alternative community states maintained by fire in the Klamath Mountains, USA. *Journal of Ecology* 98:96–105.

- Odion, D. C., et al. 2014. Examining historical and current mixed-severity fire regimes in ponderosa pine and mixed-conifer forests of Western North America. *PLoS ONE* 9:e87852.
- Odion, D. C., C. T. Hanson, W. L. Baker, D. A. DellaSala, and M. A. Williams. 2016. Areas of agreement and disagreement regarding ponderosa pine and mixed conifer forest fire regimes: a dialogue with Stevens et al. *PLoS ONE* 11:e0154579.
- Paradis, E., J. Claude, and K. Strimmer. 2004. APE: analyses of phylogenetics and evolution in R language. *Bioinformatics* 20:289–290.
- Parks, S. A., C. Miller, J. T. Abatzoglou, L. M. Holsinger, M.-A. Parisien, and S. Z. Dobrowski. 2016. How will climate change affect wildland fire severity in the western US? *Environmental Research Letters* 11:035002.
- Parks, S. A., C. Miller, M.-A. Parisien, L. M. Holsinger, S. Z. Dobrowski, and J. Abatzoglou. 2015. Wildland fire deficit and surplus in the western United States, 1984–2012. *Ecosphere* 6:275.
- Peterson, D. W., E. K. Dodson, and R. J. Harrod. 2015. Post-fire logging reduces surface woody fuels up to four decades following wildfire. *Forest Ecology and Management* 338:84–91.
- Picotte, J. J., B. Peterson, G. Meier, and S. M. Howard. 2016. 1984–2010 trends in burn severity and area for the conterminous US. *International Journal of Wildland Fire* 25:413–420.
- Pinheiro, J., D. Bates, S. DebRoy, D. Sarkar, and R Core Team. 2015. nlme: linear and nonlinear mixed effects models. R package version 3.1-120. <http://CRAN.R-project.org/package=nlme>
- R Core Team. 2013. R: a language and environment for statistical computing. R Foundation for Statistical Computing, Vienna, Austria. <http://www.R-project.org>
- Raymond, C. L., and D. L. Peterson. 2005. Fuel treatments alter the effects of wildfire in a mixed-evergreen forest, Oregon, USA. *Canadian Journal of Forest Research* 35:2981–2995.
- Rhodes, J. J., and W. L. Baker. 2008. Fire probability, fuel treatment effectiveness and ecological tradeoffs in western U.S. public forests. *Open Forest Science Journal* 1:1–7.
- Rollins, M. G. 2009. LANDFIRE: a nationally consistent vegetation, wildland fire, and fuel assessment. *International Journal of Wildland Fire* 18: 235–249.
- Schoennagel, T., T. T. Veblen, and W. H. Romme. 2004. The interaction of fire, fuels, and climate across Rocky Mountain forests. *BioScience* 54:661–676.
- Sherriff, R. L., R. V. Platt, T. T. Veblen, T. L. Schoennagel, and M. H. Gartner. 2014. Historical, observed, and modeled wildfire severity in montane forests of the Colorado Front Range. *PLoS ONE* 9:e106971.
- Spies, T. A., M. A. Hemstrom, A. Younglodd, and S. S. Hummel. 2006. Conserving old-growth forest diversity in disturbance-prone landscapes. *Conservation Biology* 20:351–362.
- Stephens, S. L., J. K. Agee, P. Z. Fulé, M. P. North, W. H. Romme, T. W. Swetnam, and M. G. Turner. 2013. Managing forests and fire in changing climates. *Science* 342:41–42.
- Stephens, S. L., and B. M. Collins. 2004. Fire regimes of mixed conifer forests in the north-central Sierra Nevada at multiple spatial scales. *Northwest Science* 78:12–23.
- Stephens, S. L., J. M. Lydersen, B. M. Collins, D. L. Fry, and M. D. Meyer. 2015. Historical and current landscape-scale ponderosa pine and mixed conifer forest structure in the Southern Sierra Nevada. *Ecosphere* 6:79.
- Stephens, S. L., and J. J. Moghaddas. 2005. Experimental fuel treatment impacts on forest structure, potential fire behavior, and predicted tree mortality in a mixed conifer forest. *Forest Ecology and Management* 215:21–36.
- Stephens, S. L., et al. 2009. Fire treatment effects on vegetation structure, fuels, and potential fire severity in western U.S. forests. *Ecological Applications* 19:305–320.
- Swanson, M. E., J. F. Franklin, R. L. Beschta, C. M. Crisafulli, D. A. DellaSala, R. L. Hutto, D. Lindenmayer, and F. J. Swanson. 2011. The forgotten stage of forest succession: early-successional ecosystems on forest sites. *Frontiers in Ecology and the Environment* 9:117–125.
- Swetnam, T., and C. Baisan. 1996. Historical fire regime patterns in the southwestern United States since AD 1700. Pages 11–32 in C. D. Allen, editor. *Fire Effects in Southwestern Forests: Proceedings of the 2nd La Mesa Fire Symposium*. General Technical Report RM-GTR-286. USDA Forest Service, Rocky Mountain Research Station, Fort Collins, Colorado, USA.
- Taylor, A. H., and C. N. Skinner. 1998. Fire history and landscape dynamics in a late-successional reserve, Klamath Mountains, California, USA. *Forest Ecology and Management* 111:285–301.
- Tepley, A. J., and T. T. Veblen. 2015. Spatiotemporal fire dynamics in mixed-conifer and aspen forests in the San Juan Mountains of southwestern Colorado, USA. *Ecological Monographs* 85:583–603.
- Thompson, J. R., T. A. Spies, and L. M. Ganio. 2007. Reburn severity in managed and unmanaged vegetation in a large wildfire. *Proceedings of the National Academy of Sciences of the United States of America* 104:10743–10748.

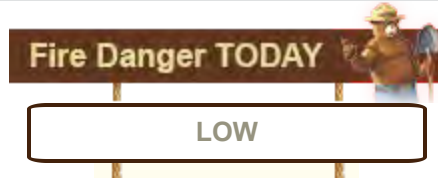
ATTACHMENT D

BRADLEY ET AL.

- US Environmental Protection Agency (EPA). 2013. Level III ecoregions of the conterminous United States. U.S. EPA Office of Research and Development (ORD)–National Health and Environmental Effects Research Laboratory (NHEERL). ftp://ftp.epa.gov/wed/ecoregions/us/Eco_Level_III_US.html
- U.S. Geological Survey (USGS) Gap Analysis Program (GAP). 2012. Protected areas database of the United States (PADUS) version 1.3. <http://gapanalysis.usgs.gov/PADUS/o>
- USDA Forest Service. 2002. National fire plan. http://www.fs.fed.us/database/budgetoffice/NFP_final32601.pdf
- USDA Forest Service. 2004. Sierra Nevada forest plan amendment, final environmental impact statement and record of decision. U.S. Forest Service, Pacific Southwest Region, Vallejo, California, USA.
- USDA Forest Service. 2009. The National Strategy: the final phase in the development of the national cohesive wildland fire management strategy. <https://www.forestsandrangelands.gov/strategy/thestrategy.shtml>
- USDA Forest Service. 2014. Scoping notice for forest plan revisions, Sierra, Inyo, and Sequoia National Forests (August 25, 2014). U.S. Forest Service, Pacific Southwest Region, Vallejo, California, USA.
- USDA Forest Service. 2015. Final environmental impact statement for the four-forest restoration initiative, with errata and objection resolution modifications. U.S. Forest Service, Coconino and Kaibab National Forests, Flagstaff, Arizona.
- USDA Forest Service. 2016. Blue Mountains forest resiliency project, notice of intent to prepare an environmental impact statement. U.S. Forest Service, Umatilla, Ochoco, and Wallowa-Whitman National Forests, Pendleton, Oregon.
- van Wageningen, J. W., K. A. van Wageningen, and A. E. Thode. 2012. Factors associated with the severity of intersecting fires in Yosemite National Park, California, USA. *Fire Ecology* 8: 11–32.
- Whitlock, C., D. A. DellaSala, S. Wolf, and C. T. Hanson. 2015. Climate change: uncertainties, shifting baselines, and fire management. Pages 265–289 in D. A. DellaSala and C. T. Hanson, editors. *The ecological importance of mixed-severity fires: nature's phoenix*. Elsevier, Waltham, Massachusetts, USA.
- Williams, M. A., and W. L. Baker. 2012a. Spatially extensive reconstructions show variable-severity fire and heterogeneous structure in historical western United States dry forests. *Global Ecology and Biogeography* 21:1042–1052.
- Williams, M. A., and W. L. Baker. 2012b. Comparison of the higher-severity fire regime in historical (A.D. 1800s) and modern (A.D. 1984–2009) montane forests across 624,156 ha of the Colorado Front Range. *Ecosystems* 15:832–847.
- Wimberly, M. C., M. A. Cochrane, A. D. Baer, and K. Pabst. 2009. Assessing fuel treatment effectiveness using satellite imagery and spatial statistics. *Ecological Applications* 19:1377–1384.

SUPPORTING INFORMATION

Additional Supporting Information may be found online at: <http://onlinelibrary.wiley.com/doi/10.1002/ecs2.1492/full>

[InciWeb - Incident Information System](#)[Kalispell Interagency Dispatch Center](#)[Montana Fire Restrictions Information](#)

Alerts & Warnings

[Food/Wildlife Attractant Storage Special Order](#)[View All Forest Alerts](#)

2017 Holland Lake Land Acquisition

The Partnership



Partnerships are a critical part of land acquisition projects for the U.S. Forest Service.

Partners and cooperators in this project include Missoula County, Montana Fish, Wildlife and Parks, Montana Department of Natural Resources, Montana Trout Unlimited, Swan Ecosystems Center, Northwest Connections, Montana Wilderness Association, Vital Ground, Backcountry Hunters and Anglers, The Trust for Public Land, The Nature Conservancy, the Rocky Mountain Elk Foundation, and

Montana Governor Steve Bullock.

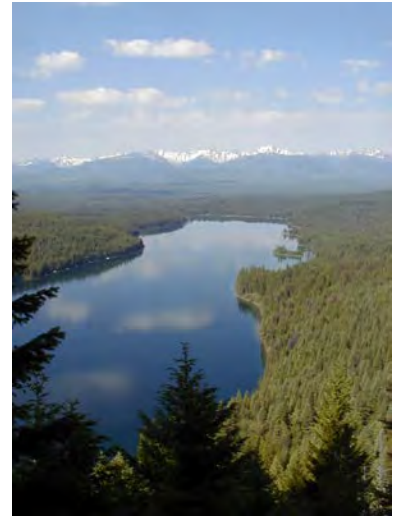
The Project

The Holland Lake Acquisition received 2017 funding from the Land and Water Conservation Fund (LWCF).

"This property lies within the popular Holland Lake recreational area of the scenic Swan Valley and there was some pressure to develop it," said Blake Henning, RMEF chief conservation officer. "We appreciate the

landowners for recognizing the wildlife values of the land and reaching out to us to help conserve it."

Situated within the internationally recognized Crown of the Continent Ecosystem, and 64-miles north of Missoula, this 640-acre parcel in the Swan Valley will contribute to national efforts to provide multiple recreation opportunities to the public. Additionally, acquisition of this parcel helps the Forest Service foster resilient, adaptive ecosystems, strengthen communities, and connect people with the outdoors. The parcel lies west of the Swan Mountains and Holland Lake Recreation Area, and east of the Mission Mountain Wilderness.



The Land

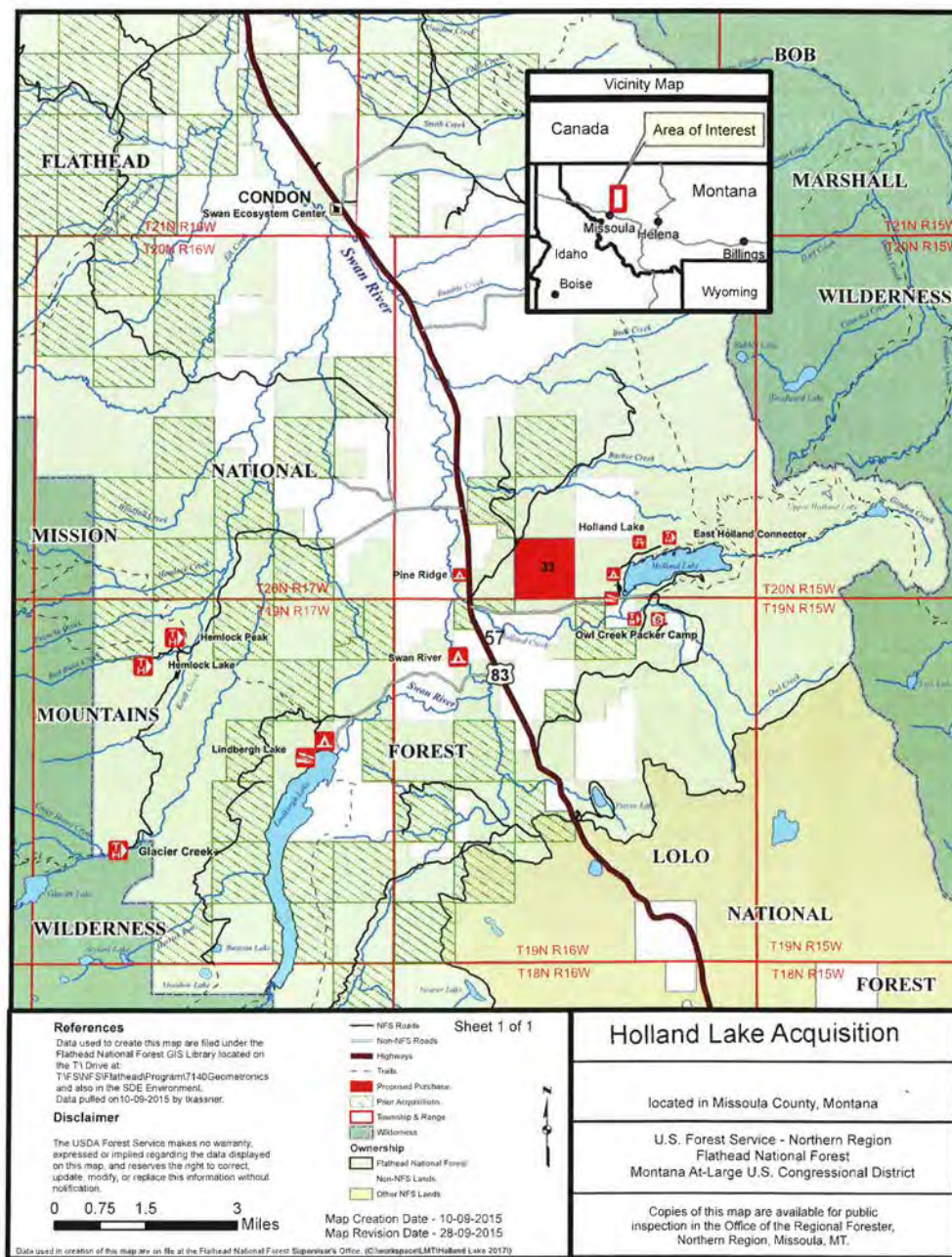


The acquisition of public land, previously threatened by development, in the Swan Valley contributes to the protection of prime wetland habitat as a result of its proximity to Holland Lake, the Swan River and its tributaries. This area provides connectivity from the Swan to the Mission Mountains and offers vital habitat for species protected by the Endangered Species Act. This area supports populations of federally threatened bull trout, grizzly bear, and Canada Lynx, as well as gray wolves, elk, moose, deer, mountain lions and wolverines.

The Crown of the Continent has been described as one of the premier mountain regions of

the world and contains many of the largest remaining blocks of roadless lands in the contiguous US. This landscape is a remarkable assemblage of peaks, dense conifer forest, cold clear rivers, and native grasslands. The full suite of native forest carnivores are found within this ecosystem, including wolf, wolverine, pine marten, fisher, bobcat, Canada lynx, mountain lion, black and grizzly bear. On a larger scale, this Crown of the Continent area links the Canadian Rockies with the Greater Yellowstone Ecosystem, Selway-Bitterroot Wilderness, and proposed Great Burn Wilderness. Acquisition of this parcel will prevent residential development and fractionation of this critical area.





[Return to top](#)

[Recreation.gov](#)

[askUSDA](#)

[Report Fraud on USDA Contracts](#)

[Accessibility Statement](#)

[WhiteHouse.gov](#)

[Policies and Links](#)

[Visit OIG](#)[Privacy Policy](#)[eGov](#)[Our Performance](#)[Plain Writing](#)[Non-Discrimination Statement](#)[Anti-Harassment Policy](#)[No FEAR Act Data](#)[Open Government](#)[Careers](#)[FOIA](#)[Information Quality](#)[USA.gov](#)

Flathead National Forest

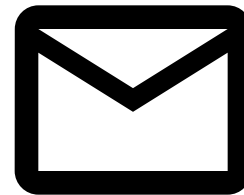
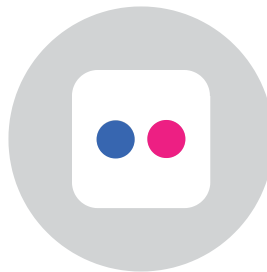
Supervisor's Office

650 Wolfpack Way

Kalispell, MT 59901

(406) 758-5208

Visit or Call our
Ranger District Offices



Contact Us



Forest Service

U.S. Department of Agriculture

